IL
NUOVO CIMENTO
ORGANO DELLA SOCIETÀ ITALIANA DI FISICA
SOTTO GLI AUSPICI DEL CONSIGLIO NAZIONALE DELLE RICERCHE
E DEL COMITATO NAZIONALE PER L'ENERGIA NUCLEARE

VOL. XXI, N. 3 *Serie decima* 1° Agosto 1961

On Static Solutions in General Relativity.

P. OLIJNYCHENKO

Institute of Physics - Madrid

(ricevuto il 14 Novembre 1960)

Summary. — The solution with cylindrical symmetry given by Weyl is examined by direct calculation of R_{ik}. The result is that Weyl's variational method is insufficient and there is no static solution for the assumed form of T^{ik}. This is generalized for any distribution of matter.

1. – Introduction.

One attempt to solve the field equations for continuous distribution of matter (with cylindrical symmetry) was made by WEYL [1]; his result is

$$ds^2 = h(dr^2 + dz^2) + \frac{r^2}{f}\,d\varphi^2 + f\,du^2\,, \qquad (u = ict),$$

$$\tfrac{1}{2}\ln f = \psi\,, \qquad \tfrac{1}{2}\ln(hf) = \gamma\,,$$

$$\Delta\psi = \tfrac{1}{2}\varrho\,; \qquad \Delta\gamma = -\operatorname{grad}^2\psi$$

(r, z and φ are cylindrical co-ordinates; Δ is the operator

$$\operatorname{div}\operatorname{grad} = \frac{\partial^2}{\partial r^2} + \frac{1}{r}\frac{\partial}{\partial r} + \frac{\partial^2}{\partial z^2}\,;$$

ϱ, the density of matter. WEYL supposed that matter is at rest; according to the conventional definition

$$T^{ik} = \varrho\,\frac{dx^i}{ds}\,\frac{dx^k}{ds} = \varrho\left(\frac{dt}{ds}\right)^2 v^i v^k\,,$$

T^{ik} has then only one component different from 0: $T^{44} = \varrho/g_{44}$).

(1) H. WEYL: *Ann. d. Phys.*, **54**, 117 (1917).

Actually there is no static solution of this form for $\varrho \neq 0$. One of Weyl's errors was to use the variational principle and to take a diagonal form of g_{ik} before calculating the components of R_{ik}; in this way some equations are missed (2).

2. – General form of R_{ik}.

(Instead of $\partial/\partial x^i$, $\partial/\partial x'^j$, $\mathrm{d}x^i$ it is written $\partial/\partial i$, $\partial/\partial j'$, $\mathrm{d}i$, etc In any single component of a tensor, the indices are denoted by the corresponding letters; for instance, g_{rr}, $g_{\varphi\varphi}$, $g_{r\varphi}$ instead of g_{11}, g_{22}, g_{12} in polar co-ordinates.)

$$
(1)\qquad
\begin{cases}
R_{ik} = \dfrac{\partial \Gamma^{\alpha}_{i\alpha}}{\partial k} - \dfrac{\partial \Gamma^{\alpha}_{ik}}{\partial \alpha} - \Gamma^{\alpha}_{ik}\Gamma^{\beta}_{\alpha\beta} + \Gamma^{\beta}_{i\alpha}\Gamma^{\alpha}_{k\beta}\,, \\[2ex]
\Gamma^{\alpha}_{i\alpha} = \dfrac{1}{2}\dfrac{\partial}{\partial i}\ln g = \dfrac{\partial}{\partial i}\ln\sqrt{\bar g}\,; \qquad \Gamma^{\beta}_{\alpha\beta} = \dfrac{\partial}{\partial \alpha}\ln\sqrt{\bar g} = \dfrac{1}{\sqrt{\bar g}}\dfrac{\partial\sqrt{\bar g}}{\partial\alpha}\,, \\[2ex]
\dfrac{\partial \Gamma^{\alpha}_{ik}}{\partial\alpha} + \Gamma^{\alpha}_{ik}\Gamma^{\beta}_{\alpha\beta} = \dfrac{1}{\sqrt{\bar g}}\dfrac{\partial}{\partial\alpha}\left(\sqrt{\bar g}\,\Gamma^{\alpha}_{ik}\right), \\[2ex]
R_{ik} = \dfrac{\partial^2}{\partial i\,\partial k}\ln\sqrt{\bar g} - \dfrac{1}{\sqrt{\bar g}}\dfrac{\partial}{\partial\alpha}\left(\sqrt{\bar g}\,\Gamma^{\alpha}_{ik}\right) + \Gamma^{\beta}_{i\alpha}\Gamma^{\alpha}_{k\beta}\,.
\end{cases}
$$

3. – Diagonal form of g_{ik} (3).

If i, k, l denote different indices, the diagonal form is defined by $g_{ik} = 0$, and then ($\gamma_i = \ln g_{ii}$)

$$
g^{ii} = \frac{1}{g_{ii}}\,, \qquad g^{ik} = 0\,,
$$

$$
\Gamma^{i}_{ii} = \frac{1}{2}\,g^{ii}\frac{\partial g^{ii}}{\partial i} = \frac{1}{2}\frac{\partial\gamma_i}{\partial i}\,,
$$

$$
\Gamma^{i}_{ll} = -\frac{1}{2}\,g^{ii}\frac{\partial g_{ll}}{\partial i} = -\frac{1}{2}\frac{g_{ll}}{g_{ii}}\frac{\partial\gamma_i}{\partial i}\,,
$$

$$
\Gamma^{i}_{il} = \frac{1}{2}\,g^{ii}\frac{\partial g_{ii}}{\partial l} = \frac{1}{2}\frac{\partial\gamma_i}{\partial l}\,; \qquad \Gamma^{i}_{kl} = 0\,.
$$

(2) The variational principle is

$$
R_{ik} = \frac{\partial}{\partial\alpha}\frac{\partial L}{\partial \bar g^{ik}_{\alpha}} - \frac{\partial L}{\partial \bar g^{ik}} \qquad (\bar g^{ik} = \sqrt{\bar g}\,g^{ik});
$$

if g_{ik} is assumed to be diagonal, L cannot be derived with respect to g^{zr} and R_{zr} is missed; if g_{rr} is made equal to g_{zz}, R_{rr} or R_{zz} is missed.

(3) The formula for R_{ik} with diagonal g_{ik}, quoted by Tolman in *Relativity, Thermodynamics and Cosmology* is too long.

4. – R_{il} for $i \neq l$.

The second term of (1) is different from 0 only when $\alpha = i$ or $\alpha = l$:

$$(2a) \qquad -\frac{1}{\sqrt{g}}\frac{\partial}{\partial \alpha}(\sqrt{g}\,\Gamma^{\alpha}_{il}) = -\frac{1}{\sqrt{g}}\left\{\frac{\partial}{\partial i}(\sqrt{g}\,\Gamma^{i}_{il}) + \frac{\partial}{\partial l}(\sqrt{g}\,\Gamma^{l}_{il})\right\} =$$

$$= -\frac{1}{2\sqrt{g}}\left\{\frac{\partial}{\partial i}\left(\sqrt{g}\,\frac{\partial \gamma_i}{\partial l}\right) + \frac{\partial}{\partial l}\left(\sqrt{g}\,\frac{\partial \gamma_l}{\partial i}\right)\right\}.$$

In the third term there are the possibilities:

1) $\beta \neq i$ and $\neq l$; then α must be equal to l or to β, otherwise $\Gamma^{\alpha}_{i\beta} = 0$:

$$1a) \qquad \alpha = l\,, \qquad \Gamma^{\beta}_{i\alpha} = \Gamma^{\beta}_{il} = 0\,;$$

$$1b) \qquad \alpha = \beta\,, \qquad \Gamma^{\beta}_{i\alpha} = \Gamma^{\alpha}_{i\alpha} \neq 0\,;$$

$$\Gamma^{\beta}_{i\beta}\Gamma^{\beta}_{l\beta} = \frac{1}{4}\sum_{\beta}\frac{\partial \gamma_\beta}{\partial i}\frac{\partial \gamma_\beta}{\partial l}\,. \qquad (\beta \neq i, l):$$

2) $\beta = i$; α can be i or l:

$$\Gamma^{i}_{i\alpha}\Gamma^{\alpha}_{li} = \Gamma^{i}_{ii}\Gamma^{i}_{li} + \Gamma^{i}_{il}\Gamma^{l}_{li} = \frac{1}{4}\left(\frac{\partial \gamma_i}{\partial i}\frac{\partial \gamma_i}{\partial l} + \frac{\partial \gamma_i}{\partial l}\frac{\partial \gamma_l}{\partial i}\right).$$

3) $\beta = l$:

$$\Gamma^{l}_{i\alpha}\Gamma^{\alpha}_{ll} = \Gamma^{l}_{ii}\Gamma^{i}_{ll} + \Gamma^{l}_{il}\Gamma^{l}_{ll} = \frac{1}{4}\left(\frac{\partial \gamma_i}{\partial l}\frac{\partial \gamma_l}{\partial i} + \frac{\partial \gamma_l}{\partial i}\frac{\partial \gamma_i}{\partial l}\right),$$

and then

$$(2b) \qquad \Gamma^{\beta}_{i\alpha}\Gamma^{\alpha}_{l\beta} = \frac{1}{4}\sum_{\delta}\frac{\partial \gamma_\delta}{\partial i}\frac{\partial \gamma_\delta}{\partial l} + \frac{1}{2}\frac{\partial \gamma_i}{\partial l}\frac{\partial \gamma_l}{\partial i}\,.$$

δ denotes all indices including i and l.

5. – R_{ik} for $i = k$ (R_{ll}).

In the second term of R_{ll} α is arbitrary. If $\alpha = l$, $\Gamma^{\alpha}_{ll} = \frac{1}{2}(\partial \gamma_l/\partial l)$; if $\alpha = \varepsilon \neq l$, $\Gamma^{\varepsilon}_{ll} = -\frac{1}{2}(g_{ll}/g_{\varepsilon\varepsilon})(\partial \gamma_l/\partial \varepsilon)$, and

$$(3a) \qquad -\frac{1}{\sqrt{g}}\frac{\partial}{\partial \alpha}(\sqrt{g}\,\Gamma^{\alpha}_{ll}) = -\frac{1}{2\sqrt{g}}\frac{\partial}{\partial l}\left(\sqrt{g}\,\frac{\partial \gamma_l}{\partial l}\right) + \frac{1}{2\sqrt{g}}\sum_{\varepsilon \neq l}\frac{\partial}{\partial \varepsilon}\left(\sqrt{g}\,\frac{g_{ll}}{g_{\varepsilon\varepsilon}}\frac{\partial \gamma_l}{\partial \varepsilon}\right).$$

In the third term

$$\Gamma^{\beta}_{l\alpha}\Gamma^{\alpha}_{l\beta} = \Gamma^{l}_{l\alpha}\Gamma^{\alpha}_{ll} + \Gamma^{b}_{l\alpha}\Gamma^{\alpha}_{l\beta} = \Gamma^{l}_{ll}\Gamma^{l}_{ll} + \Gamma^{l}_{la}\Gamma^{a}_{ll} + \Gamma^{b}_{ll}\Gamma^{l}_{bl} + \Gamma^{b}_{la}\Gamma^{a}_{lb},$$

a and b denote any index different from l. The second and the third term of this sum are equal, as one can put b for a. In the fourth a must be equal to b:

$$(3b) \qquad (\Gamma^{l}_{ll})^2 + 2\Gamma^{l}_{lb}\Gamma^{b}_{ll} + (\Gamma^{b}_{lb})^2 = \frac{1}{4}\left(\frac{\partial\gamma_l}{\partial l}\right)^2 - \frac{1}{2}\sum_{b\neq l}\frac{g_{ll}}{g_{bb}}\left(\frac{\partial\gamma_l}{\partial b}\right)^2 + \\ + \frac{1}{4}\sum_{b\neq l}\left(\frac{\partial\gamma_b}{\partial l}\right)^2 = \frac{1}{4}\sum_{\beta}\left(\frac{\partial\gamma_b}{\partial l}\right)^2 - \frac{1}{2}\sum_{b\neq l}\frac{g_{ll}}{g_{bb}}\left(\frac{\partial\gamma_l}{\partial b}\right)^2.$$

6. – The equations of the case of Sect. 1.

If $g_{rr} = g_{zz} = h$, $g_{\varphi\varphi} = r^2/f$, $g_{uu} = f$ $\quad(\ln h = \eta,\ \ln f = \Phi)$

$$\sqrt{g} = rh\,, \qquad \ln\sqrt{g} = \eta + \ln r\,,$$

$$\gamma_r = \gamma_z = \eta\,, \qquad \gamma_\varphi = 2\ln r - \Phi\,, \qquad \gamma_u = \Phi\,.$$

Besides,

$$\frac{\partial g_{ik}}{\partial\varphi} = 0\,, \qquad \frac{\partial g_{ik}}{\partial u} = 0\,.$$

Of the non-diagonal components of R_{ik} only R_{rz} is different from 0:

$$R_{rz} = \frac{\partial^2}{\partial r\,\partial z}(\eta + \ln r) - \frac{1}{2rh}\left\{\frac{\partial}{\partial r}\left(rh\frac{\partial\eta}{\partial z}\right) + \frac{\partial}{\partial z}\left(rh\frac{\partial\eta}{\partial r}\right)\right\} + \\ + \frac{1}{2}\frac{\partial\eta}{\partial r}\frac{\partial\eta}{\partial z} + \frac{1}{4}\left(2\frac{\partial\eta}{\partial r}\frac{\partial\eta}{\partial z} - \left(\frac{2}{r} - \frac{\partial\Phi}{\partial r}\right)\frac{\partial\Phi}{\partial z} + \frac{\partial\Phi}{\partial r}\frac{\partial\Phi}{\partial z}\right) = -\frac{1}{2r}\left(\frac{\partial\eta}{\partial z} + \frac{\partial\Phi}{\partial z}\right) + \frac{1}{2}\frac{\partial\Phi}{\partial r}\frac{\partial\Phi}{\partial z}.$$

The diagonal components are

$$R_{rr} = \frac{\partial^2}{\partial r^2}(\eta + \ln r) - \frac{1}{2rh}\frac{\partial}{\partial r}\left(rh\frac{\partial\eta}{\partial r}\right) + \frac{1}{2rh}\frac{\partial}{\partial z}\left(rh\frac{\partial\eta}{\partial z}\right) + \\ + \frac{1}{4}\left\{2\left(\frac{\partial\eta}{\partial r}\right)^2 + \left(\frac{2}{r} - \frac{\partial\Phi}{\partial r}\right)^2 + \left(\frac{\partial\Phi}{\partial r}\right)^2\right\} - \frac{1}{2}\left(\frac{\partial\eta}{\partial z}\right)^2 = \frac{1}{2}\Delta\eta - \frac{1}{r}\left(\frac{\partial\eta}{\partial r} + \frac{\partial\Phi}{\partial r}\right) + \frac{1}{2}\left(\frac{\partial\Phi}{\partial z}\right)^2,$$

$$R_{zz} = \frac{\partial^2}{\partial z^2}(\eta + \ln r) - \frac{1}{2rh}\frac{\partial}{\partial z}\left(rh\frac{\partial\eta}{\partial z}\right) + \frac{1}{2rh}\frac{\partial}{\partial r}\left(rh\frac{\partial\eta}{\partial r}\right) + \\ + \frac{1}{4}\left\{2\left(\frac{\partial\eta}{\partial z}\right)^2 + \left(-\frac{\partial\Phi}{\partial z}\right)^2 + \left(\frac{\partial\Phi}{\partial z}\right)^2\right\} - \frac{1}{2}\left(\frac{\partial\eta}{\partial r}\right)^2 = \frac{1}{2}\Delta\eta + \frac{1}{2}\left(\frac{\partial\Phi}{\partial z}\right)^2,$$

$$R_{\varphi\varphi} = \frac{1}{2rh}\frac{\partial}{\partial r}\left(r\frac{\partial}{\partial r}\frac{r^2}{f}\right) + \frac{1}{2rh}\frac{\partial}{\partial z}\left(r\frac{\partial}{\partial z}\frac{r^2}{f}\right) -$$

$$-\frac{1}{2}\frac{r^2}{fh}\left\{\left(\frac{\partial}{\partial r}\ln\frac{r^2}{f}\right)^2 + \left(\frac{\partial}{\partial z}\ln\frac{r^2}{f}\right)^2\right\} = \frac{1}{2h}\left\{\Delta\frac{r^2}{f} - \frac{r^2}{f}\left(\frac{1}{r} - \frac{\partial\Phi}{\partial r}\right)^2 - \frac{r^2}{f}\left(\frac{\partial\Phi}{\partial z}\right)^2\right\},$$

$$R_{uu} = \frac{1}{2h}\left\{\Delta f - f\left(\frac{\partial\Phi}{\partial r}\right)^2 - f\left(\frac{\partial\Phi}{\partial z}\right)^2\right\},$$

$R_{\varphi\varphi}$ and R_{uu} are simplified according to the formula

$$\Delta e^{\xi} = e^{\xi}\left\{\Delta\xi + \left(\frac{\partial\xi}{\partial r}\right)^2 + \left(\frac{\partial\xi}{\partial r}\right)^2\right\},$$

so that

$$R_{\varphi\varphi} = \frac{r^2}{2hf}\Delta(2\ln r - \Phi) = -\frac{r^2}{2hf}\Delta\Phi,$$

as $\Delta \ln r = 0$;

$$R_{uu} = \frac{f}{2h}\Delta\Phi.$$

Then [4]

$$R_{rr} = -\frac{1}{2}g_{rr}\varkappa T = -\frac{\varkappa hT}{2},$$

$$R_{zz} = -\frac{1}{2}g_{zz}\varkappa T = -\frac{\varkappa hT}{2},$$

$$R_{\varphi\varphi} = -\frac{1}{2}g_{\varphi\varphi}\varkappa T = -\frac{r^2}{2f}\varkappa T,$$

$$R_{uu} = \frac{1}{2}g_{uu}\varkappa T = \frac{\varkappa fT}{2},$$

$$R_{zr} = -\tfrac{1}{2}g_{zr}\varkappa T = 0.$$

The third and the fourth equation are equivalent. The final result is [5]

$$\Delta\eta - \frac{2}{r}\frac{\partial}{\partial r}(\eta + \Phi) + \left(\frac{\partial\Phi}{\partial r}\right)^2 = -\varkappa h\varrho, \tag{4a}$$

$$\Delta\eta + \left(\frac{\partial\Phi}{\partial z}\right)^2 = -\varkappa h\varrho, \tag{4b}$$

$$\Delta\Phi = \varkappa h\varrho, \tag{4c}$$

$$-\frac{1}{r}\frac{\partial}{\partial z}(\eta + \Phi) + \frac{\partial\Phi}{\partial r}\frac{\partial\Phi}{\partial z} = 0. \tag{4d}$$

[4] The equations are taken here in the form $R_{ik} = \varkappa(T_{ik} - \frac{1}{2}g_{ik}T)$.

[5] $T = T_4^4 = \varrho$.

7. – Impossibility of solution for $\varrho \neq 0$.

According to the identity $\nabla_\alpha G^{\alpha\beta} = \nabla_\alpha (R^{\alpha\beta} - \frac{1}{2} g^{\alpha\beta} R) \equiv 0$

$$\nabla_\alpha T^{\alpha\beta} = \frac{\partial}{\partial \alpha} T^{\alpha\beta} + \Gamma^{\alpha}_{\gamma\alpha} T^{\gamma\beta} + \Gamma^{\beta}_{\alpha\gamma} T^{\alpha\gamma} = 0 .$$

If $\beta \neq u$, the first and the second term are equal to 0, and

$$\Gamma^{\beta}_{\alpha\gamma} T^{\alpha\gamma} = \Gamma^{\beta}_{uu} T^{uu} = 0 .$$

Even if g_{ik} were not diagonal,

$$\Gamma^{\beta}_{uu} = \frac{1}{2} g^{\beta\gamma} \left(2 \frac{\partial g_{\gamma u}}{\partial u} - \frac{\partial g_{uu}}{\partial \gamma} \right) = - \frac{1}{2} g^{\beta\gamma} \frac{\partial g_{uu}}{\partial \gamma} ,$$

as $\partial g_{ik}/\partial u = 0$; multiplying by $g_{\delta\beta}$,

$$\frac{\partial g_{uu}}{\partial \delta} T^{uu} = \varrho g^{uu} \frac{\partial g_{uu}}{\partial \delta} = 0 ; \quad \text{either} \quad g_{uu} = \text{const} \quad \text{or} \quad \varrho = 0 .$$

In the first case, from (4*c*) $\Delta \Phi = 0$, $\varrho = 0$.

8. – Generalization.

If the distribution of matter is arbitrary and $ds^2 = X\,dx^2 + Y\,dy^2 + Z\,dz^2 + f\,du^2$, $\partial g_{ik}/\partial u = 0$, from (1) and (3)

$$R_{uu} = \sum_{\varepsilon \neq u} \left\{ \frac{1}{2\sqrt{g}} \frac{\partial}{\partial \varepsilon} \left(\sqrt{g} \frac{g_{uu}}{g_{\varepsilon\varepsilon}} \frac{\partial \gamma_u}{\partial \varepsilon} \right) - \frac{1}{2} \frac{g_{uu}}{g_{\varepsilon\varepsilon}} \left(\frac{\partial \gamma_u}{\partial \varepsilon} \right)^2 \right\} .$$

As $\partial g_{ik}/\partial u = 0$ and $g_{uu} = \text{const}$ (according to Section 7), $\gamma_u = \text{const}$, $R_{uu} = 0$; from $R_{uu} = \frac{1}{2} g_{uu} \varkappa T = g_{uu} \varkappa \varrho / 2$, $\varrho = 0$.

RIASSUNTO (*)

Esamino mediante il calcolo diretto di R_{ik} la soluzione a simmetria cilindrica data da Weyl. Risulta che il metodo variazionale di Weyl è insufficiente e che non c'è soluzione statica per la forma adottata di T^{ik}. Ciò viene generalizzato per qualsiasi distribuzione della materia.

(*) *Traduzione a cura della Redazione.*

Rotational Mechanical Moments of Electrolite Solutions in a Rotating High-Frequency Electric Field.

E. Grossetti

Istituto di Fisica Sperimentale dell'Università - Napoli

(ricevuto il 20 Gennaio 1961)

Summary. — In the present paper measurements are reported from which it results that electrolite solutions placed in a rotating high-frequency ($\nu = 100$ MHz) electric field show remarkable rotational moments, although in this frequency range the theory of the torque depending on the conductivity does not foresee any effect. The measurements have been made against the dilution (defining the dilution as the inverse of the concentration and expressing it in dm^3/g eq). While the conductivity Λ of such solutions, already for dilutions of the order of $10^2\ \Omega^{-1}\ cm^{-1} \cdot (g\ eq)/l$, acquires a value which practically does not change with the dilution, the torque due to the presence of dipoles, still tends to increase even when the dilution has reached values of the order of $10^3\ \Omega^{-1}\ cm^{-1} \cdot (g\ eq)/l$. Furthermore it has been shown that the torque is proportional to the square of the electric field. The dipendence of this moment on the frequency is characteristic of each solution.

In previous works [1,2] it has been shown that, apart from a rotational mechanical moment M_B (Born effect) which depends on the fact that there exists a phase displacement between the axis of the dipoles and the direction of the rotating field, a moment M_C appears in a liquid placed in a rotating electric field; this moment is in relation with the electrical conductivity of the liquid itself. However these moments M_B and M_C show a different behaviour at the variation of the frequency.

(1) E. Grossetti: *Nuovo Cimento*, **10**, 193 (1959).
(2) E. Grossetti: *Nuovo Cimento*, **13**, 350 (1959).

It may be said, *e.g.* that for low frequencies (50, 180, 100 Hz) [3] only the mechanical moment M_c, which depends on the conductivity, appears. Such moment is inversely proportional to the conductivity itself (Lampa's formula) [4], while, for frequencies of the order of $3 \cdot 10^5$ Hz and higher the effect which appears is that depending only on the presence of the dipoles; that is, the moment M_B (Born formula) [5] results experimentally in agreement with the theory itself. Moreover the determination of the coefficient of proportionality between the mechanical moment M_c and E^2 the square of the field intensity allows to determine, in a completely different manner the coefficients η of the liquid's viscosity, once the electrical moment m of the liquid molecules under consideration is known, whose value may obtained from the study of the polarization in relation to temperature.

According to Debye's theory, one obtains at first, in an electrolite solution a condensation of the dipoles around the ions, a phenomenon which causes characteristic behaviours, and furthermore, on the basis of the fundamental concepts of this theory, every ion is surrounded by an ionic cloud. The presence of this ionic cloud causes a variation of the conductivity with relation to the dilution, different from the one which could be expected on the basis of the classical theory, and on the appearance of a variation of the conductivity in relation to frequency. We wanted to find out whether these peculiarities, which are foreseen in electrolitic solutions, on the basis of Debye's theory, could influence the rotational effect of the dipoles which, as is known, show themselves by means of the appearance of a mechanical moment in a rotating electric field.

The condensation of the dipoles around the ions, in the last analysis causes a decrease of the dipole's mobility. And again, since they are placed radially around the centre of the ion, it causes decrease of the polarizability of the medium, which apparently has as consequence a decrease in the value of the mechanical moment. On the other hand, the formation of the ionic cloud, on the basis of Debye's theory, brings essentially to a mobility decrease of the system of dipoles, which, in the last analysis, equals a viscosity increase in the sense in which the dipoles are less free to orientate themselves. On the basis of this effect the mechanical moment should then increase.

The decrease depending on the first cause tends to lessen with the dilution and the increase due to the second cause also tends to decrease with the dilution.

Therefore, according to the entity and to the prevalence of one effect over the other a variation of the torque is to be foreseen. For this reason we

(3) A. Carrelli and M. Marinaro: *Nuovo Cimento*, **11**, 262 (1959).
(4) A. Lampa: *Wien Ber.*, **115** (2*a*), 1659 (1906).
(5) M. Born: *Zeit. f. Phys.*, **22**, 1920 (1920)

have made experiences in respect to frequencies of the order of 100 MHz, that is, for very high frequencies in order to make sure that the solutions could not present any rotational moment due to the conductivity, as is foreseen in Lampa's theory.

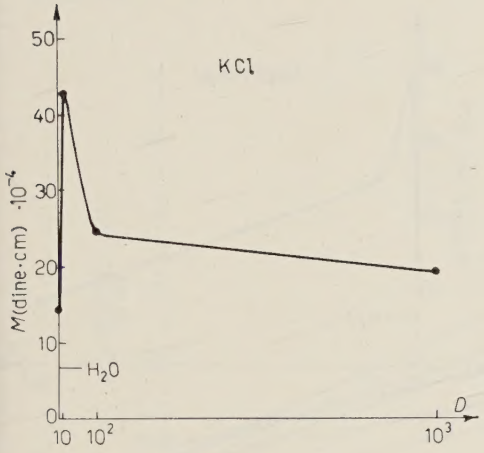

Fig. 1.

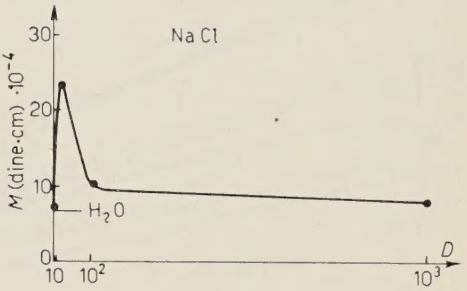

Fig. 2.

The aqueous electrolite solutions, which we have studied at such frequencies, have shown instead a very remarkable mechanical moment M_c (for certain concentrations even ten times bigger than that of water). Measurements have been taken for the following solutions: normal solution N; $N \cdot 10^{-1}$; $N \cdot 10^{-2}$; $N \cdot 10^{-3}$ of KCl, NaCl; $MgSO_4$, KOH, $Al(NO_3)_3$, $Mg(NO_3)_2$; the results obtained, that is the mechanical moments M_c measured for the various solutions, with respect to a given

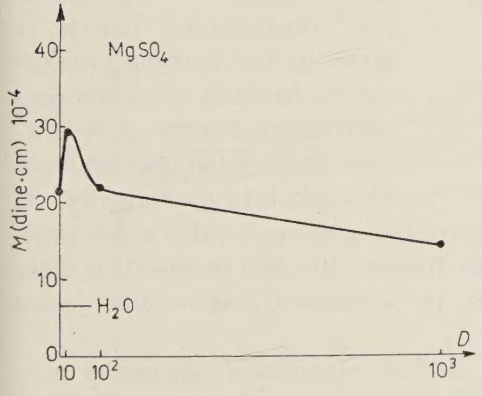

Fig. 3.

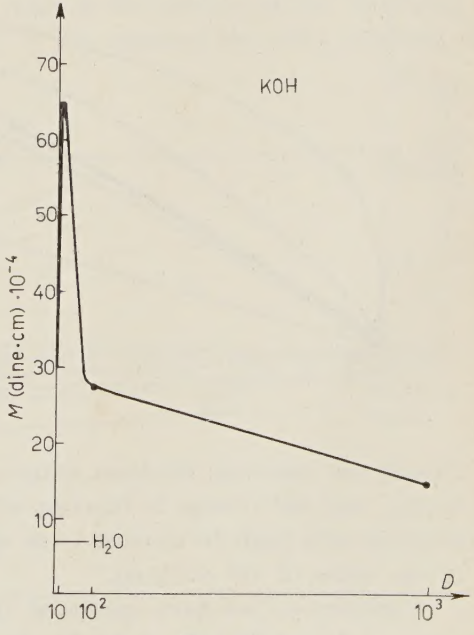

Fig. 4.

value of the electric field E, are plotted in Fig. 1, 2, 3, 5 and 6; the abscissae give the corresponding dilutions D (solution volume in dm^3/g-equivalent).

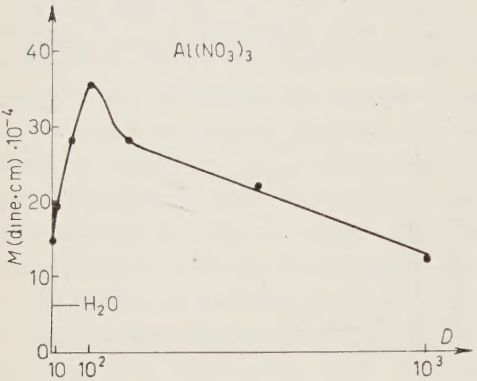

Fig. 5.

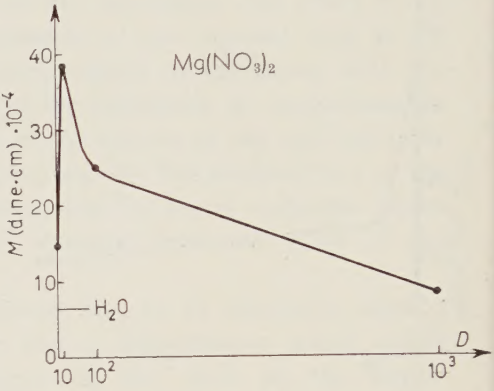

Fig. 6.

In the above named figures also the value of the water's mechanical moment is reported. In Fig. 7 and 8, shown on different scale, are reported similarly the plots which give the behaviour of the MD product *vs.* D for the studied solutions.

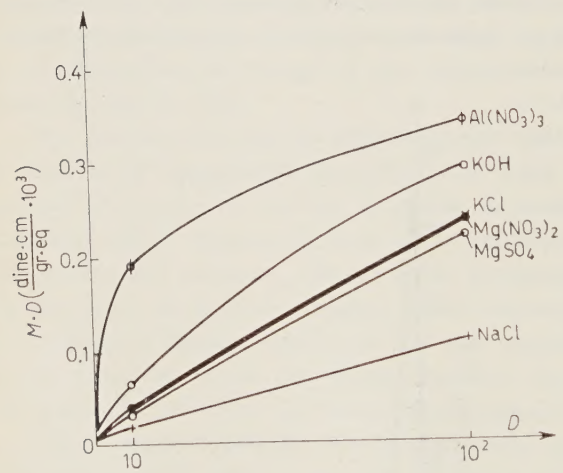

Fig. 7.

As it can be seen, the effect depends on the presence of the ions in the liquid. The quotient: mechanical torque M_e over the concentration C (that is, the MD product) grows at the increase of the dilution D, as it happens for the equivalent conductivity (which is given by the quotient: electrical conductivity over the concentration) (Fig. 9). It is however to be noted that, while in the case of the conductivity, Λ, already for molecular dilutions of the order of 10^2, acquires a value which practically does not change in function of the dilution, the MD product, for these solutions still tends to increase even when the dilution D has reached values of the order of 10^3 cm^3/g-eq.

Furthermore we have measured the mechanical moments generated in a same solution with respect to the intensity of the rotating electric field and

we have found that the values of the rotational moments of the solutions increase with the square of the field intensity, that is as given by the Born formula.

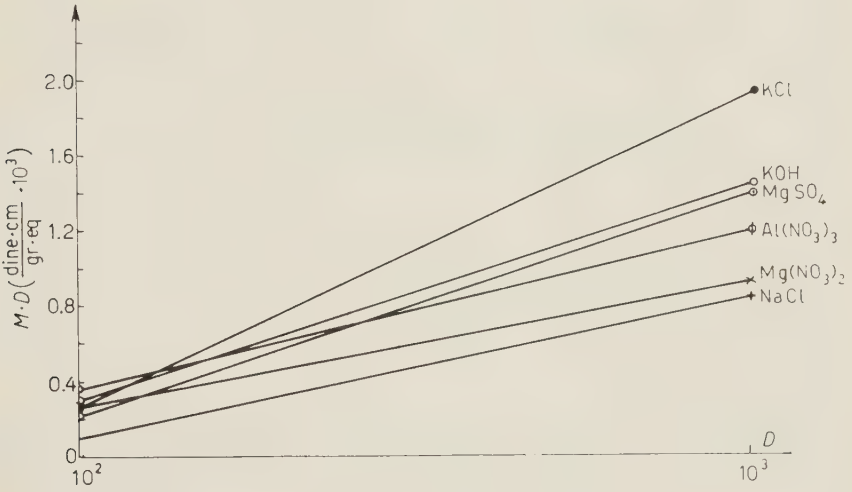

Fig. 8.

Measurements have also been taken in order to see how the mechanical moment M_c, of the different solutions varies at the increase of the frequency ν of the rotating electric field. In Fig. 10 are reported the plots obtained for

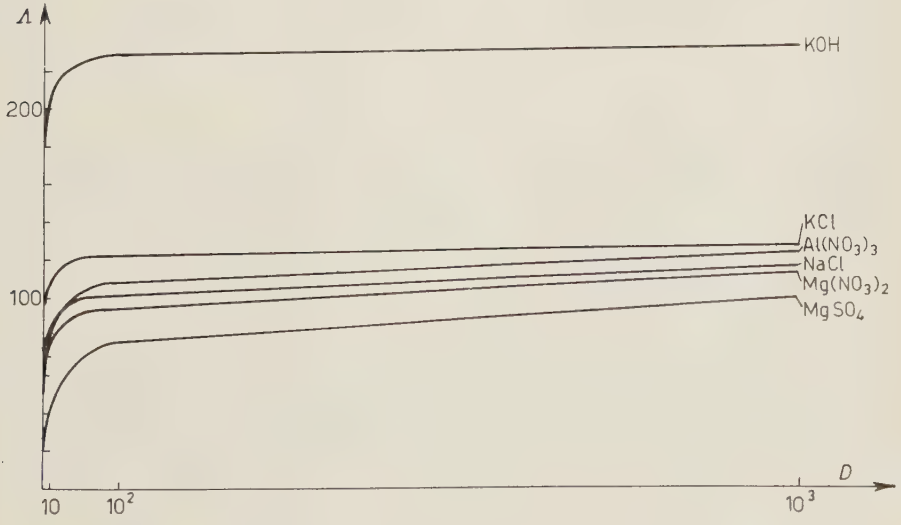

Fig. 9.

the various solutions studied; the abscissae indicate the logarithms of the ν frequencies, and the ordinates indicate the logarithms of the moments M_c determined experimentally.

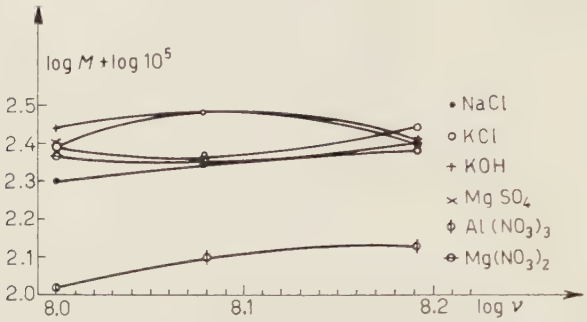

Fig. 10.

In examining these plots it is observed that for certain electrolitic solutions the mechanical moment grows with frequency, but some of the studied solutions show a different behaviour.

As it can be seen this type of research may bring some new elements in the study of electrical conductivities.

* * *

We owe thanks to Prof. A. Carrelli, Director of the Institute, for the advice he gave and for the interest he took in the work.

RIASSUNTO (*)

In questo articolo riferisco alcune misurazioni dalle quali risulta che soluzioni elettrolitiche poste in un campo elettrico rotante ad alta frequenza ($\nu = 100$ MHz) presentano un notevole momento rotazionale, quantunque per questo ordine di frequenze la teoria della torsione dipendente dalla conduttività non preveda alcun effetto. Le misure sono state eseguite rispetto alla diluizione (definendo la diluizione come l'inverso della concentrazione ed esprimendola in dm^3/g eq). Mentre la conduttività Λ di tali soluzioni, già per diluizioni dell'ordine di $10^2\ \Omega^{-1}\ cm^{-1} \cdot (g\ eq)/l$ raggiunge un valore che praticamente non cambia colla diluizione, la torsione dovuta alla presenza di dipoli, tende ancora a crescere quando la diluizione ha raggiunto valori dell'ordine di $10^3\ \Omega^{-1}\ cm^{-1} \cdot (g\ eq)/l$. Inoltre dimostro che la torsione è proporzionale al quadrato del campo elettrico. La dipendenza di questo momento della frequenza è una caratteristica di ciascuna soluzione.

(*) *Traduzione a cura della Redazione.*

Photon-Proton Collision at (250÷800) MeV.

S. Minami

Department of Physics, Osaka City University - Osaka

(ricevuto il 30 Gennaio 1961)

Summary. — A simple analysis of the experimental results for photoproduction of pions at (250÷800) MeV is made and photon-proton scattering at these energies is described in terms of shadow scattering due to photoproduction of pions. The total cross-sections for photon-proton scattering show the existence of a strong and broad resonance corresponding to the second resonance for photoproduction of pions at about 750 MeV. Since the resonance behavior is strongly reflected in photon-proton scattering, this process may be regarded as one of the most suitable reactions to study the character of the second resonance.

1. – Introduction.

Recent measurements on photoproduction of single and multiple pions in the photon energy region extending from 500 to 1000 MeV have shown the following remarkable results [1-6]:

1) there exists a broad and strong resonance level at about 750 MeV;

2) the angular distributions for $\gamma + p \to \pi^0 + p$ up to 800 MeV are quite compatible with $(2 + 3\sin^2\theta)$;

3) the angular distributions for $\gamma + p \to \pi^+ + n$ have a strong $\cos\theta$ term in the region (600÷800) MeV;

---

(1) O. Piccioni: *CERN Conference on High Energy Nuclear Physics* (1958).

(2) J. W. De Wire, H. E. Jackson and R. Littauer: *Phys. Rev.*, **110**, 1208 (1958).

(3) P. C. Stein and K. C. Rogers: *Phys. Rev.*, **110**, 1209 (1958).

(4) M. Heinberg, W. M. McClelland, F. Turkot, W. M. Woodward, R. R. Wilson and D. M. Zipoy: *Phys. Rev.*, **110**, 1211 (1958).

(5) J. M. Sellen, G. Cocconi, V. T. Cocconi and E. L. Hart: *Phys. Rev.*, **113**, 1323 (1959).

(6) J. I. Vette: *Phys. Rev.*, **111**, 622 (1958).

4) the differential cross-sections for $\gamma+p\to\pi^+ + n$ and $\gamma+p\to\pi^0+p$ at 90° are, respectively, 8 μb/sr and 4 μb/sr at 750 MeV. This ratio of 2 is in agreement with a resonance state of isotopic spin $I=\frac{1}{2}$;

5) the fact that the resonance at 750 MeV is due to a strong $d_{\frac{3}{2}}$-state interaction in the pion-nucleon system seems to be established by measurements on polarization of the recoil nucleon [7];

6) in the region (500÷800) MeV the magnitude of the cross-section for $\gamma+p\to\pi^+ + \pi^- + p$ is of the same order with that for single π^+ or single π^0 production (cf. Fig. 1 and Fig. 2).

In photon-proton collision pion photo-production processes play the most important role. Therefore it is expected that the process of photon-proton scattering can be described in terms of shadow scattering due to the absorption (*). In Section 2 we try to perform a simple analysis of the experimental results for pion photoproduction In Section 3 the cross-sections for photon-proton scattering in the region (250÷800) MeV (**) are estimated on the basis of the results in Section 2.

2. – Phenomenological analysis of pion photoproduction.

First of all let us pay attention to the angular distribution for $\gamma+p\to\pi^0+p$ (cf. Fig. 1). As is well known this reaction in the low-energy region (up to about 350 MeV) can mostly be described in terms of $p_{\frac{3}{2}}$-resonance. Since the angular distributions for this process up to 800 MeV are quite compatible with $(2+3\sin^2\theta)$, it is natural for us to assume that $M1$ $(J=\frac{3}{2})$ and $E1(J=\frac{3}{2})$-states which correspond respectively to $p_{\frac{3}{2}}$ and $d_{\frac{3}{2}}$-states in pion-nucleon system are mainly responsible for this process in the region (250÷750) MeV. We denote the reaction amplitude of the $\gamma+p\to n\pi+N$ process for the state of magnetic 2^l-pole (or electric 2^l-pole), total angular momentum J and isotopic spin I as

$$(1)\qquad \begin{cases} R^{n\pi}_{2I,2J}(Ml) = |R^{n\pi}_{2I,2J}(Ml)|\exp\big(2i\delta^{n\pi}_{2I,2J}(Ml)\big) \\ R^{n\pi}_{2I,2J}(El) = |R^{n\pi}_{2I,2J}(E\,l)|\exp\big(2i\delta^{n\pi}_{2I,2J}(E\,l)\big). \end{cases}$$

(7) G. SALVINI: *10th Rochester Conference on High Energy Physics* (1960).

(*) Photon-proton scattering at low energy (up to about 300 MeV) has been studied from a similar viewpoint [8-9].

(8) Y. YAMAGUCHI: *Prog. Theor. Phys.*, **12**, 111 (1954).

(9) S. MINAMI and Y. YAMAGUCHI: *Prog. Theor. Phys.*, **17**, 651 (1957).

(**) Experimental data for photon-proton scattering up to about 300 MeV have been reported by YAMAGATA [10].

(10) T. YAMAGATA (unpublished paper).

Then the angular distributions which have not any remarkable forward-backward asymmetry may be interpreted in such a meaning that

$$\cos 2\{\delta_{33}^{1\pi}(M1) - \delta_{13}^{1\pi}(E1)\}$$

in the interference term

$$(2) \qquad (2\sqrt{2}/3)\,|R_{33}^{1\pi}(M1)|\cdot|R_{13}^{1\pi}(E1)|\cos 2\{\delta_{33}^{1\pi}(M1) - \delta_{13}^{1\pi}(E1)\}$$

turns out to be negligibly small although $|R_{33}^{1\pi}(M1)\cdot R_{13}^{1\pi}(E1)|$ has a certain large value. This interpretation is consistent with the experimental results (7) that the values of polarization of the recoil proton are remarkably large in the energy region (500 ÷ 800) MeV, because these states contribute to the polarization of the recoil proton with

$$(3) \qquad |R_{33}^{1\pi}(M1)|\cdot \cdot|R_{13}^{1\pi}(E1)|\sin 2\{\delta_{33}^{1\pi}(M1) - \delta_{13}^{1\pi}(E1)\}$$

apart from trivial factors.

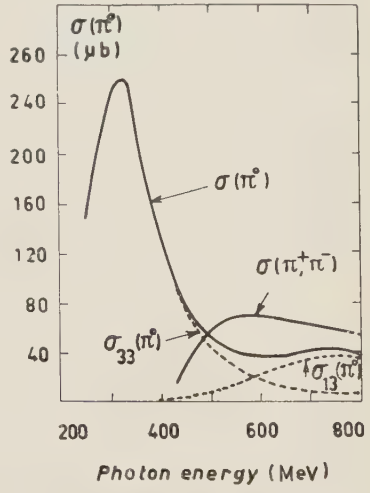

Fig. 1. – Total cross-section for π^0 production. $\sigma(\pi^0)$ represents the experimental value; $\sigma_{33}(\pi^0)$ and $\sigma_{13}(\pi^0)$ are due to the $(\frac{3}{2}, \frac{3}{2})$ and $(\frac{1}{2}, \frac{3}{2})$ resonant states respectively.

The cross-section $\sigma_{33}(\pi^0)$ due to the $M1$ $(J=\frac{3}{2})$, $I=\frac{3}{2}$-state is estimated on the basis of one level formula with resonance energy 345 MeV and width 140 MeV. Then the contribution $\sigma_{13}(\pi^0)$ from $E1$ $(J=\frac{3}{2})$, $I=\frac{1}{2}$-state to π^0 production can be estimated by $\sigma_{13}(\pi^0)=\sigma(\pi^0)-\sigma_{33}(\pi^0)$ under the assumption that $\sigma(\pi^0)$ in the energy region (250 ÷ 800) MeV is expressed in terms of the strong interactions of $M1$ $(J=\frac{3}{2})$, $I=\frac{3}{2}$ and $E1$ $(J=\frac{3}{2})$, $I=\frac{1}{2}$-states, where $\sigma(\pi^0)$ represents the experimental value of the total cross-section for $\gamma + p \to \pi^0 + p$. The curves of $\sigma_{33}(\pi^0)$ and $\sigma_{13}(\pi^0)$ are illustrated in Fig. 1, (*), where

$$(4) \qquad \sigma_{33}(\pi^0) = (2/3)(\pi/k^2)\,|R_{33}^{1\pi}(M1)|^2 = (2/3)\,\sigma_{33}(\pi)\,,$$

$$(5) \qquad \sigma_{13}(\pi^0) = (1/3)(\pi/k^2)\,|R_{13}^{1\pi}(E1)|^2 = (1/3)\,\sigma_{13}(\pi)\,.$$

Now let us try to discuss the problems of the $\gamma + p \to \pi^+ + n$ process. Since the contributions from $M1$ $(J=\frac{3}{2})$, $I=\frac{3}{2}$ and $E1$ $(J=\frac{3}{2})$, $I=\frac{1}{2}$-states to π^+

(*) In order to get a smooth curve of $\sigma_{13}(\pi^0)$, we make small correction for the curve of $\sigma_{33}(\pi^0)$ paying attention to the experimental results for polarization of recoil nucleon.

production can easily be given by $\sigma_{33}(\pi^+) = (1/2)\,\sigma_{33}(\pi^0) = (1/3)\,\sigma_{33}(\pi)$ and $\sigma_{13}(\pi^+) = 2\sigma_{13}(\pi^0) = (2/3)\,\sigma_{13}(\pi)$ respectively, we can express the cross-sections due to other states by $\sigma'(\pi^+) = \sigma(\pi^+) - \sigma_{33}(\pi^+) - \sigma_{13}(\pi^+)$, where $\sigma(\pi^+)$ indicates the experimental value for $\gamma + p \to \pi^+ + n$ reaction. These values are shown in Fig. 2.

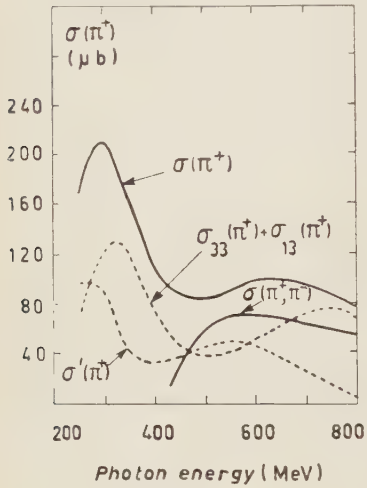

Fig. 2. – Total cross-section for π^+ production. $\sigma(\pi^+)$ represents the experimental value. $\sigma_{33}(\pi^+)$, $\sigma_{13}(\pi^+)$ and $\sigma'(\pi^+)$ are due to the $(\frac{3}{2}, \frac{3}{2})$, $(\frac{1}{2}, \frac{3}{2})$ resonant states and the other states respectively. The main part of $\sigma'(\pi^+)$ may be regarded as the contributions from $E1(J=\frac{1}{2})$ and $M1(J=\frac{1}{2})$ states.

In order to discuss what kind of states are responsible for $\sigma'(\pi^+)$, it is necessary to consider the angular distributions for $\gamma + p \to \pi^+ + n$ which have a strong $\cos\theta$ term in the region $(600 \div 800)$ MeV. It is well known that the $E1$ $(J=\frac{1}{2})$-state through which s-wave pions are produced contributes considerably to π^+ production up to 300 MeV at least. The angular distributions for this process at low energy could be explained in terms of strong interactions both of $M1$ $(J=\frac{3}{2})$ and of $E1$ $(J=\frac{1}{2})$-states. But the case is different in the phenomena at energies $(600 \div 800)$ MeV. Instead of the $M1$ $(J=\frac{3}{2})$-state it is the $E1$ $(J=\frac{3}{2})$-state that plays the most important role in photoproduction of pions at these energies. The strong forward-backward asymmetry of positive pions should be attributed to the interference between $E1$ $(J=\frac{3}{2})$ and some states among the following three ones if we take the states up to $J=\frac{3}{2}$ into consideration, $M1$ $(J=\frac{1}{2})$, $M1$ $(J=\frac{3}{2})$ and $E2$ $(J=\frac{3}{2})$-states, because the interference terms between $E1$ $(J=\frac{3}{2})$ and other states are expressed by the form

$$(6)\ (^*) \qquad (1/4k^2)\,\mathrm{Re}\big[R^*_{J=\frac{3}{2}}(E1)\{R_{J=\frac{1}{2}}(M1) - R_{J=\frac{3}{2}}(M1)\}\cos\theta + \\ + R^*_{J=\frac{3}{2}}(E1)\{R_{J=\frac{1}{2}}(E1) - \sqrt{3}\,R_{J=\frac{3}{2}}(M2)\}(1 - 3\cos^2\theta)/2 + \\ + \sqrt{3}\,R^*_{J=\frac{3}{2}}(E1)\cdot R_{J=\frac{3}{2}}(E2)\cos\theta(2 - 3\cos^2\theta)\big]\,.$$

If the form of asymmetry can be expressed in terms of $\cos\theta$ terms only, we shall be able to exclude the possibility of strong interaction in $E2$ $(J=\frac{3}{2})$-state. As was mentioned in our discussion about the γ-π^0 process (cf. eq. (2)),

(*) See the Table VI in reference [11].

(11) S. HAYAKAWA, M. KAWAGUCHI and S. MINAMI: *Prog. Theor. Phys. Supplement*, **5**, 41 (1958).

the interference between $E1\,(J=\frac{3}{2})$, $I=\frac{1}{2}$ and $M1\,(J=\frac{3}{2})$, $I=\frac{3}{2}$-states does not give rise to any remarkable effect because the magnitude of $\cos 2\{\delta_{33}^{1\pi}(M1) - \delta_{13}^{1\pi}(E1)\}$ is very small. If the strong $\cos\theta$-term is due to the interference between $E1\,(J=\frac{3}{2})$, $I=\frac{1}{2}$ and $M1\,(J=\frac{3}{2})$, $I=\frac{1}{2}$-states, the angular distributions for $\gamma+\mathrm{p}\to\pi^0-\mathrm{p}$ should have some character of asymmetry. Thus it may be said that the interference effect between $E1\,(J=\frac{3}{2})$ and $M1\,(J=\frac{1}{2})$-states is one of the most important reasons of asymmetry, although any definite conclusion can not be derived without more detailed knowledge about the experimental data. As the interpretation for $\sigma'(\pi^-)$ there may be the following possibility. A main part of $\sigma'(\pi^+)$ in the low-energy region is attributed to the contributions from the $E1\,(J=\frac{1}{2})$-state and that in the high-energy region is attributed to those from the $M1\,(J=\frac{1}{2})$-state. Since the $E1\,(J=\frac{1}{2})$ and $M1\,(J=\frac{1}{2})$-states have no large effect on π^0 production,

$$|\sqrt{\tfrac{1}{3}}R_{31}^{1\pi}(E1)+\sqrt{\tfrac{2}{3}}R_{11}^{1\pi}(E1)|\gg|\sqrt{\tfrac{2}{3}}R_{31}^{1\pi}(E1)-\sqrt{\tfrac{1}{3}}R_{11}^{1\pi}(E1)|, \tag{7}$$

$$|\sqrt{\tfrac{1}{3}}R_{31}^{1\pi}(M1)+\sqrt{\tfrac{2}{3}}R_{11}^{1\pi}(M1)|\gg|\sqrt{\tfrac{2}{3}}R_{31}^{1\pi}(M1)-\sqrt{\tfrac{1}{3}}R_{11}^{1\pi}(M1)|. \tag{8}$$

From eq. (7) and (8) it follows that

$$\sigma'(\pi^+)\cong\sigma'(\pi^+)+\sigma'(\pi^0)=\sigma'(\pi)\,, \tag{9}$$

where $\sigma'(\pi^0)$ means the cross-section of π^0 production due to the interactions in $E1\,(J=\frac{1}{2})$ and $M1\,(J=\frac{1}{2})$-states.

With regard to the cross-section for double pion production we have only experimental results for $\gamma+\mathrm{p}\to\pi^++\pi^-+\mathrm{p}$. WILSON [12] has estimated the branching ratios of the decay of the state $\mathcal{N}^{**}$ into the following decay modes:

$$\begin{cases} \mathcal{N}^{**}\to\pi^+ + \mathcal{N}^* & [\frac{1}{6}] \\ \qquad\pi^0 + \mathcal{N}^* & [\frac{1}{3}] \\ \qquad\pi^- + \mathcal{N}^* & [\frac{1}{2}] \end{cases} \tag{10}$$

$$\begin{cases} \qquad\pi^+ + \pi^- + \mathrm{p} & [\frac{1}{2}] \\ \qquad\pi^0 + \pi^+ + \mathrm{n} & [\frac{1}{3}] \\ \qquad\pi^0 + \pi^0 + \mathrm{p} & [\frac{1}{6}] \end{cases} \tag{11}$$

where $\mathcal{N}^{**}$ and $\mathcal{N}^*$ indicate the $(\frac{1}{2},\frac{3}{2})$ and $(\frac{3}{2},\frac{3}{2})$ isobaric states of the nucleon, respectively. If we adopt the above model, the value of $\sigma(\pi^+,\pi^-)$ is nearly equal to half of the total cross-section $\sigma_{13}(2\pi)$ for double pion production through

(12) R. R. WILSON: *Phys. Rev.*, **110**, 1212 (1958).

the process via $(\frac{1}{2}, \frac{3}{2})$ isobar.

$$\sigma(\pi^+, \pi^-) = (\tfrac{1}{2})(\pi/k^2)\,|\,R_{13}^{2\pi}(E1)\,|^2 = \sigma_{13}(2\pi)/2\ . \tag{12}$$

The curves of $\sigma_{33}(\pi)$ and $\sigma_{13}(\pi)+\sigma_{13}(2\pi)$ are shown in Fig. 3. For the sake of comparison, the curves for total cross-sections given by WILSON [12] are illustrated in Fig. 4 (*).

There may be some possibility of overestimation about $\sigma_{13}(2\pi)$ when its magnitude is estimated by the relation (12). Therefore it may be necessary to change the value of $\sigma_{13}(2\pi)$. Here the following cases are examined although the case iii) may not be expected.

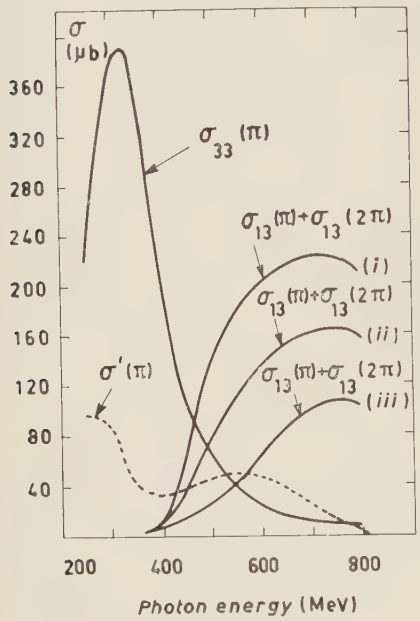

Fig. 3. – The curves show the total cross-section for excitation of $(\frac{3}{2}, \frac{3}{2})$ isobaric state and of $(\frac{1}{2}, \frac{3}{2})$ isobaric state plotted as a function of photon energy, where $\sigma_{33}(\pi)=\sigma_{33}(\pi^0)+\sigma_{33}(\pi^+)$, $\sigma_{13}(\pi)=\sigma_{13}(\pi^0)+\sigma_{13}(\pi^+)$. $\sigma_{13}(2\pi)$ means the total cross-section for double pion production due to $(\frac{1}{2}, \frac{3}{2})$ isobaric state. The curves (i), (ii) and (iii) show $\sigma_{13}(\pi)+\sigma_{13}(2\pi)$ in the following cases respectively (i) $\sigma_{13}(2\pi) = 2\sigma(\pi^+, \pi^-)$, (ii) $\sigma_{13}(2\pi)=\sigma(\pi^+, \pi^-)$, (iii) $\sigma_{13}(2\pi)=0$.

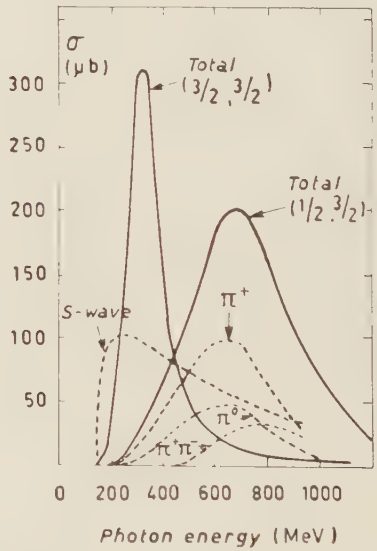

Fig. 4. – The values of $\sigma_{33}(\pi)$ and $\sigma_{13}(\pi)+\sigma_{13}(2\pi)$ estimated by Wilson (see ref [12]).

$$\text{(12)} \qquad \text{i)} \qquad \sigma_{13}(2\pi) = 2\sigma(\pi^+, \pi^-)\ ,$$

$$\text{(12)}' \qquad \text{ii)} \qquad \sigma_{13}(2\pi) = \sigma(\pi^+, \pi^-)\ ,$$

$$\text{(12)}'' \qquad \text{iii)} \qquad \sigma_{13}(2\pi) = 0\ .$$

(*) It is impossible to reproduce the experimental results shown in Fig. 1 and Fig. 2 by making use of the curves given by WILSON [12].

3. – Photon-proton scattering.

Making use of the results obtained in Section 2 we try to evaluate the cross-sections for photon-proton scattering. The contributions from the $(\frac{3}{2}, \frac{3}{2})$ and $(\frac{1}{2}, \frac{3}{2})$-resonant states to cross-sections for this process are expressed by the following forms respectively,

$$\text{(13)} \qquad \begin{cases} \dfrac{\mathrm{d}\sigma_{33}(\gamma\text{-p})}{\mathrm{d}\Omega} = \dfrac{1}{8k^2}\,|1 - A\exp[2i\alpha]|^2\,(7 + 3\cos^2\theta)/4\,, \\ \sigma_{33}(\gamma\text{-p}) = (\pi/k^2)(1 + A^2 - 2A\cos 2\alpha)\,, \end{cases}$$

$$\text{(14)} \qquad \begin{cases} \dfrac{\mathrm{d}\sigma_{13}(\gamma\text{-p})}{\mathrm{d}\Omega} = \dfrac{1}{8k^2}\,|1 - B\exp[2i\beta]|^2\,(7 + 3\cos^2\theta)/4\,, \\ \sigma_{13}(\gamma\text{-p}) = (\pi/k^2)(1 + B^2 - 2B\cos 2\beta)\,, \end{cases}$$

where

$$\text{(15)} \qquad A = \sqrt{1 - |R_{33}^{1\pi}(M1)|^2 - |R_{33}^{2\pi}(M1)|^2} = \sqrt{1 - |R_{33}(M1)|^2}\,,$$

$$\text{(16)} \qquad B = \sqrt{1 - |R_{13}^{1\pi}(E1)|^2 - |R_{13}^{2\pi}(E1)|^2} = \sqrt{1 - |R_{13}(E1)|^2}\,.$$

Since the process of pions' photoproduction plays the most important role in photon-proton collision, the effects of real phase shifts α and β may be neglected approximately. Then $\sigma_{33}(\gamma\text{-p})$ and $\sigma_{13}(\gamma\text{-p})$ are expressed as follows:

$$\text{(17)} \qquad \sigma_{33}(\gamma\text{-p}) = (\pi/k^2)(1 - A)^2 = (\pi/k^2)\big(1 - \sqrt{1 - |R_{33}(M1)|^2}\big)^2\,,$$

$$\text{(18)} \qquad \sigma_{13}(\gamma\text{-p}) = (\pi/k^2)(1 - B)^2 = (\pi/k^2)\big(1 - \sqrt{1 - |R_{13}(E1)|^2}\big)^2\,.$$

It can easily be seen that both $\sigma_{33}(\gamma\text{-p})$ and $\sigma_{13}(\gamma\text{-p})$ are underestimated by our approximation because the differences between the values in eq. (13), (14) and those in eq. (17), (18) are respectively

$$\text{((19)} \qquad \Delta\sigma_{33}(\gamma\text{-p}) = (2\pi/k^2)A(1 - \cos 2\alpha) \geqslant 0\,,$$

$$\text{(20)} \qquad \Delta\sigma_{13}(\gamma\text{-p}) = (2\pi/k^2)B(1 - \cos 2\beta) \geqslant 0\,.$$

Both $|R_{33}(M1)|^2$ and $|R_{13}(E1)|^2$ are of the order of 10^{-2}, so eq. (17) and (18) may approximately be expressed as follows:

$$\text{(21)} \qquad \sigma_{33}(\gamma\text{-p}) \cong (\pi/k^2)\big(|R_{33}(M1)|^4\big)/4 \cong (\pi/k^2)\big(|R_{33}^{1\pi}(M1)|^4\big)/4\,,$$

$$\text{22)} \qquad \sigma_{13}(\gamma\text{-p}) \cong (\pi/k^2)\big(|R_{13}(E1)|^4\big)/4\,.$$

The expressions for scatterings due to other states can easily be written down in a similar way. But the contributions from these states to photon-proton scattering turn out to be much smaller than the sum of those from $(\frac{3}{2}, \frac{3}{2})$ and $(\frac{1}{2}, \frac{3}{2})$-resonant states (*) because the effect of each state on scattering is proportional to the square of $|R_{2I,2J}(Ml)|^2$ or $|R_{2I,2J}(El)|^2$. This fact makes it possible to describe the main feature of photon-proton scattering in the region $(300 \div 800)$ MeV in terms of the shadow scattering due to the resonance phenomena in photoproduction of pions.

Since the interference term between $E1$ $(J = \frac{3}{2})$ and $M1$ $(J = \frac{3}{2})$-states contributes to angular distributions with the form of $\cos\theta$, there is no need to take into account this interference term when we discuss the differential cross-sections at 90°. Therefore

$$(23)\ (**) \qquad \frac{d\sigma(\gamma\text{-p})}{d\Omega}_{\text{at } 90^\circ} \simeq (7/32k^2)[|R_{33}(M1)|^4 + |R_{13}(E1)|^4]/4\,.$$

We show in Fig. 5 our results obtained by this method. Moreover the results based on the values of $\sigma_{33}(\pi)$ and $\sigma_{13}(\pi) - \sigma_{13}(2\pi)$ estimated by WILSON (see Fig. 4) are also shown in Fig. 5 by the dotted line.

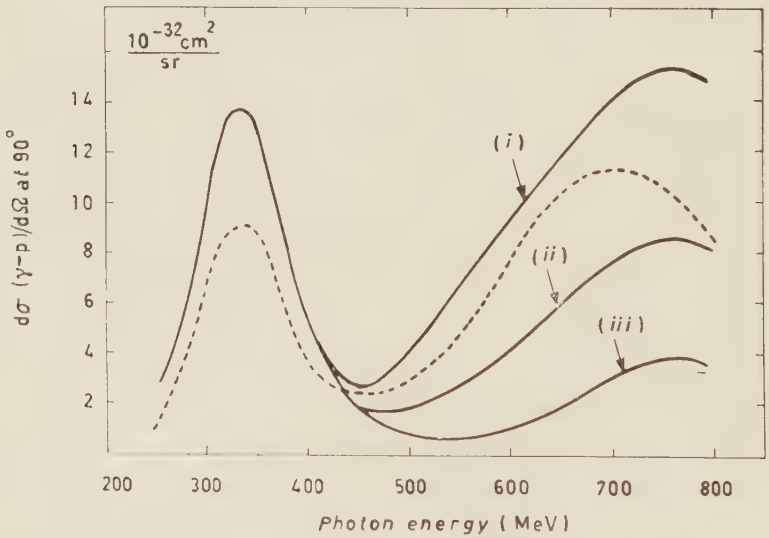

Fig. 5. – The curves (i), (ii) and (iii) show the differential cross-section at 90° for the process $\gamma + p \to \gamma + p$ corresponding respectively to those in Fig. 3. The dotted line represents the results based on $\sigma_{33}(\pi)$ and $\sigma_{13}(\pi) + \sigma_{13}(2\pi)$ in Fig. 4.

(*) Cf. Fig. 3.
(**) Cf. eq. (13) and (14).

The cross-sections for photon-proton scattering have a remarkable peak corresponding to the second resonance for the process of pion's photoproduction. Strictly speaking $\sigma_{13}(\gamma\text{-p})$ in eq. (22) is proportional to $k^2[\sigma_{13}(\pi) + \sigma_{13}(2\pi)]^2$ because $|R_{13}(E1)|^2$ is proportional to $k^2[\sigma_{13}(\pi) + \sigma_{13}(2\pi)]$ (cf. eq. (5), (12) and (16)). This k^2-dependence of $\sigma_{13}(\gamma\text{-p})$ is the very reason why $\sigma(\gamma\text{-p})$ may have a large value at the energy of the second resonance rather than the first resonance in spite of the fact that $\sigma_{13}(\pi) + \sigma_{13}(2\pi)$ at about 750 MeV is smaller than $\sigma_{33}(\pi)$ at 325 MeV. Thus the resonance behavior due to the strong interaction of the $d_{\frac{3}{2}}$-state is strongly reflected in the process of $\gamma + p \to \gamma + p$. This process may be regarded as one of the most suitable reactions to study the character of the second resonance. As is illustrated in Fig. 5, the cross-sections values in the neighbourhood of the second resonance depend strongly on $\sigma_{13}(2\pi)$. We should like to get reliable experimental data for double pion production by γ-rays.

RIASSUNTO (*)

Faccio una semplice analisi dei risultati sperimentali nella fotoproduzione di pioni a (250÷800) MeV e descrivo lo scattering fotone-protone a queste energie in funzione dello scattering ombra dovuto alla fotoproduzione di pioni. La sezione d'urto totale per lo scattering fotone-protone indica l'esistenza di una forte e larga risonanza a circa 750 MeV in corrispondenza della seconda risonanza per la fotoproduzione di pioni. Poichè il comportamento della risonanza viene fortemente rispecchiato nello scattering fotone-protone, questo processo può esser considerato una delle reazioni più adatte per lo studio del carattere della seconda risonanza.

(*) *Traduzione a cura della Redazione.*

Circular Polarization of Bremsstrahlung Emitted by a Longitudinally Polarized Electron in Weizsäcker-Williams Method.

Sasabindu Sarkar

Indian Association fot the Cultivation of Science, Department of Theoretical Physics - Jadavpur, Calcutta

(ricevuto il 6 Febbraio 1961)

Summary. — The method of Weizsäcker and Williams is applied here to calculate the circular polarization of bremsstrahlung produced in the field of nucleus by a longitudinally polarized electron. This method, valid only for extremely high energy of the electron, simplifies the calculations by reducing the problem to one of Compton scattering in a suitable Lorentz frame.

Introduction.

The longitudinal polarization of the electrons emitted in β-decay or μ-e decay is detected by observing circular polarization of the bremsstrahlung produced by the electrons themselves. This phenomenon has been investigated by McVoy [1], Banerjee [2], Fronsdal and Überall [3] all of whom have made the calculation by the laborious perturbation method. The object of the present paper is to see whether the same result can be achieved by the very much simpler method of Weizsäcker [4] and Williams [5] which consists in choosing a Lorentz frame in which the colliding electron is at rest and the field of the nucleus now moving is represented by a set of photons of different fre-

(1) Mc Voy: *Phys. Rev.*, **106**, 828 (1957).
(2) H. Banerjee: *Phys. Rev.*, **111**, 532 (1958).
(3) C. Fronsdal and H. Überall: *Phys. Rev.*, **111**, 580 (1958).
(4) C. F. v. Weizsäcker: *Zeits. f. Phys.*, **88**, 612 (1934).
(5) E. J. Williams: *Kgl. Dansk. Vid. Selsk.*, **13**, No. 4 (1935).

quencies. The photons suffer Compton scattering at the electron. An exactly opposite Lorentz transformation brings us back to the initial position and the scattered photons become the bremsstrahlung. For high-energy collisions Weizsäcker and Williams' method gives results of correct order. Lipps and Tolhoek [6] have made calculations for the different types of polarization of light scattered by an electron polarized in any direction. Taking their results we investigate the phenomenon of circular polarization of bremsstrahlung emitted by a longitudinally polarized electron by the method of Weizsäcker [4] and Williams [5].

We first choose a co-ordinate system in which the electron is initially at rest while the nucleus is moving past the electron with a high velocity. Following Batdorf and Thomas [7] we neglect collisional impacts of the electron within the nuclear radius $\sim hZ^{\frac{1}{3}}/mc$ (h, Z, m are the Planck's constant, charge number of nucleus and mass of the electron respectively) and analyse the contracted Coulomb field by means of virtual quanta. The differential cross-section of Compton scattering for initially polarized electrons according to Lipps and Tolhoek [4] is

$$\frac{\mathrm{d}\varphi}{\mathrm{d}\Omega} = \left(\frac{e^2}{mc^2}\right)^2 \frac{k^2}{k_0^2}\{\Phi_0 + \Phi_1(\xi) + \Phi_2(\xi, \zeta_0)\}\,, \tag{1}$$

where

$$\begin{cases} \Phi_0 = \dfrac{1}{8}\left[\dfrac{k_0}{k} + \dfrac{k}{k_0} - \sin^2\alpha\right], \\ \Phi_1(\xi) = \dfrac{1}{8}\xi_1 \sin^2\alpha\,, \\ \Phi_2(\xi, \zeta_0) = -\dfrac{1}{8}\xi_3(1-\cos\alpha)\,\boldsymbol{\zeta}_0\cdot(\boldsymbol{k}\cos\alpha + \boldsymbol{k}_0)\,, \\ k = \dfrac{mc^2 k_0}{mc^2 + k_0(1-\cos\alpha)}\,. \end{cases} \tag{2}$$

k_0 is the energy of the incident virtual quantum and k that of the scattered quantum, e is the charge of the electron, α is the angle of scattering and $\mathrm{d}\Omega$ is the differential solid angle of the scattered quantum. $\boldsymbol{\xi}$ and $\boldsymbol{\zeta}_0$ the polarization vectors of the scattered light quantum and the initial electron respectively. The three components of $\boldsymbol{\xi}$ known as Stokes' parameters, determine the state of polarization of the photon completely. Let the general expression for the

---

[6] F. W. Lipps and H. A. Tolhoek: *Physica*, **20**, 395 (1954).
[7] S. B. Batdorf and R. Thomas: *Phys. Rev.*, **59**, 621 (1941).

wave function of the photon be

$$(3)\qquad \begin{cases} \boldsymbol{A}\exp[i\,\boldsymbol{k}\cdot\boldsymbol{x}] = \boldsymbol{A}_1 a_1 \exp[i\,\boldsymbol{k}\cdot\boldsymbol{x}] + \boldsymbol{A}_2 a_2 \exp[\boldsymbol{k}\cdot\boldsymbol{x}]\,, \\ |a_1|^2 + |a_2|^2 = 1\,, \end{cases}$$

where unit vectors $\boldsymbol{A}_1$ and $\boldsymbol{A}_2$ (perpendicular to the wave-number $\boldsymbol{k}$) denote the two basic polarization states of the photon. Then

$$(4)\qquad \xi_1 = |a_1|^2 - |a_2|^2\,, \quad \xi_2 = a_1 a_2^* + a_2 a_1^*\,, \quad \xi_3 = i(a_1 a_2^* - a_2 a_1^*)\,.$$

In particular when $a_2 = i\,\delta a_1$ (δ is $+1$ or -1 according to whether the light is right-handed or left-handed circularly polarized)

$$(5)\qquad \xi_1 = \xi_2 = 0 \qquad \text{and} \qquad \xi_3 = \delta\,,$$

ξ_3, ξ_1 and ξ_2 denote the probabilities of circular polarization, and the two linear polarization respectively.

The number of incident quanta of energy k_0 to $k_0 + \mathrm{d}k_0$ to pass the particle is

$$(6)\qquad C(k_0) = \frac{2}{\pi}\frac{e^2}{\hbar c} Z^2 \frac{\mathrm{d}k_0}{k_0} \int_{\hbar Z^{\frac{1}{3}}/mc}^{E\hbar/mck_0} \frac{\mathrm{d}r}{r} = \frac{2}{\pi}\frac{e^2}{\hbar c} Z^2 \frac{\mathrm{d}k_0}{k_0} \ln \frac{E}{k_0 Z^{\frac{1}{3}}}\,.$$

where E is the electron energy and Z the nuclear charge number.

The energy of the scattered quantum, k' and the angle of scattering α' in the laboratory system are given by

$$(7)\qquad k' = k\left(1 - \frac{v}{c}\cos\alpha\right) E/mc^2\,,$$

and

$$(8)\qquad \cos\alpha' = \frac{\cos\alpha - v/c}{1 - (v/c)\cos\alpha}\,,$$

where v is the velocity of the electron.

Writing $k' = \varepsilon E$ and using the relation (2) we obtain

$$\frac{k}{k_0} = 1 - \frac{1 - \cos\alpha}{1 - (v/c)\cos\alpha}\,\varepsilon\,.$$

The probability of emission of a quantum of energy k' is given by

$$(9)\qquad \frac{\mathrm{d}\sigma}{\mathrm{d}\Omega} = C(k_0)\frac{\mathrm{d}\varphi}{\mathrm{d}\Omega}\,.$$

After making the transformations (7) and (8) and writing $\theta = \pi - \alpha'$ we obtain the probability of circular polarization of bremsstrahlung of a longitudinally polarized electron as ($\hbar = c = 1$)

$$\frac{\mathrm{d}\sigma}{\mathrm{d}\Omega} = \frac{1}{2}\frac{\mathrm{d}\sigma_1}{\mathrm{d}\Omega} - \frac{1}{2}\delta\frac{\mathrm{d}\sigma_2}{\mathrm{d}\Omega}, \tag{10}$$

where

$$\frac{\mathrm{d}\sigma_1}{\mathrm{d}\Omega} = C(k_0)\left[2 - \frac{1 - v^2/c^2}{(1 - (v/c)\cos\theta)^2}\sin^2\theta + \varepsilon^2\frac{(1+\cos\theta)^2}{1 + v/c - \varepsilon(1+\cos\theta)}\frac{1}{1+v/c}\right].$$

and

$$\frac{\mathrm{d}\sigma_2}{\mathrm{d}\Omega} = C(k_0)\frac{1+\cos\theta}{1+v/c}\varepsilon\left[\frac{1}{C(k_0)}\frac{\mathrm{d}\sigma_1}{\mathrm{d}\Omega} + \varepsilon\frac{1+\cos\theta}{1+v/c}\right],$$

The formula (10) for the case of circular polarization is derived from (1) and (9) by substituting particular values for the Stokes' parameters as given in (5) or directly by using the expression $a_1(\boldsymbol{A}_1 + i\delta\boldsymbol{A}_2)\exp[i\,\boldsymbol{k}\cdot\boldsymbol{x}]$ for the vector potential of the emitted photon in the matrix element.

The expression for the circular polarization is given by

$$P_c = (\mathrm{d}\sigma_2/\mathrm{d}\Omega)/(\mathrm{d}\sigma_1/\mathrm{d}\Omega)\,. \tag{11}$$

In Fig. 1 the circular polarization for 100% longitudinally polarized electron of initial energy $E = 6$ (≈ 2.5 MeV) *vs.* fractional photon energy $k/(E-1)$, (energy is measured in units of rest energy of electron) is plotted and compared with the corresponding graph of FRONSDAL and ÜBERALL [3] for various photon emission angles. The agreement between the two graphs is satisfactory.

Eq. (11) shows that the cross-section for right-handed circular polarization is larger or smaller than that of the left-handed circular polarization of the bremsstrahlung according as the polarization of the electron is parallel or antiparallel to its momentum. The circular polarization

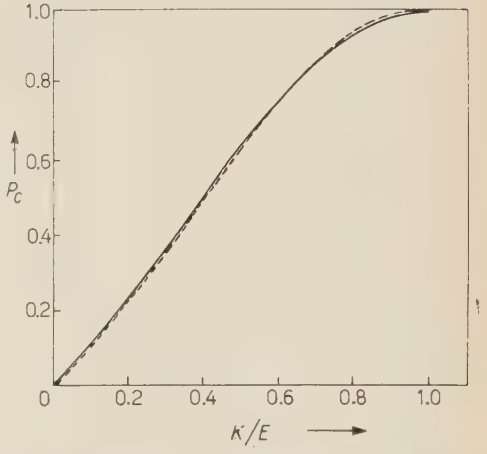

Fig. 1. – Circular polarization P_c (for 100% longitudinally polarized electron) for initial electron energy $E = 6$ (≈ 2.5 MeV) *vs.* fractional photon energy $k/(E-1)$ for emission angles of 0° and 30°. Our result is shown in broken line and that of Fronsdal and Überall in solid line.

P_c of the bremsstrahlung emitted by 100% longitudinally polarized electron varies from zero for soft radiation to almost 100% at the high spectral end. Further the circular polarization has got little variation with the angle of emission of the radiation.

In the case of electrons incident at extremely high energy the bremsstrahlung is mostly emitted in a small cone in the forward direction. In this case we get the average of circular polarization P_c of the entire cone of radiation by integrating (10) over the photon emission angle.

Putting $v = c$

$$\mathrm{d}\Omega = 2\pi \frac{mc^2}{k_0} \frac{\mathrm{d}\varepsilon}{(1-\varepsilon)^2},$$

$$\sigma(\varepsilon, E)\,\mathrm{d}\varepsilon = 2\,\frac{e^2}{\hbar c}\left(\frac{e^2}{mc^2}\right)^2 Z^2\,\mathrm{d}\varepsilon \int_{\varepsilon/2(1-\varepsilon)}^{E/mc^2 Z^{\frac{1}{3}}} \mathrm{d}k_0 \int_{Z^{\frac{1}{3}}}^{E/mc^2 k_0} \frac{\mathrm{d}r}{r} \cdot \tag{12}$$

$$\cdot\left[\left\{\frac{2-2\varepsilon+\varepsilon^2}{1-\varepsilon}\frac{1}{k_0^2} - \frac{2\varepsilon}{1-\varepsilon}\frac{1}{k_0^3} + \frac{\varepsilon^2}{(1-\varepsilon)^2}\frac{1}{k_0^4}\right\}(1+\varepsilon\delta) + \delta\varepsilon^2\frac{1}{k_0^2}\right] =$$

$$= 2\,\frac{e^2}{\hbar c}\left(\frac{e^2}{mc^2}\right)^2 Z^2\,\mathrm{d}\varepsilon\left\{\left[\frac{8(1-\varepsilon)+6\varepsilon^2}{3\varepsilon}(1+\varepsilon\delta) + 2\varepsilon(1-\varepsilon)\delta\right]\ln\frac{2E(1-\varepsilon)}{\varepsilon mc^2 Z^{\frac{1}{3}}} - \right.$$

$$\left. - (1+\varepsilon\delta)\,\frac{26(1-\varepsilon)+18\varepsilon^2}{9\varepsilon} - 2\varepsilon(1-\varepsilon)\delta\right\}.$$

For extremely high energy of the incident electron the part of (12) containing

$$\ln\frac{2E(1-\varepsilon)}{\varepsilon mc^2 Z^{\frac{1}{3}}},$$

as a factor is much greater than the remaining part of (12), so the circular polarization summed over all angles of emission of photon is independent of the initial energy of the electron.

Fig. 2 represents the circular polarization P_c integrated over

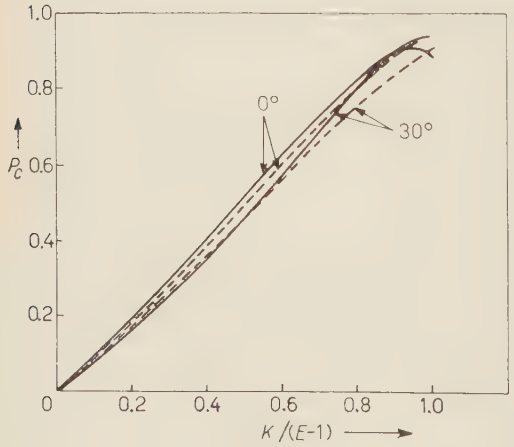

Fig. 2. – Circular polarization integrated over photon emission angles for extremely high initial electron energy *vs.* fractional photon energy k/E. Our result is shown in broken lines and that of Fronsdal and Überall in solid lines.

the emission angle as a function of the fractional photon energy; our results shown in broken lines are in good agreement with those of FRONSDAL and ÜBERALL (7) shown in solid lines.

* * *

The author is grateful to Prof. D. BASU for his constant help and guidance throughout the progress of this work.

RIASSUNTO (*)

Si applica qui il metodo di Weizsäcker and Williams per calcolare la polarizzazione circolare di bremsstrahlung prodotta nel campo del nucleo da un elettrone polarizzato longitudinalmente. Questo metodo, valido solo per altissime energie dell'elettrone, semplifica i calcoli riducendo il problema a quello dello scattering Compton in un'opportuno schema di Lorentz.

(*) *Traduzione a cura della Redazione.*

Photoproduction of π^0 in the Coulomb Field of the Electron.

P. G. Sona

Laboratori C.I.S.E. – Segrate, Milano

(ricevuto il 22 Febbraio 1961)

Summary. — Parallel to the process, studied by Primakoff, of photoproduction of π^0 in the Coulomb field of the nucleus, there exists another photoproduction process of π^0 in the Coulomb field of the electron. The total cross-section is of the same order as that of the Primakoff process, divided by Z^2. A formula is given for the angular distribution in the c. m. system. The possibility is considered of utilizing this process to determine the mean life of π^0.

1. – The purpose of this work is to study the reaction

$$\gamma + e^- \to \pi^0 + e^- \tag{1}$$

that is the photoproduction of π^0 in the Coulomb field of the electron. A few years ago [1] the existence was suggested by Primakoff of an analogous process in the Coulomb field of the nucleus; the measurement of the cross-section of this process enables us to know indirectly the mean life of the π^0-meson. Though similar substantially, kinematically the two process differ greatly. The Feynman graph relative to the process (1) is of the type shown in Fig. 1.

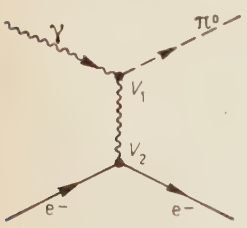

Fig. 1. – Feynman graph for process (1).

The coupling constant in the vertex V_1 is not known; but because the interaction represented by

[1] H. Primakoff: *Phys. Rev.*, **81**, 899 (1951).

the vertex V is the same that gives rise to the decay of π^0 into two photons, we may express in terms of this constant both the life τ of π^0 and the cross-section σ for the process under examination, and therefore we have a theoretical relationship between τ and σ. The most simple interaction that can be assumed for vertex V_1 (for pseudoscalar π^0) is of the type:

$$\text{cost} \cdot \Phi_{\pi^0} \cdot (\boldsymbol{E} \cdot \boldsymbol{H}) \,. \tag{2}$$

This interaction is the limiting form of a non-local interaction taking place with the intervention of a virtual intermediate state of a nucleon-antinucleon pair when the mass M of the nucleon is made to tend to ∞. Therefore the formulae that can be deduced from it for τ and σ are a good approximation only as long as the total energy of π^0 in the c.m. system is somewhat smaller than M.

The graph of Fig. 1 is topologically identical to the one relative to the decay $\pi^0 \to e^+ + e^- + \gamma$ studied by DALITZ [2], as also to that of the process $e^+ + e^- \to \pi^0 + \gamma$ considered by some authors. The difference consists only in the different classification of the four lines leaving the graph as ingoing or outgoing particles.

2. – Let us consider first the kinematics of reaction (1), assuming the target electron fixed in the laboratory system.

The threshold is at the energy of the photon $E_\gamma = 19.7$ GeV. For any value of E_γ, the π^0 can be produced only at angles $< m_e/m_\pi = 1/264$ rad, while the recoil electron can be emitted between 0° and 90°. Taking for instance $E_\gamma = 30$ GeV, the production angle of π^0 is $< 1.54 \cdot 10^{-3}$ rad. Therefore π^0 is emitted in a narrow cone around the direction of the incident γ-ray. For each E_γ, the maximum production angle of π^0 is given by

$$\bar{\vartheta}(E_\gamma) = \frac{2E_\gamma/m_e - (m_\pi/m_e)^2}{2(m_\pi/m_e)\, E_\gamma/m_e} \,. \tag{3}$$

In the c.m. system, π^0 is emitted with a momentum p_π^* given by

$$p_\pi^* = m_\pi \cdot \frac{2E_\gamma/m_e - (m_\pi/m_e)^2}{2(m_\pi/m_e)\sqrt{2E_\gamma/m_e}} \,. \tag{4}$$

For $E_\gamma = 30$ GeV this gives $p_\pi^* = m_\pi \cdot 0.264 \simeq 35.7$ MeV/c. In the laboratory

(2) R. H. DALITZ: *Proc. Phys. Soc.*, **64**, 667 (1951).

system, the momentum p_π of π^0 varies between two limits given by

$$(5) \qquad \begin{cases} p_{\pi\,\mathrm{min}} = \dfrac{m_\pi^2}{2m_e} = 17.9\ \mathrm{GeV/c} = \mathrm{cost}\,, \\ p_{\pi\,\mathrm{max}} = E_\gamma\,. \end{cases}$$

In the case of $E_{\pi^0} = \max = E_\gamma$, the two photons from the decay of π^0 form a minimum angle of $2m_\pi/E_\gamma$; for $E_\gamma = 30$ GeV, this angle is $\sim 9 \cdot 10^{-3}$ rad.

3. – The differential cross-section has been derived from the graph in Fig. 1, with the approximations $m_e/m_\pi \ll 1$, $m_e/\omega \ll 1$, $\omega = \sqrt{2 m_e E_\gamma}$ being the energy of the incident photon in the c.m. system. In the c.m. system we obtain

$$(6) \qquad \sigma(\vartheta)\,\mathrm{d}\Omega = \frac{\alpha^3 g^2}{(2\pi)^2}\left(\frac{\hbar}{m_\pi c}\right)^2\left(\frac{m_\pi}{M}\right)^2 \frac{1 - \frac{1}{4}s^2(1 - \cos\vartheta)^2}{1 - \cos\vartheta + \varepsilon}\,\mathrm{d}\Omega\,,$$

where: $\vartheta =$ production angle of π^0 in the c.m. system,

$$\varepsilon = \left(\frac{m_e}{m_\pi}\right)^2 \cdot \frac{(1-s)^2}{s} \cdot \left(\frac{2-s}{s}\cos\vartheta - 1\right),$$

$$s = 1 - \left(\frac{m_\pi}{2\omega}\right)^2,$$

$$\alpha = \frac{1}{137}\,,$$

$g =$ coupling constant π^0-nucleon.

The mean life τ of π^0, using the same symbols for the coupling constants, is given by

$$(7) \qquad \frac{1}{\tau} = \left(\frac{\alpha}{4\pi}\right)^2 g^2 \left(\frac{m_\pi}{M}\right)^2 \frac{m_\pi \cdot c^2}{\hbar}\,.$$

By integrating (6) we obtain for the total cross-section:

$$(8) \qquad \sigma_{\mathrm{tot}} = \frac{\alpha^3 g^2}{2\pi}\left(\frac{\hbar}{m_\pi c}\right)^2\left(\frac{m_\pi}{M}\right)^2 \left|\left(1 + \frac{3}{4}s^2 + \frac{1}{4}s^4\right)\ln\left(\frac{m_\pi^2}{m_e^2}\,\frac{s^2}{(1-s)^3}\right) - \frac{3}{2}s^2\right|.$$

This expression is not valid for E_γ values very near the threshold (the logarithm should be somewhat > 1) due to the approximations made ($m_e/m_\pi \ll 1$, $m_e/\omega \ll 1$); and, in view of what has been said above, it is no longer valid when

the energy of the π^0 in the c.m. system is near (or grater than) 1 GeV; (6) also permits us to obtain easily the energy spectrum of π^0, for each E_γ, because, due to the great forward collimation of the π^0, $\mathrm{d}\cos\vartheta/\mathrm{d}E_{\pi^0}$ is practically a constant (E_{π^0} = total energy of π^0 in the laboratory). From (6) it can be seen that σ is strongly anisotropic and peaked at small angles; correspondingly, the energy spectrum of π^0 in the laboratory is strongly concentrated towards higher energies (towards E_γ).

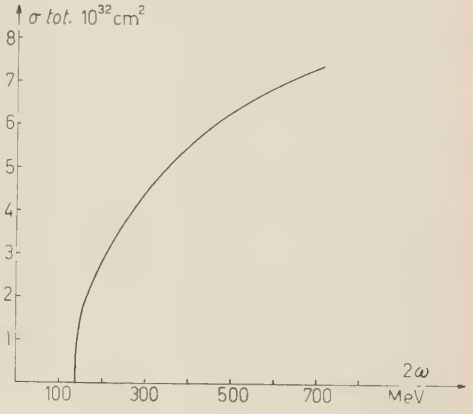

Fig. 2. – Total cross-section for process (1) for $\tau = 10^{-17}$ s, as function of E_γ = energy of the incident photon in the laboratory.

For the sake of comparison we shall give the formulae of the differential cross-section $\sigma'(\vartheta)/Z^2$ for the process of Coulomb photoproduction of π^0 from nuclei, as given by MORPURGO [3] (with some change in the symbols for coupling constants):

$$\frac{\sigma'(\vartheta)}{Z^2}\,\mathrm{d}\Omega = \frac{\alpha^3 g^2}{(2\pi)^2}\left(\frac{\hbar}{m_\pi c}\right)^2\left(\frac{m_\pi}{M}\right)^2 \frac{2v^3\sin^2\vartheta}{(1+v^2-2v\cos\vartheta)^2}\,\mathrm{d}\Omega\,, \tag{9}$$

$$\frac{\sigma'_{\mathrm{tot}}}{Z^2} = \frac{\alpha^3 g^2}{2\pi}\left(\frac{\hbar}{m_\pi c}\right)^2\left(\frac{m_\pi}{M}\right)^2\left[(1+v^2)\ln\frac{1+v}{1-v} - 2v\right], \tag{10}$$

in which the nucleus is supposed of infinite mass and $Z\cdot e$ charge, and in which v = velocity of outgoing π^0/c.

In Fig. 2, 3 and 4 are respectively shown the σ_{tot} given by eq. (8) as function of 2ω (total energy in the c.m. system), the same σ_{tot} as function of E_γ, the $\sigma'_{\mathrm{tot}}/Z^2$ given by (10); all these σ's

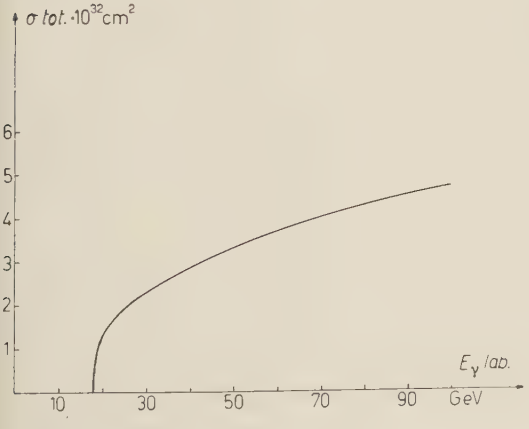

Fig. 3. – Total cross-section for process (1) for $\tau \approx 10^{-17}$ s as function of 2ω, with ω = energy of the incident photon in the c. m. system.

[3] G. MORPURGO: *Suppl. Nuovo Cimento*, **16**, 17 (1960).

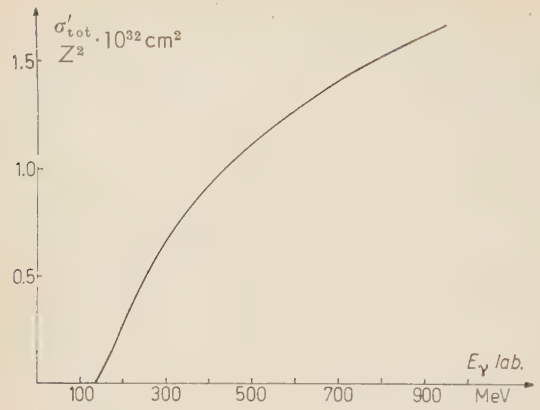

are calculated in the case of $\tau = 10^{-17}$ s.

From the comparison it can be seen that, photon energy in the c.m. system being equal, σ_{tot} is of the same order, but somewhat greater than σ'_{tot}/Z^2.

Fig. 4. – Total cross-section ($\cdot 1/Z^2$) of Primakoff process for $\tau = 10^{-17}$ s, as function of E_γ = energy of the incident photon.

4. – In principle, the study of process (1) therefore allows an indirect measurement of the mean life τ of the π^0, as one obtains for the Primakoff process. It is clear however, that the much smaller value of σ_{tot} (Z^2 cannot be varied here), the greater E_γ energies required (~ 30 GeV), and the strong collimation forward, impose severe restrictions on the possibility of studying this reaction. It should be noted however that the experimental study of the Primakoff process shows that there is a strong interference [3] between the Coulomb production and the nuclear production of π^0 which lacks completely in process (1). As far as the possibility of distinguishing experimentally process (1) from other processes is concerned, it should be observed that in a reaction of this type the total charge of the interacting particles is negative. This fact suggests the use of a technique which visualizes the track of the recoiling electron, and which gives at least the sign of the charge of this recoil.

It is easy to see that it should be possible to have a sufficient number of events of this type; but strong limitations arise from the requirement of distinguishing wanted events from other types of events, due to the same γ-ray beam itself, or to the neutron beam produced together with the γ-rays.

The angle formed by the two γ from π^0-decay, though small (see Section 2). is always quite greater than the average angle of production of secondary particles from purely electrodynamic events, for the same value of E_γ.

5. – Let us now consider the process:

(11) $$e^+ + e^- \to \gamma + \pi^0 .$$

If the negative electron is fixed in the laboratory, the kinematics of this process is practically identical to that of process (1). The matrix element that gives rise to this process is exactly the same: from simple phase-space considerations it is evident that the σ should also be of the same order of mag-

nitude, energy of the incident particle being equal. Thus, in principle, process (11) can also be used for an indirect measurement of τ, provided an intense beam of high energy ((20 ÷ 30) GeV) e^+ is available. It should be noted that if a linear accelerator of several GeV for e^- electrons (as the one proposed by NEALS and PANOFSKY [4]) could be available, it would be easy to adapt it for the production of positrons in a not-too-wide energy interval; it would be sufficient simply to insert in the accelerating tube a target of a convenient thickness on the path of the electrons, where $E_e \simeq (0.5 \div 1)$ GeV, and adjust the phase of the accelerating electric field in the second part of the accelerator in such a way as to accelerate in it the positrons produced in the target by the double collisions $e^- \to e^- + \gamma$ (bremsstrahlung), $\gamma \to e^+ + e^-$ (pair production). The same process (11) can be studied, as has been recently proposed [5,6], with a storage-ring machine in which two beams (an e^+ beam and an e^- beam) circulate continuously in the same orbit and in opposite directions; in this case the energy of the colliding electrons should be of the order of some hundred MeV.

* * *

The author wishes to thank Prof. R. DUIMIO for suggestions and discussions.

---

(4) R. B. NEAL and W. K. U. PANOFSKY: *Proc. CERN Symp. on high energy accelerators and pion physics* (1956).

(5) B. TOUSCHEK: *Nota interna n. 57 dei Lab. Naz. di Frascati del C.N.E.N.*

(6) G. GHIGO: *Nota interna n. 62 dei Lab. Naz. di Frascati del C.N.E.N.*

RIASSUNTO

In analogia al processo di fotoproduzione di π^0 nel campo coulombiano del nucleo, studiato da PRIMAKOFF, esiste anche un processo di fotoproduzione di π^0 nel campo coulombiano dell'elettrone. La sezione d'urto totale è dello stesso ordine di quella del processo di Primakoff, divisa per Z^2; viene data la formula per la distribuzione angolare nel sistema del c. di m. Viene considerata la possibilità di principio di utilizzare questo processo per la determinazione indiretta della vita media del π^0.

The Mass of the Muon's Neutrino (*).

J. Bahcall and R. B. Curtis

Indiana University - Bloomington, Ind.

(ricevuto il 16 Marzo 1961)

Summary. — We investigate the effects, on free muon production and decay, of a non-zero mass for the muon's neutrino. The quantity most sensitive to the mass of the muon's neutrino is the shape of the electron spectrum from isotropic μ^+-decay near the maximum electron energy. A probable upper limit of 5 electron masses is set on the neutrino's mass using data on the maximum electron energy, but a more accurate evaluation is possible, with current experimental techniques, if data are obtained on the shape of the isotropic electron spectrum.

1. – Introduction.

The form of the electron-neutrino coupling has been spelled out in detail by a series of beautiful experiments in allowed β-decay (1), but a corresponding phenomenological determination of the muon-neutrino coupling has not been possible. Observations made on decay electrons have been essentially the only source of experimental information concerning the muon-neutrino coupling, whereas in β-decay crucial observations have also been made on the initial and final nuclei. Moreover, radioactive nuclei are more convenient experimental sources than μ-mesons, and this greater convenience has made possible a precise measurement of the mass of the β-decay neutrino (2) while a similar measurement has not been possible in muon-decay.

The fact that electrons emitted in μ-decay predominantly have energies near the maximum electron energy proves that the Pauli principle does not

(*) Supported in part by the National Science Foundation.

(1) E. J. Konopinski: *Ann. Rev. Nucl. Sci.*, **9**, 99 (1959).

(2) L. Langer and D. Moffat: *Phys. Rev.*, **88**, 689 (1952).

operate between the two neutral particles that participate in μ-decay. We know, therefore, that the two neutral particles are either a particle and its anti-particle or two different species of neutral particles. There is no experimental information indicating which of these alternatives is correct.

The assumption that the muon's neutrino, ν_μ, is different from the electron's neutrino, ν_β, has been made by a number of authors [3], primarily to forbid unobserved μ-decay modes. This assumption implies that the precise measurements of the β-decay neutrino's helicity and mass tell us nothing about the experimental properties of the muon's neutrino. There is almost no direct information available on the helicity of the muon's neutrino [4] and published estimates on the mass of the muon's neutrino only set a probable upper limit of 8 or 9 electron masses [5].

Experiments are currently underway to measure the helicity of ν_μ; we shall discuss the effects, on muon production and decay, of a non-zero mass, m_ν, for the muon's neutrino. The experiment most sensitive to m_ν is a measurement of the shape of the electron spectrum from isotropic μ-decay near the maximum electron energy.

We assume that the mass of the β-decay neutrino is zero and that the $V-A$ theory is correct. Our results are valid, however, for either a right-handed or a left-handed ν_μ and for a large class of experimentally possible interactions.

2. – Production of muons.

There are three ways in which a non-zero m_ν would affect muon production.

2·1. *Muon-electron branching ratios.* – The muon-electron branching ratio from pion (kaon) decay is

$$(1) \qquad B_\pi \equiv \frac{w(\pi \to e + \nu_\beta)}{w(\pi \to \mu + \nu_\mu)} = \frac{\mathscr{P}_e(E_e E_{\nu_\beta} - \mathscr{P}_e^2)}{\mathscr{P}_\mu(E_\mu E_{\nu_\mu} - \mathscr{P}_\mu^2)} \approx$$

$$\approx \left(\frac{m_e}{m_\mu}\right)^2 \left(\frac{m_\pi^2 - m_e^2}{m_\pi^2 - m_\mu^2}\right) \left[1 - \left(\frac{m_\nu}{m_\pi}\right)^2 \frac{(1-3\chi^4)}{\chi^2(1-\chi^2)^2}\right],$$

---

[3] See, for example, T. D. Lee and C. N. Yang: *Phys. Rev.*, **119**, 1410 (1959); T. Kinoshita: *Phys. Rev., Lett.*, **4**, 379 (1960); S. P. Rosen: *Phys. Rev. Lett.*, **4**, 613 (1960).

[4] See, however, A. T. Alikanov, Tu. V. Galaktionov, Yu. V. Gorodkov, G. P. Eliseyev and V. A. Lyubinov: *Proc. High Energy Physics Conference at Rochester*, 539 (1960); W. A. Love, S. Marder, J. Nadelhaft and R. T. Sugel: *Phys. Rev. Lett.*, **4**, 382 (1960).

[5] W. Dudziak, R. Sagane and J. Vedder: *Phys. Rev.*, **114**, 336 (1959).

where

$$\chi = \left(\frac{m_\mu}{m_\pi}\right).$$

The muon-electron branching ratio from kaon decay can be obtained from the above formula by replacing m_π by m_K.

The experimentally significant quantities are:

$$\frac{\Delta B_\pi}{B_\pi^0} = -2\cdot 10^{-6}\left(\frac{m_\nu}{m_e}\right)^2, \tag{2}$$

and

$$\frac{\Delta B_K}{B_K^0} = -3\cdot 10^{-5}\left(\frac{m_\nu}{m_e}\right)^2. \tag{3}$$

where B_π^0 and B_K^0 refer to the case $m_\nu = 0$. The effect of m_ν on muon-electron branching ratios is therefore not observable.

2·2. *Longitudinal polarization of muons.* – The longitudinal polarization of muons produced in π^--decay is (in the rest frame of the pions):

$$\frac{\Gamma_-}{\Gamma_+} = \left(\frac{E_\mu + \mathscr{P}}{E_\nu + \mathscr{P}}\right)^2\left(\frac{m_\nu}{m_\mu}\right)^2, \tag{4}$$

where

$$E_\mu = \left(\frac{m_\pi^2 + m_\mu^2 - m_\nu^2}{2m_\pi}\right) = \sqrt{m_\mu^2 + \mathscr{P}^2}, \tag{5}$$

and

$$E_\nu = (m_\nu^2 + p^2)^{\frac{1}{2}}. \tag{6}$$

Γ_-/Γ_+ is the ratio of the number of left-handed to right-handed muons that are produced. The result for π^+-decay (or for a right-handed ν_μ in π^--decay) is obtained from formula (4) by reversing the roles of $+$ and $-$, and the results for K-decay are obtained by changing m_π to m_K in formula (5).

Putting the appropriate numbers into (4) we find:

$$\left(\frac{\Gamma_-}{\Gamma_+}\right)_{\pi^-} \approx 1.3\left(\frac{m_\nu}{m_e}\right)^2\cdot 10^{-4}, \tag{7}$$

and

$$\left(\frac{\Gamma_-}{\Gamma_+}\right)_{K^-} \approx 0.3\left(\frac{m_\nu}{m_e}\right)^2\cdot 10^{-4}. \tag{8}$$

The effect of a non-zero m_ν on the longitudinal polarization of muons is therefore too small to be observed.

2·3. *Muon energy.* – The energy of muons produced in pion (kaon) decay from rest has been given in formula (5). To set an upper limit of 5 electron masses on m_ν using this result would require a muon energy measurement of better than 0.02%, and thus is not a practical method.

3. – Muon decay.

We discuss three ways in which a non-zero m_ν would affect muon decay.

3·1. *Electron end-point energy.* – The maximum electron energy from μ-decay at rest is

$$E_{\max} = \frac{m_\mu^2 + m_e^2 - m_\nu^2}{2m_\mu}. \tag{9}$$

DUDZIAK *et al.* [5] have, using formula (9), set a probable (accurate to one standard deviation) upper limit on m_ν of 8 or 9 electron masses. This estimate may be lowered by combining their results on the electron end-point energy with the recent precision measurements on the mass of the muon [6]. We find a probable upper limit of 5 electron masses on m_ν.

It is difficult to obtain an accurate measurement of m_ν using data only on the end-point energy, since all the experimental information (and error) is contained in a single number, $E_{\max}$.

3·2. *Electron spectrum.* – The electron spectrum for μ^+-decay is (in the muon's rest frame)

$$\frac{\Gamma}{A} = \mathscr{P} E \, \mathrm{d}E \, \mathrm{d}\Omega (1-\alpha)^2 \left[\left\{ 3(W_0 - E) + \frac{\mathscr{P}^2}{E} + \alpha \left(3W_0 - E - \frac{2m_e^2}{E} \right) \right\} + \right. \tag{10}$$

$$\left. + \frac{P\mathscr{P}\cos\theta}{E} \left\{ \left(W_0 - 2E + \frac{m_e^2}{m_\mu} \right) - \alpha \left(E + W_0 - \frac{2m_e^2}{m_\mu} \right) \right\} \right],$$

where

$$A = \frac{G^2}{12\pi^4 \hbar^7 c^6} W_0^5, \qquad W_0 = \frac{m_\mu^2 + m_e^2}{2m_\mu},$$

$$\alpha = \frac{m_\nu^2}{2m_\mu (W_0 - E)}.$$

---

[6] J. F. LATHROP, R. A. LUNDY, V. L. TELEGDI, R. WINSTON and D. D. YOVANOVITCH: *Nuovo Cimento*, **17**, 109 (1960); J. F. LATHROP, R. A. LUNDY, S. PENMAN, V. L. TELEGDI, R. WINSTON and D. D. YOVANOVITCH: *Nuovo Cimento*, **17**, 114 (1960).

The electron momentum and energy are denoted by $\mathscr{P}$ and E, and θ is the angle between the electron's momentum and the direction of motion of the muon as seen from the pion's rest frame. The polarization P, if the muons are not depolarized between production and decay, is

$$P = \frac{\Gamma_- - \Gamma_+}{\Gamma_- + \Gamma_+}, \tag{11}$$

where Γ_+, Γ_- are defined by eq. (4). The results for μ^--decay (or for a right-handed ν_μ) can be obtained from formulae (10) and (11) by reversing the roles of $+$ and $-$ in formula (11). For $m_\nu = 0$ ($\alpha = 0$), eq. (10) reduces to the spectrum given by MICHEL and BOUCHIAT (7) except for the term m_e^2/m_μ in the asymmetric part of Γ. The value of the muon lifetime computed from (10)

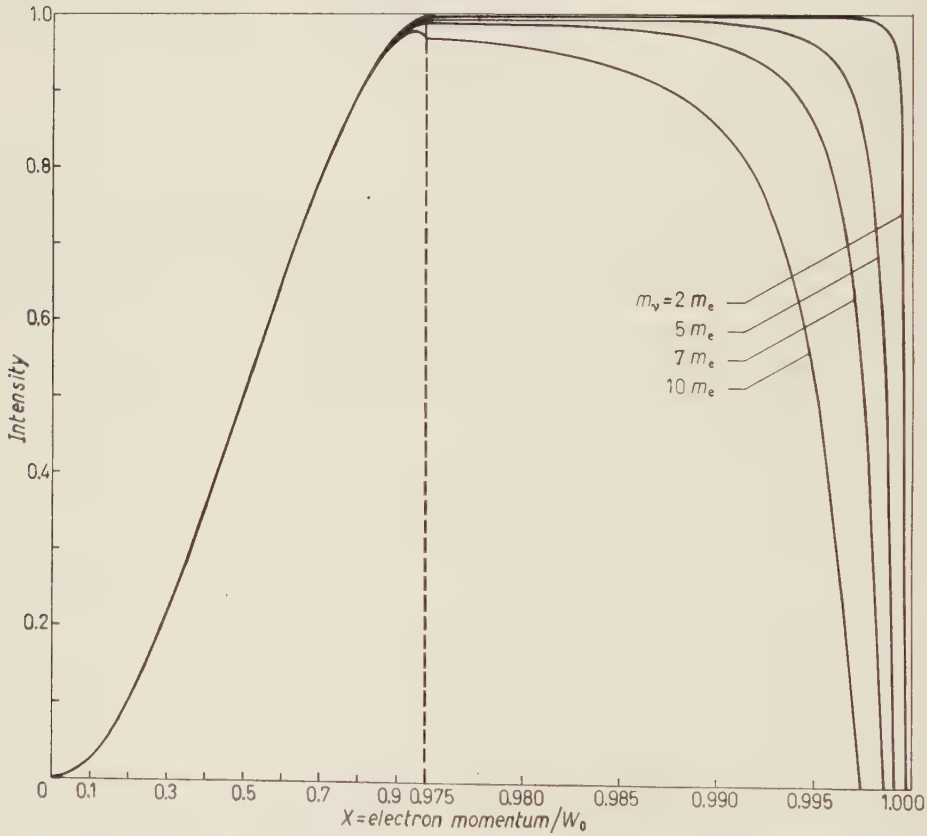

Fig. 1. – The electron spectrum for isotropic muon decay is shown for several values of the mass of the muon's neutrino.

(7) C. BOUCHIAT and L. MICHEL: *Phys. Rev.*, **106**, 170 (1957). There are some minor errors in eq. (45) of the excellent paper by L. MICHEL: *Proc. Phys. Soc.* (*London*), **63** A, 514 (1950), in which the isotropic spectrum for $m_\nu \neq 0$ is given.

with $m_\nu = 5$ electron masses is lower than the value computed for $m_\nu = 0$ by less than 1%.

The most accurate method for determining m_ν is the investigation of the form of the electron spectrum from the isotropic decay of μ^+. The shape of this spectrum near the maximum electron energy, $W_0 - (m_\nu^2/2m_\mu)$ depends strongly on the value of m_ν. For $m_\nu = 0$, the electron spectrum is a monotonically increasing function of E which attains its maximum at $E = W_0$, but for $m_\nu \neq 0$, the spectrum goes to zero rapidly as E approaches E_{max}. The peak of the spectrum is shifted below W_0 by an amount $\approx m_\nu/2$. For values of the neutrino mass which are not already excluded by experiment, the important electron energy region is about 1 MeV wide, from W_0 (= 52.8 MeV) to $W_0 - 2m_e$. The form of the isotropic spectrum in this sensitive region is plotted for several values of m_ν, in Fig. 1.

The form of the spectrum (10) will not be qualitatively changed by radiative corrections, but these corrections, which have been calculated by several authors [8], and the resolution function of the measuring apparatus, must be folded into (10). The corrected spectrum, containing m_ν as a parameter, can then be compared directly with the observed electron spectrum, and the magnitude of m_ν determined by adjusting m_ν to yield the lowest χ^2 value when comparing theoretical and experimental curves.

Measuring the electron spectrum shape is a more accurate method of determining m_ν than measuring the electron end-point energy, since the shape measurement depends on a qualitative change in the form of the spectrum. More measurements are relevant for the determination of m_ν using the shape method and thus the accuracy required of each measurement is less.

3·3. *Longitudinal polarization of decay electrons.* – The longitudinal polarization of electrons emitted from unpolarized muons is described (in the muon's rest frame) by

$$(12) \qquad \frac{\Gamma}{A} = \mathscr{P} E \, dE \, d\Omega (1-\alpha)^2 \left[\left(1 \mp \frac{\boldsymbol{v}\cdot\boldsymbol{\sigma}_e}{c} \right) (3W_0 - 2E + \alpha(3W_0 - E)) - \right.$$
$$\left. - \frac{m_e^2 c^2}{E} \left(1 \mp \frac{\mathscr{P}\cdot\boldsymbol{\sigma}_e}{m_\mu c} \right) (1 + 2\alpha) \right],$$

where the constants have been defined in the previous section. The upper sign refers to electrons and the lower sign to positrons.

The non-zero mass of the electron causes a correction to the usual formula [9] that is most important at low electron energies and is of order m_e/m_μ;

---

[8] R. E. Behrends, R. J. Finkelstein and A. Sirlin: *Phys. Rev.*, **101**, 866 (1956); T. Kinoshita and A. Sirlin: *Phys. Rev.*, **107**, 593 (1957); **108**, 844 (1957).

[9] H. Überall: *Nuovo Cimento*, **6**, 376 (1957); T. Kinoshita and A. Sirlin: *Phys. Rev.* **106**, 1110 (1957).

the correction for a finite mass of m_ν is most important at high energies and is of order $(m_e/m_\mu)^2$. The effect of a non-zero m_ν on the polarization of electrons from polarized muons is also small.

4. – Speculation [10].

The only experimental reason for assigning the negative muon and electron the same lepton number is that the Pauli principle has been found not to act between the two neutral particles emitted in muon decay. If ν_μ is assumed different from ν_β, then lepton number -1 may be assigned to μ^- and ν_μ and lepton number $+1$ to e^- and ν_β. All observed decays then satisfy lepton conservation, and moreover the apparently unobserved processes, $\mu \to e + (\gamma)$ and $\mu \to e + e^+ + e^-$ are absolutely forbidden, as in the original proposal of KONOPINSKI and MAHMOUD [11]. This assignment of lepton numbers is valid for either a right-handed or left-handed ν_μ. The scheme suggested here differs from the original proposal in two ways: 1) ν_μ is different from ν_β and 2) one is forced to conserve separately both muon and electron lepton charge, if present ideas regarding weak currents are correct. The non-existence of an intermediate boson cannot be inferred from the lack of occurrence of $\mu \to e + (\gamma)$ but rather this lack of occurrence may be regarded as evidence for the assumption that $\nu_\mu \neq \nu_\beta$.

5. – Conclusions.

The most accurate way to detect a possible non-zero value of m_ν is to examine the shape of the electron spectrum from isotropic muon decay near the maximum electron energy. Current experimental techniques are adequate for obtaining a much improved estimate of m_ν.

* * *

We are grateful to Dr. E. J. KONOPINSKI and Dr. R. G. NEWTON for clarifying discussions and valuable suggestions.

---

[10] These ideas have undoubtedly occurred to many people. We include them here to make more plausible the assumption that $\nu_\mu \neq \nu_\beta$.

[11] E. J. KONOPINSKI and H. MAHMOUD: *Phys. Rev.*, **92**, 1045 (1953).

Appendix

The formula

$$\iint \frac{\mathrm{d}^3\boldsymbol{s}\,\mathrm{d}^3\boldsymbol{t}}{s_0 t_0}(s\cdot a)(t\cdot b)\delta^4(k-s-t) =$$

$$= \frac{\pi}{6}(1-\alpha)^2\theta(k^2-m_t^2)\left[k^2(a\cdot b)+2(k\cdot a)(k\cdot b)-\alpha(k^2(a\cdot b)-4(k\cdot a)(k\cdot b))\right],$$

where

$$s\cdot s = 0\,, \qquad t\cdot t = m_t^2\,,$$

and

$$\alpha = \frac{m_t^2}{k^2}\,,$$

has been used to evaluate all integrals that occurred in our calculations. This formula is especially convenient because of its covariant form.

Note added in proof.

We are grateful to Professor S. Bludman for bringing to our attention his discussion (Gatlinburg Conference on Weak Interactions (1958)) of the possibility that $\nu_\mu \neq \nu_\beta$. He investigated, among other things, the change in the effective ϱ value caused by a non-zero m_ν (*Bull. Am. Phys. Soc.*, **4**, 80 (1959)).

RIASSUNTO (*)

Studiamo gli effetti di una massa non nulla del neutrino del muone, sulla produzione e sul decadimento del muone libero. La caratteristica che subisce di più l'influenza della massa del neutrino del muone è la forma dello spettro degli elettroni derivati dal decadimento isotropico del μ^+ nei pressi della massima energia degli elettroni. Poniamo un probabile limite superiore di 5 masse elettroniche alla massa del neutrino. usando i dati sull'energia massima degli elettroni, ma è possibile fare una valutazione più accurata, con le tecniche sperimentali usuali, se si ottengono dei dati sulla forma dello spettro elettronico isotropico.

(*) *Traduzione a cura della Redazione.*

Decay Scheme of ^{212}Pb.

M. Giannini, D. Prosperi and S. Sciuti

Centro Studi Nucleari della Casaccia - Roma

(ricevuto il 4 Aprile 1961)

Summary. — Some experimental results concerning ^{212}Pb $\rightarrow$ ^{212}Bi decay are reported. The investigation of the ^{212}Pb decay scheme is of some interest because until now it is not known whether or not the shell model holds in the lead region boundary. Coincidence spectra and γ, γ angular correlations have been employed in order to measure the intensities of weakest transitions, and to make spin assignments. A decay scheme has been proposed. Further, the doubtful existence of a 177 keV γ-ray has been unambiguously demonstrated.

1. – Introduction.

The lead region is particularly interesting as far as nuclear structure is concerned. In the middle of this region there is ^{208}Pb whose core is particularly stable, due to the fact that it has a double closed shell ($Z = 82$, $N = 126$)

By adding or subtracting one or two nucleons from this core, nuclear structures can be obtained for which the first levels are due to the excitation of the added particles (or holes). For such nuclei the shell model holds quite correctly, if one takes into account—by means of a perturbation theory—both the interactions between nucleons outside the closed shells and the coupling to the collective oscillations of the nuclear surface. This argument has already been treated in a theoretical work by Blomqvist and Wahlborn [1] and in a review article by Bergström and Andersson [2].

[1] J. Blomqvist and S. Wahlborn: *Ark. f. Fys.*, **16**, 545 (1959).
[2] I. Bergström and G. Andersson: *Ark. f. Fys.*, **12**, 415 (1957).

By adding three or four particles (or holes) to ^{208}Pb, the following difficulties arise:

1) the configuration mixings cannot be neglected;

2) the strength of the coupling increases and makes possible collective vibrations characterized by phonon energies of 1 MeV or less. In this case the presence of motions of the nuclear surface produces remarkable perturbations to the single particle levels.

By adding to ^{208}Pb more than four particles or holes, it is not generally possible to employ the shell model. It is not yet clear whether nuclei with $|\Delta Z|+|\Delta N|=4$ can be described. Of those, just a few have been theoretically studied (^{204}Pb, ^{206}Bi). Furthermore, the experimental work on these nuclei is still incomplete. In order to obtain more data for theoretical investigations, we decided to improve the experimental knowledge of excited levels belonging to some of these nuclei. In the present work, some experimental results concerning the decay scheme of ^{212}Pb are described. The essential characteristics of ^{212}Bi levels were known ([3,4]), while the spins and the intensities of the weakest transitions were not yet well known.

2. – Intensity and conversion coefficients of γ-transitions in ^{212}Bi.

A chemically pure source was obtained at the beginning of each measurement by separating ^{212}Pb from a RdTh solution by means of the dithizone method ([5]). In all measurements no source has been employed for more than 15 minutes in order that the ^{212}Bi formed was not more than 25% of the ^{212}Bi content at equilibrium.

The experimental set up (Fig. 1) consists of a fast-slow spectrometer to which a Hoogenboom sum-circuit can be added ([6]). The detectors are two $(1\frac{1}{2}\times 1)$ in. NaI(Tl) crystals, coupled to 56 AVP Philips photomultipliers. Anode and dinode outputs are provided for coincidence and proportional pulses. The coincidence resolving time was $\tau=10$ ns. The proportional outputs were fed, through non-overloading amplifiers, to the analysis circuits. The spectra were displayed on a 200 channel pulse height analyser (LABEN).

([3]) E. M. Krisjuk, A. G. Sergeyev, G. D. Latyshev and V. D. Vorobyov: *Nucl. Phys.*, **4**, 579 (1957).

([4]) P. G. Roetling, W. P. Ganley and G. S. Klaiber: *Nucl. Phys.*, **20**, 347 (1960).

([5]) L. A. Haddock: *Analyst*, **163**, 59 (1934).

([6]) A. M. Hoogemboom: *Nucl. Instr.*, **3**, 57 (1958).

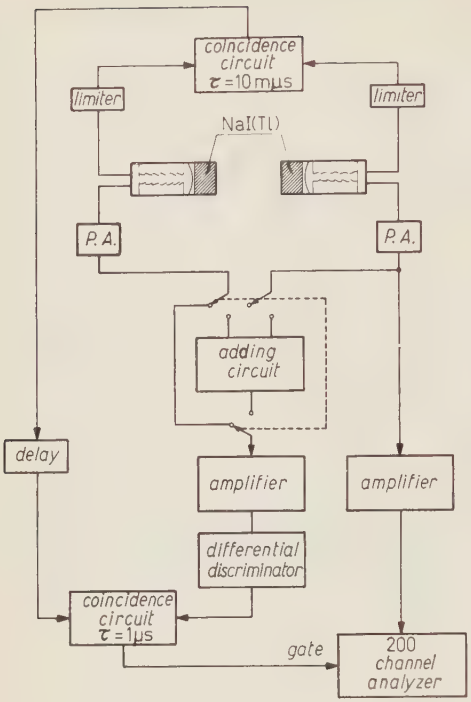

Fig. 1. – Block diagram of the experimental arrangement.

The total γ-ray spectrum of ^{212}Bi is shown in Fig. 2, in which the contributions from the ^{212}Bi daughters have been subtracted. After a careful analysis γ-rays of 115, 177, 239, 300 and 415 keV were found. The 80 keV line is due to the X-rays following internal conversion processes. The existence of the 177 keV γ-ray is of particular interest, since, according to KRISJUK *et al.* ([3]), the corresponding transition was supposed to be *E*0. In Fig. 3, 4, 5, 6 the spectra in coincidence with the 80 keV X-rays and 115, 239, 300 keV γ-rays are shown. In these spectra, the 115, 239 and 300 keV, γ-lines allow a good evaluation of both intensities and conversion coefficients. However, there is a considerable uncertainty in the intensity of the 177 keV line, the existence of which is doubtful according to many authors. In order to clear up this point, we have added to the fast-slow spectrometer a sum-circuit set for a total energy release of 415 keV. The result is shown in Fig. 7. From the spectrum analysis the existence of a 177, 239 keV cascade is proved in an unambiguous way. As far as the apparent existence of a 80, 335 keV cascade is concerned, it turns out that it is due to the coincidence between 80 keV X-rays following the 115 keV γ-conversion and the tail of the 300 keV peak in the 335 keV region. The presence of this apparent cascade is a direct consequence

TABLE I.

Energy (keV)	γ-rays relative intensities	Absolute intensities (photons per ^{212}Pb decay)
80	73 ±4	$(3.4 \pm .7) \cdot 10^{-1}$
115	1.4 ±0.3	$(6.6 \pm 1.8) \cdot 10^{-3}$
177	0.50 ±0.10	$(2.4 \pm .7) \cdot 10^{-3}$
239	100	$(4.7 \pm .9) \cdot 10^{-1}$
300	6.9 ±0.4	$(3.2 \pm .7) \cdot 10^{-2}$
415	0.33 ±0.05	$(1.6 \pm .4) \cdot 10^{-3}$

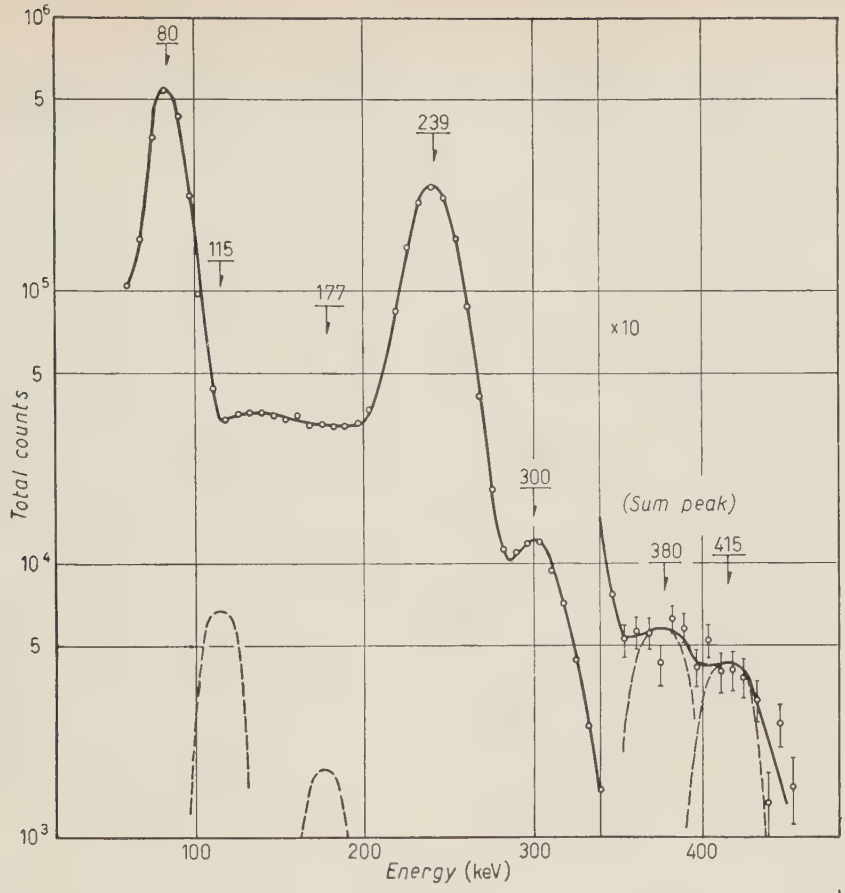

Fig. 2. – Total γ-ray spectrum of ^{212}Bi (daughter contribution subtracted).

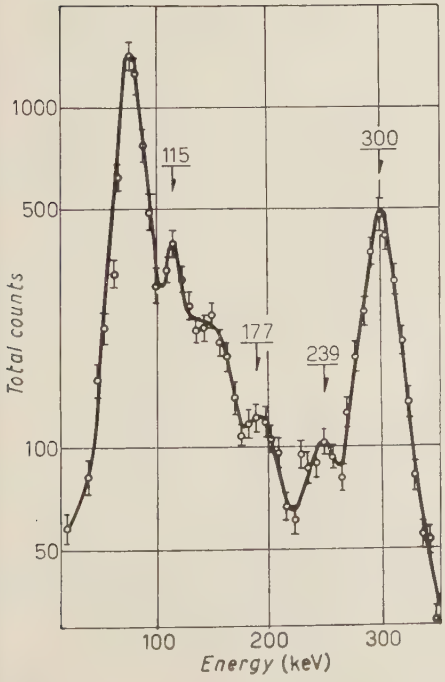

Fig. 3. – Spectrum in coincidence with 80 keV X-rays.

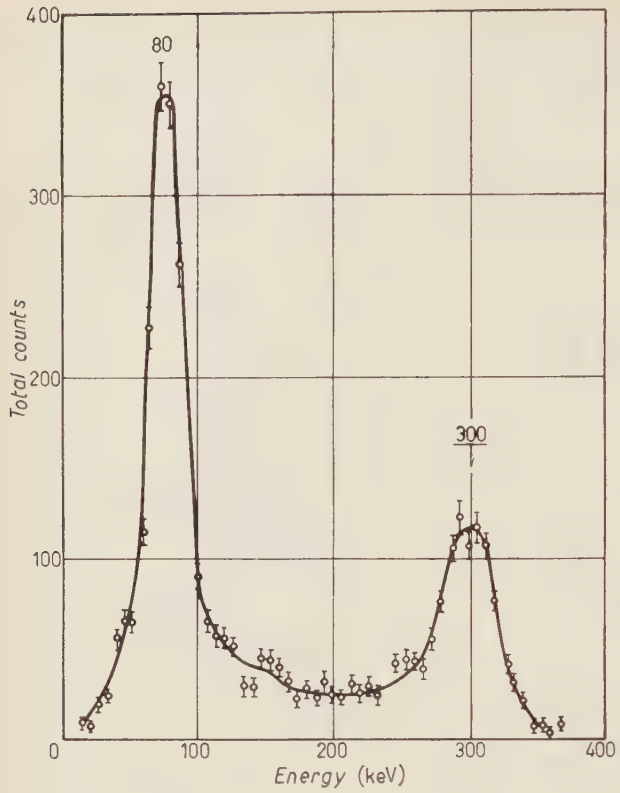

Fig. 4. – Spectrum in coincidence with 115 keV γ-rays.

Fig. 5. – Spectrum in coincidence with 239 keV γ-rays, showing the existence of 177 keV γ-rays. The upper curve refers to a ^{212}Pb source with some daughter contaminations. The 240 keV γ-line is due to chance coincidences while the 115 keV line is due to true coincidences with the tail of the 300 keV line. The lower curve refers to a ^{212}Bi source and has been normalized to the upper one.

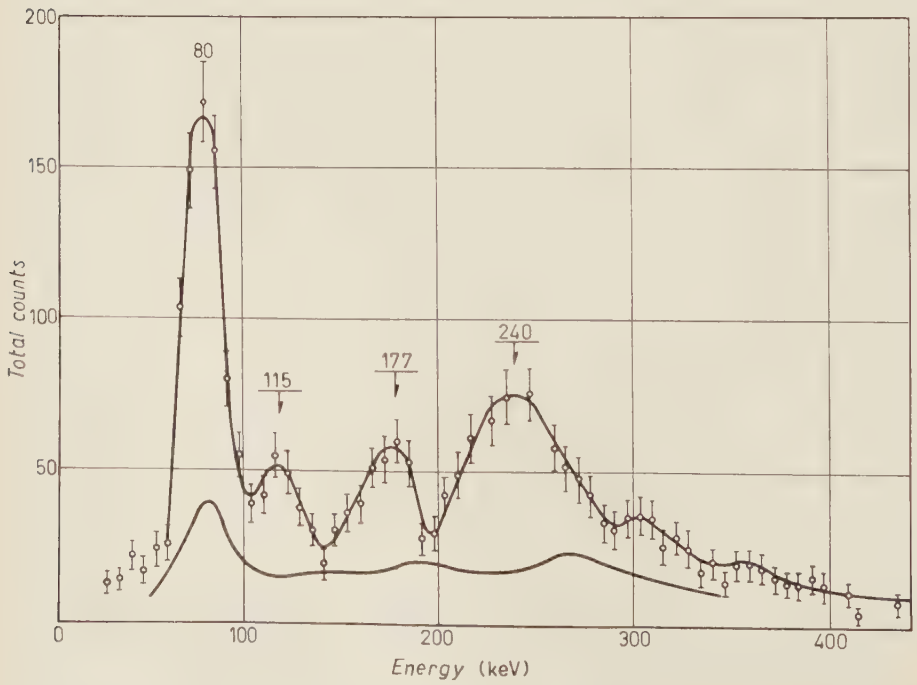

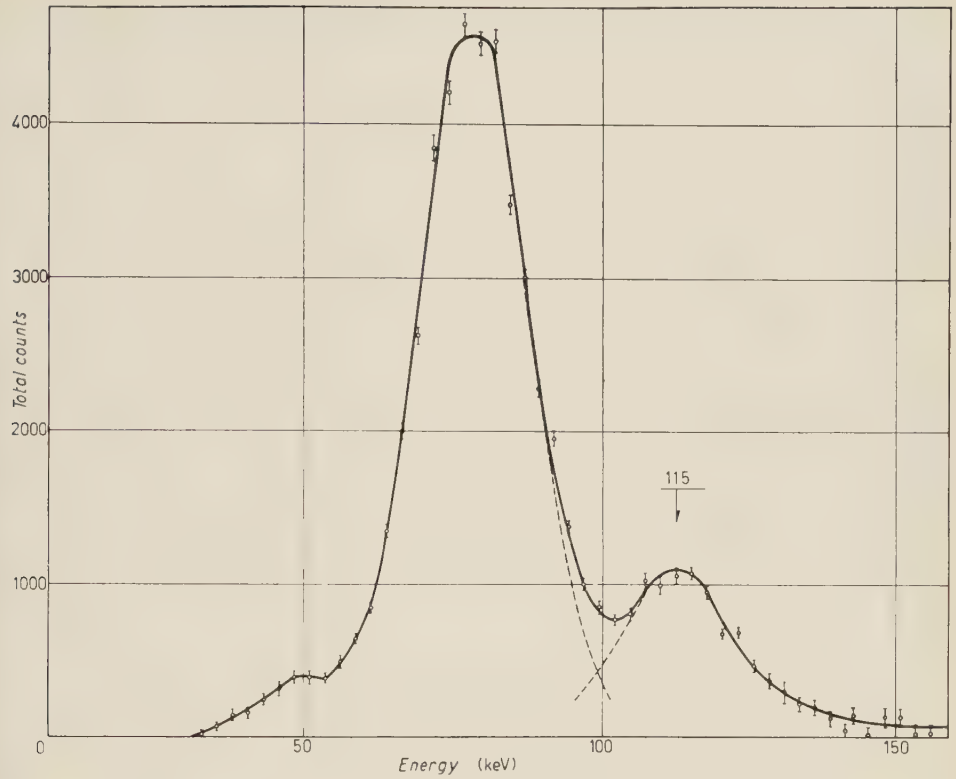

Fig. 6. – Spectrum in coincidence with 300 keV γ-rays.

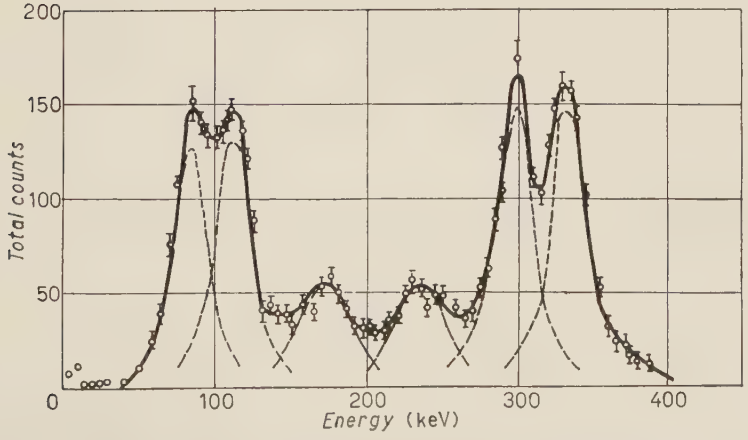

Fig. 7. – Sum-coincidence spectrum referred to a total energy release of 415 keV. The existence of a 177, 239 keV cascade is clearly shown.

of the selection criterion introduced by the sum-circuit. In the second column of Table I the relative intensities of the γ-transitions and of the X-line are listed. The values concerning the 80, 239, 300 and 415 keV peaks have been deduced from Fig. 2. The intensity of 115 keV transition has been deduced from the spectrum of Fig. 3, while the sum-coincidence spectrum of Fig. 7 was employed to deduce the 177 keV γ-ray intensity.

In third column are listed the absolute intensities deduced from the intensity ratio $I(239)/I(2\,610) = 1.31 \pm 0.25$ [7] and the branching value $\alpha/(\alpha+\beta) = 0.359 \pm 0.001$ averaged from the results obtained by several authors [8].

Since the X-line is almost entirely due to the k-conversion of the 239 γ-ray, it is possible to calculate the conversion coefficient of this transition, correcting for the existence of other converted γ-rays and for the fluorescent yield. The k-conversion coefficients of the remaining weakest transitions can be calculated from the data of Table I, together with the intensity ratios of the corresponding conversion lines reported by KRISJUK *et al.* These values are listed in the second column of Table II. In the third column are reported the values obtained by means of the coincidence spectra of Fig. 3, 4, 5, and 6.

TABLE II.

Energy	k-conversion coefficients	
	Deduced from Table I and from KRISJUK [3]	Deduced from Figs. 3, 4, 5, 6
115	3.7 $\pm$1.0	4.8 $\pm$.4
177	0.43 $\pm$ .10	1.5 $\pm$.3
239	0.68 $\pm$ .05	—
300	0.38 $\pm$ .05	0.45 $\pm$.07
415	0.021 $\pm$ .005	—

Our coefficients are in agreement with the ones measured by EMERY and KANE [7] and by ROETLING *et al.* [4].

[7] G. T. EMERY and W. R. KANE: *Phys. Rev.*, **118**, 755 (1960).

[8] F. E. SENFTLE T. A. FARLEY and N. LAZAR: *Phys. Rev.*, **104**, 1629 (1956); D. PROSPERI and S. SCIUTI: *Nuovo Cimento*, **9**, 734 (1958); P. MARIN, G. R. BISHOP and M. HALBORN: *Proc. Phys. Soc.*, **66**, 607 (1953); P. RICE EVANS and N. J. FREEMAN: *Proc. Phys. Soc.*, **72**, 300 (1958); G. SHUPP, M. DANIEL, G. W. EAKINS and E. N. JENSEN: *Phys. Rev.*, **120**, 189 (1960).

3. – Spin determination of the 300 keV level in ^{212}Bi.

In order to give a complete assignment of spins and parities of the levels, an angular correlation measurement for 300, 115 keV cascade has been carried out. The experimental device employed the same electronic equipment described above. The solid angles subtended by the detectors were each about 0.58 sr. The attenuation coefficient, G_2, has been evaluated to be 0.89. The well-known γ, γ angular correlation in ^{60}Ni has been employed to test the allignment of the device.

The spectrum in coincidence with the 300 keV peak was displayed at each angle on a 200 channel analyzer. In this way it is possible to evaluate the contribution to the 115 keV peak due to the 80 keV X-rays. After correcting for this effect, the coincidence rate at various angles was least squares fitted to a $1+a_2\cos^2\theta$ form. This is shown in Fig. 8. The errors listed are both

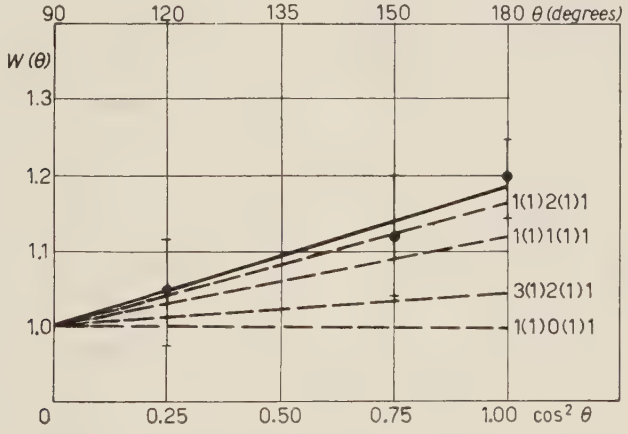

Fig. 8. – Angular correlation between 115, 300 keV γ-rays. The full line is the curve fitted by least-squares. The theoretical attenuated curves for different cascades are shown by the dotted lines.

statistical and due to the uncertainty of the X-ray correction. In Fig. 8 are also shown the theoretical curves including the solid angle attenuation of the counters corresponding to 1(1)0(1)1, 1(1)1(1)1, 1(1)2(1)1, 3(1)2(1)1 cascades. The experimental value

$$W^{\text{exp}}(\vartheta) = 1 + (0.19 \pm .05)\cos^2\theta$$

is in good agreement with a 1(1)2(1)1 cascade whose correlation function is $W^{\text{th}}(\vartheta) = 1 + (0.17)\cos^2\vartheta$. Our result is in agreement with the corresponding result quoted by ROETLING *et al.* [4] who employed similar techniques.

4. – Conclusions.

The above reported results allow us to uniquely assign the spins and parities of levels in ^{212}Bi. The curves of the conversion coefficients in Bi ($Z = 83$) for several multipolarities (9) are shown in Fig. 9 together with the averaged experimental values obtained from the columns of Table II. The 115, 239 and 300 keV transitions turn out to be $M1$ almost pure. In Table III the maximum values of the $E2$ admixtures (δ^2) compatible with our experimental results and those quoted by KRISJUK *et al.* are reported.

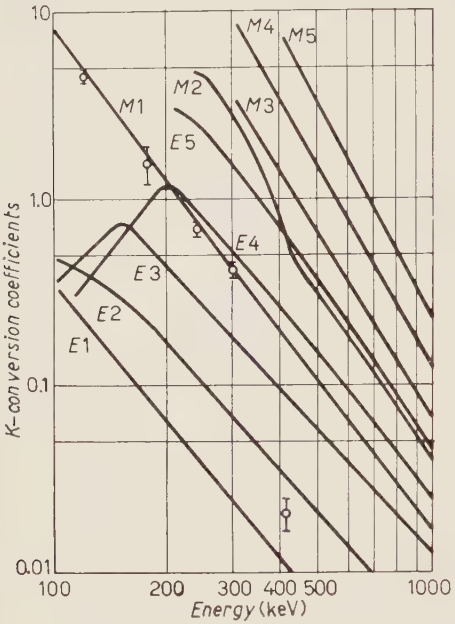

Fig. 9. – Conversion coefficients in Bi ($Z = 83$) for several multipolarities. The average experimental points are deduced from the columns of Table II.

The 415 keV transition seems to be $E2$. Such attribution is not in agreement with the generally assumed level schemes. Because of the agreement between our intensity value and the corresponding value quoted by ROETLING, we can suppose that our figure is correct. At present it is not possible to explain the disagreement with the generally assumed level scheme. A similar consideration holds for the 177 keV transition. In this case, however, also a direct evaluation of α_k can be

TABLE III.

Energy (keV)	δ^2_{max} (%)	
	present work (from α_k)	KRISJUK *et al.* (from α_k/α_L)
115	16	0.1
239	15	0.3
300	6	~ 0

(9) M. E. ROSE: *Internal Conversion Coefficients* (Amsterdam, 1958).

performed by means of the spectrum in Fig. 3. The value so obtained turns out to be in a better agreement with the α_k value expected for a $M1$ transition.

In order to obtain further information on spins, we analyzed the *ft* values of β-transitions in ^{212}Pb. In Table IV these values, deduced from conversion coefficients and from our γ-intensities are listed.

TABLE IV.

E_β (MeV)	Level energy (keV)	log *ft*	Spins and parities
580	0	6.7	1^-, 2^-
340	239	5.1	0^-
280	300	6.7	1^-, 2^-
160	415	5.6	0^-, 1^-

The spins and parities in Table IV have been deduced from a comparison between the experimental data and the systematic behaviour of *ft* values in the lead region (Fig. 10).

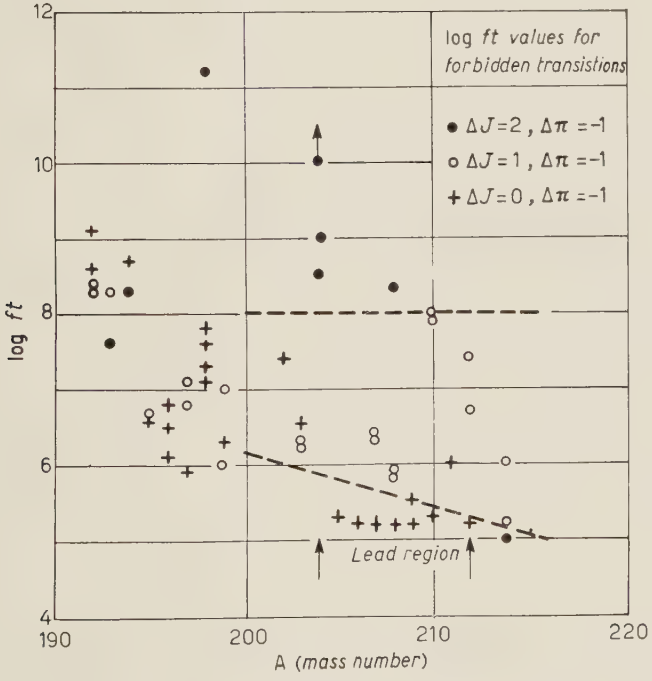

Fig. 10. – Log *ft* values for forbidden transition in the lead region.

From the data reported in the present work, we can propose the decay scheme shown in Fig. 11.

Our scheme is in agreement with that proposed by ROETLING *et al.* [4] while it is different from that proposed by KRISJUK *et al.* as far as the assignment of some spins and the existence of 177 keV γ-ray are concerned.

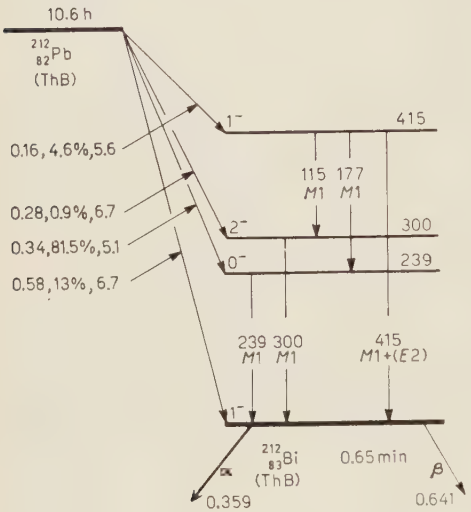

Fig. 11. – Decay scheme of ^{212}Pb (β-energies in MeV, γ-energies in keV).

All levels must have the same parity ($\pi = -1$, as predicted by the shell model), since all the transitions are $M1$.

Spin assignments 1^-, 0^- and 1^- respectively to the ground state and to 239, 415 keV levels are deduced from log ft and γ-multipolarity knowledges. The spin assignment 1^- to the ground state is also confirmed by α, γ angular correlations [10], while 0^- assignment to the 415 keV level is rejected due to the 177 keV γ-ray existence and to the γ, γ angular correlation results. The 2^- assignment to the 300 keV level is essentially due to 115, 300 keV angular correlation results.

The relative intensities of 415, 177 and 115 keV $M1$ transitions turn out to be 0.24 : 0.67 : 1 in evident disagreement with the 40.5 : 3.6 : 1 values deduced from the Weisskopf estimate. This disagreement, according to KRISJUK, can be explained only if level configuration assignments are taken into consideration. *I.e.* with the configuration assignment $(h\,9/2)_p(i\,11/2)^3_h \to 1^-$, $(h\,9/2)_p \cdot (i\,11/2)^2_h (g\,9/2)_h \to 0^-$, $(p\,7/2)_p\,(i\,11/2)_n\,(g\,9/2)^2_n \to 2^-$, $(h\,9/2)_p\,(i\,11/2)_n\,(g\,9/2)^2_p \to 1^-$ one can explain the slowing of 415 keV transition because it would result a two-particle transition. The noticeable slowing of 177 keV transition, can be interpreted by means of the configuration mixings which turn out to be very important when levels are very close together as in the present case. In the above example the ground state configuration has been assigned according to some considerations due to KRISJUK *et al.* in analogy with ^{210}Bi.

---

[10] J. W. HORTON: *Phys. Rev.*, **101**, 717 (1956); I. I. FILIMONOV and G. A. PETROV: *Izv. Acad. Nauk SSSR, Sez. Fiz.*, **20**, 1434 (1956).

* * *

The authors wish to thank Prof. Franco Salvetti of « Istituto di Chimica Generale dell'Università degli Studi di Roma » who prepared the ^{212}Pb source.

RIASSUNTO (*)

Riferiamo alcuni risultati relativi al decadimento ^{212}Pb $\rightarrow$ ^{212}Bi. La ricerca dello schema di decadimento del ^{212}Pb ha qualche interesse perchè sinora non si sa se il modello a guscio sia valido nei dintorni della regione del piombo. Per misurare le intensità delle transizioni più deboli e per assegnare gli spin abbiamo adoperato gli spettri di coincidenza e le correlazioni angolari γ, γ. Proponiamo uno schema di decadimento. Inoltre abbiamo dimostrato senza incertezze l'esistenza, sinora dubbia, del raggio γ di 177 keV.

(*) *Traduzione a cura della Redazione.*

Definition of Uniform Acceleration and its Conformal Invariance.

VACHASPATI and L. M. BALI

Physics Department, University of Lucknow - Lucknow

(ricevuto il 16 Aprile 1961)

Summary. — The usual equation defining uniform acceleration of a particle in special relativity, namely $(1-u^2)\boldsymbol{u}''+3(\boldsymbol{u}\boldsymbol{u}')\boldsymbol{u}'=0$ where $\boldsymbol{u}$ is the velocity and primes denote differentiation with respect to time, is shown to be equivalent to (i) $\ddot{v}_\mu=Kv_\mu$, $\mu=0, 1, 2, 3$ where v_μ is the four-velocity, dots denote differentiation with regard to the proper time, τ, and K is a costant. On integration this gives (ii) $v_\mu=\alpha_\mu \exp[\lambda\tau]+\beta_\mu \exp[-\lambda\tau]$ and (iii) $x_\mu-\xi_\mu=(1/\lambda)[\alpha_\mu \exp[\lambda\tau]-\beta_\mu \exp[-\lambda\tau]]$ where $\lambda=\sqrt{K}$ and $\alpha_\mu, \beta_\mu, \xi_\mu$ are integration constants. Three-dimensional forms of these equations are given. The invariance of these equations is examined and it is shown that under the infinitesimal conformal transformations of the coordinates $\delta x_\mu=(ax)x_\mu-\frac{1}{2}x^2a_\mu$, $[(ax)=a^\alpha x_\alpha]$, they are invariant provided K, ξ_μ, α_μ and β_μ transform suitably, namely according to $\delta K=-2K(a\xi)$, $\delta\xi_\mu=(a\xi)\xi_\mu-\frac{1}{2}\xi^2a_\mu+(1/K)(\frac{1}{2}a_\mu-2C_\mu)$, $\delta\alpha_\mu=(\alpha a)\xi_\mu-(\alpha\xi)a_\mu$ $\delta\beta_\mu=(\beta a)\xi_\mu-(\beta\xi)a_\mu$, $C_\mu=(a\beta)\alpha_\mu+(a\alpha)\beta_\mu$. Since the transformation law for ξ_μ is inhomogeneous, it follows that the constants ξ_μ cannot be taken zero, nor are either K or α_μ or β_μ absolute constants. It is interesting that the eq. (i) for $\ddot{v}_\mu$ is invariant only if we consider it together with its integral (ii); in turn, (ii) is invariant only if we consider it together with its integral (iii). Taken by themselves alone, neither (i) nor (ii) are conformally invariant, but (iii) is.

Introduction.

The problem of a relativistic particle in uniform accelerated motion has given rise to considerable discussion in the last fifty years. The work of BORN [1] in 1909 and PAULI's comment [2] that a uniformly accelerated charged

[1] M. BORN: *Ann. Phys.*, **30**, 1 (1909).

[2] W. PAULI: *Enzyklopädie der Mathematischen Wissenschaften*: vol. 5 (Leipzig, 1918), p. 539, p. 647. Translated as W. PAULI: *Theory of Relativity* (New York, 1958), p. 93.

particle should not give rise to any radiation, have been a matter of good deal of controversy. Pauli's argument has found support in the discovery that Maxwell's equations are invariant under relativistic conformal transformations which form a wider group than that of Lorentz transformations. Since this group contains, in particular, the transformation from rest to uniformly accelerated motion, it is concluded that such a motion cannot be associated with (irreversible) emission of radiation. Pauli's proof has been disputed by DRUKEY ([3]), BONDI and GOLD ([4]), and recently by FULTON and ROHRLICH ([5]) who have given also a historical account of this problem.

To decide this question, it is necessary first to define what we mean by uniform acceleration. It seems that the usual definition of a uniformly accelerated particle is rather clumsy. Therefore, in this paper we have tried to put it in an equivalent but simpler form. The solution of our defining equation is immediate and we show how it leads to hyperbolic motion. We then examine the invariance of this equation and show that the definition is, indeed invariant against conformal transformations. The transformation laws for the various quantities that occur in the equivalent definitions are found out. It is hoped that this work will facilitate examination of the interesting but intricate question of radiationless orbits in relativity.

The work is divided in two sections, one connected with the definition of uniform acceleration, and the other examining the conformal invariance of the defining equations.

1. – Definition of uniform acceleration.

1·1. *Three-dimensional definition.* – After the work of EINSTEIN, MINKOWSKI, BORN and SOMMERFELD in one dimension, to which reference can be found in the book by PAULI ([2]), the three dimensional definition of a particle in uniformly accelerated motion was given by HILL ([6]) in 1947. It is:

Definition. The motion of a particle will be considered to be uniformly accelerated if the time rate of change of its acceleration, as measured in an instantaneous rest-system, vanishes identically.

To put the definition in a mathematical form HILL considered two coordinate systems, the laboratory system S and another system $\bar{S}$, con-

([3]) D. L. DRUKEY: *Phys. Rev.*, **76**, 543 (1949).

([4]) M. BONDI and T. GOLD: *Proc. Roy. Soc.*, A **229**, 416 (1955).

([5]) T. FULTON and F. ROHRLICH: *Ann. Phys.*, **9**, 499 (1960). This paper contains a good list of references.

([6]) E. L. HILL: *Phys. Rev.*, **67**, 358 (1945); **72**, 143 (1947).

nected to each other by the general homogeneous Lorentz transformation

$$\bar{\boldsymbol{r}} = \boldsymbol{r} - \boldsymbol{u}_0 \left[\frac{(\boldsymbol{r}\boldsymbol{u}_0)}{u_0^2} (1 - g_0^{-\frac{1}{2}}) + t\, g_0^{-\frac{1}{2}} \right], \tag{1a}$$

$$\bar{t} = [t - (\boldsymbol{r}\boldsymbol{u}_0)] g_0^{-\frac{1}{2}} \qquad (g_0 = 1 - u_0^2), \tag{1b}$$

where $\boldsymbol{u}_0$ represents the velocity with which S is moving with respect to $\bar{S}$ and we have taken the speed of light as unity. It is then easy to compute the time rate of change of acceleration of a particle as observed in the $\bar{S}$ system; it is

$$\bar{\boldsymbol{u}}'' = g_1^{-5} \left[g_1 \boldsymbol{f}^{(2)} + 3 g_1 (\boldsymbol{u}_0 \boldsymbol{u}') \boldsymbol{f}^{(1)} + (\boldsymbol{u}_0,\, g_1 \boldsymbol{u}'' + 3(\boldsymbol{u}_0 \boldsymbol{u}') \boldsymbol{u}') (\boldsymbol{f}^{(0)} - g_0 \boldsymbol{u}_0) \right], \tag{2}$$

where

$$\left\{ \begin{array}{l} \bar{\boldsymbol{u}}'' = \dfrac{\mathrm{d}^3 \bar{\boldsymbol{r}}}{\mathrm{d}\bar{t}^3}, \qquad \boldsymbol{u} = \dfrac{\mathrm{d}\boldsymbol{r}}{\mathrm{d}t} = \boldsymbol{u}^{(0)} \qquad \boldsymbol{u}' = \dfrac{\mathrm{d}\boldsymbol{u}}{\mathrm{d}t} = \boldsymbol{u}^{(1)}, \qquad \boldsymbol{u}'' = \dfrac{\mathrm{d}\boldsymbol{u}'}{\mathrm{d}t} = \boldsymbol{u}^{(2)}. \\ g_0 = 1 - u_0^2, \qquad g_1 = 1 - (\boldsymbol{u}_0 \boldsymbol{u}), \\ \boldsymbol{f}^{(n)} = g_0^{\frac{3}{2}} \boldsymbol{u}^{(n)} + g_0 (1 - g_0^{\frac{1}{2}}) \dfrac{(\boldsymbol{u}_0 \boldsymbol{u}^{(n)})}{u_0^2} \boldsymbol{u}_0, \qquad n = 0, 1, 2. \end{array} \right. \tag{3}$$

Requiring that $\bar{S}$ be the instantaneous rest-system for the particle and applying the definition of uniform acceleration, we have

$$\bar{\boldsymbol{u}} = 0, \qquad \boldsymbol{u}_0 = \boldsymbol{u}, \qquad \bar{\boldsymbol{u}}'' = 0. \tag{4}$$

When (4) is used in (2), we get

$$(1 - u^2) \boldsymbol{u}'' + 3(\boldsymbol{u}\boldsymbol{u}') \boldsymbol{u}' = 0. \tag{5}$$

This equation is usually taken as the characteristic differential equation of uniformly accelerated motion.

1·2. *Four-dimensional form of the definition.* – The eq. (5) which characterizes uniform acceleration, looks rather complicated. To put it in a simpler form we introduce as parameter, instead of the laboratory time t, the particle's proper time τ:

$$\mathrm{d}\tau = \mathrm{d}x_0 \sqrt{1 - u^2}. \qquad (x_0 = t,\ \boldsymbol{r} = (x_1, x_2, x_3)). \tag{6}$$

We denote differentiations with regard to the proper time by dots, and

easily find

$$(7)\qquad \begin{cases} u_i = \dfrac{\dot{x}_i}{\dot{x}_0}, \quad 1 - u^2 = \dfrac{1}{\dot{x}_0^2}, \\ u_i' = (\ddot{x}_i \dot{x}_0 - \dot{x}_i \ddot{x}_0)/\dot{x}_0^3, \\ u_i'' = (\dot{x}_0^2 \dddot{x}_i - \dot{x}_0 \ddot{x}_0 \dot{x}_i - 3\dot{x}_0 \ddot{x}_0 \ddot{x}_i + 3\ddot{x}_0^2 \dot{x}_i)/\dot{x}_0^5 . \end{cases}$$

Writing (*)

$$(8)\qquad v_\mu = \frac{\mathrm{d}x_\mu}{\mathrm{d}\tau}, \qquad \mu = 0, 1, 2, 3,$$

and using (7) in (5), we now get

$$(9)\qquad v_0 \ddot{v}_i = \ddot{v}_0 v_i \qquad i = 1, 2, 3.$$

The eq. (9) is exactly the same as (5). We can now generalize (9) to read

$$(10)\qquad v_\mu \ddot{v}_\nu = \ddot{v}_\mu v_\nu .$$

Since this equation is manifestly relativistic and, moreover, looks simpler than (5), we can take it to be our definition of uniform acceleration.

1˙3. *Alternative form of the definition.* – If one of the suffixes in (10) is zero, it becomes the same as (9). If neither of the two suffixes is zero, (10) seems, at first sight, to give the new relations

$$\ddot{v}_i v_j = \ddot{v}_j v_i \qquad i, j = 1, 2, 3,$$

which are not contained in (9). However, a simple consideration shows that this is not so: if we write (9) as

$$\frac{\ddot{v}_i}{v_i} = \frac{\ddot{v}_0}{v_0},$$

or

$$(11)\qquad \frac{\ddot{v}_1}{v_1} = \frac{\ddot{v}_2}{v_2} = \frac{\ddot{v}_3}{v_3} = \frac{\ddot{v}_0}{v_0},$$

(*) Grek indices run from 0 to 3; Latin suffixes take values 1, 2, 3 only. We denote contravariant quantities by lower suffixes. Our metric is $g^{00}=1$, $g^{11}=g^{22}=g^{33}=-1$. Summation convention is followed as usual. We frequently denote scalar product of two four-vectors by round brackets, and that of a vector with itself by writing it as a square; thus $(AB)=A^\alpha B_\alpha$, $A^2=A^\alpha A_\alpha$.

we see that the eq. (10) implies no more and no less than (11). The former is therefore completely equivalent to the latter and hence to (9).

The eq. (11) lead to another form for the definition of uniform acceleration. If we equate each of the expressions in (11) to K, we get

$$\dot{v}_\mu = K v_\mu \,. \tag{12}$$

Here K may be a function of (x_0, x_1, x_2, x_3), their derivatives, etc. etc. To find it, we multiply both sides of (12) by v^μ and use

$$v^2 = 1\,, \quad (v\dot{v}) = 0\,, \quad (v\ddot{v}) + \dot{v}^2 = 0\,. \tag{13}$$

This yields

$$K = -\,\dot{v}^2\,. \tag{14}$$

On the other hand, if we multiply (12) by $\dot{v}^\mu$ and use (13), we get

$$(\ddot{v}\,\dot{v}) = 0$$

or

$$\frac{\mathrm{d}\dot{v}^2}{\mathrm{d}\tau} = 0\,.$$

Substitution of (14) in this equation shows that K must be independent of τ and, hence, it must be a constant.

We shall now consider (12), with K as a constant, as the characteristic differential equation defining uniform acceleration.

1'4. *Three-dimensional form of the new definition.* – The three-dimensional form of the new definition of uniform acceleration, namely (12), can be easily found by a procedure similar to that of Sect. **1**'2. We get in this way:

For $\mu = 0$.

$$\Delta = 0\,, \tag{15}$$

where

$$\Delta = (\boldsymbol{\pi u}) + (1 - u^2)u'^2 + (\boldsymbol{u u'})^2 - K(1 - u^2)^3\,, \tag{16}$$

$$\boldsymbol{\pi} = (1 - u^2)\boldsymbol{u''} + 3(\boldsymbol{u u'})\boldsymbol{u'}\,. \tag{17}$$

For $\mu = 1, 2, 3$.

$$(1 - u^2)\boldsymbol{\pi} + \Delta \boldsymbol{u} = 0\,. \tag{18}$$

If we use (15) in (18), we obtain

$$\boldsymbol{\pi} = 0 \tag{19}$$

which is the same as (5).

On the other hand, if we use (19) in (16), we find, on account of (15),

$$(1 - u^2)u'^2 + (\boldsymbol{u}\boldsymbol{u}')^2 = K(1 - u^2)^3 . \tag{20}$$

This equation does not involve the second time-derivative of velocity.

1'5. *Solution of the new equation.* – The eq. (12), which defines constant acceleration, can be solved at once giving

$$v_\mu = \alpha_\mu \exp[\lambda\tau] + \beta_\mu \exp[-\lambda\tau] , \tag{21}$$

where $\lambda = \sqrt{K}$ may be real or imaginary, and α_μ and β_μ are constants. If λ is imaginary, we should have α_μ and β_μ complex; otherwise they are real. Since $v^2 = 1$, we have

$$\alpha_\mu \alpha^\mu = \beta_\mu \beta^\mu = 0 \tag{22a}$$

and

$$2(\alpha\beta) = 1 . \tag{22b}$$

The eq. (21) can be integrated again giving

$$x_\mu - \xi_\mu = \frac{1}{\lambda}\left(\alpha_\mu \exp[\lambda\tau] - \beta_\mu \exp[-\lambda\tau]\right) , \tag{23}$$

where ξ_μ are integration constants. The relation

$$\lambda^2(x_\mu - \xi_\mu) = \dot{v}_\mu \tag{24}$$

which follows from (23) will be useful later (see eq. (42) and (43)).

If we take $\mu = 0$ in (23) we get the relation between the laboratory time t and the proper time τ. Solving it for τ we obtain

$$\exp[\pm\lambda\tau] = \frac{1}{2\alpha_\pm}\cdot\left[\{\lambda^2(t - \xi_0)^2 + 4\alpha_0\beta_0\}^{\frac{1}{2}} \pm \lambda(t - \xi_0)\right] , \tag{25}$$

where

$$\alpha_+ = \alpha_0 , \qquad \alpha_- = \beta_0 .$$

We can now express the three-dimensional velocity $\boldsymbol{u}$ as a function of t. From (21) and (25) we readily get

$$\boldsymbol{u} = \boldsymbol{u}_{(0)} + \frac{1}{2}\left(\frac{\boldsymbol{\alpha}}{\alpha_0} - \frac{\boldsymbol{\beta}}{\beta_0}\right)\frac{\lambda(t-\xi_0)}{\sqrt{\lambda^2(t-\xi_0)^2 + 4\alpha_0\beta_0}}, \tag{26}$$

where

$$\boldsymbol{u}_{(0)} = \frac{1}{2}\left(\frac{\boldsymbol{\alpha}}{\alpha_0} + \frac{\boldsymbol{\beta}}{\beta_0}\right). \tag{27}$$

For $t \to -\infty$, we get

$$\boldsymbol{u} = \boldsymbol{\beta}/\beta_0 .$$

If we require that the particle should be at rest in the distant past, $t \to -\infty$, a condition which is usually assumed in electrodynamics, we see that $\boldsymbol{\beta}/\beta_0$ should vanish. From (22*a*, *b*) we then see that all the components β_μ must vanish and α_μ must be infinite. This initial condition is therefore inadmissible. Similarly $\boldsymbol{u}$ cannot be made to vanish in the distant future, $t \to +\infty$. The simplest boundary condition is then to suppose that $\boldsymbol{u}$ vanishes at $t = \xi_0$. This means that we take

$$\frac{\boldsymbol{\beta}}{\beta_0} = -\frac{\boldsymbol{\alpha}}{\alpha_0}, \tag{28}$$

and (26) then becomes

$$\boldsymbol{u} = \frac{\boldsymbol{\alpha}}{\alpha_0}\frac{\lambda(t-\xi_0)}{\sqrt{\lambda^2(t-\xi_0)^2 + 4\alpha_0\beta_0}}. \tag{29}$$

From (22*a*), (22*b*) and (28) we now get

$$\alpha_0\beta_0 = \tfrac{1}{4}. \tag{30}$$

Thus α_0 and β_0 must have the same sign. If we now consider the zeroth component of (21), we see that v_0 has the same sign as α_0. However, the definition of the proper time, eq. (6), implies that v_0 must be positive. Hence α_0 is positive, as well as β_0. Therefore, according to (28) and (30), we can write

$$(\beta_0, \boldsymbol{\beta}) = \frac{1}{4\alpha_0^2}(\alpha_0, -\boldsymbol{\alpha}), \tag{31}$$

$$\alpha_0 = |\boldsymbol{\alpha}| > 0 . \tag{32}$$

Notice that while α_0 and β_0 both have the same sign and, in fact, are positive, the spacial components, $\boldsymbol{\alpha}$ and $\boldsymbol{\beta}$, have opposite signs.

If we substitute (25) in (23), we get for the spacial components the expression

$$\boldsymbol{x}-\boldsymbol{\xi}=\boldsymbol{u}_{(0)}(t-\xi_0)+\frac{1}{2}\left(\frac{\boldsymbol{\alpha}}{\alpha_0}-\frac{\boldsymbol{\beta}}{\beta_0}\right)\left[(t-\xi_0)^2+\frac{4\alpha_0\beta_0}{\lambda^2}\right]^{\frac{1}{2}}, \tag{33}$$

which becomes, on using (28) and (30),

$$\boldsymbol{x}-\boldsymbol{\xi}=\frac{\boldsymbol{\alpha}}{\alpha_0}\left[(t-\xi_0)^2+\frac{1}{\lambda^2}\right]^{\frac{1}{2}}, \tag{34}$$

while, on using (30), (29) gives

$$\boldsymbol{u}=\frac{\boldsymbol{\alpha}}{\alpha_0}\frac{t-\xi_0}{[(t-\xi_0)^2+1/\lambda^2]^{\frac{1}{2}}}, \tag{35}$$

where $\alpha_0=|\boldsymbol{\alpha}|$. (Cf. (5)).

2. – Conformal invariance.

2·1. *Conformal invariance of the new definition* (12). – We shall examine the invariance of the eq. (12) under infinitesimal conformal transformations,

$$\bar{x}_\mu=x_\mu+\delta x_\mu, \tag{36}$$

with (7)

$$\delta x_\mu=(ax)x_\mu-\tfrac{1}{2}x^2a_\mu, \tag{37}$$

retaining only the terms linear in a_μ for consideration in this section. From (36) it follows that

$$\mathrm{d}\bar{\tau}^2=\mathrm{d}\bar{x}_\mu\,\mathrm{d}\bar{x}^\mu=\mathrm{d}\tau^2+2\,\mathrm{d}x^\mu\,\mathrm{d}\delta x_\mu$$

and we easily get

$$\begin{cases}\dot{\bar{\tau}}=1+v_\alpha\dot{\delta}x^\alpha=1+(ax),\\ \ddot{\bar{\tau}}=(av)\,, \qquad \dddot{\bar{\tau}}=(a\dot{v})\,;\end{cases} \tag{38}$$

(7) E. Cunningham: *Proc. London Math. Soc.*, **8**, 77 (1910); H. Bateman: *Proc. London. Math. Soc.*, **8**, 223 (1910); Vachaspati and M. Jauhari: *Proc. Nat. Inst. Sci. India*, A **26**, 115 (1960); Vachaspati: *Proc. Nat. Inst. Sci. India*: A **26**, 254 (1960); A **26**, 326 (1960); A **26**, 355 (1960); *Proc. Summer School of Theoretical Physics held at Mussoorie*, Pt, I, 27-32 (1958), printed by INSDOC, NPL, New Delhi. See also Vachaspati and L. M. Bali: *Proc. Low Energy Nucl. Phys. Symp., Bombay*, 512 (1961) (organized by Dept. of Atomic Energy, Govt. of India).

$$
(39)\quad \begin{cases}
\bar{v}_\mu = \dfrac{d\bar{x}_\mu}{d\bar{\tau}} = \dfrac{1}{\dot{\bar{\tau}}}(v_\mu + \dot{\delta}x_\mu) = \dfrac{1}{\dot{\bar{\tau}}}\left[\{1 + (ax)\}v_\mu + (av)x_\mu - (xv)a_\mu\right], \\[2ex]
\dot{\bar{v}}_\mu = \dfrac{d\bar{v}_\mu}{d\bar{\tau}} = \dfrac{1}{\dot{\bar{\tau}}^3}\left[(\dot{v}_\mu + \ddot{\delta}x_\mu)\dot{\bar{\tau}} - v_\mu\ddot{\bar{\tau}}\right] = \\[2ex]
\qquad\qquad = \dfrac{1}{\dot{\bar{\tau}}^3}\left[\{1 + 2(ax)\}\dot{v}_\mu + (av)v_\mu + (a\dot{v})x_\mu - \{1 + (xv)\}a_\mu\right], \\[2ex]
\ddot{\bar{v}} = \dfrac{d\dot{\bar{v}}_\mu}{d\bar{\tau}} = \dfrac{1}{\dot{\bar{\tau}}^4}\left[(\ddot{v}_\mu + \dddot{\delta}x_\mu)\dot{\bar{\tau}} - v_\mu\dddot{\bar{\tau}} - 3\dot{v}_\mu\ddot{\bar{\tau}}\right] = \\[2ex]
\qquad\qquad = \dfrac{1}{\dot{\bar{\tau}}^4}\left[\{1 + 2(ax)\}\ddot{v}_\mu + 2(a\dot{v})v_\mu + (a\ddot{v})x_\mu - (x\ddot{v})a_\mu\right];
\end{cases}
$$

$$
(40)\quad \begin{cases}
\dot{\delta}x_\mu = (av)x_\mu + (ax)v_\mu - (xv)a_\mu, \\
\ddot{\delta}x_\mu = (a\dot{v})x_\mu + 2(av)v_\mu + (ax)\dot{v}_\mu - \{1 + (x\dot{v})\}a_\mu, \\
\dddot{\delta}x_\mu = (ax)\ddot{v}_\mu + (a\ddot{v})x_\mu - (x\ddot{v})a_\mu + 3(av)\dot{v}_\mu + 3(a\dot{v})v_\mu.
\end{cases}
$$

Hence we get

$$
(41)\quad \ddot{\bar{v}}_\mu - \bar{K}\bar{v}_\mu = \frac{1}{\dot{\bar{\tau}}^4}\left[\{1 + 2(ax)\}\ddot{v}_\mu + 2(a\dot{v})v_\mu + (a\ddot{v})x_\mu - (x\ddot{v})a_\mu - \right.
$$
$$
\left. - \bar{K}\{1 + 4(ax)\}v_\mu - \bar{K}\{(av)x_\mu - (xv)a_\mu\}\right],
$$

where $\bar{K}$ is a constant which, we shall presently see, may be different from K. When the eq. (12) is satisfied, this becomes

$$
(42)\quad \ddot{\bar{v}}_\mu - \bar{K}\bar{v}_\mu = \frac{v_\mu}{\dot{\bar{\tau}}^4}\left[K - \bar{K} + 2(a, \dot{v} - Kx)\right].
$$

On using (24), since $\lambda^2 = K$, we get

$$
(43)\quad \ddot{\bar{v}}_\mu - \bar{K}\bar{v}_\mu = -\frac{v_\mu}{\dot{\bar{\tau}}^4}\left[\delta K + 2K(a\xi)\right],
$$

where

$$
(44)\quad \delta K = \bar{K} - K.
$$

From this equation we notice that our definition of uniform acceleration, (12), is invariant if we take

$$
(45)\quad \delta K = -2K(a\xi).
$$

It is thus seen that, unless $\xi_\mu = 0$, $\bar{K}$ is not the same as K. Thus K is not an absolute constant in the sense that it remains unaltered through the co-ordinate transformations; however, it is a constant in the sense that, in any system, it is independent of the appropriate proper time, *i.e.*

$$\frac{\mathrm{d}K}{\mathrm{d}\tau} = 0 , \qquad \frac{\mathrm{d}\bar{K}}{\mathrm{d}\bar{\tau}} = 0 .$$

We shall see below that ξ_μ, α_μ and β_μ also are constants only in this sense.

2·2. *Special cases*, $K = 0$ *and* $K = \pm\infty$. – Two special cases should be mentioned here, namely i) $K = 0$, and ii) $K = \pm\infty$, or $1/K = 0$.

Case i), $K = 0$.

If $K = 0$, the eq. (12) becomes

$$\ddot{v}_\mu = 0 . \tag{46}$$

From (41) we see by putting $\bar{K} = 0$ and using (46) that

$$\ddot{\bar{v}}_\mu = \frac{1}{\dot{\bar{\tau}}^4}[2v_\mu(a\dot{v})] \neq 0 .$$

This shows that the eq. (46) in which $K = 0$ is not invariant, unless we take the constant arising from the integration of (46) to be zero. This, however, is not permissible because it is not a conformally invariant procedure (cf. next section).

Case ii), $K = \pm\infty$. – If $1/K = 0$, (12) becomes

$$v_\mu = 0 . \tag{47}$$

Now, from (39)

$$\bar{v}_\mu = \frac{1}{\dot{\bar{\tau}}}(v_\mu + \dot{\delta}x_\mu) = \frac{1}{\dot{\bar{\tau}}}\left(v_\mu + \frac{\partial \delta x_\mu}{\partial x_\alpha} v_\alpha\right).$$

If we use (47), the right-hand side becomes zero for arbitrary δx_μ. Thus the eq. (47), if true in one co-ordinate system, would be true in any other co-ordinate system obtained from the former by arbitrary infinitesimal transformations. The eq. (47) is, however, impossible in relativity theory.

We thus see that both the possibilities, $K = 0$ and $K = \pm\infty$, are ruled out, the former because the eq. (46) is not conformally invariant, and the latter because (47) is inadmissible in relativity theory.

2·3. *Invariance of the equation* (24) *and transformation law of* ξ_μ. – In proving that our definition (12) is conformally invariant, we had to use, in passing over from (42) to (43), the eq. (24), namely

$$\dot{v}_\mu = K(x_\mu - \xi_\mu)\,. \tag{48}$$

Since (12) can be derived from this equation by differentiating it with respect to τ, one would suppose that (48) would be an equally suitable starting point for the definition of uniform acceleration. We shall now show that (48) is, indeed, conformally invariant provided we use its integral (23) also and transform K and ξ_μ suitably; the transformation law for K is already given by (45) and that for ξ_μ will be derived presently.

From (38), (39) and (40) it follows that

$$\bar{\dot{v}}_\mu - \bar{K}(\bar{x}_\mu - \bar{\xi}_\mu) = \frac{1}{\dot{\tau}^3}[\dot{v}_\mu + (g_{\mu\alpha} - v_\mu v_\alpha)\ddot{\delta}x^\alpha + (\dot{v}_\mu v_\alpha - v_\mu \dot{v}_\alpha)\dot{\delta}x^\alpha] - \bar{K}(x_\mu + \delta x_\mu - \bar{\xi}_\mu) =$$

$$= \frac{1}{\dot{\tau}^3}\left[\dot{v}_\mu - K(x_\mu - \xi_\mu) + 2(ax)\dot{v}_\mu + (av)v_\mu + \{(a\dot{v}) - 4K(ax) - \delta K\}x_\mu - \right.$$

$$\left. - \{1 + (x\dot{v}) - \tfrac{1}{2}Kx^2\}a_\mu + K\,\delta\xi_\mu + \{\delta K + 3K(ax)\}\,\xi_\mu\right],$$

where

$$\delta\xi_\mu = \bar{\xi}_\mu - \xi_\mu\,.$$

Taking into account the eq. (48) and the one obtained from it by multiplication with x_μ, *viz.*

$$(\dot{v}x) = K\{x^2 - (x\xi)\}\,,$$

we get

$$\bar{\dot{v}}_\mu - \bar{K}(\bar{x}_\mu - \bar{\xi}_\mu) = \frac{1}{\dot{\tau}^3}\left[(av)v_\mu - \{K(a,\, x + \xi) + \delta K\}\,a_\mu - \right. \tag{49}$$

$$\left. - \{1 + \tfrac{1}{2}K(x - \xi)^2 - \tfrac{1}{2}K\xi^2\}\,a_\mu + K\,\delta\xi_\mu + \{\delta K + K(ax)\}\,\xi_\mu\right].$$

To eliminate v_μ from this expression, we have to employ the integral of (48), *i.e.* the eq. (23):

$$x_\mu - \xi_\mu = \frac{1}{\lambda}\left[\alpha_\mu \exp\,[\lambda\tau] - \beta_\mu \exp\,[-\lambda\tau]\right].$$

From this it follows, on using (22*a*, *b*), that

$$(x - \xi)^2 = -\frac{1}{\lambda^2} = -\frac{1}{K}\,, \tag{50}$$

and

$$(av)v_\mu = K(a, x-\xi)(x_\mu - \xi_\mu) + 2C_\mu , \tag{51}$$

where

$$C_\mu = (a\beta)\alpha_\mu + (a\alpha)\beta_\mu . \tag{52}$$

Hence (49) becomes

$$\bar{\dot{v}}_\mu - \bar{K}(\bar{x}_\mu - \bar{\xi}_\mu) = \frac{1}{\bar{\tau}^3}\left[2C_\mu - \{\delta K + 2K(a\xi)\}x_\mu - \tfrac{1}{2}(1 - K\xi^2)a_\mu + \right.$$
$$\left. + K\delta\xi_\mu + \{\delta K + K(a\xi)\}\,\xi_\mu\right] .$$

Employing the transformation law for K, *viz.* (45), we find

$$\bar{\dot{v}}_\mu - \bar{K}(\bar{x}_\mu - \bar{\xi}_\mu) = \frac{1}{\bar{\tau}^3}\left[2C_\mu - \tfrac{1}{2}(1 - K\xi^2)\,a_\mu + K\,\delta\xi_\mu - K(a\xi)\,\xi_\mu\right] .$$

This will be zero, and consequently the eq. (48) will be invariant, if

$$\delta\xi_\mu = (a\xi)\,\xi_\mu - \frac{1}{2}\,\xi^2\,a_\mu + \frac{1}{K}\left(\frac{1}{2}\,a_\mu - 2C_\mu\right). \tag{53}$$

This provides the transformation law for ξ_μ; we notice that it is inhomogeneous. Hence, even if $\xi_\mu = 0$, ξ_μ is not zero; in fact

$$\bar{\xi}_\mu = \frac{1}{K}\left(\frac{1}{2}\,a_\mu - 2C_\mu\right).$$

Therefore, invariance with regard to conformal transformations makes it essential to keep the term ξ_μ in (23) and hence, according to (45), $\bar{K}$ is different from K. (Cf. Sect. 2·2).

We can simplify C_μ, eq. (52), if we employ the relation (31), namely

$$\beta_\mu = \frac{1}{4\alpha_0^2}\,\alpha_\mu^* , \tag{54}$$

where

$$(\alpha_0^*, \boldsymbol{\alpha}^*) = (\alpha_0, -\boldsymbol{\alpha}) , \tag{55}$$

which is valid when the particular choice of initial condition on the velocity, characterized by the vanishing of $\boldsymbol{u}_{(0)}$, eq. (27), is made. Then (52) yields

$$(C_0, \boldsymbol{C}) = \frac{1}{2\alpha_0^2}(a_0\alpha_0^2, (\boldsymbol{a}\boldsymbol{\alpha})\boldsymbol{\alpha}) . \qquad (\alpha_0 = |\boldsymbol{\alpha}|). \tag{56}$$

2·4. *Invariance of the eq.* (23) *and transformation laws for* α_μ *and* β_μ. – Instead of taking (12) or (24), we can as well take (23) as our basic equation. In any case, the requirement of conformal invariance of this equation will enable us to find the transformation laws for α_μ and β_μ under the infinitesimal transformations (37).

The equation (23) is

$$A_\mu \equiv x_\mu - \xi_\mu - \frac{1}{\lambda}(\alpha_\mu \exp[\lambda\tau] - \beta_\mu \exp[-\lambda\tau]) = 0 . \tag{57}$$

Of the four eq. (57), the one with $\mu = 0$ defines τ in terms of x_0 and enables us to express $\delta\tau$ in terms of δx_0:

$$\delta x_0 - \delta\xi_0 = -\frac{\delta\lambda}{\lambda^2}(\alpha_0 \exp[\lambda\tau] - \beta_0 \exp[-\lambda\tau]) + \left(\delta\tau + \tau\frac{\delta\lambda}{\lambda}\right)\cdot$$

$$\cdot(\alpha_0 \exp[\lambda\tau] + \beta_0 \exp[-\lambda\tau]) + \frac{1}{\lambda}(\delta\alpha_0 \exp[\lambda\tau] - \delta\beta_0 \exp[-\lambda\tau]) ,$$

or

$$v_0\left(\delta\tau + \tau\frac{\delta\lambda}{\lambda}\right) = \delta x_0 - \delta\xi_0 + \frac{\delta\lambda}{\lambda}(x_0 - \xi_0) - \frac{1}{\lambda}(\delta\alpha_0 \exp[\lambda\tau] - \delta\beta_0 \exp[-\lambda\tau]) \tag{58}$$

(using (57) and (21)), where

$$\delta\tau = \bar{\tau} - \tau , \qquad \delta\lambda = \bar{\lambda} - \lambda ,$$

$$\delta\alpha_\mu = \bar{\alpha}_\mu - \alpha_\mu , \qquad \delta\beta_\mu = \bar{\beta}_\mu - \beta_\mu .$$

Also, on employing (57) and (50), we get

$$\delta x_\mu = (ax)x_\mu - \frac{1}{2}x^2 a_\mu = (a\xi)\,\xi_\mu - \frac{1}{2}\left(\xi^2 - \frac{1}{\lambda^2}\right)a_\mu - \frac{1}{\lambda^2}C_\mu + \tag{59}$$

$$+\frac{1}{\lambda}\exp[\lambda\tau]\left[(a\xi)\alpha_\mu + (a\alpha)\,\xi_\mu - (\alpha\xi)a_\mu\right] - \frac{1}{\lambda}\exp[-\lambda\tau]\left[(a\xi)\beta_\mu + (a\beta)\,\xi_\mu - (\beta\xi)a_\mu\right] +$$

$$+\frac{1}{\lambda^2}\left[(a\alpha)\alpha_\mu \exp[2\lambda\tau] + (a\beta)\beta_\mu \exp[-2\lambda\tau]\right] .$$

We are now in a position to find out $\bar{A}_\mu$. On account of (58), it is seen that $\bar{A}_0$ is automatically zero and what remains is to examine $\bar{A}_i$ with $i = 1, 2, 3$. Now

$$\bar{A}_i = \bar{x}_i - \bar{\xi}_i - \frac{1}{\lambda}(\bar{\alpha}_i \exp[\bar{\lambda}\bar{\tau}] - \bar{\beta}_i \exp[-\bar{\lambda}\bar{\tau}]) = \tag{60}$$

$$= \delta x_i - \delta\xi_i + \frac{\delta\lambda}{\lambda}(x_i - \xi_i) - \left(\delta\tau + \tau\frac{\delta\lambda}{\lambda}\right)v_i - \frac{1}{\lambda}(\delta\alpha_i \exp[\lambda\tau] - \delta\beta_i \exp[-\lambda\tau]) ,$$

where A_i that occurred in the right-hand side has been replaced by zero in accordance with (57). On substituting $(\delta\tau+\tau\,\delta\lambda/\lambda)$ by the expression obtained from (58), we get

$$\bar{A}_i = \frac{1}{v_0}\Big[v_0\delta x_i - v_i\delta x_0 - (v_0\delta\xi_i - v_i\delta\xi_0) + \frac{\delta\lambda}{\lambda}\{v_0(x_i-\xi_i) - (x_0-\xi_0)v_i\} - \\ - \frac{1}{\lambda}\{(v_0\delta\alpha_i - v_i\delta\alpha_0)\exp[\lambda\tau] - (v_0\delta\beta_i - v_i\delta\beta_0)\exp[-\lambda\tau]\}\Big].$$

When we use (59) and (57) in this, we find

$$\begin{aligned}(61)\qquad \bar{A}_i = \frac{1}{v_0}\Big[&\exp[\lambda\tau]\Big\{(a\xi)(\alpha_0\xi_i-\xi_0\alpha_i) - \frac{2}{\lambda^2}(a\alpha)(\alpha_0\beta_i-\beta_0\alpha_i) - \\ &-\frac{1}{2}\Big(\xi^2-\frac{1}{\lambda^2}\Big)(\alpha_0 a_i - a_0\alpha_i) - (\alpha_0\delta\xi_i - \alpha_i\delta\xi_0)\Big\} + \\ &+\exp[-\lambda\tau]\Big\{(a\xi)(\beta_0\xi_i-\xi_0\beta_i) - \frac{2}{\lambda^2}(a\beta)(\beta_0\alpha_i-\alpha_0\beta_i) - \\ &-\frac{1}{2}\Big(\xi^2-\frac{1}{\lambda^2}\Big)(\beta_0 a_i - a_0\beta_i) - (\beta_0\delta\xi_i - \beta_i\delta\,\xi_0)\Big\} + \\ &+\frac{1}{\lambda}\exp[2\lambda\tau]\{(a\alpha)(\alpha_0\xi_i-\xi_0\alpha_i) - (\alpha\xi)(\alpha_0 a_i - a_0\alpha_i) - (\alpha_0\delta\alpha_i - \alpha_i\delta\alpha_0)\} - \\ &-\frac{1}{\lambda}\exp[-2\lambda\tau]\{(a\beta)(\beta_0\xi_i-\xi_0\beta_i) - (\beta\xi)(\beta_0 a_i - a_0\beta_i) - (\beta_0\delta\beta_i - \beta_i\delta\beta_0)\} + \\ &-\frac{2}{\lambda}(a\xi)(\beta_0\alpha_i-\alpha_0\beta_i) + \frac{1}{\lambda}(a\alpha)(\beta_0\xi_i-\xi_0\beta_i) - \frac{1}{\lambda}(a\beta)(\alpha_0\xi_i-\xi_0\alpha_i) - \\ &-\frac{1}{\lambda}(\alpha\xi)(\beta_0 a_i - a_0\beta_i) + \frac{1}{\lambda}(\beta\xi)(\alpha_0 a_i - a_0\alpha_i) + 2\frac{\delta\lambda}{\lambda^2}(\beta_0\alpha_i-\alpha_0\beta_i) - \\ &-\frac{1}{\lambda}(\beta_0\delta\alpha_i - \beta_i\delta\alpha_0) + \frac{1}{\lambda}(\alpha_0\delta\beta_i - \alpha_i\delta\beta_0)\Big].\end{aligned}$$

If we use the transformation rule for ξ_μ, eq. (53), the coefficients of $\exp[\lambda\tau]$ and $\exp[-\lambda\tau]$ in (61) vanish. In order that the coefficient of $\exp[2\lambda\tau]$ also becomes zero, we must have (on a little re-arrangement of terms)

$$(62)\qquad \alpha_0[(a\alpha)\xi_i - (\alpha\xi)a_i - \delta\alpha_i] - \alpha_i[(a\alpha)\xi_0 - (\alpha\xi)a_0 - \delta\alpha_0] = 0\,.$$

Similarly, consideration of the coefficient of $\exp[-2\lambda\tau]$ shows that

$$(63)\qquad \beta_0[(a\beta)\xi_i - (\beta\xi)a_i - \delta\beta_i] - \beta_i[(a\beta)\xi_0 - (\beta\xi)a_0 - \delta\beta_0] = 0\,.$$

Lastly, we consider the constant term in (61). Since $K = \lambda^2$ and

$$\delta K = -2K(a\xi)$$

from (45), it follows that

$$\frac{\delta\lambda}{\lambda} = (a\xi) .$$

and the constant term gives

$$\beta_0\,\delta\alpha_i - \beta_i\,\delta\alpha_0 - (\alpha_0\,\delta\beta_i - \alpha_i\,\delta\beta_0) = (a\alpha)(\beta_0\xi_i - \xi_0\beta_i) - \tag{64}$$
$$- (\alpha\xi)(\beta_0 a_i - a_0\beta_i) - (a\beta)(\alpha_0\xi_i - \xi_0\alpha_i) + (\beta\xi)(\alpha_0 a_i - a_0\alpha_i) .$$

The eq. (62), (63) and (64) can be satisfied by assuming

$$\delta\alpha_\mu = (a\alpha)\xi_\mu - (\alpha\xi)a_\mu \tag{65a}$$

and

$$\delta\beta_\mu = (a\beta)\xi_\mu - (\beta\xi)a_\mu . \tag{65b}$$

These equations provide the transformation laws for α_μ and β_μ under the infinitesimal co-ordinate transformations (37).

2·5. *Summary and concluding remarks.* – We summarize here the main results of this work.

We have shown that the differential equation

$$(1 - u^2)\boldsymbol{u}'' + 3(\boldsymbol{u}\boldsymbol{u}')\boldsymbol{u}' = 0 , \tag{5}$$

[$\boldsymbol{u} = \mathrm{d}\boldsymbol{x}/\mathrm{d}t$; primes indicate differentiation with respect to time t] which is usually taken to characterize uniformly accelerated motion can be written in the form

$$\ddot{v}_\mu = Kv_\mu \qquad (\mu = 0, 1, 2, 3), \tag{12}$$

where dots denote differentiation with regard to the proper time, τ, of the particle, $v_\mu = \dot{x}_\mu$, and K is a constant in the sense that it is independent of τ. On integration, (12) gives

$$v_\mu = \alpha_\mu \exp[\lambda\tau] + \beta_\mu \exp[-\lambda\tau] , \tag{21}$$

where $\lambda = \sqrt{K}$ and α_μ and β_μ are constants satisfying (22a, b). A further

integration yields

$$x_\mu - \xi_\mu = \frac{1}{\lambda}\left[\alpha_\mu \exp\left[\lambda\tau\right] - \beta_\mu \exp\left[-\lambda\tau\right]\right], \tag{23}$$

(ξ_μ are integration constants). The three-dimensional forms of these equations are given by (34) and (35) which are valid if $\boldsymbol{u}$ is assumed to be zero at $t = \xi_0$.

The eq. (12) is conformally invariant if, when the infinitesimal conformal transformations

$$\delta x_\mu = (ax)x_\mu - \tfrac{1}{2}x^2 a_\mu \tag{37}$$

are made on the co-ordinates, K is simultaneously transformed according to

$$\delta K = -2K(a\xi)\,. \tag{45}$$

The requirements of relativity and of conformal invariance necessitate that K should be neither infinite nor zero (Sect. 2·2). Moreover, we cannot make $\delta K = 0$ by choosing $\xi_\mu = 0$ because of the following reason. Consideration of the invariance of the eq. (21) demands that ξ_μ should transform according to

$$\delta\xi_\mu = (a\xi)\,\xi_\mu - \frac{1}{2}\,\xi^2 a_\mu + \frac{1}{K}\left(\frac{1}{2}\,a_\mu - 2C_\mu\right), \tag{53}$$

where C_μ is defined in (52). The first two terms of this expression resemble δx_μ, eq. (37), but the last term is independent of ξ_α. This reminds one of the transformation law for affine connection in Riemannian geometry and shows that we cannot take $\xi_\mu = 0$ consistently with the invariance condition on (21).

The transformation laws for α_μ and β_μ that occur in (23) are found in Sect. 2·4. They are

$$\delta\alpha_\mu = (\alpha a)\xi_\mu - (\alpha\xi)a_\mu \tag{65a}$$

and

$$\delta\beta_\mu = (\beta a)\xi_\mu - (\beta\xi)a_\mu\,. \tag{65b}$$

It is to be noticed that the transformation laws for K, α_μ and β_μ contain ξ_μ in an essential way; if ξ_μ could be taken zero, $\overline{K}$, $\overline{\alpha}_\mu$, $\overline{\beta}_\mu$ would all be equal to K, α_μ, β_μ.

The novel feature of this analysis is that the eq. (12) or (21) are by themselves not conformally invariant; they become invariant only if we consider them together with their integrals. On the other hand, their solution, namely the eq. (23), is invariant by itself provided we suitably transform the constants that occur in it.

* * *

One of the authors, L. M. BALI, gratefully acknowledges the award of a junior Research Fellowship by the Atomic Energy Departement of the Government of India.

RIASSUNTO (*)

Mostriamo che la solita equazione che in relatività speciale definisce l'accelerazione uniforme di una particella, cioè $(1-u^2)\boldsymbol{u}''+3(\boldsymbol{u}\boldsymbol{u}')\boldsymbol{u}'=0$, in cui $\boldsymbol{u}$ è la velocità e gli apici indicano derivazione rispetto al tempo, è equivalente a (1) $\ddot{v}_\mu = K v_\mu$, $\mu=0, 1, 2, 3$ in cui v_μ è la quadri-velocità, i punti indicano la differenziazione rispetto al tempo proprio, τ, e K è una costante. Integrando si ottiene (2) $v_\mu=\alpha_\mu \exp[\lambda\tau]+ +\beta_\mu \exp[-\lambda\tau]$ e (3) $x_\mu \geqslant \xi_\mu=(1/\lambda)[\alpha_\mu \exp[\lambda\tau]-\beta_\mu \exp[-\gamma\tau]]$, in cui $\gamma=\sqrt{K}$ ed α_μ, β_μ, ξ_μ sono costanti di integrazione. Diamo le forme tridimensionali di queste equazioni. Esaminiamo l'invarianza di queste equazioni e mostriamo che per trasformazioni conformi infinitesime delle coordinate $\delta x_\mu = (ax)\, x_\mu - \frac{1}{2}x^2 a_\mu$, $[(ax) = \alpha_\mu x_\mu]$, esse sono invarianti purchè K, ξ_μ, α_μ e β_μ si trasformino opportunamente, cioè in accordo con $\delta K = -2K(a\xi)$, $\delta\xi = (a\xi)\xi_\mu - \frac{1}{2}\xi^2 a_\mu + (1/K)(\frac{1}{2}\alpha_\mu - 2c_\mu)$, $\delta\alpha_\mu = (\alpha a)\xi_\mu - (\alpha\xi)a_\mu$, $\delta\beta_\mu = (\beta a)\xi_\mu - (\beta\xi)a_\mu$, $C_\mu = (a\beta)\alpha_\mu + (a\alpha)\beta_\mu$. Poichè la legge di trasformazione di ξ_μ non è omogenea, segue che non si può dare valore zero alle costanti ξ_μ, e che nè K, nè α_μ, nè β_μ sono costanti assolute. È interessante il fatto che l'eq. (1) per v_μ è invariante solo se la consideriamo in unione con il suo integrale (2); a sua volta (2) è invariante solo se la consideriamo in unione con il suo integrale (3). Prese da sole in se stesse, nè la (1), nè la (2) sono conformemente invarianti, mentre lo è la (3).

(*) *Traduzione a cura della Redazione.*

IL NUOVO CIMENTO Vol. XXI, N. 3 1° Agosto 1961

Observations on the Long-Range Interactions of Pions.

I. Preliminary Results on the Coherent Production of two Charged Pions by Pions at 14 GeV.

F. Baldassarre, A. Caforio, D. Ferraro, A. Ferilli, M. Merlin, D. H. Perkins (*) and S. Semeraro

Istituto di Fisica dell'Università - Bari (**)

J. C. Combe, W. M. Gibson (*) and W. O. Lock

CERN - Geneva

A. Bonetti, M. Di Corato, A. Fedrighini, A. J. Herz, A. E. Sichirollo, L. Tallone, G. Vegni and E. Villar (***)

Istituto di Fisica dell'Università - Milano
Istituto Nazionale di Fisica Nucleare - Sezione di Milano

(ricevuto il 27 Aprile 1961)

Summary. — A stack of nuclear emulsion exposed to 14 GeV/c negative pions has been examined by along-the-track scanning. Events with three outgoing relativistic tracks (« tridents ») were analysed to see whether their features are consistent with those to be expected for interactions in which an additional pion pair is produced in a process in which the nucleus acts coherently. Examples of such proposed processes are diffraction dissociation and electromagnetic production. Coherent events are characterized by extremely low momentum transfer to the « target » nucleus, and by the absence of any evidence of nuclear excitation. In 168 metres of track, 13 trident events were found in which none of the three outgoing particles is an electron. Five of these satisfy the criteria for diffraction dissociation, and of these one also falls within the narrower criteria for Coulomb production of a pion pair. From these

(*) Present address: H. H. Wills Physical Laboratories, University of Bristol.
(**) The work at Bari was supported by grants from N.A.T.O. and the Istituto Nazionale di Fisica Nucleare.
(***) I.A.E.A. Fellow, permanent address: Centro de Fisica Fotocorpuscular, Faculdad de Ciencias, Valencia.

3027

figures, only *upper limits* to the cross-sections can be deduced, for other, incoherent, processes can give rise to spurious events. If it is assumed that the one possible case of electromagnetic production is an example of the particular mechanism proposed by FERRETTI [1], one can deduce an upper limit of 440 mb to the pion-pion cross-section at the $T=1$, $J=1$ resonance.

1. – Introduction.

Considerable interest has recently been shown in a specific kind of nuclear interaction of high-energy particles in which other particles are created, but in which the target nucleus receives a negligibly small momentum transfer.

Several mechanisms have been suggested for these processes which belong to the class of long-range interactions: the nucleus may interact with the incident particle via the exchange of a virtual photon [1,2], or diffraction dissociation of the incident particle may take place [3,4]. Other types of interaction have been described [5] which involve pion exchange with single nucleons and which may also give rise to very low nuclear excitation.

It is the purpose of this report to describe experimental observations related to a particular type of such interaction: the production of a pair of charged pions by an incident pion in collisions in which the target nucleus may have acted coherently.

For the case of the Coulomb interaction, the magnitude of the cross-section for the transition π + nucleus $\to 3\pi$ + nucleus has been calculated by FERRETTI [1] who supposed that the transition probability would be appreciable only for those final-state interactions where the created pion pair is emitted in a resonant state with $J=1$ and $T=1$ and with an energy of approximately $4m_\pi$. With these restrictions, the expression given by FERRETTI for the total cross-section, valid for primary energies between 10 GeV and 25 GeV, is (private communication)

$$\sigma_{\pi,3\pi} = 10^{-8}\,\frac{Z^2}{A^{\frac{2}{3}}}\left(\frac{p}{m_\pi}\right)^2 \sigma_{\pi\pi} \tag{1}$$

where the momentum of the incident pion is denoted by p; Z and A are the atomic number and mass number of the target nucleus and $\sigma_{\pi\pi}$ is the total

[1] B. FERRETTI: *Nuovo Cimento*, **19**, 193 (1961) and private communications.
[2] M. L. GOOD and W. D. WALKER: *Phys. Rev.*, **120**, 1855 (1960).
[3] E. L. FEINBERG and I. POMERANČUK: *Suppl. Nuovo Cimento*, **3**, 652 (1956),
[4] M. L. GOOD and W. D. WALKER: *Phys. Rev.*, **120**, 1857 (1960).
[5] For a discussion of processes of this type see, for example, F. SALZMAN and G. SALZMAN: *Phys. Rev.*, **120**, 599 (1960).

pion-pion cross-section at the assumed resonance. The experimental results can thus yield information on the magnitude of $\sigma_{\pi\pi}$.

In general the distinguishing features of the processes under discussion are the following:

i) the only secondaries are three charged pions,

ii) the total energy of the three secondaries is very nearly equal to that of the incident pion, the energy transfer to the recoil nucleus being only a few hundred keV at most, and

iii) both the longitudinal and the lateral components of the momentum transfer q to the target nucleus are small.

The limitation on the momentum transfer stems from the two requirements that *a*) the nucleus must act as a whole, and *b*) in the processes considered here the momentum transfer must be too small to lead to disintegration.

For diffraction dissociation ([3,4]) the upper limit to the longitudinal momentum transfer is set by requirement *a*):

$$q_{\parallel\,\max} \simeq m_\pi A^{-\frac{1}{3}} \qquad (\hbar = c = 1). \tag{2}$$

The upper limit to the transverse momentum transfer is set ([3]) by requirement *b*) at

$$q_{\perp\,\max} \approx m_\pi \,. \tag{3}$$

In calculations concerning the Coulomb process ([1,6]) on the other hand it is assumed that requirement *a*) restricts the momentum transfer irrespective of direction so that condition (2) should apply to both components of q.

In the work reported here we have searched for evidence of interactions with the features described above.

2. – Experimental details and results.

In this experiment we have analysed « trident events » produced by high-energy negative pions in nuclear emulsions (*). For silver the value of $q_{\perp\,\max}$ (eq. (2)) is 30 MeV/c and for the light elements (C, N, O) it is ~ 60 MeV/c. These values must be kept in mind when one considers diffraction dissociation.

([6]) G. N. Fowler: private communication.

(*) Interactions of this type in which the number of heavy tracks $N_h = 0$ and the number of relativistic « shower » particles $n_s = 3$ are usually referred to as type $(0+3)_\pi$; the subscript π indicates a pion primary.

Eq. (1) predicts a $Z^2A^{-\frac{2}{3}}$ dependence for the electromagnetic process suggested by FERRETTI [1], and this leads to a weighted mean value $q_{\max} = 36$ MeV/c.

The emulsions were Ilford K-5 pellicles, 600 μm thick, stacked together and exposed to a beam of negative particles of momentum 14 GeV/c from the CERN proton synchrotron. This beam was set up by VON DARDEL to whom, and to whose group, we are indebted for assistance and co-operation. VON DARDEL *et al.* have shown that the proportion of strongly-interacting particles other than pions in this beam is very low. The calculated muon contamination was only 6%. Contamination of the beam by electrons appeared to be negligible: no evidence of loss of energy by bremsstrahlung was found during scattering measurements on a sample of 77 non-interacting beam tracks, each longer than 6 cm in emulsion (2 radiation lengths). It can therefore be assumed that virtually all the beam tracks followed were produced by 14 GeV/c negative pions.

In order to assess the reliability of our measurements and the quality of our emulsion stack, routine measurements of multiple scattering were performed on *a*) the primaries of all nuclear interactions and *b*) one in five of all the beam tracks followed. The results obtained by means of these checks show that the measured values of $p\beta$ are reliable within the statistical limits stated. They also allowed the elimination of measurements made in some isolated regions of the stacks where distortion was present.

A summary of the results of scanning along the beam tracks is given in Table I. Details of the trident events are given in Table II. There the events are divided into 3 groups:

TABLE I. – *Results of scanning: total track length scanned* 167.5 m.

Event type	Number found	Mean free path (**)	
		(cm)	(g cm^{-2})
All stars (*)	509	32.9	126
White stars (**)	85	197	754
$(0+0)_\pi$ (stops, charge exchanges)	3	5580	21400
$(0+1)_\pi$ (inelastic scatters)	1	16750	64000
$(0+2)_\pi$	16	1047	4010
$(0+3)_\pi$ (***)	27	620	2370
High-energy knock-on electrons (89 m of track only)	62	—	—

(*) All events recorded with the exception of knock-on electrons, single scatters and pairs starting next to the tracks.

(**) Events in which all prongs have a blob density less than (1.5±0.15) the plateau value. This criterion corresponds to a pion kinetic energy of 90 MeV.

(***) All events of type $(0+3)_\pi$, including electron pairs produced by pions.

(**) Not corrected for effect of muon contamination.

Group A consists of those events which were not accepted for measurement as one or more of the tracks had an angle of dip greater than 20°.

Group B contains events in which at least one of the secondary particles was identified as an electron. In all these cases two of the secondaries were, in fact, found to be electrons.

Group C comprises those events in which none of the secondaries was an electron.

TABLE II. – *Events of the type* $(0+3)_\pi$.

	Numbers of events	
A) *Tridents which could not be analysed*		3
B) *Electron events* (*)		
Direct pair production by pions		
pair energy < 100 MeV	7	
pair energy $\geqslant 100$ MeV	3	
pair production with deflection of pion	1	
Hence total number of electron events		11
C) *Pion events* (**)		
« Possible » events, all secondaries measured	4	
« Possible » events; two secondaries measured, one interacts	1	
Hence total number of « possible » events		5
Number of events rejected because sum of secondary energies small	5	
Because momentum transfers too large	3	
Hence total number of rejected events		8
Total number of pion events		13
Total number, events of type $(0+3)_\pi$		27

(*) Electron events were classified as direct pair production only if no deflection of the primary pion could be detected within the errors of measurements.
(**) See text for definitions.

In general it was not possible to prove that the secondaries were pions. However one third of the number of the secondary particles had momenta less than 1 GeV/c and scattering and grain density measurements showed that none of them were protons.

In Table III are listed some of the results of measurements and calculations concerning the events of group C, Table II. The errors, where given, are equivalent to statistical standard deviations. We estimate the standard

TABLE III. – *I*

Event no.	Class	$\sum (p\beta)_{sec}$ GeV/c	$q_\perp$ MeV/c	$q_\parallel$ MeV/c	γ_c	M^* MeV/c²	m^* MeV/c²	$(p\beta)_1$ GeV/c	α_1
21-42	Poss.	$14.2^{+3.5}_{-1.9}$	192^{+58}_{-53}	27	16.8	886	432	$6.8^{+1.4}_{-1.1}$	2° 24′
21-50	Poss.	8.5^{+6}_{-2}	131^{+108}_{-68}	25	10.1	847	351	$0.7^{+0.6}_{-0.2}$	6° 48′
125 A	Poss.	15^{+4}_{-2}	60^{+64}_{-38}	42	13.8	1093	307	$5.8^{+2}_{-1.2}$	0° 9′
146 A	Poss.	$11.9^{+2.6}_{-1.5}$	138^{+111}_{-78}	57	9.4	1276	822	$2.7^{+0.3}_{-0.2}$	7° 44′
142	Poss.	Interacts	186^{+110}_{-82}	36	13.1	1017	632	$0.63^{+0.11}_{-0.08}$	12° 54′
53 A	Reject	$8.4^{+1.1}_{-0.9}$	31^{+48}_{-48}	23	10.3	816	457	$2.4^{+0.4}_{-0.3}$	6° 15′
22-7	Reject	$9.9^{+4}_{-1.3}$	320^{+113}_{-55}	29	10.9	910	491	$0.7^{+0.2}_{-0.2}$	9° 48′
6-51	Reject	$7.6^{+1.3}_{-0.8}$	332^{+106}_{-72}	23	9.3	818	449	$3.0^{+0.8}_{-0.5}$	3° 18′
15-34	Reject	$5.9^{+1.2}_{-0.7}$	433^{+50}_{-28}	26	6.8	872	—	$3.9^{+0.9}_{-0.6}$	2° 24′
6-72	Reject	$14.6^{+1.9}_{-1.6}$	396^{+72}_{-69}	99	8.7	1671	—	$0.58^{+0.07}_{-0.05}$	20° 12′
16-99	Reject	13^{+3}_{-2}	607^{+146}_{-106}	37	12.6	1030	395	$3.4^{+1.2}_{-0.9}$	6°
196	Reject	9.8^{+2}_{-1}	394^{+217}_{-143}	44	8.7	1123	810	$4.2^{+1.4}_{-0.9}$	8° 49′
87	Reject	Interacts	582^{+78}_{-60}	38	13.4	1046	—	$2.3^{+0.5}_{-0.4}$	2° 45′

x_i = space angle of the i-th secondary with the direction of the primary;
ψ_i = azimuth angle of the i-th secondary in the plane perpendicular to the direction of the prim

deviation of the q to be about 10 MeV/c. The values of q were calculated using the approximation $q \simeq (M^{*2} - m_\pi^2)/2p$, which implies that the target is appreciably more massive than a nucleon. The values of M^* (see also further below) are derived directly from the measured $p\beta$'s, assuming all outgoing particles are pions.

Of the total of thirteen events in this group, six show a measured total energy ($\approx \sum p\beta$) of the secondaries which lies within one standard deviation of the primary energy of 14 GeV. These events are therefore consistent with criteria i) and ii) above. In two of the six, however, the transverse momentum transfer q is very large, leaving four which satisfy the less restrictive criterion (3). Of these only two satisfy all the conditions discussed earlier; in

events.

)	α_2	ψ_2	$(p\beta)_3$ (GeV/c)	α_3	ψ_3	$\cos\alpha_1^*$	$\cos\beta_2^*$	$\cos\alpha_3^*$	Remarks
	0° 30′	229°	$0.7^{+0.3}_{-0.1}$	6° 54′	330°	0.593	0.769	−0.957	
	0° 45′	217°	$0.8^{+0.8}_{-0.3}$	9° 18′	272°	−0.868	0.996	−0.816	
	0° 59′	277°	$0.41^{+0.11}_{-0.07}$	14° 19′	114°	0.991	0.930	−0.975	
	2° 41′	231°	$3.1^{+0.9}_{-0.6}$	7° 54′	127°	−0.350	0.774	−0.297	Blob
ts	2° 4′	11° 19′	$5.4^{+3.1}_{-1.3}$	1° 48′	223°	−0.936	0.813	0.428	
	2° 36′	230° 15′	$1.3^{+0.3}_{-0.2}$	5° 48′	116° 20′	−0.291	0.637	−0.525	
	4° 18′	149°	$5.4^{+3.2}_{-1.2}$	3° 6′	234°	−0.885	0.421	0.616	
	5° 42′	199°	$0.8^{+0.3}_{-0.2}$	8° 48′	341°	0.498	0.470	−0.801	
	8° 48′	14°	$0.51^{+0.17}_{-0.11}$	26°	114°	0.893	−0.034	−0.883	Auger? + dirt
	3° 18′	313°	$1.8^{+0.4}_{-0.1}$	9° 36′	120°	−0.897	0.864	−0.565	
	1° 18′	243°	$2.0^{+1.0}_{-0.5}$	9° 6′	319°	−0.079	−0.390	−0.534	
	2° 10′	236°	$1.6^{+0.7}_{-0.4}$	6° 9′	316°	−0.032	0.345	−0.760	
ts	4° 6′	191°	$1.0^{+0.4}_{-0.2}$	6° 39′	324°	−0.410	0.703	−0.847	

ψ_i = angle of the i-th secondary in the c.m. of the three outgoing particles. The other symbols have the meaning given in the text.

one of the remaining two the total secondary energy lies only just within one standard deviation of 14 GeV, and in the other the longitudinal momentum transfer q is more than one standard deviation (10 MeV/c) in excess of the limit according to relation (2). We label all these four events as « possible ». A further event, 142, is classed as « possible » in spite of the fact that one of its secondaries interacts after traversing such a short distance in emulsion that significant scattering measurements are not possible. The assumption that the total secondary energy is 14 GeV brings this event into the « possible » class, and we accept it, like the other doubtful cases in this class, as we are trying to establish an upper limit to the cross-section.

We are thus left with five events which satisfy the less restrictive of the

criteria. If, instead, we accept only events in which neither $q_\perp$ nor $q_\parallel$ exceed 36 MeV c by more than one standard deviation, we remain with one candidate: 125 A. Since the total secondary energy and resultant transverse momentum are, for all practical purposes, independent quantities, the condition that the measured values of both shall lie within one standard deviation of the required ones might lead to the inclusion of as few as 70% of genuine events. Hence the true number of events satisfying the criteria may be about seven (or about 1.4 if the more restrictive criterion is adopted). The contribution from the events which were not measured is negligible.

3. – Discussion and conclusions.

One can conclude from these preliminary results that the number of events consistent with the less restrictive of the criteria given above is not more than seven in 168 metres of tracks, 8% of all white stars, a rather large proportion. This upper limit is reduced to 1.4 in 168 metres (about 1.6% of white stars) if the more restrictive criteria appropriate to the Coulomb process are applied. The latter corresponds to a mean free path of 120 m in nuclear emulsion.

Hence, for the particular process envisaged by FERRETTI [1] we can deduce an upper limit of 8.4 mb for the cross-section *in lead* for the production of tridents. Eq. (1) gives for lead and an incident pion momentum of 14 GeV c $\sigma_{\pi\pi} = 52\sigma_{\pi,3\pi}$, so that we find $\sigma_{\pi\pi} \leqslant 440$ mb at the hypothetical ($J=1$, $T=1$) resonance.

It is clear that the above figures for the numbers of events and cross-sections represent rough upper limits. In fact, the Ferretti model is only one of various possible interpretations of this kind of event. Also, the statistical errors associated with the energy measurements are large (typically 20%) so that the apparent balance of energy and transverse momentum in a particular event certainly does not exclude the emission of low-energy π^0-mesons, neutrons or other neutral particles. The transverse momentum of individual secondary particles generated in nuclear interactions at these energies is typically 200 MeV/c, and the possibility that three of the secondaries should by chance have a very small resultant transverse momentum is by no means remote.

Because of the possibility of the existence of virtual bound states of two or three pions we have also calculated the following quantities:

i) the value of $\gamma_c = (1-\beta_c^2)^{-\frac{1}{2}}$ of the centre-of-momentum system of the three secondary particles;

ii) the total energy M^*c^2 of the three outgoing particles in their c.m. system. If a virtual three-pion bound state exists and can be excited in the processes considered here, the calculated values of M^*c^2 should cluster around the mass of this state;

iii) the total energy m^*c^2 in their own barycentric system of those two of the three secondaries which have closely similar momenta in the laboratory system. If a virtual two-pion state with mass around $4m_\pi$ exists, one would expect m^*c^2 to peak at about that value;

iv) the angular distribution of the outgoing secondaries in their own c.m. system. Given are the space angles α_i^* between the lines of flight of the particles and of the c.m.

All this information is displayed in Table III.

Clearly, no definite conclusions can be drawn at this stage, for while the values of M^* are all of the same order, there is no significant difference between the mean M^* for the accepted events (1024 MeV/c^2) and the mean for all thirteen pion events (1031 MeV/c^2). Similarly, while the values of m^* are entirely consistent with the existence of a resonance in the expected region ($4m_\pi = 560$ MeV/c^2), the agreement is of no significance as a calculation of m^* taking all possible permutations of two tracks from the thirteen pion events gave values in the same range.

* * *

In conclusion we wish to acknowledge our indebtedness to Professor B. Ferretti and Dr. M. L. Good for helpful discussions and communications, and to Professor G. Bernardini for drawing our attention to Professor Ferretti's work. We are grateful to Prof. P. T. Matthews, Dr. F. Selleri and Dr. G. N. Fowler for discussions. We wish to express out gratitude to Prof. C. C. Dilworth and to Dr. L. Scarsi for their generous assistance and criticisms, and to Drs. H. Aly, C. Fisher, and W. Venus (Bristol) for discussions and work on ten of the events. It is a pleasure to acknowledge the contribution made by Mr. Bertram Stiller who took a major part in the processing of the emulsion stack during a visit to the Milan laboratory. One of us, (E.V.), wishes to thank the International Atomic Energy Authority for a fellowship.

RIASSUNTO

Un pacco di emulsioni nucleari esposte al fascio di mesoni π negativi di 14 GeV/c del protosincrotone del CERN è stato esplorato per traccia, e sono state registrate le interazioni delle particelle primarie (stelle, stops, diffusioni anelastiche). Il libero cammino medio, non corretto per la contaminazione di mesoni μ del fascio ($\sim 6\%$) è risultato di cm 32.9 su un totale di 168 metri di traccia. Un'analisi dettagliata delle

interazioni è stata iniziata, prendendo in considerazione innanzi tutto gli eventi in cui tre particelle relativistiche emergono dal punto di interazione con forte collimazione e senza eccitazione visibile del nucleo colpito (tridenti). Processi di questo ripo, in cui le tre particelle emergenti sono pioni, e in cui il nucleo bersaglio può aver reagito coerentemente con assorbimento trascurabile di energia e quantità di moto, sono stati descritti teoricamente come dissociazione diffrattiva della particella primaria, o come interazione elettromagnetica con scambio di fotoni virtuali. In quest'ultimo caso è stato data da FERRETTI una formula esplicita che (nel caso di un ipotetico stato risonante $T = 1$, $J = 1$) lega la sezione d'urto per produzione di una coppia di pioni da pioni su nuclei complessi alla sezione d'urto pione-pione. 10 dei 27 « tridenti » osservati sono risultati casi di produzione diretta di coppie di elettroni. In 5 dei rimanenti casi il bilancio energetico e della quantità di moto è risultato compatibile con l'ipotesi di un'interazione coerente con un nucleo complesso; in uno in particolare sono rispettate nei limiti degli errori le condizioni più restrittive imposte dall'interazione col campo coulombiano del nucleo. I dati attuali possono fornire solo grossolani limiti superiori per le sezioni d'urto, poichè altri processi, non coerenti, possono concorrere alla produzione di eventi del tipo qui descritto. Con questa avvertenza, e ammettendo che l'evento compatibile con l'interazione elettromagnetica sia un esempio del particolare processo proposto da FERRETTI, si ricava un limite superiore di 440 mb per la sezione d'urto pione-pione alla risonanza ($T = 1$, $J = 1$).

IL NUOVO CIMENTO Vol. XXI, N. 3 1° Agosto 1961

Experimental Results on the Proton-Nucleus Collisions at 27 GeV in Emulsion.

A. Barbaro-Galtieri, A. Manfredini and B. Quassiati (*)

Istituto di Fisica dell'Università - Roma
Istituto nazionale di Fisica Nucleare - Sezione di Roma

C. Castagnoli (**), A. Gainotti and I. Ortalli

Istituto di Fisica dell'Università - Parma

(ricevuto il 16 Maggio 1961)

Summary. — We are examining the caracteristics of 3226 stars produced by collisions of 27 GeV protons against emulsions nuclei. We obtain the mean multiplicities $n_s = 6.6 \pm 0.1$, $n_h = 7.2 \pm 0.2$. The mean energy of the secondary shower particles is 2.3 ± 0.2 GeV. The energy transfer to the secondary mesons in the l.s. is $K \sim 0.6$. From the study of the angular distribution we obtain the mean number of collisions inside the nucleus to be 1.1 and 2 7 for light anf heavy nuclei respectively. The mean free path for absorption is $\lambda = 38.0 \pm 1.0$ which according to an optical model corresponds to a nuclear mean free path $\lambda_n = (4.3 \pm 0.3)$ fermi.

1. – Introduction.

In this work some features of the 27 GeV protons' interactions with nuclei in nuclear emulsion have been investigated. The beam of protons is produced by the CERN Proton Synchrotron in Geneva.

The results concerning the p-nucleon collisions obtained from the same exposition will be analysed in collaboration with other laboratories.

(*) On leave from Istituto di Fisica, Università di Torino.
(**) Now at the Istituto di Fisica, Università di Torino.

The main aim of the present investigation is to give a general description of the stars and to obtain some information on the energy spectrum of the secondary mesons, on the inelasticity of the interaction and on the mean number of collisions inside the nuclei of nuclear emulsion.

2. – Irradiation, scanning, efficiency.

The so-called « Bern beam » has been used (1), that is, a proton beam scattered out from the CERN proton synchrotron working nominally at 28 GeV. The emulsions used are G-5 600 μm thick 3 in. × 3 in. size.

The momentum spectrum of the beam has been studied (2) with a magnetic analysis at a lower energy; by means of these measurements we can evaluate the mean energy of protons in our stack to be: $E_p = 27$ GeV.

The scanning was performed by area and track following methods; the scanning rate per man day was 1 m by the track and 0.5 cm² by the area method.

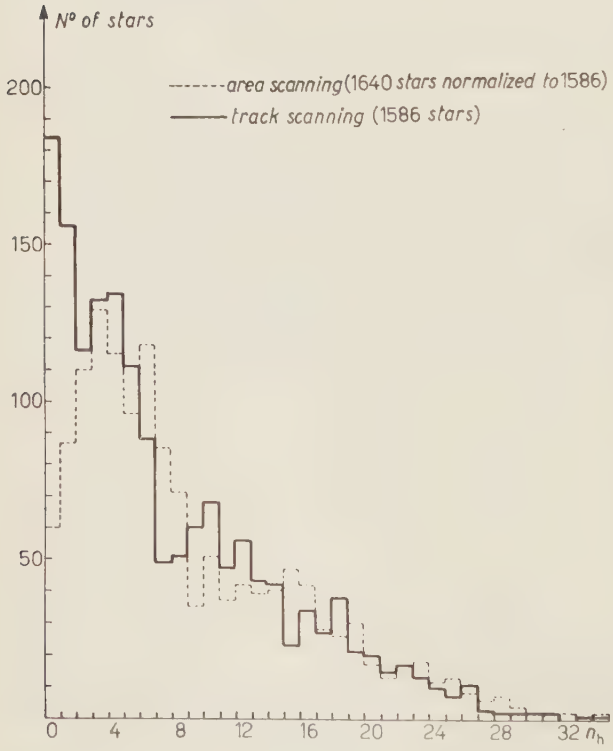

Fig. 1. – n_h distributions of stars from track and area scanning.

The analysis reported hereafter refers to a total of 1586 stars collected on 603 m of track and 1640 stars collected on 33 cm² of area scanned. The scanning was performed with a magnification of 50×, 8×; special care was taken to avoid the losses of charged shower particles produced in the primary direction. All scatterings with pro-

(1) B. Dayton, W. Koch, M. Nikolić, H. Winzeler, J. C. Combe, W. M. Gibson, W. O. Lock, M. Schneeberger and G. Vanderhaeghe: *Helv. Phys. Acta*, **33**, 544 (1960).

(2) G. Cocconi, A. N. Diddens, E. Lillethun and A. M. Wetherell: *Phys. Rev. Lett.*, **6**, 231 (1961).

jected angle on the emulsion plane $> 2°$ and $> 5°$ in the perpendicular plane have been recorded.

The tracks with a ionization $b/b_0 < 1.4$ (where b_0 is the blob density at plateau ionization) corresponding to a $\beta \gtrsim 0.7$ were classified as shower tracks n_s. This evaluation was made by sight and can be a source of error in the n_s and n_h multiplicities; but a control on a sample of 100 stars shows that the error is certainly $< 1\%$.

All the tracks with $b/b_0 > 1.4$ were defined as black tracks n_h. An evaluation of the efficiency by the area scanning method can be deduced by comparison of the n_s and n_h distributions shown in Fig. 1 and 2. The agreement is quite satisfactory; a loss appears only for $n_h = 0$, 1 stars in the area scanning. However, we have defined these stars as due to p-nucleon collisions and we are not considering these events in this paper. The mean efficiency for the shower tracks is $\varepsilon = 1.0$ for all the stars measured for angular distribution of shower particles and $\varepsilon = 0.9$ for all the unmeasured stars.

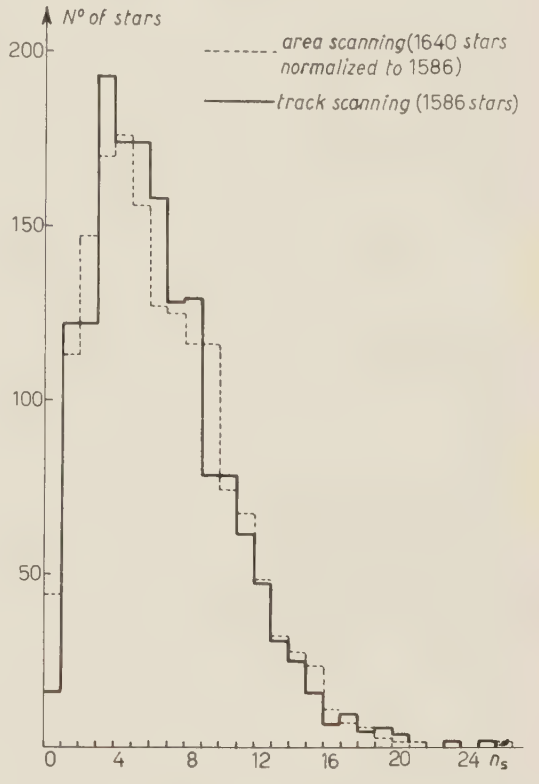

Fig. 2. – n_s distributions of stars from track and area scanning.

3. – Mean free path, n_s and n_h multiplicities.

The mean free path by track following, concerning stars and scatterings $> 5°$, discarding electromagnetic events (K.O., pairs), is

$$\lambda = (38.0 \pm 1.0) \text{ cm} .$$

The comparison between this value and those found by other authors [3] is shown in Table I.

[3] *a*) A. Winzeler, B. Klaiber, W. Koch, N. Nikolić and M. Scheeberger: *Nuovo Cimento*, **17**, 8 (1960); *b*) N. P. Bogachev, S. A. Bunjatov, T. P. Merckov

TABLE I. – *Mean free path.*

GeV	cm	References
6.2	38.2 ± 1.5	(3) *a*)
9	37.1 ± 1.0	(3) *b*)
23.5	36.6 ± 1.0	(3) *c*)
27	38.0 ± 1.0	present work
250	41 ± 10	(3) *d*)

The mean values of n_s and n_h found in the area and track scanning are respectively:

by area scanning $\quad \overline{n}_h = 8.5 \pm 0.2 \qquad \overline{n}_s = 6.1 \pm 0.1$

by track scanning $\quad \overline{n}_h = 7.2 \pm 0.2 \qquad \overline{n}_s = 6.1 \pm 0.1$

The maximum number of shower tracks found is $n_s = 26$. The above mentioned $\overline{n}_s$ value corrected for efficiency is

$$\overline{n}_s = 6.6 \pm 0.1 \, .$$

That value together with the multiplicity $\overline{n}_s$ obtained by various authors (4) at different kinetic energies E_p of the incident proton are shown in Fig. 3.

We note that the percentage $\eta(E)$ of stars with $n_s > 6$ is 49%; this value and those given by BRICMAN *et al.* (4) *f*) seem to indicate a linear dependence of $\eta(E)$ with respect to E_p.

This fact is in agreement with a similar observation of ZHDANOV (5) at a

and V. M. SIDOROV: *Dokl. Akad. Nauk USSR*, **121**, 617 (1958); *c*) G. CVIJANOVICH, B. DAYTON, P. EGLI, B. KLAIBER, W. KOCH, M. NICOLIĆ, R. SCHNEEBERGER, H. WINZELER, J. C. COMBE, W. M. GIBSON, W. O. LOCK, M. SCHNEEBERGER and G. VANDERHAEGE: *Nuovo Cimento*, **20**, 1012 (1961); *d*) M. W. TEUCHER and E. LOHMANN: (unpublished: reported by CIRJANOVICH).

(4) *a*) W. R. JOHNSON: *Phys. Rev.*, **99**, 1049 (1955); *b*) M. SCHEIN, D. M. HASKIN and R. G. GLASSER: *Nuovo Cimento*, **3**, 131 (1956); *c*) (3) *a*); *d*) P. L. JAIN and H. C. GLAHE: *Phys. Rev.*, **116**, 458 (1959); *e*) I. M. GRAMENITSKII, M. IA. DANYSH, V. B. LIUBIMOV, M. I. PODGORETSKII and D. TUVDENDORZH: *Soviet Phys. JEPT*, **8** (35), 381 (1959); V. S. BARASHENKOV, V. A. BELIAKOV, V. V. GLAGOLEV, N. DALKHAZHAV, YAO TSYNG SE, L. F. KIRILLOVA, R. M. LEBEDEV, V. M. MALTSEV, P. K. MARKOV, N. G. SHAFRANOVA, K. D. TOLSTOV, E. N. TSIGANOV and WANG SHOU FENG: *Nucl. Phys.*, **14**, 522 (1960); *f*) C. BRICMAN, M. CSEJTHEY-BARTH, J. P. LAGNAUX and J. SACTON: *Nuovo Cimento*, **20**, 1017 (1961); *g*) present work.

(5) *a*) C. W. SMITH, C. P. LEAVITT, A. M. SHAPIRO, C. E. SWARTZ and M. WIDGOFF: *Phys. Rev.*, **92**, 851 (1953); *b*) (4) *a*); *c*) (4) *b*); *d*) (3) *a*); *e*) G. L. BAYATJAN, I. M. GRAMENITSKII, A. A. NOMOFILOV, N. I. PODGORETSKII and E. S. SKRZYPEZAK: *Soviet Phys. JEPT*, **9** (36), 483 (1959); *f*) (4) *e*); *g*) (4) *f*); *h*) (3) *c*); *i*) present work.

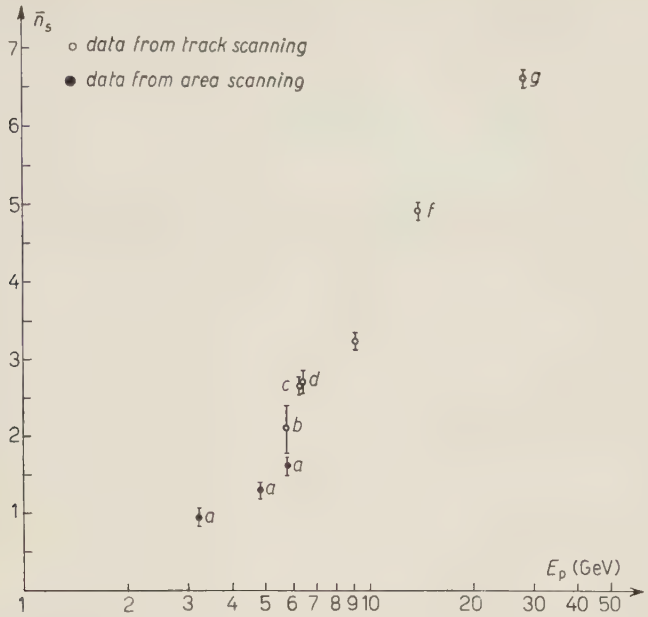

Fig. 3. – $\bar{n}_s$ from p-emulsion nucleus interaction as a function of incident kinetic energy.

lower energy. Quite different is the behaviour of $\bar{n}_h$ *vs.* E_p as is shown in Fig. 4. In fact $\bar{n}_h$ seems to be nearly constant with respect to E_p and the apparent decrease is perhaps due only to efficiency in star detection with $n_n = 0, 1$ in the area scanning data.

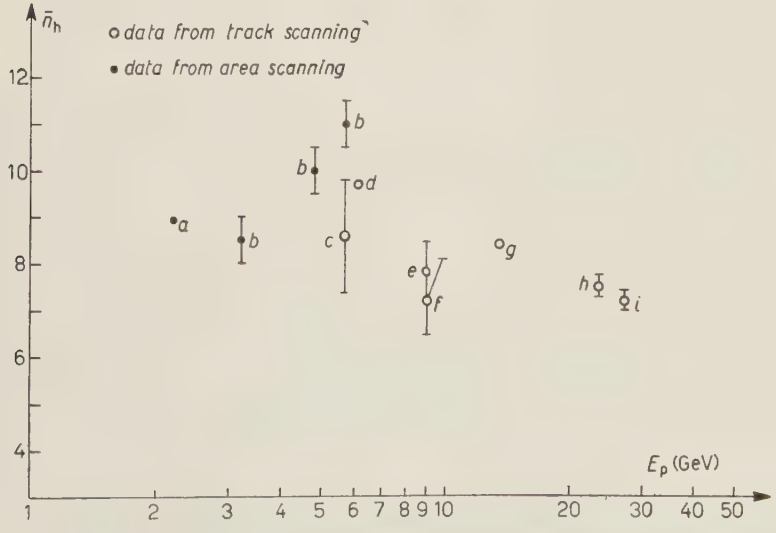

Fig. 4. – $\bar{n}_h$ from p-emulsion nucleus interaction as a function of incident kinetic energy.

However we note that the percentage of stars found in the track scanning with $n_h \geq 20$ is at our energy 6.7% compared with (10 : 11)% in the energy interval between 6.2 and 14 GeV. Also taking into account only the data of the area scanning, where the efficiency for $n_h = 0, 1$ is quite low, our percentage is 8.8%.

Moreover the percentage of stars with $n_h \geq 6$ ((48 ÷ 50)%) is constant in the total energy interval above mentioned. At our energy the dependence of $\bar{n}_s$ on n_h is shown in Fig. 5 for $n_s \geq 0$ and for $n_s \geq 4$, the values have been corrected for efficiency.

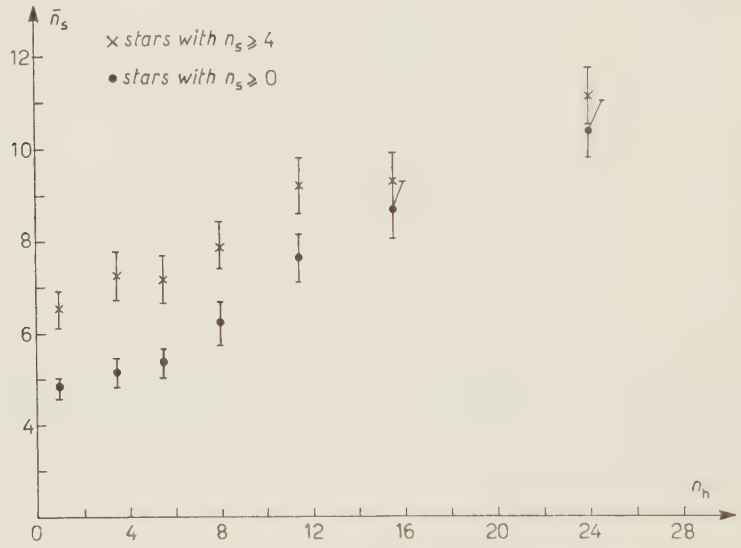

Fig. 5. – $\bar{n}_s$ *vs.* n_h for stars with $n_s \geq 4$ and $n_s \geq 0$.

Since $\bar{n}_s$ increases almost uniformly with n_h, no criteria can be derived from this plot to distinguish between events due to heavy nuclei and events due to light nuclei as was suggested at lower energy ([6]).

Also from the integral spectrum of n_h, shown in Fig. 6, it is not possible to distinguish between light and heavy nuclei; in fact there is no indication of a «knee» for $n_h = 7 : 8$, as observed in the analogous spectrum obtained by cosmic radiation. This different behaviour is probably due to the energy spectrum of the primaries. But in the absence of more reliable criteria, we accept the distinction suggested by FRIEDLÄNDER ([7]): $n_h \leq 4$ for the light nuclei (L-stars), $n_h \geq 7$ for the heavy nuclei (H-stars).

([6]) G. B. ZHDANOV, P. K. MARKOV, V. N. STRELSTSOV, M. I. TRETYAKOVA, CHENG-PU-YING and M. G. SHAFRANOVA: *Soviet Phys. JEPT*, **10** (37), 433 (1960).

([7]) E. M. FRIEDLÄNDER: *Nuovo Cimento*, **14**, 796 (1959).

The distribution in multiplicity of these L and H stars is shown in Fig. 7. The ratio between the mean multiplicities results to be:

$$r = \frac{(\bar{n}_s)_H}{(\bar{n}_s)_L} = \frac{8.2 \pm 0.2}{5.0 \pm 0.2} = 1.6 \pm 0.3 .$$

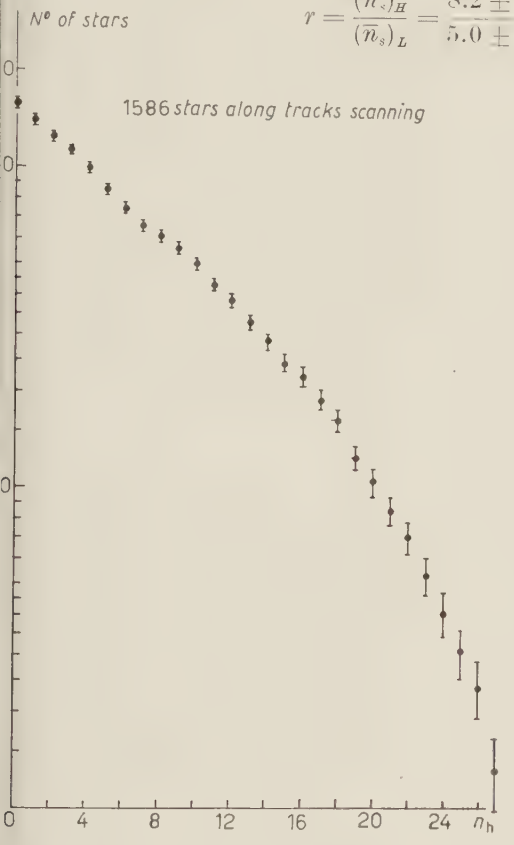

Fig. 6. – Integral distribution of black prongs n_h.

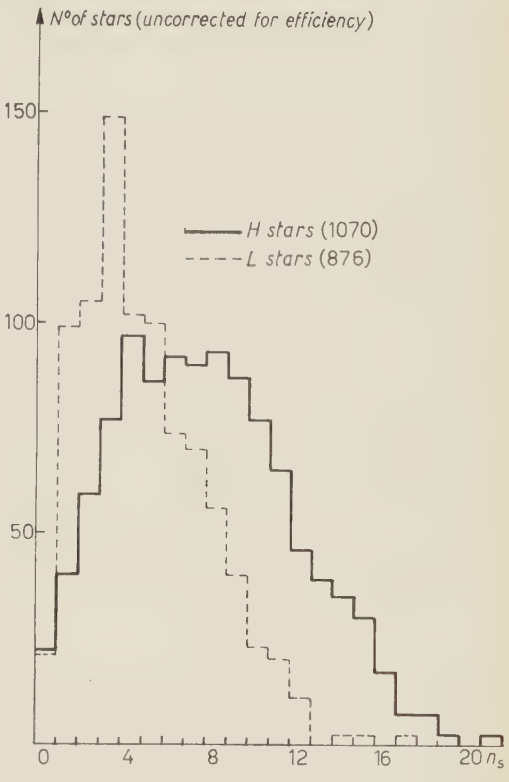

Fig. 7. – $\bar{n}_s$ distribution for L and H stars.

From the hydrodynamic theory (8) one finds that with a good approximation the ratio r is given by

$$r = \frac{1.55\,(A_{\mathrm{AgBr}}^{\frac{1}{3}} - 0.25)^{\frac{3}{2}}}{0.84\,(A_{\mathrm{CNO}}^{\frac{1}{3}} + 1)} = 1.62 \qquad \begin{array}{l} A_{\mathrm{AgBr}} = 94, \\ A_{\mathrm{CNO}} = 14, \end{array}$$

As one can see, the agreement is quite satisfactory; this result is also in agreement with that obtained at 9 GeV (7) and it is significantly different from what one could expect from a plural-type cascade process $r = 2 \div 3$, as is pointed out by FRIEDLÄNDER (7).

(8) S. Z. BELEN'KJI and G. A. MILEKHIN: *Soviet Phys. JEPT*, **2** (29), 14 (1956); S. Z. BELEN'KJI and L. D. LANDAU: *Suppl. Nuovo Cimento*, **3**, 15, (1956).

4. – On the energy of the charged shower particles.

Scattering measurements performed on the secondary tracks are, at this energy, very difficult and the errors due to the spurious noise and the statistical ones are very high. Therefore we have tried to determine this energy by the study of the secondary stars. Since the proton beam has a narrow angular distribution (the mean spread being 10′), we shall define as secondary stars produced by charged particles all the events showing an incoming relativistic track at a projected angle $2° < \alpha < 60°$ with the mean primary direction. The lower limit was chosen taking into account the spread of the primary beam (see Fig. 8), the scattering effect and uncertainties in the angular measurements. The 60° upper limit (needed to avoid stars produced by neutrons) was chosen taking into account the angular distribution of the shower prongs of the primary stars.

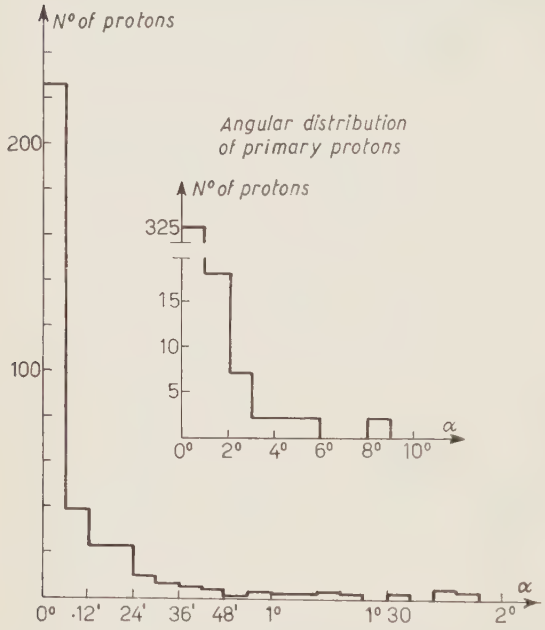

Fig. 8. – Distribution of projected angle α of primary protons at the edge of the stack.

We have compared the angular distribution of the particles producing the secondary stars with the angular distribution of the pion from primary proton stars. No evidence appears of a possible bias deriving from the geometry of the stack.

The scanning was performed on 33 cm² of emulsion; Fig. 9 shows the frequency distribution of the n_s multiplicity of the collected secondary stars. If we reasonably assume that the charged particles producing secondary stars are π-mesons, and if we take into account the known [9] experimental results

[9] *a*) M. Blau and A. R. Oliver: *Phys. Rev.*, **102**, 489 (1956); *b*) Rome group: unpublished results; *c*) [4] *b*); *d*) Shutt-Kalbach: in press; *e*) C. Besson, J. Crussard, V. Fouché, J. Hennessy, G. Kayas, V. R. Parikh and G. Trilling: *Nuovo Cimento*, **6**, 1168 (1959); *f*) H. H. Aly, J. G. M. Duthie and C. M. Fisher: *Phil. Mag.*, **4**, 993 (1959); *g*) E. M. Friedländer, M. Marcu and M. Spirchez: *Nuovo Cimento*, **18**, 623 (1960); *h*) Rome group: in press.

on $\bar{n}_s$ *vs.* E for π-mesons (see Fig. 10), then we can convert the multiplicity spectrum into the energy spectrum. From Fig. 3 one can see that the contamination of secondary protons would not affect considerably the energy spectrum so determined. We emphasize that in converting the multiplicity in energy spectrum we must use the smooth line of Fig. 9. This fact introduces some arbitrarity; however, any reasonable alteration of the line produces no noticeable alteration in

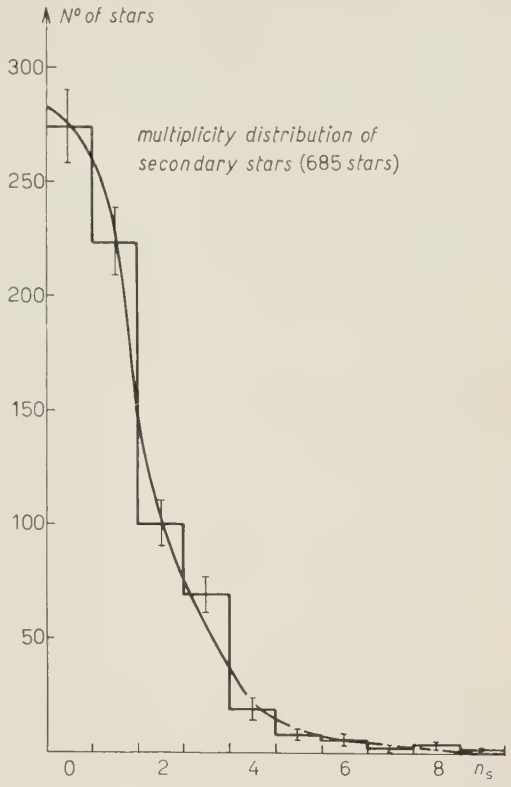

Fig. 9. – Multiplicity distribution of secondary stars produced by the charged minimum tracks. The smooth curve has been drawn to best fit the experimental spectrum.

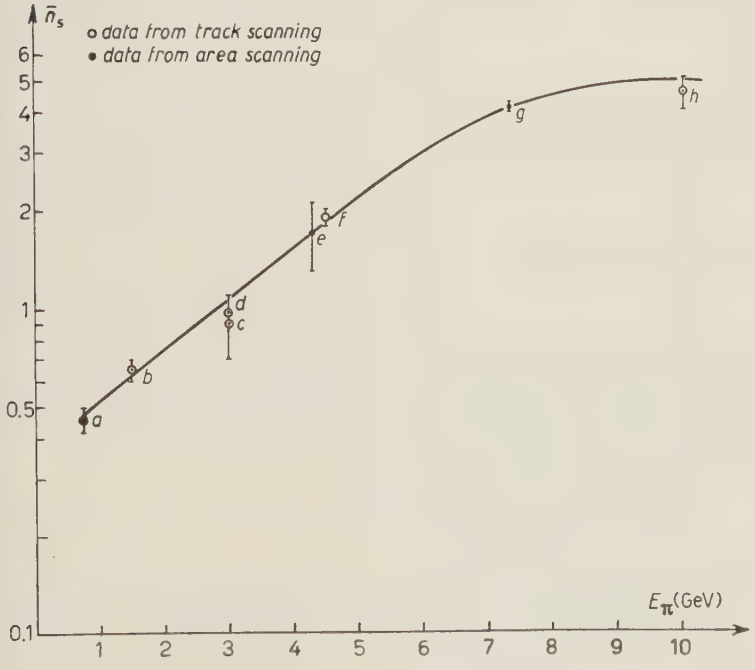

Fig. 10. – $\bar{n}_s$ *vs.* kinetic energy of pions E_π. The line has been drawn to best fit the experimental points.

the energy spectrum. The latter spectrum should, however, be corrected on the basis of the following arguments.

First, since in the area scanning there is a loss for small stars, we have corrected the n_s multiplicity spectrum according to the efficiency appearing from track and area scanning.

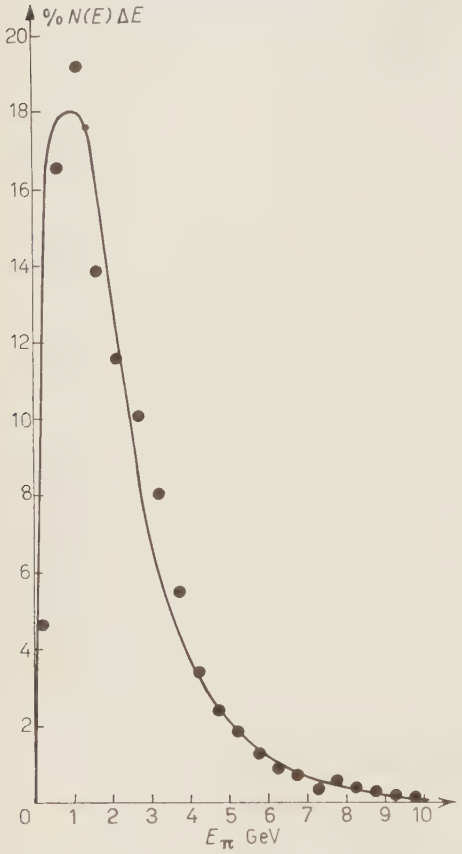

Fig. 11. – Pion spectrum of statistical theory (Hagedorn). The points represent our results.

A second correction is due to the spread of the primary proton beam (4% of the primary protons have a projected angle $> 2°$ to the mean direction of the beam). Then the primary protons of 27 GeV produce only 2% of the stars defined as secondary ones. The calculated correction on $\bar{E}_\pi$ can be neglected.

In Fig. 11 the spectrum of pions produced in a p-nucleon collision as calculated by HAGEDORN [10] by the statistical theory, is compared with the points obtained from the Fig. 9 with the procedure previously discussed. We have integrated the statistical spectrum in the angular interval between 2° and 60°. As one can see, the agreement between the spectra is satisfactory in spite of the several limitations of the method. To evaluate the mean energy $\bar{E}_\pi$ of the secondary pions one should take into account the correction due to the cut-offs at 2° and 60°. This correction can be done on the basis of the theoretical spectrum, which seems to be in agreement with the experimental one. That means a correction of 10% for $\alpha > 60°$ with a mean energy of 0.5 GeV and a 2.5% correction for $\alpha < 2°$ with a mean energy of 3 GeV.

The end result for nucleon-nucleus collisions is

$$E_{\pi^\pm} = 2.3 \pm 0.2$$

[10] R. HAGEDORN: *Nuovo Cimento*, **15**, 434 (1960).

compared with the mean value of 2.2 GeV obtained by the statistical theory for the nucleon-nucleon collisions. The error is only the statistical one.

5. – Inelasticity.

One can evaluate the fraction K' of the energy transferred in the laboratory system to secondary pions by the primary proton. If the mean multiplicity of charged pions on all nuclei of the emulsion is

$$\overline{n}_{\pi\pm} = \overline{n}_s - 2 = 4.6$$

and the mean kinetic energy is 2.3 GeV, we deduce for the total energy transferred in pion production

$$W_\pi = \tfrac{3}{2} W_{\pi\pm} n_{\pi\pm} = 16.5 \text{ GeV} .$$

Since the kinetic energy of primary protons is 27 GeV, we obtain

$$K' \sim 0.6 .$$

The error $\Delta K'/K'$ evaluated roughly as 30%, is due to several sources. First, the number of protons in $\overline{n}_s$ is perhaps different from 2; for instance in p-p collisions the Hagedorn calculation gives 1.2. This number is difficult to evaluate in p-nucleus collisions without mass measurements. A second uncertainty is due to the error on E_π, about 6.5%. One can remark that at 9 GeV some authors ([11]) have obtained $K' = 0.45 \pm 0.15$ and others ([6]) 0.33 ± 0.09, or ([12]) $0.33 < K' < 0.44$.

One can also evaluate the inelasticity in the c.m. system by means of the angular distributions. Since however these distributions depend also on the number of secondary interactions inside the nucleus, we prefer to use these distributions for this last problem.

6. – Angular distributions and collisions inside the nucleus.

The angular measurements on secondary prongs were performed on a sample of 284 stars of $n_s \geqslant 4$ reproducing the true n_s multiplicity spectrum.

For each star we have calculated the value:

$$\xi = \frac{1}{n_s} \sum_{i=1}^{n_s} \log |\operatorname{ctg} \theta_i| . \tag{1}$$

([11]) N. P. BOGACHEV, S. A. BUNJATOV, T. VISHKI, YU P. MEREKOV, V. M. SIDOROV and V. A. YARBA: *Soviet Phys. JEPT*, **11** (38), 317 (1960).

([12]) W. S. BARASHENKOV *et al.*: ([4]) *e*).

Since the distortion can influence the angular measurements of the prongs, we evaluate this error $|\Delta\xi|$ in our experimental conditions. The Fig. 12 shows the results obtained on a sample of 33 jets in unfavourable conditions on which was made the correction. One can see that the errors due to the distortion can be neglected towards the statistical ones. Fig. 13 shows the experimental value of ξ for interval $\Delta\xi = 0.05$. From the two hystograms it appears that the two distributions are picked for different values of ξ.

Fig. 12. – Correction on the $\log \gamma_c$ for the distortion effect.

If one considers multiple collisions inside the nucleus, the c.m.s. Lorentz factor is a function of the number ν of the target nucleons:

$$\gamma_c = (\gamma_0 + \nu)(1 + \nu^2 + 2\gamma_0\nu)^{-\frac{1}{2}}, \tag{2}$$

where γ_0 is the Lorentz factor of the primary proton in the l.s. γ_c should have a set of discrete values. Using the $\log \gamma_c = \xi$ from the spectrum-independent approximation ([13]) one should find the frequency distribution of ξ to be a superimposition of gaussian curves corresponding to the different γ_c values, with peaks on the values given by eq. (1), as pointed out by FRIEDLÄNDER ([7]).

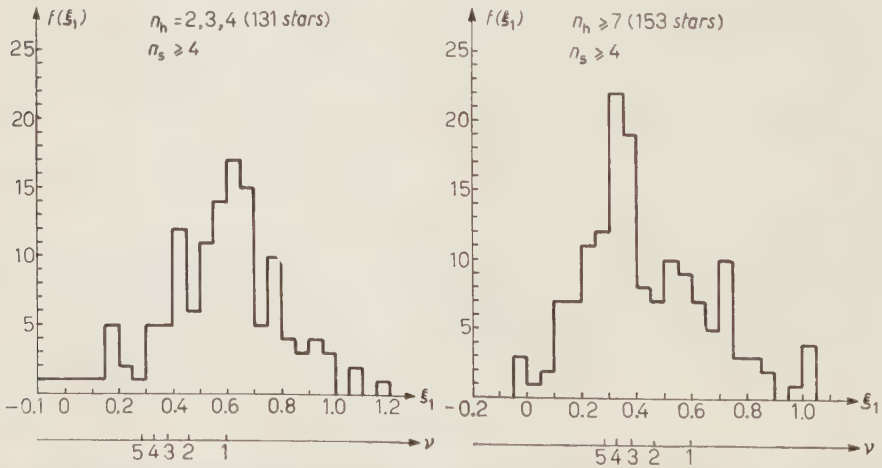

Fig. 13. – ξ_1 distribution for *L*-stars and *H*-stars. The ν axis is determined by formula (2).

([13]) C. CASTAGNOLI, G. CORTINI, A. MANFREDINI and D. MORENO: *Nuovo Cimento*, **10**, 1539 (1960).

Our ξ experimental distributions do not allow us to derive a statistically significant evidence for such « fine structure ». We can try to evaluate only the mean value $\bar{\nu}$ of the number of collisions for the two classes of events. We obtain from (1)

$$\langle \xi \rangle_L = 0.59 \pm 0.02 , \qquad \langle \xi \rangle_H = 0.38 \pm 0.02 ,$$

that is

$$\bar{\nu}_L = 1.0 \pm 0.1 , \qquad \bar{\nu}_H = 3.0 \pm 0.3 .$$

If we give to each ξ the corresponding value ν, we calculate, taking into account the maximum length of the tunnel, the mean values:

$$\bar{\nu}'_L = 1.3 \pm 0.2 , \qquad \bar{\nu}'_H = 2.7 \pm 0.3 .$$

A similar result can be obtained from the plot $\bar{\xi}$ *vs.* n_s (see Fig. 14), where the $\bar{\xi}$ was calculated on a « composite star » containing all the tracks of the stars with the same multiplicity. The result is: $\bar{\nu}_H = 2.7$.

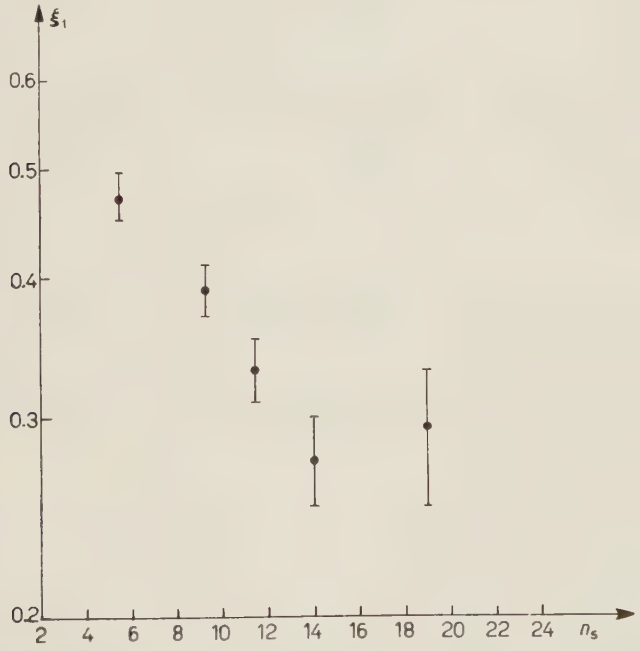

Fig. 14. – ξ_1 *vs.* n_s for the H-stars with $n_s \geqslant 4$.

From a similar plot we obtain $\bar{\nu}_L = 1.0$. These values are not statistically independent; but the different elaboration gives consistent values.

We can remark that the behaviour of $\bar{\xi}$ *vs.* n_h is similar to that abobe mentioned *vs.* n_s.

The ratio $\nu_L/\nu_H \sim 2.5$ is not in disagreement with the $(A_H/A_L)^{\frac{1}{3}} = 1.9$ from the tunnel theory. By means of the tunnel model [14], this ratio is 2.3.

It is possible, taking into account the absorption mean free path λ_a, to evaluate the mean free path in nuclear matter λ_n. We use the optical model square well with $r_0 = 1.35$ fermi and we can calculate the absorption cross-section:

$$\sigma_A \sim \frac{1}{\lambda_a} = \pi R^2 \{1 - \sum 1 - (1 + 2KR) \exp[-2KR] I/2K^2R^2\},$$

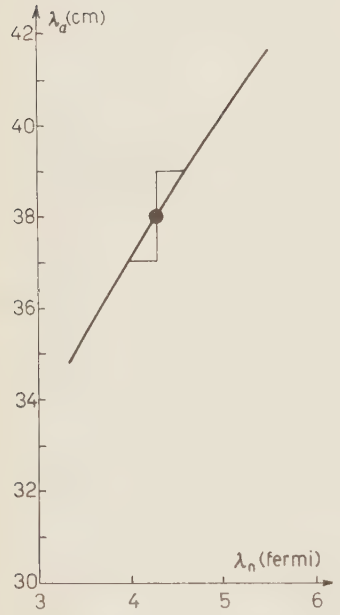

Fig. 15. – Mean free path in nucleon matter as a function of λ_a for a square well model with $r_0 = 1.35$ fermi.

when $K = 1/\lambda_n$ and $R = r_0 A^{\frac{1}{3}}$ for all the nuclei of the emulsions.

For the mean composition of the Ilford G-5 emulsion we have obtained the curve of Fig. 15.

The mean free path in nuclear matter λ_n results

$$\lambda_n = (4.3 \pm 0.3) \text{ fermi} .$$

Utilizing a similar calculation performed by BARASHENKOV [15] we obtain the cross-section for proton-nucleon σ_t averaged over p-p and p-n interactions, by the reduction (using the optical model) of the λ_a experimental value. We obtain

$$\sigma_{tot}(\text{p-nucleon}) = (32 \pm 1) \text{ mb} .$$

This cross sections is in good agreement with the value obtained in our direct preliminary measurement [16] on the proton-proton interaction $\sigma = (32 \pm 2)$ mb. From the λ_n value one derives, in a way independent from the preceeding one,

$$\bar{\nu} = 1.0 \pm 0.1 , \qquad \bar{\nu} = 0.1 \pm 1.9 .$$

7. – Conclusion.

1) For the stars produced by protons of 27 GeV in emulsion we obtain $\bar{n}_s = 6.6 \pm 0.1$, $\bar{n}_H = 7.2 \pm 0.2$. The ratio between the $\bar{n}_s$ multiplicities in H and L nuclei is $r = 1.6 \pm 0.3$, in agreement with the hydrodynamic theory.

[14] T. GOZANI and K. SITTE: *Nuovo Cimento*, **11**, 26 (1959).
[15] V. S. BARASHENKOV: *Sov. Phys. Usp.*, **3**, 689 (1961).
[16] LIÈGE, PARIS, PARMA, ROME GROUPS: in press.

2) The mean energy of the secondary shower particles is (2.3 ± 0.2) GeV. This evaluation was made by means of the multiplicity of the secondary stars. The mean value and the form of the energy spectrum are not in disagreement with the predictions of the statistical theory.

3) The energy transfer to the secondary mesons in the l.s. is $K \sim 0.6$ with an error of about 30%; compared with the values ~ 0.4 found at 9 GeV.

4) The study of the angular distributions of the shower tracks does not allow a statistically significant analysis of the features of the p-nucleus collisions. By means only of the mean value of ξ, we obtain for the mean number of collisions inside the nucleus

$$\sim 1.1 \text{ for } L \text{ nuclei}, \qquad \sim 2.7 \text{ for } H \text{ nuclei}.$$

5) The mean free path for absorption in emulsions is 38.0 ± 1.0, to which, according to an optical model, corresponds a nuclear mean free path $\lambda_n = (4.3 \pm 0.3)$ fermi.

* * *

We are greatly indebted to the emulsion Staff of CERN for the exposure facilities.

One of us (B.Q.) wishes to thank the Sezione di Torino dell'I.N.F.N. for the kind support for her stay in Rome.

RIASSUNTO

Abbiamo esaminato le caratteristiche di 3 226 stelle prodotte da protoni di 27 GeV contro nuclei delle emulsioni. Per le molteplicità medie si è ottenuto $n_s = 6.6 \pm 0.1$; $n_h = 7.2 \pm 0.2$. L'energia media dei secondari è stata valutata con un metodo indiretto ed è risultata di 2.3 ± 0.2 GeV. La frazione di energia trasferita ai mesoni secondari nel s.l. è $K \sim 0.6$. Dallo studio della distribuzione angolare abbiamo ricavato che il numero medio di collisioni all'interno del nucleo è di 1.1 e 2.7 rispettivamente per i nuclei leggeri e pesanti. Il cammino libero medio di assorbimento è $\lambda = 38.0 \pm 1.0$ da cui con un modello ottico, si ottiene un λ_n in materia nucleare uguale a 4.3 ± 0.3 fermi.

On the Theory of « Spiking » in Neutron Multiplying Systems.

S. E. Corno

AGIP Nucleare - San Donato, Milano

(ricevuto il 22 Maggio 1961)

Summary. — The main purpose of the work is to develop a theory suitable for dealing with those neutron multiplying structures in which a small number of highly reactive blocks — the so called « spikes » — are embedded into a finite subcritical medium; this basic medium is assumed to be homogeneous from the standpoint of neutron migration and multiplication. It is shown how the theory can be worked out by performing a proper inversion of the integral operator, which describes the thermal flux distribution. The problem is solved by giving it the same form which one encounters when treating — along the lines of the heterogeneous theory — a « reactor with a small number of blocks ». Cylindrical multiplying structures are examined in great detail: the resulting treatment - within the limits of the age-diffusion or multigroup theory — can be considered as the exact one, at least for those systems is which the spikes can be taken as line singularities of the neutron field. Spiked structures — even if the basic multiplying medium is left unchanged — possess as many degrees of freedom as the number of « classes » of spikes which constitute the system, times the number of parameters charactering each spike. An *optimization* theory is worked out for such types of nuclear reactors in order to fulfill, by a proper choice of the free parameters, the criticality condition together with a set of additional requirements.

Introduction.

Let us consider a finite neutron multiplying structure, which can be assumed to be homogeneous from the standpoint of neutron migration and multiplication. Obviously the further requirement that the structure is subcritical will be added.

A problem of considerable interest, both for its practical and theoretical

implication, is that of making critical such a structure by addition of few and highly reactive lumps of fissionable material.

In other words, we introduce into the homogeneous subcritical structure some highly enriched blocks, the so called « *spikes* », which « ignite » the system, compensating for losses and parasitic absorptions. The neutron flux, if stationary conditions can be achieved, shall thus result from the complicated interactions of the spikes with each other, and also from the interactions of the spikes themselves with the basic multiplying and moderating medium.

The main purpose of this work is to develop a selfconsistent theory for criticality calculations expecially suitable to treat what we shall simply call the « spiked structures ».

Furthermore a method will be worked out for the optimization of such kinds of nuclear reactors, in order to fulfill, together with criticality condition, some additional requirements. Special attention will be devoted to the problem of flattening the power distribution.

1. – The general theory.

1·1. *The integral equation of the problem.* – To write down properly the neutron balance equation for a spiked structure:

a) We start by considering a system in which the spikes are embedded into a *pure moderator*, of given capture cross-section.

Let us consider the k-th spike, located at $\boldsymbol{r}_k$, acting as a fast neutron source of intensity q_k and as a sink of thermal neutrons of intensity I_k. Each localized neutron absorption will be considered as the emission of a « negative » neutron, according to the well known heterogeneous theory techniques.

As a consequence, if M spikes are present, the thermal flux, at any point $\boldsymbol{r}$ of our simplified structure, will be given by

$$\Phi_{\text{Mod}}(\boldsymbol{r}) = \sum_1^M{}_k [q_k \cdot F_{\text{Mod}}(\boldsymbol{r}, \boldsymbol{r}_k) - I_k \cdot f_{\text{Mod}}(\boldsymbol{r}, \boldsymbol{r}_k)] , \tag{1.1}$$

where the function $F_{\text{Mod}}(\boldsymbol{r}, \boldsymbol{r}_k)$ stands for the thermal flux at $\boldsymbol{r}$ due to a unit point source, stationary in time, releasing fast neutrons near $\boldsymbol{r}_k$, while $f_{\text{Mod}}(\boldsymbol{r}, \boldsymbol{r}_k)$ is the diffusion kernel for a unit thermal source at $\boldsymbol{r}_k$.

b) If a thermal neutron absorber is uniformly added to the moderator considered above, an equation of the same form of (1.1) is still valid, provided that a proper change is made in the capture cross-section and—eventually—in the thermalization parameters which appear in $F_{\text{Mod}}(\boldsymbol{r}, \boldsymbol{r}_k)$ and in $f_{\text{Mod}}(\boldsymbol{r}, \boldsymbol{r}_k)$.

c) Let's suppose now that the additional capture cross-section referred to in *b*) is—at least partially—*a fission cross-section.*

This fact causes the moderator, we have been starting with, to change into an homogeneous multiplying medium. A distributed fast neutron source will thus arise into the system.

If the resonance captures by the homogeneous medium can be assumed to take place in the same point in which the multiplication occurs, the thermal neutron flux shall satisfy the following integral equation:

$$\Phi(\boldsymbol{r}) = k_\infty \Sigma_a \iiint F(\boldsymbol{r}, \boldsymbol{r}') \Phi(\boldsymbol{r}') \, \mathrm{d}\boldsymbol{r}' + \sum_1^M{}_k I_k \cdot [\eta_k \cdot F(\boldsymbol{r}, \boldsymbol{r}_k) - f(\boldsymbol{r}, \boldsymbol{r}_k)] \,. \tag{1.2}$$

The most striking feature of eq. (1.2) is a lack of symmetry in the description of the thermal neutron absorptions: when a capture occurs into the k-th block, its effect appears as a depletion of the thermal flux in the surrounding medium, and $f(\boldsymbol{r}, \boldsymbol{r}_k)$ represents this localized sink.

On the other hand, the neutrons absorbed by the distributed fissionable materials have been properly accounted for when the fission cross-section has been added to the moderator's absorption cross-section, which appears in F, f and, explicitly, as a factor in the integral term of (1.2).

Further assumptions are implicit in eq. (1.2):

α) The fission energy spectrum is the same for neutrons born into the blocks and for neutrons born in the homogeneous medium.

In effect, the age-diffusion or multigroup kernel F, used to describe the positive contribution to the neutron population, caused by the presence of the spikes, appears unchanged under the sign of integration.

This assumption, however, is not essential for the future development of the theory and could be easily removed.

β) The emission of q_k fast neutrons from a block appears in (1.2) as a consequence of the absorption of I_k thermal neutrons into the spike itself. The parameter η_k can be taken as an overall measure of the multiplying properties of a spike.

In order to save the neutron balance we shall include in η_k a factor accounting for the resonance escape probability in the homogeneous medium. We simply write

$$q_k = \eta_k \cdot I_k \,.$$

γ) The spikes are acting as *rigid sources and sinks*: in other words—at least for the moment—the values of I_k are independent of the neutron flux present in the system.

δ) No attention is given to the geometrical dimensions of the spikes. They have been simply considered as point—or line—singularities of the neutron field. The theory worked out below could be extended in principle to account for spikes of any geometrical structure.

1·2. *Formal solution of the thermal flux equation.* – If we still assume the rigid source-sink approximation, disregarding for the moment the relation between the thermal neutron population and the intensity of absorption in the spikes, eq. (1.2) immediately appears as a non-homogeneous integral equation, in which the term under the summation sign stands for a known function.

Let us rewrite it in a standard form:

$$(\mathbf{I} - \nu\mathbf{K})\cdot\Phi(\boldsymbol{r}) = \psi(\boldsymbol{r})\,, \tag{1.2'}$$

where **I** is the identity operator; ν is the number of secondaries per fission in the basic multiplying medium, and could be taken as the eigenvalue of the integral equation itself. The integral operator **K** is defined by

$$\mathbf{K} = \Sigma_f\cdot\varepsilon\cdot p\cdot\iiint F(\boldsymbol{r}, \boldsymbol{r}')\ldots \mathrm{d}\boldsymbol{r}'\,, \tag{1.3}$$

Σ_f being the macroscopic fission cross-section of the homogeneous medium, ε its fast fission factor and p its resonance escape probability. We want to remember explicitly the previous assumptions i) that no resonance capture occurs in the blocks, and ii) that the spatial distribution of thermal neutrons is unaffected by the spatial distribution of the epithermal captures. Both these hypotheses are quite reasonable and one can easily understand that neither of them could be removed without destroing the formal simplicity of the theory. The meaning of the right hand side of eq. (1.2') is obvious:

$$\psi(\boldsymbol{r}) \equiv \sum_1^M{}_k I_k\cdot[\eta_k\cdot F(\boldsymbol{r}, \boldsymbol{r}_k) - f(\boldsymbol{r}, \boldsymbol{r}_k)]\,. \tag{1.4}$$

We just recall that $\psi(\boldsymbol{r})$ is always a function of $\boldsymbol{r}$ belonging to the class L^2.

Supposed now that the inverse integral operator of (1.3) has been found; we shall than have

$$\Phi(\boldsymbol{r}) = (\mathbf{I} + \nu\cdot\mathbf{H}_\nu)\,\psi(\boldsymbol{r}) \tag{1.5}$$

and, due to the linearity of the problem and the particular form of $\psi(\boldsymbol{r})$,

$$\Phi(\boldsymbol{r}) = \sum_1^M{}_k I_k\cdot(\mathbf{I} + \nu\mathbf{H}_\nu)[\eta_k\cdot F(\boldsymbol{r}, \boldsymbol{r}_k) - f(\boldsymbol{r}, \boldsymbol{r}_k)]\,. \tag{1.5'}$$

The thermal flux still appears formally as a sum of positive and negative contributions, arising from the singularities.

Eq. (1.4) supplies us with a solution of the problem, provided that the operator $\mathbf{H}_\nu$ exists: it happens in practice, as it will become clear in Section **2**, that the conditions for the existence of $\mathbf{H}_\nu$—the convergence of a Neumann series, say—possess a deep physical significance. Anyhow they can always be fulfilled by a formal change in the parameter ν, in order to prevent it from being a spectral point of the operator $\mathbf{K}$. This formal change however is meaningless on the physical ground: in practice the composition of the basis medium or the dimensions of the system will have to be modified whenever the inversion of $\mathbf{K}$ proves to be impossible.

1·3. *The critical condition.* – The solution (1.5), if it exists, refers to the ideal case of rigid sources and sinks. But, if a stationary flux distribution has to be entertained in the system, the spikes themselves will be required to compensate for losses.

The easiest way of imposing this condition is to calculate $\Phi(\boldsymbol{r})$ by means of eq. (1.5) at a certain spatial point $\boldsymbol{r}$ and let then $\boldsymbol{r}$ to approach a point $\boldsymbol{r}_h$ on the boundary of the h-th spike.

According to the well-known techniques of the heterogeneous method, the linear dependence of I_h on $\Phi(\boldsymbol{r}_h) \equiv \Phi_h$ is then taken into account:

$$\Phi_h = \gamma_h \cdot I_h = \sum_1^M{}_k I_k \cdot (\mathbf{I} + \nu \mathbf{H}_\nu)[\eta_k \cdot F(\boldsymbol{r}_h, \boldsymbol{r}_k) - f(\boldsymbol{r}_h, \boldsymbol{r}_k)] \,. \tag{1.6}$$

The parameter γ_h is dependent on the nuclear characteristics of the spike and on the properties of the surrounding medium. It can be easily related to the extrapolation length λ_h for thermal neutrons.

As $\boldsymbol{r}_h$ in (1.6) can indicate the position of any spike, the formula (1.6) is to be taken as an homogeneous system of linear equations in the M unknowns $I_1, I_2, \ldots, I_M$.

We can give (1.6) the following concise form:

$$\gamma_h \cdot I_h = \sum_1^M{}_k I_k \cdot \Gamma_{hk}(\eta_k; k_\infty) \equiv \sum_1^M{}_k I_k \cdot [a_{hk}(k_\infty) \cdot \eta_k - b_{hk}(k_\infty)] \quad (h = 1, 2, \ldots, M). \tag{1.6'}$$

The assumption that ν be a « regular value » of the operator $\mathbf{K}$ implies in practive the choice of the geometrical dimensions, and of the parameters k_∞, Σ_a, L^2, τ ... characterizing the homogeneous medium to be made into a bounded domain « D ». But, as soon as this restricted choice has been made, the conditions for the consistency of the system of linear eq. (1.6) can be identified with the conditions which allow eq. (1.2) to possess a stationary and self-consistent solution.

In other words the vanishing of the determinant of the coefficients for eq. (1.6′)

$$\|\Gamma_{hk}(\eta_k; k_\infty) - \gamma_h \cdot \delta_{hk}\| = 0 \tag{1.7}$$

can be taken as *the critical equation of the spiked structure.*

To satisfy eq. (1.7), when the geometry of the system has been chosen in advance, one can in principle change the values of the parameters η's and γ's characterizing the spikes.

But it should be remembered that each γ_k is depending on the corresponding η_k, and, furthermore, that a chosen set of eigenvalues has to be acceptable on physical ground. Even the nuclear constants of the basic multiplying medium can be taken as eigenvalues, provided that the choice is made inside the bounded domain « D », defined above.

It appears clearly at this point that one free parameter alone could be sufficient to satisfy the critical equation. In Section 3 of this work the problem of using the remaining $(2M-1)$ degrees of freedom (and the parameter of the basic medium) in order to optimize the spiked reactor will be discussed.

2. – The cylindrical « spiked » structure.

2·1. *The application of the general theory.* – To show how the method outlined above can be applied in practical cases, we shall work out in detail the calculations for a bare cylindrical reactor of infinite height.

In ref. [1] it has been shown that $F(\boldsymbol{r}, \boldsymbol{r}')$, in the age-diffusion approximation, has the following form, for the two-dimensional cylindrical systems:

$$F(\boldsymbol{r}, \boldsymbol{r}') = \frac{1}{\pi R^2} \sum_{-\infty}^{+\infty m} \cos m(\theta - \theta') \sum_{1}^{\infty j} \frac{\exp\left[-(\alpha_{mj}^2/R^2)\tau\right] J_m((\alpha_{mj}/R)r) J_m((\alpha_{mj}/R)r')}{D((\alpha_{mj}^2/R^2) + \varkappa^2)(J'_m(\alpha_{mj}))^2} \tag{2.1}$$

while, the diffusion kernel is given by

$$f(\boldsymbol{r}, \boldsymbol{r}') = \frac{1}{\pi R^2} \sum_{-\infty}^{+\infty m} \cos m(\theta - \theta') \sum_{1}^{\infty j} \frac{J_m((\alpha_{mj}/R)r) J_m((\alpha_{mj}/R)r')}{D((\alpha_{mj}^2/R^2) + \varkappa^2)(J'_m(\alpha_{mj}))^2}, \tag{2.2}$$

R being the extrapolated radius of the cylinder, τ the neutron age to thermal, $\varkappa^2 = 1/L^2 = \Sigma_a/D$ the inverse diffusion length in the homogeneous medium. We still want to point out explicitly that the macroscopic absorption cross-section Σ_a of the uniform medium includes the distributed fission cross-section as well.

The constants α_{mj} stand for the j-th positive root of the transcendental equation $J_m(x) = 0$.

---

[1] S. E. Corno: *Nuovo Cimento*, **17**, 580 (1960). *Note*: In this work the factor $(1+\delta_{m0})/2$ has to be taken as equal 1 wherever it appears.

We can write (1.2′) in the form

$$\Phi(\boldsymbol{r}) = \nu \mathbf{K}\, \Phi(\boldsymbol{r}) + \psi(\boldsymbol{r}) \tag{2.3}$$

and seek its solution $\Phi(\boldsymbol{r})$ in term of Neumann's series expansion, the function $\psi(\boldsymbol{r})$ being assumed to be known.

We take as a first approximation of $\Phi(\boldsymbol{r})$

$$\varphi_1(\boldsymbol{r}) = \psi(\boldsymbol{r}) \equiv \sum_1^M{}_k I_k \cdot [\eta_k \cdot F(\boldsymbol{r}, \boldsymbol{r}_k) - f(\boldsymbol{r}, \boldsymbol{r}_k)] \tag{2.4}$$

and then

$$\left\{\begin{aligned} &\varphi_2(\boldsymbol{r}) = \psi(\boldsymbol{r}) + \nu \mathbf{K}\, \psi(\boldsymbol{r}) \\ &\quad . \quad . \quad . \quad . \quad . \quad . \quad . \quad . \quad . \quad . \quad . \quad . \quad . \quad . \\ &\varphi_n(\boldsymbol{r}) = \psi(\boldsymbol{r}) + \nu \mathbf{K}\, \varphi_{n-1}(\boldsymbol{r}) \\ &\qquad = \psi(\boldsymbol{r}) + \nu \mathbf{K} \psi + \nu^2 \mathbf{K}^2 \psi + \ldots + \nu^{n-1} \mathbf{K}^{n-1} \psi \,. \end{aligned}\right. \tag{2.5}$$

This iteration procedure just involves successive integrations of the following type:

$$\begin{aligned} \nu\, \Sigma_f\, \varepsilon p \int_0^{2\pi} \int_0^R F(\boldsymbol{r}, \boldsymbol{r}')[\eta_k \cdot F(\boldsymbol{r}', \boldsymbol{r}_k) - f(\boldsymbol{r}', \boldsymbol{r}_k)]\, \mathrm{d}\theta' r'\, \mathrm{d}r' = \\ = \frac{1}{\pi R^2} \sum_{-\infty}^{+\infty}{}_m \cos m(\theta - \theta_k) \sum_1^\infty{}_j \left[\frac{\nu\, \Sigma_f\, \varepsilon p \exp\left[-(\alpha_{mj}^2/R^2)\tau\right]}{D((\alpha_{mj}^2/R^2) + \varkappa^2)}\right] \cdot \\ \cdot \frac{(\eta_k \exp\left[-(\alpha_{mj}^2/R^2)\tau\right] - 1) J_m((\alpha_{mj}/R) r) \cdot J_m((\alpha_{mj}/R) r_k)}{D((\alpha_{mj}^2/R^2) + \varkappa^2) \cdot (J'(\alpha_{mj}))^2} \,. \end{aligned} \tag{2.6}$$

Let us simply call β_{mj} the following set of ∞^2 constants:

$$\beta_{mj} \quad \frac{\nu\, \Sigma_f\, \varepsilon p \cdot \exp\left[-(\alpha_{mj}^2/R^2)\tau\right]}{D((\alpha_{mj}^2/R^2) + \varkappa^2)} - \frac{k_\infty \exp\left[-(\alpha_{mj}^2/R^2)\tau\right]}{1 + L^2(\alpha_{mj}^2/R^2)} \,. \tag{2.7}$$

It can be easily proved that any successive iteration just causes the factor β_{mj} appearing in (2.6) to be multiplied by β_{mj} itself under the summation signs. So, the final expression of $\varphi_n(\boldsymbol{r})$, by inverting the order of the sums, can be given the following form:

$$\begin{aligned} \varphi_n(\boldsymbol{r}) = \sum_1^M{}_k I_k \frac{1}{\pi R^2} \sum_{-\infty}^{+\infty}{}_m \cos m(\theta - \theta_k) \sum_1^\infty{}_j \left\{\sum_0^{n-1}{}_s \beta_{mj}^s\right\} \cdot \\ \cdot \frac{(\eta_k \exp\left[-(\alpha_{mj}^2/R^2)\tau\right] - 1)}{D((\alpha_{mj}^2/R^2) + \varkappa^2) \cdot (J_m'(\alpha_{mj}))^2} \cdot J_m\left(\frac{\alpha_{mj}}{R} r\right) \cdot J_m\left(\frac{\alpha_{mj}}{R} r'\right) \,. \end{aligned} \tag{2.8}$$

Obviously the exact solution of (2.3) is given by the limit function

$$\Phi(\boldsymbol{r}) = \lim_{n\to\infty} \varphi_n(\boldsymbol{r}) \tag{2.9}$$

provided that such a limit exists.

To secure the convergence of the Neumann series, we require as a *sufficient condition* any one of the infinite geometrical series appearing in (2.8) under the sign $\sum_0^\infty{}_s$ to be convergent.

This implies all of the β_{mj} to be less than one. It appears immediately that the maximum value of β_{mj} occurs for $m=0$, and $j=1$. So we can write, by remembering that for a bare cylinder the geometrical buckling B^2 simply equals $\alpha_{01}^2/R^2 = (2.4048)^2/R^2$,

$$\beta_{01} = \frac{k_\infty \cdot \exp\left[-(\alpha_{01}^2/R^2)\tau\right]}{1+L^2(\alpha_{01}^2/R^2)} = \frac{k_\infty \cdot \exp\left[-B^2\tau\right]}{1+L^2B^2} < 1\,. \tag{2.10}$$

The inequality (2.10) requires *the starting homogeneous core* to be *subcritical* before introducing the spikes. As soon as (2.10) has been satisfied, the geometrical series appearing as factors in (2.8) can be summed up quite simply and the resulting flux distribution will be

$$\Phi(\boldsymbol{r}) = \sum_1^M{}_k I_k \frac{1}{\pi R^2} \cdot \sum_0^\infty{}_m \varepsilon_m \cos m(\theta-\theta_k) \sum_1^\infty{}_j \frac{1}{D((\alpha_{mj}^2/R^2)+\varkappa^2) - k_\infty \Sigma_a \exp\left[-(\alpha_{mj}^2/R^2)\tau\right]} \cdot \tag{2.11}$$

$$\cdot (\eta_k \cdot \exp\left[-(\alpha_{mj}^2/R^2)\tau\right] - 1) \frac{J_m((\alpha_{mj}/R)r)\cdot J_m((\alpha_{mj}/R)r_k)}{(J'_m(\alpha_{mj}))^2}\,, \quad (\varepsilon_0 = 1;\ \varepsilon_1 = \varepsilon_2 = \ldots = 2).$$

As to the convergence of the series (2.11) we note that, asymptotically, the difference between its terms and the corresponding terms of the expansion of $\psi(\boldsymbol{r})$ is $O(\alpha_{mj}^{-4})$. In effect we have

$$\lim_{\substack{m\to\infty \\ j\to\infty}} \left[\frac{1}{D((\alpha_{mj}^2/R^2)+\varkappa^2) - k_\infty \Sigma_a \exp\left[-(\alpha_{mj}^2/R^2)\tau\right]} - \frac{1}{D((\alpha_{mj}^2/R^2)+\varkappa^2)} \right] = O\left(\frac{1}{\alpha_{mj}^2}\right), \tag{2.12}$$

so that the difference between (2.11) and $\psi(\boldsymbol{r})$ is an absolutely and uniformly convergent series.

This fact causes the convergence of (2.11) to be the same as for the series representing $\psi(\boldsymbol{r})$. We may then conclude that the flux $\Phi(\boldsymbol{r})$ given by (2.11) possesses logarithmic singularities at all the points where the spikes are located.

When imposing now the consistency condition for the flux distribution we

shall find a critical equation, whose matrix elements, still using the nomenclature of (1.6′), are given by

$$(2.13)\qquad \Gamma_{hk}(\eta_k;\, k) = \frac{1}{\pi R^2} \sum_0^\infty{}_m \varepsilon_m \cos m(\theta_h - \theta_k) \cdot$$

$$\cdot \sum_1^j \frac{\{\eta_k \cdot \exp[-(\alpha_{mj}^2/R^2)\tau] - 1\}}{\{D((\alpha_{mj}^2/R^2) + \varkappa^2) - k_\infty \Sigma_a \exp[-(\alpha_{mj}^2/R^2)\cdot\tau]\}} \cdot \frac{J_m((\alpha_{mj}/R)r_h)\cdot J_m((\alpha_{mj}/R)r_k)}{(J'_m(\alpha_{mj}))^2} .$$

Particular attention has to be devoted to the diagonal elements of the critical matrix, because of the logarithmic singularity occurring in their negative components. A suitable procedure will be outlined below, in order to avoid the appearance of unlimited terms in the critical equation.

A further obvious remark can be made on formula (2.13).

If we suppose ν, the number of secondary neutrons per fission, tend to zero, then k_∞ also goes to zero. And the critical matrix of our spiked core goes over into the corresponding matrix for an heterogeneous reactor « with a small number of rods ». This can be checked by comparing (2.12) with (3.8) of ref. (1).

2·2. *On the convergence of the series representing the flux.* – Starting from the remarks made when discussing eq. (2.12), one can easily see that the second double series in the left hand side of (2.11) is not uniformly convergent on the whole domain $0 \leqslant r \leqslant R$.

Furthermore, even for $\boldsymbol{r} \neq \boldsymbol{r}_k$, its convergence is extremely slow. On the other hand we know that the logarithmic singularities which are located at any spike place $\boldsymbol{r} = \boldsymbol{r}_k$ are of the same kind as those occurring in the Green's function $G(\boldsymbol{r}, \boldsymbol{r}_k)$ related to the two dimensional diffusion equation in an infinite moderator:

$$(2.14)\qquad G(\boldsymbol{r}, \boldsymbol{r}_k) = \frac{1}{2\pi D} K_0(|\boldsymbol{r} - \boldsymbol{r}_k| \varkappa) .$$

This fact suggests the idea of taking out the singularities from the series (2.11) by adding and subtracting the Green's function (2.14) itself. To carry out this program we will expand first of all $G(\boldsymbol{r}, \boldsymbol{r}_k)$ in a series of the orthonormal eigenfunctions

$$(2.15)\qquad u_{mj}(r, \theta) = \sqrt{\frac{\varepsilon_m}{\pi}} \cdot \frac{J_m((\alpha_{mj}/R)r)}{RJ'_m(\alpha_{mj})} \cos m(\theta - \theta_k) ,$$

the same reference system of the Hilbert space in terms of which the flux $\Phi(\boldsymbol{r})$, as given by (2.11), happens to be expressed.

By performing the expansion we can easily show that

$$(2.16)\quad -\frac{1}{2\pi D}K_0(|\boldsymbol{r}-\boldsymbol{r}_k|\varkappa)+\frac{1}{\pi R^2}\sum_0^\infty{}_m\,\varepsilon_m\cos m(\theta-\theta_k)\cdot$$
$$\cdot\sum_1^\infty{}_j\frac{J_m((\alpha_{mj}/R)r)}{D((\alpha_{mj}^2/R^2)+\varkappa^2)(J'_m(\alpha_{mj}))^2}\left\{J_m\left(\frac{\alpha_{mj}}{R}r_k\right)-\alpha_{mj}J'_m(\alpha_{mj})\,I_m(\varkappa r_k)K_m(\varkappa R)\right\}=0\,.$$

Then, by simply defining the constants

$$(2.17)\qquad H_{mj}\equiv k_\infty\,\Sigma_a\exp\left[-\frac{\alpha_{mj}^2}{R^2}\tau\right],$$

and adding the left-hand side of eq. (2.16) to the series expansion of $\Phi(\boldsymbol{r})$, we shall have, instead of (2.11),

$$(2.18)\quad \Phi(\boldsymbol{r})=\sum_1^M{}_k\,I_k\cdot$$
$$\cdot\left\{-\frac{1}{2\pi D}K_0(|\boldsymbol{r}-\boldsymbol{r}_k|\varkappa)+\frac{1}{\pi R^2}\sum_0^\infty{}_m\,\varepsilon_m\cos m(\theta-\theta_k)\sum_1^\infty{}_j\frac{J_m((\alpha_{mj}/R)r)J_m((\alpha_{mj}/R)r_k)}{(J'_m(\alpha_{mj}))^2}\cdot\right.$$
$$\cdot\left[\frac{\eta_k\cdot\exp\left[-(\alpha_{mj}^2/R^2)\tau\right]}{D((\alpha_{mj}^2/R^2)+\varkappa^2)-H_{mj}}-\frac{H_{mj}}{D((\alpha_{mj}^2/R^2)+\varkappa^2)\left[D((\alpha_{mj}^2/R^2)+\varkappa^2)-H_{mj}\right]}\right]+$$
$$\left.+\frac{1}{2\pi D}\sum_0^\infty{}_m\,\varepsilon_m\cos m(\theta-\theta_k)I_m(\varkappa r_k)K_m(\varkappa R)\sum_1^\infty{}_i\frac{(-2)\cdot\alpha_{mi}\cdot J_m((\alpha_{mi}/R)r)}{R^2((\alpha_{mi}^2/R^2)+\varkappa^2)J'_m(\alpha_{mi})}\right\}.$$

A remarkable simplification can be reached in this formula by carrying out the summation which appears in the rightmost position, under the sign $\sum_i$.

The symplest way of doing this is looking at this series as an inverse Hankel transform of some unknown function of r.

By means of standard properties of the integrals involving Bessel functions the inverse transformation referred to above can be given its explicit form and, as a final result, we have

$$(2.19)\qquad \frac{I_m(\varkappa r)}{I_m(\varkappa R)}=-\frac{2}{R^2}\sum_1^\infty{}_i\frac{\alpha_{mj}J_m((\alpha_{mi}/R)r)}{((\alpha_{mi}^2/R^2)+\varkappa^2)J'_m(\alpha_{mi})}\,.$$

So, the last double series of (2.18) may be written as a simple one in the form

$$(2.20)\qquad \frac{1}{2\pi D}\sum_0^\infty{}_m\,\varepsilon_m\cos m(\theta-\theta_k)\frac{I_m(\varkappa r)}{I_m(\varkappa R)}I_m(\varkappa r_k)K_m(\varkappa R)\,,$$

and this series can easily be shown to be absolutely and uniformly convergent, provided that $r_k < R$.

In effect, for $r \leqslant R$, the asymptotic relation

$$\cos m(\theta - \theta_k) \frac{I_m(\varkappa r)}{I_m(\varkappa R)} = O(1),$$

$m \to \infty$, is self-evident and, furthermore, for large values of m $(m \gg \frac{1}{4}z^2)$ the following expansions hold

$$K_m(z) \sim \left(\frac{2}{z}\right)^m \frac{(m-1)!}{2} \left\{1 - \frac{(\frac{1}{2}z)^2}{(m-1)} + \frac{(\frac{1}{2}z)^4}{2!(m-1)(m-2)}\right\};$$

$$I_m(z) \sim \left(\frac{z}{2}\right)^m \frac{1}{m!} \left\{1 + \frac{(\frac{1}{2}z)^2}{(m+1)} + \frac{(\frac{1}{2}z)^4}{2!(m+1)(m+2)}\right\} <$$

$$< \left(\frac{z}{2}\right)^m \frac{1}{m!} \left\{1 + \frac{(\frac{1}{2}z \cdot R/r_k)^2}{(m-1)} + \frac{(\frac{1}{2}z \cdot R/r_k)^4}{2!(m-1)(m-2)}\right\}.$$

As a consequence, for large values of m one can write

$$I_m(\varkappa r_k) K_m(\varkappa R) \sim \frac{1}{2} \left(\frac{r_k}{R}\right)^m \cdot \frac{1}{m} \cdot \left[1 + O\left\{\left[\frac{1}{2} \varkappa R \cdot \frac{1}{m}\right]^4\right\}\right],$$

and the series (2.20) appears immediately as an absolutely and uniformly convergent one in the whole domain $0 \leqslant |\boldsymbol{r}| \leqslant R$, provided that $r_k < R$, *i.e.* no spike is allowed to lie in the contour of the reactor.

It has to be pointed out in addition that all of the other series which appear in (2.18) are absolutely and uniformly convergent.

This fact shows clearly how the formula (2.18)—as compared with (2.11)—is taking advantages from the fact that the singularities have been « collected » in the closed terms K_0's.

Furthermore, when computing the diagonal elements of the critical determinant for our problem, starting from the flux represented by means of (2.18) and (2.20), we can easily avoid the appearance of unlimited terms: it will be sufficient to take into account the finite radius—say ϱ_k—of any spike in evaluating the Bessel function K_0.

So on the main diagonal we shall have terms like $-(1/2\pi D) \cdot K_0(\varkappa \varrho_k)$, while in the off-diagonal positions the finite dimensions of the spikes will be disregarded. Thus the matrix elements for our neutron multiplying structure can

be given the following form:

$$(2.21)\quad \Gamma_{hk}(\eta_k;\, k_\infty) = \frac{1}{\pi R^2} \sum_0^\infty{}_m\, \varepsilon_m \cos m(\theta_h - \theta_k) \cdot$$

$$\cdot \left\{ \sum_1^\infty{}_j \frac{J_m((\alpha_{mj}/R) r_h)\, J_m((\alpha_{mj}/R) r_k)}{(J'_m(\alpha_{mj}))^2} \left[\frac{\eta_k \cdot \exp\left[-(\alpha_{mj}^2/R^2)\tau\right]}{D((\alpha_{mj}^2/R^2) + \varkappa^2) - H_{mj}} - \right.\right.$$

$$\left.\left. - \frac{H_{mj}}{D((\alpha_{mj}^2/R^2) + \varkappa^2)\left[D((\alpha_{mj}^2/R^2) + \varkappa^2) - H_{mj}\right]} \right] + \frac{R^2}{2D} \cdot \frac{I_m(\varkappa r_h) I_m(\varkappa r_k)}{I_m(\varkappa R)} K_m(\varkappa R) \right\} -$$

$$- \frac{1}{2\pi D} K_0\left(\sqrt{r_h^2 + r_k^2 - 2 r_h r_k \cos(\theta_h - \theta_k)} \cdot \varkappa\right),$$

depending on the polar co-ordinate of the two points $\boldsymbol{r}_h$ and $\boldsymbol{r}_k$, the whole set of the nuclear parameters and the geometrical dimensions of the system.

Formula (2.21) is now suitable for calculation by means of a high speed computer.

We want to remark here the summation procedure for slowly convergent series outlined above, can be applied also in the case described in ref. [1], formula (3.8).

3. – The optimum spiking in neutron multiplication.

The most attractive feature of lumping the enriched fissionable material in blocks seems to be related to the fact that the resulting « spiked structures » posses so many degrees of freedom as to allow the fulfilment of almost any required optimum condition.

By changing the local position and the mutual enrichment of the spikes, one can obtain in principle any desired neutron flux distribution in the system: so the « *minimum critical mass* condition » for instance can be approximated, as well as the fuel temperature distribution which is most suitable for a safe heat removal.

3·1. *The flux flattening problem.* – To give an idea of the wide range of possibilities open by the spiking techniques, let us solve the following problem.

A subcritical structure, fueled by natural uranium, has to be made critical by addition of spikes, located in some given positions $\boldsymbol{r}_k$. We want to find out the multiplying properties of that system of spikes, which leads to the most uniform power distribution *on the natural fuel.*

The assumption is made that, by changing independently the dimensions and the enrichment, one can build spikes having the same blackness for thermal neutrons *i.e.* the same value of the parameter γ, and different values for η.

The critical equation for the present problem will be given in a form consistent with (1.6′):

$$\Delta \equiv \| a_{hk}(k_\infty) \cdot \eta_k - b_{hk}(k_\infty) - \gamma \cdot \delta_{hk} \| = 0 \,. \tag{3.1}$$

The meaning of a_{hk} and b_{hk} may be derived from (2.21) in the case of cylindrical structures.

The required uniform flux distribution, if realised in the system, will imply as a consequence that spikes of different characteristics, but possessing the same absorption capacity, do effectively absorb the same number of neutrons in the unit time.

The mathematical problem is thus reduced to that of determining simultaneously a set of values η_k^* for the η's ($\eta = 1, 2, \ldots, M$) and a unique value γ^* for the parameter γ such that:

i) the critical eq. (3.1) is satisfied;

ii) all the corresponding unknowns, *i.e.* the intensities of absorption, $I_1, I_2, \ldots, I_M$, take the same numerical value.

So, to determine our optimum condition, we shall have to solve the following coupled system of $(M+1)$ algebraic equations

$$\left| \begin{array}{l} \sum_1^M{}_k \, a_{hk} \cdot \eta_k^* = B_h + \gamma^* \,, \qquad (3.2) \\ \Delta \equiv \| a_{hk} \cdot \eta_k^* - b_{hk} - \gamma^* \cdot \delta_{hk} \| = 0 \qquad (3.3) \end{array} \right.$$

the first M being linear and the last one of the M-th order.

The constants B_h obviously stand for $\sum_1^M{}_k \, b_{hk}$.

Let the coupled linear eq. (3.2) be written in matrix form

$$\{A\}(\eta^*) = (Y) \tag{3.4}$$

the elements of $\{A\}$ being the $a_{hk}(k_\infty)$ defined before and the components of the vector (Y) being given by

$$Y_h = B_h + \gamma^* \,. \tag{3.5}$$

As soon as the inverse matrix $\{A\}^{-1}$ is found, one can get (η^*) as a function of γ^*

$$\eta_k^* = \sum_1^M{}_j \, (a^{-1})_{kj} (B_j + \gamma^*) \tag{3.6}$$

so that eq. (3.3) can be expressed in a form depending only on γ^*:

$$\|a_{hk} \cdot \sum_{1}^{M}{}_{j} A_{jk}(B_j + \gamma^*) - (\|A\|) \cdot b_{hk} - (\|A\|)\gamma^* \cdot \delta_{hk}\| = 0 \,. \tag{3.3'}$$

A_{jk} is the cofactor of a_{jk} in the matrix $\{A\}$ and $\|A\|$ the determinant of $\{A\}$.

Among the M roots of (3.3') we will choose the positive one which is physically significant, *i.e.* the root which leads to a vector (η^*) consisting of all positive components.

An even more stringent condition should be imposed in practice, namely that all the components of (η^*) be larger that one, in order to prevent each spike in turn from acting as a neutron absorber.

3·2. *The extrema of functions of the spike parameters.* – The critical equation for the spiked structure has been given the same form as that describing a reactor with a small number of blocks.

This allows the optimization theory worked out in ref. (1), (Sec. 3·3) for the above mentioned heterogeneous reactors to be extended also to the case of spiked structures.

Any function of the system of spikes—their spatial distribtuion being given—will ultimately appear, in the following form:

$$G = G(\eta_1, \eta_2, ..., \eta_M; \gamma_1, \gamma_2, ..., \gamma_M) \,. \tag{3.7}$$

For each spike the characteristic parameters η and γ happen to be related to each other and the following M functions

$$\gamma_k = \chi_k(\eta_k; \delta_1, \delta_2, ..., \delta_N) \tag{3.8}$$

are assumed to be known. The δ's stand here for a set of additional variables, mainly dependent upon the enrichment, the presence of cladding materials and the geometrical shape of the spike itself. The functions χ can be determined by means of detailed transport theory or Monte Carlo calculations, as well as from experiments (2,3).

We want to find out now the spike configuration which makes critical the multiplying structure, causing at the same time the function G to take an extremum value, say a minimum.

---

(2) *a*) J. W. Zink: *Use of small source theory in the determination of the critical size of heterogeneous thermal reactors*, NAA-SR-3222; *b*) J. W. Zink and G. W. Rodeback: *Nucl. Sci.*, **9**, 16 (61).

(3) S. M. Feinberg *et al.*: *Large-scale heterogenity of the core*, Part III of the paper P/2145 URSS, P.I.G.C., **13**, 376 (1958).

The problem is actually reduced to that of a conditional minimum, which can be dealt with by the well-known Lagrange's method of multipliers.

Let us consider the following linear combination

$$H(\eta_1, \eta_2, \ldots, \eta_M; \gamma_1, \gamma_2, \ldots, \gamma_M; \lambda) \equiv G + \lambda \Delta \,, \tag{3.9}$$

Δ being the critical determinant as defined in (3.1), and λ a further parameter to be determined. The function χ's being given, H can now be taken as just depending on the $(M+1)$ variables $\eta_1, \eta_2, \ldots, \eta_M$ and λ. For a conditional minimum of G to be present, the following set of equations has to be necessarily satisfied:

$$\begin{cases} \dfrac{\partial H}{\partial \eta_k} = \dfrac{\partial G}{\partial \eta_k} + \dfrac{\partial G}{\partial \gamma_k} \cdot \dfrac{\partial \chi_k}{\partial \eta_k} + \lambda \cdot \sum_1^M{}_j D_{jk} \left[a_{jk} - \dfrac{\partial \chi_k}{\partial \eta_k} \cdot \delta_{jk} \right] = 0 \,, \quad (k = 1, 2, \ldots, M) \\ \dfrac{\mathrm{d}H}{\partial \lambda} = \Delta = 0 \,. \end{cases} \tag{3.10}$$

The function D_{jk} stands for the cofactor of the (jk)-th element in the determinant Δ, and as such is dependent on all of the η's, except η_k.

Let us examine the following simplified case: if a change in the values of the η's could be made without altering the γ's, *i.e.* if any χ_h where constant with respect to η_h, the mathematical difficulties of the optimization problem summarized in eq. (3.10) would be simply reduced to make equal to zero the critical determinant together with M linear combinations, each involving M of the $(M-1)$-th order minors of Δ.

In practice, as the χ's are not constant, the solution of (3.3) represents a more elaborate problem. But, as in the practical cases the spikes of a system can be grouped in classes, according to their nuclear characteristics and geometrical positions, the order of the determinant Δ is quite low, say four of five as a maximum, and the optimization procedure outlined above can be safely afforded by means of digital computers, taking into account its full generality.

RIASSUNTO

Scopo di questo lavoro è la formulazione di una teoria della criticità adatta per strutture moltiplicanti di neutroni, costituite da un piccolo numero di « blocchi » (spikes), altamente arricchiti, immersi in un mezzo moltiplicante finito, praticamente

omogeneo. La teoria è fondata sulla soluzione dell'equazione integrale che descrive la distribuzione del flusso neutronico termico nel sistema. Il problema viene formalmente ricondotto ad una equazione critica analoga a quella che si incontra, trattando col metodo eterogeneo reattori aventi un piccolo numero di elementi di combustibile. Si esaminano in dettaglio le strutture moltiplicanti cilindriche assialmente infinite e la trattazione che ne risulta può considerarsi rigorosa nell'ambito della teoria dell'età-diffusione. La generalizzazione a più gruppi è da ritenersi immediata. Tutti i gradi di libertà delle strutture contenenti spikes vengono infine vincolati tramite una opportuna teoria dell'ottimizzazione. Ciò consente di ottenere le più favorevoli distribuzioni della potenza nel sistema critico, oppure di estremare una qualunque funzione dipendente dalle caratteristiche degli « spikes ».

Double Pion Production in K-$\mathcal{N}$ Collisions.

Chia Hwa Chan

Department of Physics, Imperial College - London

(ricevuto il 27 Maggio 1961)

Summary. — Recent experiments (1) showed a fair probability of single pion production in high energy K-$\mathcal{N}$ collisions. This process has been calculated (2,3) in the peripheral interaction with a K′ isobar model and found in good agreement with experiments. Here we report the calculation of double pion production in a similar model, particularly for the process (*): $K^- + p \to K^- + p + \pi^+ + \pi^-$ since this is the easiest to be detected experimentally.

Recent experiments (1) showed a fair probability of single pion production in high energy K-$\mathcal{N}$ collisions. This process has been calculated (2,3) in the peripheral interaction with a K′ isobar model and found in good agreement with experiments. Here we report the calculation of double pion production in a similar model, particularly for the process (*):

$$K^- + p \to K^- + p + \pi^+ + \pi^-$$

since this is the easiest to be detected experimentally.

Double pion production involves considerable complication because there are four outgoing particles. We shall make the following assumptions to facilitate the calculation.

(1) M. Alston *et al.*: *Phys. Rev. Lett.*, **6**, 300 (1961).

(2) M. A. B. Beg and P. C. De Celles: *Phys. Rev. Lett.*, **6**, 145, 428 (1961).

(3) C. H. Chan: *Phys. Rev. Lett.*, **6**, 383 (1961).

(*) For other different charge states, they are related to this process by charge independence and the total cross-sections differ only by a constant factor.

1) The process takes place through the excited K-meson state K′ (4), which decays strongly into a K-meson and a pion:

$$K^- + p \to \overline{K}^{0\prime} + p + \pi^- \to K^- + \pi^+ + p + \pi^- .$$

This assumption reduces the calculation of the cross-section essentially to that of 3 outgoing particles, provided that the width of K′ is small. If K′ has isotopic spin $\frac{1}{2}$ (3),

$$\sigma(K^- + p \to K^- + p + \pi^+ + \pi^-) = \tfrac{2}{3}\sigma(K^- + p \to \overline{K}^{0\prime} + p + \pi^-) .$$

2) The peripheral interaction dominates (5), *i.e.* we shall neglect all diagrams except the one in which only a single pion is exchanged between the incoming K-meson and the nucleon.

3) The pion production from the nucleon is through the (33) resonant state. This assumption is good provided that the incoming K-meson's kinetic energy does not exceed 1600 MeV in the laboratory system, so that the total energy of the pion-nucleon system in their own c.m. system is within the (33) resonant energy range. In the calculation, the amplitude of the virtual pion-nucleon scattering in (33) state is substituted by a real (33) resonant scattering amplitude; this is exact only at $\Delta^2 = -\mu^2$ (6), but may be valid for small Δ^2 as argued by several authors (7).

In the above approximation the reaction in question is represented by one Feynman diagram:

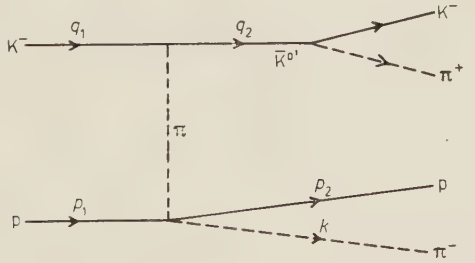

Fig. 1. – The Feynman diagram of double pion production from K⁻-p collision.

(4) J. TIOMNO: *Proceedings of the 1960 Annual International Conference on High Energy Physics at Rochester* (New York, 1960), p. 508.

(5) F. SALZMAN and G. SALZMAN: *Phys. Rev.*, **120**, 599 (1960); F. BONSIGNORI and F. SELLERI: *Nuovo Cimento*, **15**, 465 (1960); F. SELLERI: *Phys. Rev. Lett.*, **6**, 64 (1961).

(6) G. F. CHEW and F. E. LOW: *Phys. Rev.*, **113**, 1640 (1959).

(7) *E.g.* F. SALZMAN and G. SALZMAN: *Phys. Rev. Lett.*, **5**, 377 (1960).

The cross-section reads

$$\sigma(K^- + p \to K^- + p + \pi^+ + \pi^-) = \tfrac{2}{3}\sigma(K^- + p \to \overline{K}^{0\prime} + p + \pi^-) =$$

$$= \left(\frac{G_V^2}{4\pi}\right)\frac{1}{9\pi U^2 |q_1|_U^2 m_0^2}\int dA^2\, dW\, |k|_W W^2[(m_0^2 + A^2 + m^2)^2 - 4m_0^2 m^2]\cdot$$

$$\cdot\sigma_{\pi^- + p\to\pi^- + p}(W^2)\frac{1}{(A^2+\mu^2)^2},$$

for vector K′, and

$$= \left(\frac{m^2 G_S^2}{4\pi}\right)\frac{1}{9\pi U^2 |q_1|_U^2}\int dA^2\, dW\, |k|_W W^2 \sigma_{\pi^- + p\to\pi^- + p}(W^2)\frac{1}{(A^2+\mu^2)^2},$$

for scalar K′; where

$$\left(\frac{G_V^2}{4\pi}\right) = \frac{4\lambda m_0^5}{[(m_0^2 - m^2 - \mu^2)^2 - 4m^2\mu^2]^{\frac{3}{2}}},$$

$$\left(\frac{m^2 G_S^2}{4\pi}\right) = \frac{4\lambda m_0^3}{3[(m_0^2 - m^2 - \mu^2)^2 - 4m^2\mu^2]^{\frac{1}{2}}},$$

M, m_0, m, μ are the masses of the nucleon, K′, K and pion respectively, λ is the total width of the K′. U is the overall c.m. energy, and W is the total outgoing pion-nucleon energy in the lower vertex in their own c.m. system. A is the energy momentum 4-vector of the virtual pion. The suffix U or W shows in which system the quantity is evaluated.

$\sigma_{\pi^- + p\to\pi^- + p}(W^2)$ is the total cross-section for the π^--p elastic scattering, for which we shall take the (33) theoretical approximation ([8-9]).

Then

$$\cdot\sigma_{\pi^- + p\to\pi^- + p}(W^2) = \frac{8\pi}{3}|f_{33}(W^2)|^2,$$

where

$$f_{33}(W^2) = \frac{1}{|k|_W}\sin\delta_{33}\exp[i\delta_{33}] \cong \frac{\Gamma(W)}{(W_r - W) - i\Gamma(W)|k|_W},$$

$$\Gamma(W) = \frac{\gamma|k|_W}{W - M}, \qquad \gamma = \frac{0.225}{\mu}, \qquad W_r = M + 2.1\mu.$$

([8]) G. F. Chew and F. E. Low: *Phys. Rev.*, **101**, 1570 (1959).

([9]) S. Bergia, F. Bonsignori and A. Stanghellini: *Nuovo Cimento*, **19**, 1073 (1960).

The limits of integration are given by

$$\Delta^2_{\max,\min} = -m^2 - m_0^2 + 2E(q_1)_U E(q_2)_U \pm 2(q_1)_U 2(q_2)_U ,$$

where

$$E(q_1)_U = \frac{U^2 - M^2 + m^2}{2U}, \qquad E(q_2)_U = \frac{U^2 - W^2 + m_0^2}{2U},$$

and

$$W_{\min} = M + \mu , \qquad W_{\max} = U - m_0 .$$

We see that if we limit the incoming K-meson kinetic energy to 1600 MeV, this corresponds to $W_{\max} \sim 1364$ MeV, which is within the (33) resonant energy range. The differential cross-sections $d\sigma/d\Delta^2$ at this particular energy for scalar and vector K′ are shown in Fig. 2, where we have taken the experimental values of the mass and width of K′ to be 885 MeV and 16 MeV respectively. The peak in the low energy-momentum transfer range corresponds to (K^--π^+) going forward and (p-π^-) going backward in the total c.m. system.

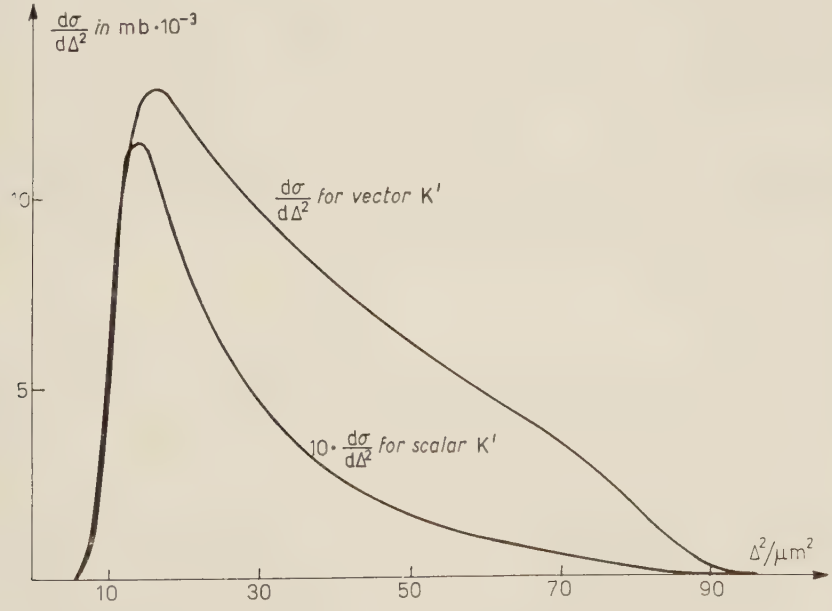

Fig. 2. – The differential cross-sections $d\sigma/d\Delta^2$ of double pion production, in which the scale for the vector case is ten times larger than that for the scalar case.

The total cross-section for this process is computed below and is compared to that of $K^- + p \to \bar{K}^0 + \pi^- + p$ ([3]) in Table I. The ratio between these two

is independent of λ, the width of K′, which experimentally is not well determined.

TABLE I.

Incoming K-meson k.e. in lab. sys. in MeV	$\sigma(K^-+p\to\to\bar{K}^0+p+\pi^-)$ in mb		$\sigma(K^-+p\to\to K^-+p+\pi^++\pi^-)$ in mb·10^{-3}		$\frac{\sigma(K^-+p\to K^-+p+\pi^++\pi^-)}{\sigma(K^-+p\to\bar{K}^0+p+\pi^-)}$ in %	
	vector K′	scalar K′	vector K′	scalar K′	vector K′	scalar K′
900	1.71	0.120				
1000	1.89	0.121	0.003	0.0002	0.0001	0.0001
1100	2.00	0.116	0.332	0.0191	0.0166	0.0165
1200	2.07	0.110	3.864	0.208	0.186	0.289
1300	2.12	0.104	16.04	0.823	0.755	0.796
1400	2.16	0.097	31.10	1.565	1.44	1.62
1500	2.18	0.091	42.26	2.102	1.93	2.32
1600	2.20	0.085	51.28	2.553	2.33	3.02

As it has been argued previously [3] from the total cross-section of $K^-+p\to K^0+p+\pi^-$, K′ may be a vector; if this is the case, the cross-section for double pion production is still small which explains why we do not see any such process yet.

* * *

The author wishes to thank Dr. A. FUJII for going through the manuscript and Prof. A. SALAM for suggesting this work.

RIASSUNTO (*)

Esperimenti recenti hanno mostrato che si ha una buona probabilità per la produzione di pioni singoli nelle collisioni K-N di alta energia. Si è calcolato questo processo nell'interazione periferica con un modello K′ isobarico e si è trovata una buona concordanza con gli esperimenti. Qui riportiamo i calcoli per la produzione di due pioni in un modello analogo, particolarmente per il processo: $K^-+p\to K^-+p+\pi^++\pi^-$, poichè questo è il più facile ad individuare sperimentalmente.

(*) *Traduzione a cura della Redazione.*

IL NUOVO CIMENTO Vol. XXI, N. 3 1° Agosto 1961

Solutions of the Coupled S and P-Wave Equations for Pion-Pion Scattering.

B. H. Bransden (*)

CERN - Geneva

J. W. Moffat (**)

RIAS - Baltimore, Md.

(ricevuto il 29 Maggio 1961)

Summary. — A method is presented for solving numerically the coupled S and P-wave equations for pion-pion scattering derived by Moffat from analyticity, crossing symmetry and unitarity on the basis of the Mandelstam representation. It is shown that apart from the pion-pion coupling constant, no further parameters enter the low-energy theory. For a range of coupling constant λ, taking negative values $|\lambda| \leqslant 0.45$, solutions exist satisfying crossing symmetry. These solutions are characterized by the existence of a low-energy resonance in the P-wave of which the position and width are entirely determined by λ. The corresponding S-wave phase shifts show that scattering in the $I=0$ isotopic spin-state is large at low energies.

1. – Introduction.

The study of pion-pion elastic scattering has received much attention recently ([1-7]). Chew and Mandelstam ([1]) have shown that, in principle, the

(*) On leave of absence from the University, Glasgow.

(**) The major part of this work was carried out while one of us (J.W.M.) was a visiting scientist at CERN, Geneva.

([1]) G. F. Chew and S. Mandelstam: *Phys. Rev.*, **119**, 467 (1960).

([2]) G. F. Chew, S. Mandelstam and H. P. Noyes: *Phys. Rev.*, **119**, 478 (1960).

([3]) G. F. Chew and S. Mandelstam: *UCRL Report* 9126 (Lawrence Radiation Laboratory, March 1960).

([4]) W. R. Frazer and J. R. Fulco: *Phys. Rev.*, **117**, 1609 (1960).

([5]) M. Cini and S. Fubini: *Ann. Phys.*, **3**, 352 (1960).

([6]) Ho Tsu-hsien, Hsien Ding-chang and W. Zoellner: preprint (Dubna, 1960).

([7]) J. G. Taylor: preprint (Cambridge University, 1960).

partial wave amplitudes may be determined from analyticity, unitarity and crossing symmetry, in the approximation where waves higher than P-waves are assumed small and contributions from four-pion and higher mass states are neglected. In practice, the N/D method developed for the solution of these equations has proved unsatisfactory. To obtain finite results when the P-wave amplitude is large, cut-offs have to be introduced for both S and P-waves. Although the number of parameters introduced in this way may be reduced by crossing symmetry, one new arbitrary parameter remains in the theory, in addition to the coupling constant λ.

An entirely different method of solution of the equations governing the partial wave amplitudes has been described by MOFFAT ([8]) ([*]). This method constructs coupled equations defining the *inverse* partial wave amplitude in a form suitable for numerical solution. In I, this method was applied in the approximation neglecting S-waves entirely, thus producing uncoupled equations for the P-wave amplitude. It was shown that a low-energy resonance in the P-wave was consistent with the Mandelstam representation. However, to define the P-wave amplitude completely, two arbitrary constants appeared, an « effective » P-wave coupling constant and a parameter related to the slope of the cross-section at zero energy.

In the present paper the coupled equations for both the S and P-waves are presented in a form in which a numerical solution may be developed by iteration. Further, it is shown that crossing symmetry implies equations relating waves of different l that determine both the P-wave constants in terms of a single pion-pion coupling constant. It is therefore clear that the equations obtained neglecting four-pion and higher mass states form a soluble system in the *low-energy* region in terms of one constant, and the introduction of further constants is a property of the method of solution employed and not of the original equations, as has been supposed ([9]).

In Section 2, the integral equations are described and the problem of the high-energy behaviour of the equations is discussed. Section 3 treats the approximate crossing conditions obtained by CHEW and MANDELSTAM ([3]). These conditions are used to reduce the number of free parameters entering the equations. In Section 4 the iteration scheme is developed which is used to obtain a numerical solution to the coupled S and P-wave equations. Finally, in Section 5, the results of the numerical iteration are described for different values of the coupling constant λ.

([8]) J. W. MOFFAT: *Phys. Rev.*, **121**, 926 (1961).

([*]) This paper is referred to as I throughout.

([9]) G. F. CHEW and S. C. FRAUTSCHI: *Phys. Rev. Lett.*, **5**, 580 (1960).

2. – The integral equations.

The implicit solution of the equations defining the pion-pion elastic scattering partial wave amplitudes, discussed in I, is (*)

$$(1) \qquad \left[\frac{1}{a_l^I} + L_l^I(\nu, \nu_0) + N_l^I(\nu, \nu_0) - (\nu - \nu_0)\sum_{n=0}^{l-1}\frac{\nu^{n-l}}{n!}\, g_l^{(n)I}(0) - iT_l^I(\nu)\right]^{-1},$$

where I denotes the isotopic spin state and l is the l-th partial wave and $a_l^I \equiv A_l^I(\nu_0)$ is the l-th partial wave subtraction constant, also

$$(2) \qquad L_l^I(\nu, \nu_0) = -\frac{(\nu - \nu_0)}{\pi} P\int_0^\infty \frac{\mathrm{d}\nu' \sqrt{\nu'/(\nu'+1)}\, R_l^I(\nu')}{(\nu' - \nu)(\nu' - \nu_0)}.$$

$$(3) \qquad N_l^I(\nu, \nu_0) = -\frac{(\nu - \nu_0)}{\pi} P\int_1^\infty \frac{\mathrm{d}\nu' K_l^I(-\nu')}{(\nu' + \nu)(\nu' + \nu_0)}.$$

The quantity $T_l^I(\nu)$ is defined by

$$(4) \qquad T_l^I(\nu) = \begin{cases} R_l^I \sqrt{\dfrac{\nu}{\nu+1}}, & \text{for } \nu > 0, \\ K_l^I(\nu), & \text{for } \nu < -1, \end{cases}$$

where $R_l^I(\nu) = \sigma_l^T(\nu)/\sigma_l^{el}(\nu)$, and $\sigma_l^T(\nu)$, $\sigma_l^{el}(\nu)$ are the total and elastic partial wave cross-sections, respectively. The fourth term on the right of (1) arises from the singularity in the inverse partial wave amplitude generated by the threshold behaviour at the origin

$$(5) \qquad A_l(\nu) = C_l \nu^l + O(\nu^{l+1}) \qquad \text{as } \nu \to 0.$$

In the l-th angular momentum state there will occur $(l+1)$ constants in the solution (1). We could equally well have divided $A_l^I(\nu)$ by ν^l in order to remove the singularity at the origin, but then $(l+1)$ subtractions would be required in the l-th angular momentum state. We shall reduce the number of free parameters by utilizing the derivative crossing conditions at the symmetry point $\nu_0 = -\frac{2}{3}$ ([3]).

In the elastic scattering region we have $R_l^I = 1$, and $L(\nu, \nu_0) = h(\nu) - h(\nu_0)$,

(*) The notation and units of I are employed throughout.

where for $\nu > 0$ and $\nu < -1$, we find that

$$h(\nu) = \frac{2}{\pi}\sqrt{\frac{\nu}{\nu+1}}\ln\left(\sqrt{|\nu|}+\sqrt{|\nu+1|}\right), \tag{6}$$

and, for $-1 < \nu < 0$,

$$h(\nu) = \frac{2}{\pi}\sqrt{\frac{-\nu}{\nu+1}}\,\mathrm{tg}^{-1}\sqrt{\frac{1+\nu}{-\nu}}. \tag{7}$$

When $\nu_0 = -\frac{2}{3}$, we have from eq. (7) that

$$h(-\tfrac{2}{3}) = \frac{2}{\pi}\sqrt{2}\,\mathrm{tg}^{-1}\frac{1}{\sqrt{2}}. \tag{8}$$

It is convenient to introduce the variable z which runs between 0 and 1 as ν covers the interval 0 to ∞. We define

$$z = \frac{1}{\sqrt{1+\nu}}, \qquad \nu > 0. \tag{9}$$

The variable x is also introduced, which runs between 0 and 1 as ν covers the interval -1 to $-\infty$:

$$x = (-\nu)^{-\frac{1}{2}}, \qquad \nu < -1. \tag{10}$$

For real phase shifts, we obtain the formula

$$\mathrm{ctg}\,\delta_l^I = \frac{1}{\sqrt{1-z^2}}\left[\frac{1}{a_l^I} + L\left(\frac{1}{z^2}-1, -\frac{2}{3}\right) + N_l^I\left(\frac{1}{z^2}-1, -\frac{2}{3}\right) - \right. \tag{11}$$
$$\left. - \left(\frac{1}{z^2}-\frac{1}{3}\right)\sum_{n=0}^{l-1}\frac{1}{n!}\left(\frac{1}{z^2}-1\right)^{n-l} g_l^{(n)I}(0)\right],$$

where

$$h\left(\frac{1}{z^2}-1\right) = \frac{2}{\pi}\sqrt{1-z^2}\ln\left|\frac{1+\sqrt{1-z^2}}{z}\right|, \tag{12}$$

and

$$N_l^I\left(\frac{1}{z^2}-1, -\frac{2}{3}\right) = -\left(1-\frac{1}{3}z^2\right)\frac{2}{\pi}P\int_0^1 \frac{\mathrm{d}x\, x K_l^I(-1/x^2)}{[z^2+x^2(1-z^2)](1-\frac{2}{3}x^2)}. \tag{13}$$

In the above equations, we have chosen the subtraction point at $\nu_0 = -\frac{2}{3}$.

The function $K_l^I(-1/x^2)$ is given by

$$K_l^I(-1/x^2) = \frac{I_l^I(-1/x^2)}{(E_l^I(-1/x^2))^2 + (I_l^I(-1/x^2))^2}, \tag{14}$$

where $\operatorname{Im} A_l^I(\nu) = I_l^I(-1/x^2)$ and $\operatorname{Re} A_l^I(\nu) = E_l^I(-1/x^2)$ for $\nu < -1$. The absorptive partial wave amplitude on the left cut will be determined by crossing symmetry in terms of the imaginary parts of the S and P-wave amplitudes on the right cut.

In the physical region

$$\operatorname{Im} A_l^I(\nu) = \frac{(1-z^2)^{-\frac{1}{2}}}{1+\operatorname{ctg}^2\delta_l^I}, \qquad \text{for } \nu > 0, \tag{15}$$

and we obtain up to and including P-waves:

$$\operatorname{Im} A_l^I(-1/x^2) = -2x^2 \int_x^1 \frac{\mathrm{d}z}{z^3} P_l\left(1-2\frac{x^2}{z^2}\right)\left\{\alpha_{I0} \operatorname{Im} A_0^0\left(\frac{1}{z^2}-1\right) + \right. \tag{16}$$

$$\left. + \alpha_{I'} \operatorname{Im} A_0^2\left(\frac{1}{z^2}-1\right) + 3\left(1-2\frac{(1/x^2)-1}{(1/z^2)-1}\right)\alpha_{I1} \operatorname{Im} A_1^1\left(\frac{1}{z^2}-1\right)\right\},$$

where the matrix $\alpha_{II'}$ is given by

$$\alpha_{II'} = \begin{pmatrix} \frac{2}{3} & 2 & \frac{10}{3} \\ \frac{2}{3} & 1 & -\frac{5}{3} \\ \frac{2}{3} & -1 & \frac{1}{3} \end{pmatrix}. \tag{17}$$

After having obtained solutions for the S and P-waves, we can check *a posteriori* that the higher partial waves do not contribute significantly to (16) within the range of convergence of the Legendre polynomial expansions.

The question arises whether the absorptive amplitude obtained from the crossing eq. (16) is consistent with the absorptive amplitude given by the defining eq. (1) in the limit as $-\nu = \omega \to \infty$. The structure of the *inverse* amplitude equations is such that we do not encounter divergence difficulties when calculating $A_l^{-1}(\nu)$. Inspection shows that in the limit as $\omega \to \infty$, (16) gives the asymptotic values

$$\operatorname{Im} A_l^I(\omega) \sim \begin{pmatrix} 12 \\ 6 \\ -6 \end{pmatrix} \int_0^\omega \frac{\mathrm{d}\nu' \operatorname{Im} A_1^1(\nu')}{\nu'} = C_l^I - 1/\log\omega, \tag{18}$$

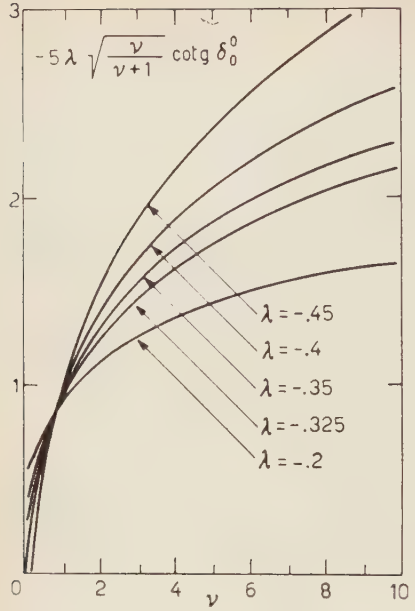

Fig. 1. – The cotangent of δ_0^0, multiplied by $(-5\lambda)\sqrt{\nu/(\nu+1)}$, as a function of $\nu=q^2/\mu^2$, for different values of λ. Note that ctg δ_0^0 for $\lambda=-.45$ becomes negative near $\nu=0$.

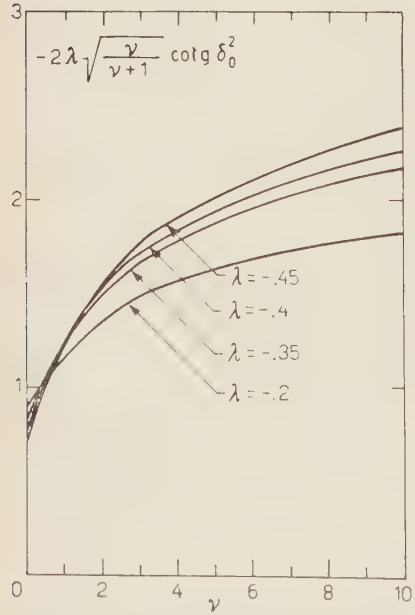

Fig. 2. – The cotangent of δ_0^2, multiplied by $(-2\lambda)\sqrt{\nu/(\nu+1)}$ for different values of λ.

where C_l^I are certain non-vanishing constants. It is clear that the absorptive amplitude obtained from the defining eq. (1) behaves as $1/(\log\omega)^2$ as $\omega\to\infty$. Thus the asymptotic behaviour of the crossing equation on the left cut is not quite the same as the one inferred from analyticity. This is not surprising as the crossing eq. (16) is not reliable in the limit as $|\nu|\to\infty$ in view of the

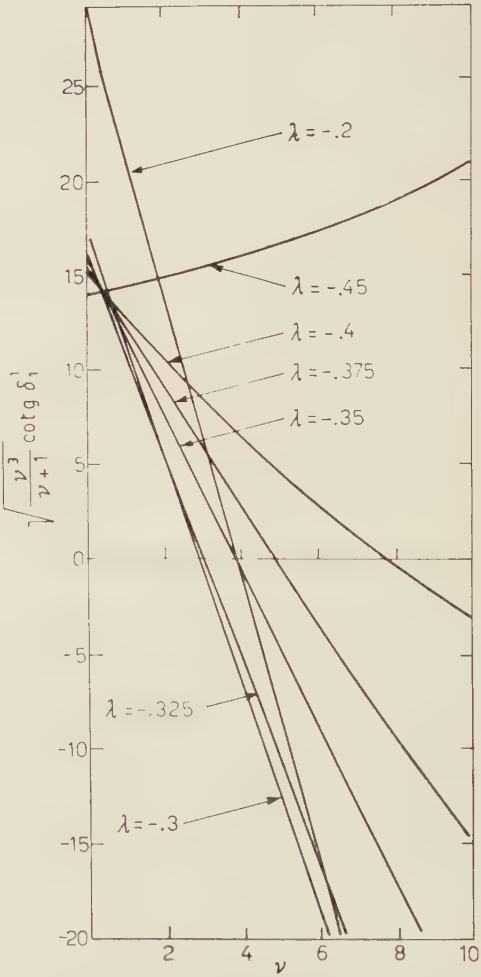

Fig. 3. – The cotangent of δ_1^1, multiplied by $\sqrt{\nu^3/(\nu+1)}$ for different values of λ.

fact that we have only taken into account a part of the double spectral function in the crossing equation. If the total absorptive amplitude used in the crossing equation is determined by the Mandelstam representation with subtracted S and P-waves, it becomes apparent that contributions associated with the double spectral functions include terms which cancel the constant part of the asymptotic limit in (18), and the asymptotic behaviour becomes consistent with analyticity and unitarity to all energies. In our present work analyticity and crossing symmetry are consistent in the low-energy range in which our approximations are valid. It is expected that the $1/(\log\,\omega)^2$ asymptotic behaviour of the absorptive amplitude provided by analyticity is the correct behaviour, because this implies a $1/\log\nu$ asymptotic behaviour as $\nu\to\infty$ for the real part of the amplitude, which would be consistent with unitarity. In the machine calculation of $(A_l^I(\nu))^{-1}$ the absorptive part $\mathrm{Im}\,A_l^I(\nu)$ on the left cut was set equal to zero for $\nu<-625$ in each cycle of the iterated equations (for the solutions described in Fig. 1, 2 and 3), and the results were compared with a calculation in which $\mathrm{Im}\,A_l^I(\nu)$ was set equal to zero for $\nu<-11$. It was found that the two sets of results differed only by a few percent. From this follows the important consequence: the calculation of $(A_l^I(\nu))^{-1}$ in the low-energy region is completely independent of $\mathrm{Im}\,A_l^I(\nu)$ for $\nu\leqslant -11$.

3. – Approximate crossing symmetry conditions.

Let us consider how many parameters enter the coupled S and P-wave equations after higher partial waves have been neglected. CHEW and MANDELSTAM [3] have shown that

$$a_0^I\approx\begin{pmatrix}-5\\-2\end{pmatrix}\lambda\,, \tag{19}$$

is a consistent approximation for the two S-wave subtraction constants in the reduced problem. In addition to λ, we have a subtraction constant a_1 in the P-wave dispersion relations, and also a constant ξ_1 generated by the P-wave threshold behaviour. We shall find that the first order derivative conditions at the symmetry point $\nu=-\frac{2}{3}$ determine the two parameters a_1 and ξ_1. Thus we have a solution to the pion-pion scattering problem in the low-energy region, containing a single pion-pion coupling constant and no further parameters.

CHEW and MANDELSTAM [3] have deduced the following exact first and second derivative crossing conditions at $\nu=-\frac{2}{3}$:

$$\frac{\partial A^0}{\partial\nu}=2\,\frac{\partial}{\partial\cos\theta}\left(\frac{A^1}{\nu}\right), \tag{20}$$

$$\frac{\partial A^2}{\partial\nu}=-\frac{\partial}{\partial\cos\theta}\left(\frac{A^1}{\nu}\right), \tag{21}$$

and

$$\frac{\partial^2 A^0}{\partial \nu^2} - \frac{5}{2}\frac{\partial^2 A^2}{\partial \nu^2} = -\frac{9}{2}\frac{\partial^2}{\partial \cos\theta\, \partial \nu}\left(\frac{A^1}{\nu}\right), \tag{22}$$

$$\frac{\partial^2}{\partial \cos^2\theta}\left(\frac{A^0}{\nu}\right) - \frac{5}{2}\frac{\partial^2}{\partial \cos^2\theta}\left(\frac{A^2}{\nu}\right) = \frac{3}{2}\frac{\partial^2}{\partial \cos\theta\, \partial \nu}\left(\frac{A^1}{\nu}\right), \tag{23}$$

$$\frac{\partial^2}{\partial \cos^2\theta}\left(\frac{A^0}{\nu^2}\right) - 7\frac{\partial^2}{\partial \cos^2\theta}\left(\frac{A^2}{\nu^2}\right) = -\frac{\partial^2 A^0}{\partial \nu^2} + \frac{\partial^2 A^2}{\partial \nu^2}. \tag{24}$$

There exists an infinite number of such derivative conditions on the scattering amplitude, but the third and higher derivative conditions involve mainly the higher l values. As long as D and higher waves are small, we have to a good approximation from eq. (20) and (21) at $\nu = -\frac{2}{3}$:

$$a_1^1 = -\frac{1}{9}\frac{\partial A_0^0}{\partial \nu} = \frac{2}{9}\frac{\partial A_0^2}{\partial \nu}. \tag{25}$$

We shall discover that in order to satisfy the two independent conditions (25) the form of the left cut contributions to the two S-waves is important. We shall seek solutions with parameters a_1 and ξ_1 which satisfy the consistency requirements (25).

Unlike the first derivative conditions, the second derivative condition (22) is more sensitive to the D-wave, while it is evident that the second derivative conditions (23), (24) depend primarily on the D-wave amplitudes. However, CHEW and MANDELSTAM have shown that if the D-waves are small, then (22) may be corrected by means of (23) to provide the following *single* condition at $\nu = -\frac{2}{3}$:

$$\frac{\partial^2 A_0^0}{\partial \nu^2} - \frac{5}{2}\frac{\partial^2 A_0^2}{\partial \nu^2} = 27 a_1 + 18\frac{\partial A_1^1}{\partial \nu}. \tag{26}$$

The extent to which the condition (26) is satisfied is a test of the consistency of the theory, and we shall see that it does *not* impose further limitations on the values of λ that are acceptable.

4. – The iteration scheme.

We shall now develop the iteration scheme for solving the coupled S and P-wave equations. The iterated solution is required to satisfy

crossing symmetry, the first two derivative conditions and the second derivative condition at $\nu = -\frac{2}{3}$.

Let us denote by $J_l^I(z)$ the absorptive amplitude on the right cut. The $(n+1)$-th iterate of this function is determined by

$$(27)\quad J_0^{0(n+1)}(z) = \sqrt{1-z^2}\left[\left\{a_0^{-1} + L\left(\frac{1}{z^2}-1, -\frac{2}{3}\right) + N_0^{0(n)}\left(\frac{1}{z^2}-1, -\frac{2}{3}\right)\right\}^2 + (1-z^2)\right]^{-1},$$

$$(28)\quad J_0^{2(n+1)}(z) = \sqrt{1-z^2}\left[\left\{a_2^{-1} + L\left(\frac{1}{z^2}-1, -\frac{2}{3}\right) + N_0^{2(n)}\left(\frac{1}{z^2}-1, -\frac{2}{3}\right)\right\}^2 + (1-z^2)\right]^{-1},$$

$$(29)\quad J_1^{1(n+1)}(z) = \sqrt{1-z^2}\left[\left\{a_1^{-1} + L\left(\frac{1}{z^2}-1, -\frac{2}{3}\right) + N_1^{1(n)}\left(\frac{1}{z^2}-1, -\frac{2}{3}\right) - \left(\frac{1-\frac{1}{3}z^2}{1-z^2}\right)\xi_1\right\}^2 + (1-z^2)\right]^{-1}.$$

The n-th iterates of the absorptive S and P-waves on the left cut are found from the equations

$$(30)\quad I_0^{0(n)}(-1/x^2) = 2x^2\int_1^x \frac{dz}{z^3}\left[\frac{2}{3}J_0^{0(n)}(z) + \frac{10}{3}J_0^{2(n)}(z) + 6\left\{1 - 2\frac{z^2(1-x^2)}{x^2(1-z^2)}\right\}J_1^{1(n)}(z)\right],$$

$$(31)\quad I_0^{2(n)}(-1/x^2) = 2x^2\int_1^x \frac{dz}{z^3}\left[\frac{2}{3}J_0^{0(n)}(z) + \frac{1}{3}J_0^{2(n)}(z) - 3\left\{1 - 2\frac{z^2(1-x^2)}{x^2(1-z^2)}\right\}J_1^{1(n)}(z)\right],$$

$$(32)\quad I_1^{1(n)}(-1/x^2) = 2x^2\int_1^x \frac{dz}{z^3}\left[\frac{2}{3}J_0^{0(n)}(z) - \frac{5}{3}J_0^{2(n)}(z) + 3\left\{1 - 2\frac{z^2(1-x^2)}{x^2(1-z^2)}\right\}J_1^{1(n)}(z)\right]\left(1 - 2\frac{x^2}{z^2}\right).$$

We also require the real parts of the S and P-wave amplitudes on the left-cut. These are given by

$$(33)\quad E_0^{0(n+1)}(-1/x^2) = [a_0^{-1} + L(-1/x^2, -\tfrac{2}{3}) + N_0^{0(n)}(-1/x^2, -\tfrac{2}{3})]\cdot [\{a_0^{-1} + L(-1/x^2, -\tfrac{2}{3}) + N_0^{0(n)}(-1/x^2, -\tfrac{2}{3})\}^2 + (K_0^{0(n)}(-1/x^2))^2]^{-1},$$

$$(34)\quad E_0^{2(n+1)}(-1/x^2) = [a_2^{-1} + L(-1/x^2, -\tfrac{2}{3}) + N_0^{2(n)}(-1/x^2, -\tfrac{2}{3})]\cdot [\{a_2^{-1} + L(-1/x^2, -\tfrac{2}{3}) + N_0^{2(n)}(-1/x^2, -\tfrac{2}{3})\}^2 + (K_0^{2(n)}(-1/x^2))^2]^{-1},$$

$$(35)\qquad E_1^{1(n+1)}(-1/x^2) = [a_1^{-1} + L(-1/x^2, -\tfrac{2}{3}) + N_1^{1(n)}(-1/x^2, -\tfrac{2}{3}) - (1-\tfrac{2}{3}x^2)\xi_1]\cdot$$
$$\cdot[\{a_1^{-1} + L(-1/x^2, -\tfrac{2}{3}) + N_1^{1(n)}(-1/x^2, -\tfrac{2}{3}) - (1-\tfrac{2}{3}x^2)\xi_1\}^2 + \left(K_1^{1(n)}(-1/x^2)\right)^2]^{-1}.$$

With the aid of these formulas, we can now write the expressions which determine the $N_l^I(\nu)$ up to and including the n-th iterate

$$(36)\qquad N_0^{0(n)}\left(\frac{1}{z^2}-1\right) = -\frac{2}{\pi}\left(1-\frac{1}{3}z^2\right)\int_0^1 \frac{\mathrm{d}x\, x K_0^{0(n)}(-1/x^2)}{[z^2 + x^2(1-z^2)](1-\frac{2}{3}x^2)},$$

$$(37)\qquad N_0^{2(n)}\left(\frac{1}{z^2}-1\right) = -\frac{2}{\pi}\left(1-\frac{1}{3}z^2\right)\int_0^1 \frac{\mathrm{d}x\, x K_0^{2(n)}(-1/x^2)}{[z^2 + x^2(1-z^2)](1-\frac{2}{3}x^2)},$$

$$(38)\qquad N_1^{1(n)}\left(\frac{1}{z^2}-1\right) = -\frac{2}{\pi}\left(1-\frac{1}{3}z^2\right)\int_0^1 \frac{\mathrm{d}x\, x K_1^{1(n)}(-1/x^2)}{[z^2 + x^2(1-z^2)](1-\frac{2}{3}x^2)}.$$

The $N_l^I(-1/x^2)$ on the left cut are obtained from (36), (37) and (38) by replacing $(1/z^2)-1$ by $-1/x^2$. Finally, the S and P-wave phase shifts will be given in terms of the calculated L and N functions by

$$(39)\qquad \operatorname{ctg}\delta_0^{0,2} = \frac{1}{\sqrt{1-z^2}}\left|a_{0,2}^{-1} + L\left(\frac{1}{z^2}-1, -\frac{2}{3}\right) + N_0^{0,2}\left(\frac{1}{z^2}-1, -\frac{2}{3}\right)\right|,$$

and

$$(40)\qquad \operatorname{ctg}\delta_1^1 = \frac{1}{\sqrt{1-z^2}}\left|a_1^{-1} + L\left(\frac{1}{z^2}-1, -\frac{2}{3}\right) - \right.$$
$$\left. - N_1^1\left(\frac{1}{z^2}-1, -\frac{2}{3}\right) - \xi_1\left\{1 - \frac{2}{3}\left(\frac{z^2}{1-z^2}\right)\right\}\right].$$

It is interesting to note that a solution of these equations exists for $\lambda = 0$ and $a_1 = 0$ for which both the S and P-wave amplitudes vanish exactly.

Starting from given values of ξ_1, a_1 and λ, the iteration scheme is used to determine the unknown functions. By varying ξ_1 and a_1 in a systematic manner until eq. (25) are satisfied, these constants were determined. Each solution was checked for consistency by inspecting whether eq. (26) was satisfied. If the calculated amplitudes are indeed to be compatible with the original Mandelstam representation, no complex poles may occur in $A_l^I(\nu)$. It has been verified that no such complex poles exist in the solutions presented in this paper.

5. – Numerical calculations and results.

The system of eq. (27)–(40) have been programmed for numerical solution on the CERN Ferranti « Mercury » computer. ([10]) In the range of integration the z variable is represented by 60 and the x variable by 30 pivotal points. The iterative cycle is entered at first by calculating the functions J_l^I with N_l^I set equal to zero. The subsequent convergence depends on the values of λ, ξ_1 and a_1. Usually from five to ten cycles determine the phase shifts to sufficient accuracy (better than 1%). As explained above, for each λ, the calculations are performed for a number of ξ_1, a_1; the final values of ξ_1 and a_1 being those for which the conditions (25) are satisfied. The calculated ξ_1 and a_1 are accurate to $(1 \div 2)\%$. In the solutions of interest a_1^{-1} and ξ_1 turn out to be of the same order of magnitude ~ -30. Reference to eq. (27)–(29) and eq. (33)–(35) shows that under these circumstances cancellation occurs in the calculations of E_l^I, J_l^I and especial care has been taken to preserve accuracy; at the same time the results become sensitive to the coupling constant λ.

Once a solution for one value of λ has been found, this solution is itself used as a trial function for a calculation with new values of λ, this device materially speeding convergence. In general, as might be expected in a method based on the *inverse* amplitude, convergence is most rapid for the larger values of λ. A typical calculation for one λ, a_1 and ξ_1 combination could be completed in 18 minutes of machine time.

For a limited range of negative λ (solutions with negative λ correspond to attractive S-wave forces) the numerical calculations have shown clearly that satisfactory solutions exist. For each negative λ with $|\lambda| \leqslant 0.5$ a single *negative* value of ξ_1 can be found such that conditions (25) are satisfied. These solutions satisfy the consistency condition (26) and therefore represent acceptable physical solutions. For values of $|\lambda| \geqslant 0.45$ a bound state in the $I = 0$ state occurs ($\operatorname{ctg} \delta_0^0$ becomes negative near zero energy), but for smaller values of $|\lambda|$ this disappears and at the same time the P-wave phase shifts become large. For each negative λ with $\lambda| \leqslant 0.5$ solutions for a single *positive* value of ξ_1 and a corresponding single negative value of a_1 are found that also satisfy conditions (25). These solutions give rise to a very small P-wave phase shift and correspond to those computed by CHEW, MANDELSTAM and NOYES ([2]). However, these solutions do not satisfy the condition (26) and do not therefore represent cases of physical interest.

Solutions of the coupled equations corresponding to repulsive S-wave forces (*i.e.* to positive λ) have not been found. For $\lambda > 0.25$ solutions, with given a_1 and ξ_1, cannot be found, that satisfy conditions (25). On the other hand,

([10]) B. H. BRANSDEN and J. W. MOFFAT: *Phys. Rev. Lett.*, **6**, 708 (1961).

for $\lambda < 0.25$ the iterative procedure adopted becomes *unstable*, and it has not been possible to determine whether a solution exists.

For the range of λ, $-0.45 \leqslant \lambda \leqslant -0.2$, the calculated values of a_1 and ξ_1 are shown in Table I, and the calculated values of

$$(-5\lambda)\sqrt{\frac{\nu}{\nu+1}}\operatorname{ctg}\delta_0^0, \quad (-2\lambda)\sqrt{\frac{\nu}{\nu+1}}\operatorname{ctg}\delta_0^2 \quad \text{and} \quad \sqrt{\frac{\nu^3}{\nu+1}}\operatorname{ctg}\delta_1^1,$$

TABLE I. – *Calculated values of* a_1^1, ξ, *resonance parameters* ν_R, Γ *and S-wave scattering lengths* α_0, α_2.

λ	a_1^1	ξ_1^1	ν_R	Γ	α_0	α_2
−0.45	−0.0529	−21.2	—	—	−68.0	1.24
−0.40	−0.0442	−22.5	7.7	6.0	33.7	1.05
−0.375	−0.0413	−22.9	4.8(5)	2.5	16.4	0.96
−0.35	−0.0397	−23.4	3.8	1.7(5)	10.8	0.87
−0.325	−0.0373	−24.1	3.0	1.0	7.5	0.79
−0.30	−0.0357	−25.5	2.9(5)	0.8	5.6	0.7
−0.20	−0.0217	−42.4	3.9	0.6	2.0	0.4

are displayed in Fig. 1, 2 and 3. For $|\lambda| < 0.45$, $\operatorname{ctg}\delta_1^1$ passes through zero from positive to negative values, so that the P-wave partial cross-section exhibits a resonance. The positions ν_R and the widths Γ of the P-wave resonant solutions are shown as a function of λ in Table I (*). The S-wave phase shifts for $I = 0$ are larger than those for $I = 2$ at low energies. The corresponding S-wave scattering lengths α_0 and α_2 are shown in Table I. To illustrate the behaviour of the amplitudes on the left cut, $I_l^I(-1/x^2)$ and $K_l^I(-1/x^2)$ are shown in Fig. 4 and 5. In view of the weighting of the absorptive amplitude on the left cut in $\operatorname{Im}(A_l^{-1}(\nu))$, the calculation of the inverse amplitude $A_l^{-1}(\nu)$ is insensitive, in the low-energy region $0 < \nu \lesssim 10$, to the behaviour of $\operatorname{Im} A_l^I(\nu)$ on the left cut for large values of $|\nu|$. In Fig. 5, it is noticed that the imaginary parts of the inverse amplitude have become *small* and constant when $\nu \sim -20$. The $\operatorname{Re} A_l^I(\nu)$ obtained from our inverse amplitude solution (1) was compared

(*) The width Γ quoted in Table I is the total width at half maximum, and is related to the reduced width γ by the formula $\Gamma = \gamma\sqrt{\nu_R^3/(\nu_R+1)}$.

with $\mathrm{Re}\, A_l^I(\nu)$ derived from the original partial-wave dispersion relations eq. (13) in I, where the integral on the left cut in eq. (13) was cut off at $\delta = -20$. A satisfactory quantitative fit was found in the low-energy region $0 < \nu \leqslant 10$ for the solutions described as functions of λ in Fig. 1, 2 and 3.

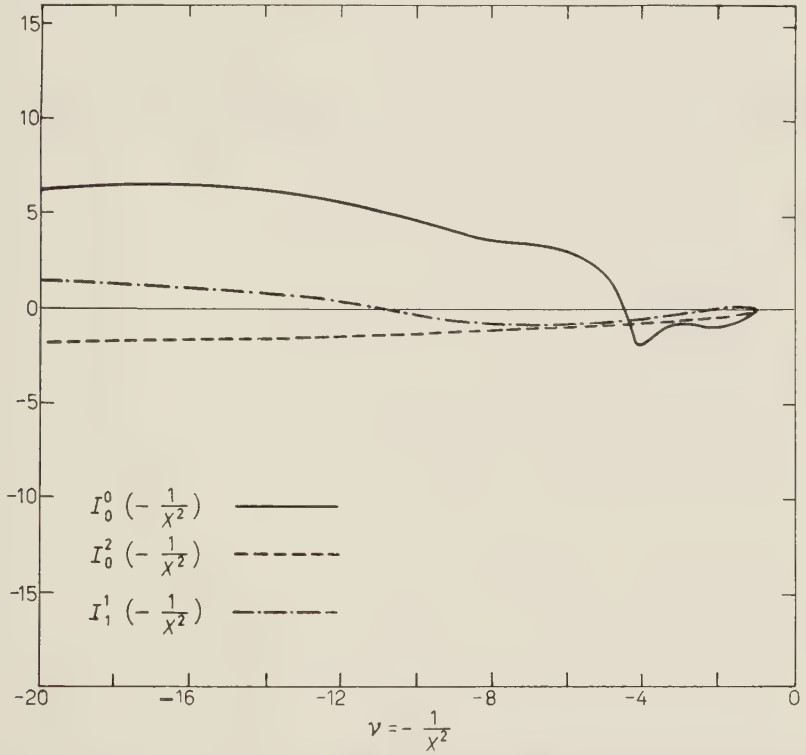

Fig. 4. – Absorptive amplitude $I_l^I(-1/x^2)$ on the left cut obtained from crossing symmetry as a function of $\nu = -1/x^2$ for $\lambda = -0.35$.

From Table I, we see that as $|\lambda|$ decreases in value the S-wave scattering lengths continually decrease in magnitude. This is consistent with the fact that the s-wave phase shifts tend to zero as $\lambda \to 0$. The resonance positions ν_R move towards zero energy until $|\lambda| = 0.325$ after which the ν_R values *increase* again, and the resonance positions move to higher energy values. At $|\lambda| = 0.2$ it is observed that $\nu_R \sim 4$ (in the total barycentric system energy $t_R \sim 20\mu^2$) and $\Gamma = 0.6$, while $\alpha_0 = 2$ and $\alpha_2 = 0.4$. This value of the resonance width Γ would appear to give a sufficiently sharp P-wave resonance to agree with the calculations on nucleon electromagnetic structure ([4,11,12]).

([11]) S. C. Frautschi: *Phys. Rev. Lett.*, **5**, 159 (1960).
([12]) J. Bowcock, W. N. Cottingham and D. Lurié: *Phys. Rev. Lett.*, **5**, 386 (1960).

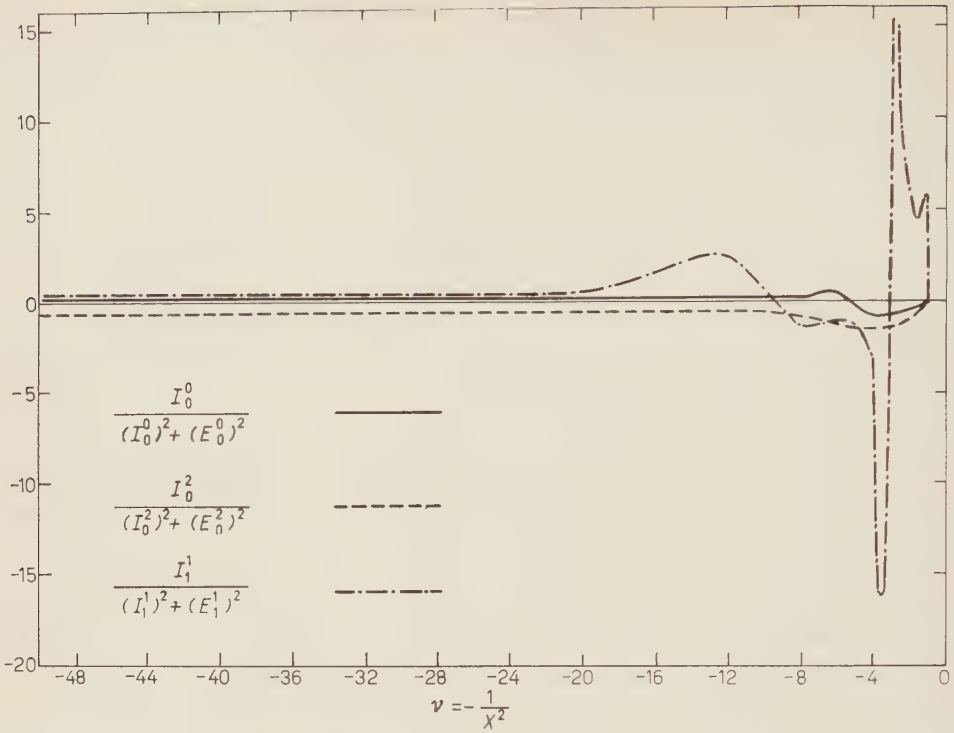

Fig. 5. – The imaginary part of the inverse amplitude $\mathrm{Im}\,[(A_l^I)^{-1}]$ on the left cut as a function of $\nu=-1/\lambda^2$ for $\lambda=-0.35$.

* * *

The authors wish to record their gratitude to CERN for its hospitality while this work was in progress, and to thank the staff of the CERN Mercury computer for their co-operation.

RIASSUNTO (*)

Presentiamo un metodo per risolvere numericamente le equazioni accoppiate delle onde S e P per lo scattering pione-pione, dedotte da Moffat dalla analiticità, dalla simmetria incrociata e dall'unitarietà sulla base della rappresentazione di Mandelstam. Mostriamo che oltre la costante di accoppiamento pione-pione, nessun ulteriore parametro entra nella teoria a bassa energia. Per un campo della costante di accoppiamento λ, prendendo valori negativi $|\lambda| < 0.45$, esistono soluzioni che soddisfano alla simmetria incrociata. Queste soluzioni sono caratterizzate dalla esistenza di una risonanza di bassa energia nell'onda P la cui posizione ed ampiezza sono completamente da λ. I corrispondenti spostamenti di fase dell'onda P mostrano che lo scattering nello stato di spin isotopico $T=0$ è grande a bassa energia.

(*) *Traduzione a cura della Redazione.*

IL NUOVO CIMENTO Vol. XXI, N. 3 1° Agosto 1961

A Natural Boundary of the Scattering Amplitude on an Unphysical Sheet.

P. G. O. Freund and R. Karplus (*)

Institute for Theoretical Physics, University of Vienna - Vienna

(ricevuto il 5 Giugno 1961)

Summary. — The scattering amplitude has a two-sheeted branch point at zero kinetic energy. It is shown that the amplitude on the second (unphysical) sheet has a natural boundary that terminates at zero total energy.

The extension of two-particle scattering amplitudes from the physical domain of their energy and angular dependence to complex and unphysical real values of these variables has been extensively studied and described [1]. During the last year it has become possible to analytically continue elastic scattering amplitudes completely around the branch point they possess at zero kinetic energy into a second (so-called unphysical) sheet of their Riemann surface [2-5]. The condition on the scattering amplitudes that allows such an extension is the one that the S-matrix be unitary. From this condition one obtains an

(*) Fulbright Research Scholar and John Simon Guggenheim Fellow on sabbatical leave from the University of California, Berkeley.

(1) See, for instance, N. N. Bogoliubov and D. V. Shirkov: *Introduction to the Theory of Quantized Fields* (Moscow, 1957), chap. IX.

(2) J. Gunson and J. G. Taylor: *Phys. Rev.*, **119**, 1121 (1961); **121**, 343 (1961)

(3) R. Oehme: *Phys. Rev.*, **121**, 1810 (1961) and preprint EFINS 61-5 (University of Chicago).

(4) R. Blankenbecler: *Proc. of the* 1960 *Rochester Conf.* (New York, 1961), p. 247. R. Blankenbecler, M. L. Goldberger, S. W. McDowell and S. B. Treiman: *Singularities of scattering amplitudes on unphysical sheets and their interpretation* (Princeton, 1961). preprint.

(5) W. Zimmermann: *Nuovo Cimento*, **21**, 249 (1961).

integral equation for the angular dependence of the function on the second sheet when its behavior on the first sheet is known.

This extension of the domain of definition of the scattering amplitude raises the question as to whether further extension around branchpoints on the second sheet is possible. The question is not a trivial one, because a branch point need not be an isolated singularity, but may be the endpoint of a natural boundary for the function. We wish to show that the negative real axis of the variable s (the square of the mass of the two-particle system) on the second sheet mentioned above is indeed such a natural boundary for all scattering angles θ. Analytic continuation around the branchpoint $s=0$ on the second sheet is therefore not possible. For our demonstration we consider the scattering of identical particles that are created in pairs. We shall assume a Mandelstam [6] representation for the amplitude on the physical sheet, but can relax this condition if we confine our attention to a region near the origin of the complex $(s, \cos\theta)$-space. For the special case of physical angles the scattering amplitude is analytic on the second sheet with cuts on the real axis. The usual kind of dispersion relation therefore exists for it, but the spectral function on the left-hand cut ($s \leqslant 0$) must contain the complication associated with the natural boundary. Since our remarks merely state corollaries of the results of others [2,4,5], we refer the reader to the cited references for algebraic details of the calculations and derivations.

We begin with a statement of the integral equation in the notation of ZIMMERMANN [5]. The scattering amplitude for the two particles of mass m is $\Phi(s, \cos\theta)$ on the physical sheet, $\Phi^{(2)}(s, \cos\theta)$ on the unphysical sheet joined to the physical sheet along the real s-axis in the region of elastic scattering $4m^2 < s < 16m^2$. Then the unitarity of the S-matrix leads to the equation

$$(1)\qquad \Phi^{(2)}(S, \cos\theta) = \Phi(s, \cos\theta) - \frac{i}{4}\left(\frac{s-4m^2}{s}\right)^{\frac{1}{2}} \cdot \int_{-1}^{1} \mathrm{d}\cos\theta' \int_{-1}^{+1} \mathrm{d}\cos\theta'' \, \frac{\Phi(s, \cos\theta')\Phi^{(2)}(s, \cos\theta'')}{\sqrt{-k(\cos\theta, \cos\theta', \cos\theta'')}} \, \theta(-k(\cos\theta, \cos\theta', \cos\theta'')) ,$$

where the function $k(x, x', x'')$ is

$$(2)\qquad k(x, x', x'') = -1 + x^2 + x'^2 + x''^2 - 2xx'x'' .$$

The singularities of $\Phi(s, \cos\theta)$ are most easily stated in terms of the inva-

---

[6] S. MANDELSTAM: *Phys. Rev.*, **112**, 1344 (1958).

riants

$$\left|\begin{array}{l} s \\ t = -\tfrac{1}{2}(s-4m^2)(1-\cos\theta) \\ u = -\tfrac{1}{2}(s-4m^2)(1+\cos\theta)\,, \end{array}\right. \tag{3}$$

which are related by

$$s+t+u = 4m^2\,. \tag{4}$$

The scattering amplitude is a symmetrical function of s, t, and u. In the Mandelstam representation, it has an isolated branch point at $s=4m^2$ and a branch cut starting at $s=16m^2$. (As yet, no properties of the spectral function in this cut are known; it seems plausible to expect, however, that the function is analytic except for a sequence of isolated branch points at $s=4m^2n^2$, $n=2, 3, \ldots$.) For t or u equal to these values, the function has the same behavior, of course. We therefore encounter three isolated branch points when

$$s=4m^2\,, \quad (s-4m^2)(1-\cos\theta) = -8m^2\,, \quad (s-4m^2)(1+\cos\theta) = -8m^2. \tag{5}$$

The presence of the other singularities does not affect the argument, so we shall ignore them for the time being.

To find the singularities of $\Phi^{(2)}(s, \cos\theta)$ we use eq. (1). It has been shown [2,4,5] that this amplitude has, in addition to the singularities of $\Phi(s, \cos\theta)$, singularities at the points

$$\cos\theta = \cos n \cos^{-1}\left[\pm\left(1+\frac{8m^2}{s-4m^2}\right)\right], \qquad n=2, 3, \ldots, \tag{6}$$

as long as s does not lie on the negative real axis. For fixed complex s these points lie on an exponential spiral in the complex $\cos\theta$-plane. As s approaches the negative real axis, the rate of growth of the spiral becomes smaller, but it always lies outside the points $\cos\theta = \pm 1$. In the limit $\operatorname{Im} s = 0$, $\operatorname{Re} s < 0$, the spiral degenerates into the real line segment determined by $\operatorname{Im}\theta = 0$. Since there is an infinite number of singular points of the form (6) on the spiral, one may expect a quite singular behavior for the function $\Phi^{(2)}(s, \cos\theta)$ on the negative real axis.

To exhibit this behavior more closely, we solve eq. (6) for s at a fixed complex value of θ; or, to simplify the discussion, we may introduce a new variable σ to replace s,

$$\sigma = 1+\frac{8m^2}{s-4m^2}\,. \tag{7}$$

In the complex σ-plane the singularities then occur at

$$\sigma = \sigma_{n,l} = \pm \cos\left|\frac{\theta}{n} + 2\pi\frac{l}{n}\right|, \qquad \begin{cases} n = 1, 2, 3, \ldots, \\ l = 0, 1, \ldots, n-1, \end{cases} \tag{8}$$

where the multiplicity described by the index l arises from the multi-valued nature of the inverse trigonometric function. For given n, these points lie on an ellipse with foci $\sigma = \pm 1$ and semi-major axis $\cosh\left((1/n)\,\mathrm{Im}\,\theta\right)$. For infinite n the ellipse degenerates to the straight line between the foci.

Now, the negative real axis in s is mapped by the transformation (7) into this real segment, $C = (-1 < \mathrm{Re}\,\sigma < 1,\ \mathrm{Im}\,\sigma = 0)$. We therefore wish to consider the analytic properties of $\Phi^{(2)}(s, \cos\theta)$ as σ approaches a point on C. It is clear that $\Phi^{(2)}(s, \cos\theta)$ may be analytically continued along a path that avoids the isolated singularities located according to eq. (8). As real values of σ are approached, however, the singularities lie closer and closer together, so that the radii of convergence of the successive Taylor series that are used to effect the continuation diminish to zero. In other words, there exists a $\sigma_{n,l}$ for each σ such that

$$|\sigma - \sigma_{n,l}| < |\sigma - \cos\varphi| \qquad \text{(all real } \varphi\text{)}. \tag{9}$$

Hence it is not possible to continue the function across the real axis. We conclude that the segment C is a natural boundary for the function. Equivalently, by eq. (7), the negative real s-axis is a natural boundary for $\Phi^{(2)}(s, \cos\theta)$.

We observe that this conclusion is independent of the value of θ as long as θ is complex. When θ becomes a real angle, the situation is somewhat different. All points $\sigma_{n,l}$ then lie on the segment C where they are everywhere densely distributed. If $\theta = 0$, for instance, the $\sigma_{n,l}$ are just equal to the cosines of all rational multiples of 2π (cf. eq. (8)). In this case, also, the line segment C, and hence the negative real axis in the s-plane, are a natural boundary of the function [7]. The function, however, has no complex singularities

[7] It may seem surprising that the partial wave amplitudes do not exhibit any trace of these singularities, that are present for all real values of θ. There are two comments to be made in this connection. First, the partial wave series does not converge on the negative real s-axis, so that the amplitude at a fixed angle can have properties different from those of any one partial wave. Second, the projection of the partial wave amplitude involves an integration that smoothes the function; the only singularities remaining are those at extremal values where $d\sigma_{n,l}/d\theta = 0$ which occur at $\sigma = \pm 1$ $(s = 0, -\infty)$. The integrand at the integration endpoints does not determine a singularity, because the integrand is periodic.

in the s-plane and can be represented by a dispersion relation of the form

$$(10) \qquad \Phi^{(2)}(s, \cos\theta) = \frac{1}{\pi}\int_{-\infty}^{0} \frac{\operatorname{Im}\Phi(s', \cos\theta)}{s' - s}\,\mathrm{d}s' + \frac{1}{\pi}\int_{4m^2}^{\infty} \frac{\operatorname{Im}\Phi(s', \cos\theta)}{s' - s}\,\mathrm{d}s'.$$

Also of interest is the case in which the momentum transfer rather than the scattering angle is held fixed. One obtains again eq. (8), but this time the angle θ depends on s (or σ). The locations of the singular points are therefore more complicated to find; nevertheless, it is possible to show that the segment C in the σ-plane is a natural boundary, because one encounters near it singularities densely distributed in the sense of eq. (9).

The higher singularities of $\Phi(s, \cos\theta)$, which we ignored earlier, will complicate the analytic properties of $\Phi^{(2)}(s, \cos\theta)$ ([4,5]). To the extent to which the function Φ has natural boundaries, $\Phi^{(2)}$ will of course have them also. It was our principal point to show that even if Φ has only isolated singularities, $\Phi^{(2)}$ has a natural boundary on the negative real axis. This particular conclusion is not modified by the existence of additional singularities of $\Phi(s, \cos\theta)$. For physical angles, the dispersion relation (10) still holds, with a spectral function unaffected by the higher singularities for $-12m^2 < s' < 0$. Our result is therefore somewhat more general than the Mandelstam representation. For a section of the negative real axis near the origin it follows from the analytic properties of the scattering amplitude as a function of two variables (s and t) derived by Mandelstam from general field theoretical considerations ([8,9]).

* * *

We have enjoyed stimulating and informative discussions concerning the problems of analytic continuation with R. Oehme and K. Johnson. W. Zimmermann kindly sent us a preprint of his paper. One of us (R.K.) is grateful to Professor W. Thirring for the hospitality of the Institute for Theoretical Physics.

([8]) S. Mandelstam: *Nuovo Cimento*, **15**, 658 (1960).
([9]) Cf. Appendix to ref. ([5]).

RIASSUNTO (*)

Studiamo le soglie anomale delle ampiezze di reazione senza far ricorso allo sviluppo in onde parziali. Mostriamo che il comportamento delle ampiezze è del tutto analogo a quello delle proiezioni delle onde parziali anche se le serie di Legendre non convergono vicino alla soglia anomala.

(*) *Traduzione a cura della Redazione.*

IL NUOVO CIMENTO Vol. XXI, N. 3 1° Agosto 1961

On a Mathematical Problem Encountered in Quantum Field Theory.

R. Omnès

Service de Physique Mathématique,
Centre d'Etudes Nucléaires de Saclay - Gif-sur-Yvette (S. et O.)

(ricevuto il 5 Giugno 1961)

Summary. — We reduce the problem of determining a unitary analytic function whose discontinuity on a cut is known to the solution of a Fredholm equation. This method leads to much simpler and physically transparent results than the N/D method by Chew and Mandelstam. The connexion between the two methods is elucidated. The ambiguity in the solution is completely displayed. The resulting form gives insight in the structure of s^* matrix under inelastic threshold.

1. – When considering applications of dispersion theory and particularly of Mandelstam representation (1), one frequently meets the following problem:

A function $h(\nu)$ of the square of a momentum $\nu = q^2$ is known to be analytic in the complex ν-plane cut from 0 to ∞ and from $-\infty$ to $-\mu^2$. It has the property $h(\nu^*) = -h^*(\nu)$. On the upper lip of the right-hand cut, it is known to have the form $h(\nu) = \exp[i\,\delta(\nu)]\sin\delta(\nu)$, where $\delta(\nu)$ is a real argument. $h(\nu) \to 0$ when $\nu \to 0$ and $|\nu| \to \infty$. The value of $h(\nu+i\varepsilon)+h(\nu-i\varepsilon)$ is a given function $i\,\Delta h(\nu)$ on the left-hand cut. The problem is to determine $h(\nu)$ in the whole complex plane from the given real function $\Delta h(\nu)$.

This problem is usually solved using the so-called N/D method due to Chew and Mandelstam (2). We want to present here another method which, in our opinion, has the following advantages:

(1) G. F. Chew and S. Mandelstam: *Phys. Rev.*, **119**, 467, (1960); UCRL 9126; W. Frazer and J. Fulco: *Phys. Rev. Lett.*, 2, 364 (1959); *Phys. Rev.*, **117**, 1609 (1960). For general reference, see G. F. Chew in *Cours de l'Ecole des Houches* (Paris, 1961).

(2) See for instance G. F. Chew in *Les Houches Lectures.*

a) it leads to simpler equations, both from the analytical and the computational point of view;

b) the physical meaning of the functions which we use is more transparent: in particular it leads to a simple interpretation of the D function;

c) it is well suited to a low-energy limit and a transition to potential scattering;

d) it gives some interesting information on the structure of s-matrix elements.

Its only drawback is to completely neglect the inelasticity parameter $r(\nu) = \sigma_i/\sigma_{\text{elas.}}$ which is assumed to be 1 for every value of ν [3].

2. – Let us first derive some well-known properties of the function

$$s(\nu) = 1 + 2i\,h(\nu)\,. \tag{1}$$

From the properties of $h(\nu)$, one immediately derives:

a) $s(\nu)$ is an analytic function of ν in the complex ν-plane cut from 0 to ∞ and from $-\infty$ to $-\mu^2$ along the real axis.

b) One has the symmetry property

$$s(\nu^*) = s^*(\nu)\,. \tag{2}$$

c) On the upper lip of the right-hand cut, one has the unitary property

$$|s(\nu)| = 1 \tag{3}$$

and we define $\delta(\nu)$:

$$s(\nu) = \exp\,[2i\,\delta(\nu)]\,. \tag{4}$$

d) One has, on the left-hand cut

$$s(\nu + i\varepsilon) + s(\nu - i\varepsilon) = 2\big(1 - \Delta h(\nu)\big)\,. \tag{5}$$

e) $$s(\nu) \to 1 \qquad \text{when} \qquad |\nu| \to \infty\,.$$

It is possible to continue analytically $s(\nu)$ through the right-hand cut by using a variant of the Schwarz's reflexion principle. The relation

$$s(\nu^*) = [s^*(\nu)]^{-1} \tag{6}$$

(3) For the use of this parameter, see preceding reference.

defines $s(\nu)$ in another Riemann sheet where $s(\nu)$ has again a cut running from $-\infty$ to $-\mu^2$. As operation (6) is reflexive, one sees that passing twice through the right-hand cut without cutting the left-hand cut one goes back to the initial « physical » sheet. The only possible singularities of $s(\nu)$ in the second Riemann sheet are poles symmetrical of the zeros of $s(\nu)$ with respect to the real axis.

These properties are made clearer if one uses the variable $q = \sqrt{\nu}$. Thus:

a) $s(q)$ is a meromorphic function in the complex q-plane cut along the imaginary axis from $-i\infty$ to $-i\mu$ and from $i\mu$ to $i\infty$: it is analytic in the upper half of the complex plane C_+ and may have poles in the lower half of the complex C_-;

b) one has the two reflexion properties corresponding respectively to (2) and (6)

$$s(-q^*) = s^*(q)\,, \tag{7}$$

$$s(q^*) = s^{*-1}(q)\,, \tag{8}$$

whence $s(q)\,s(-q) = 1$. On the real axis $s(q)$ is unitary

$$s(q) = \exp\left[2i\,\delta(q)\right], \tag{9}$$

where $\delta(q) = \delta(\nu)$ (resp. $-\delta(\nu)$) for $q > 0$ (resp < 0). $\delta(q)$ is necessarily a continuous function and even an analytic function in a neighbourhood of the real axis.

c) On the upper cut, one has

$$s(q) + s(-q^*) = 2\left(1 - \Delta h(q^2)\right) \qquad \text{for } q = ik + \varepsilon,\ k > 0. \tag{10}$$

d) $s(q) \to 1$ when $|q| \to \infty$ or zero. Thus $\delta(\nu)$ is equal to zero modulo π for $q = 0$ and ∞; we shall choose a determination of $\delta(q)$ such that

$$\delta(\infty) = 0\,, \qquad \delta(0) = -n\,\pi \tag{11}$$

n being an integer.

3. – Assuming $s(q)$ to exist let us define a function $f(q)$ with the following properties:

a) $f(q)$ is analytic in the lower half-plane C_- where it has no zero.

b) Reflextion property:

$$f(-q^*) = f^*(q)\,. \tag{12}$$

c)

$$f(q) \to 1 \qquad \text{when} \qquad |q| \to \infty \qquad \text{in } C_- . \tag{13}$$

d) Along the real axis the phase of $f(q)$ is equal to $\delta(q)$.

We shall construct explicitly $f(q)$, thus proving its existence (4).

From *a*) and *c*) we deduce that $\log f(q)$ is an analytic function of q in C_- which tends to zero when $|q| \to \infty$. We can consider it as a function of $\nu = q^2$ in a plane cut along the positive real axis. Writing a Cauchy formula for $\log f(q)$ we get the dispersion relation

$$\log f(\nu) = \frac{1}{\pi} \int_0^\infty \frac{\operatorname{Im} \log f(\nu' + i\varepsilon)}{\nu' - \nu} \, \mathrm{d}\nu' ,$$

but, from assumption *d*)

$$\operatorname{Im} \log f(\nu' + i\varepsilon) = - \delta(\nu')$$

thus

$$f(\nu) = \exp \left[- \frac{1}{\pi} \int_0^\infty \frac{\delta(\nu') \, \mathrm{d}\nu'}{\nu' - \nu} \right] . \tag{14}$$

We can thus assert that $f(q)$ exists in C_-: (14) verifies *a*), *b*), *c*), *d*).

As $\delta(\nu)$ is a continuous function, $f(q)$ is continuous for ν real and positive. However, it can be singular near $q = 0$. As one easily verifies from (11) and a limited expansion of $\delta(\nu)$ in (14), the leading singularity is in q^{2n} for $n > 0$, and in $\log q$ for $n < 0$.

Let us now continue analytically $f(q)$ in the upper half-plane C_+. To do so, we shall define

$$f'(q) = s(q) f(-q) \tag{15}$$

for $\operatorname{Im} q > 0$. This defines an analytic function $f'(q)$ in C_+. Due the property *d*) of $f(q)$, $f'(q)$ and $f(q)$ coincide on the real axis which proves that $f(q)$ is an analytic function of q in the whole complex plane cut from $i\mu$ to $i\infty$. As the possible singularity of $f(q)$ for $q = 0$ is isolated by this continuation, this singularity can only be a pole of order $2n$ if $n > 0$ or a regular point if $n < 0$ (*).

Having thus proved the existence and properties of a function $f(q)$ when $s(q)$ exists, we shall now consider the problem in the opposite way, trying first to determine $f(q)$ in order to obtain $s(q)$.

(4) This deduction follows R. G. Newton: *Journ of Math. Phys.*, **1**, 319 (1960

(*) One easily shows, using (14) that there is no term in q^{-2n+1} in $f(q)$.

4. – Let us now use (15) as an ansatz for the solution of our problem. We shall define

$$s(q) = f(q)/f(-q)\,, \tag{16}$$

where $f(q)$ is analytic in the complex plane cut from $i\mu$ to $i\infty$ and has properties *a*), *b*) and *c*) of Section **3**. It may have a pole of finite even order at the origin, we shall call $2n$ the order of this pole. Thus in the neighbourhood of the origin one has

$$f(q) = \frac{A_{2n}}{q^{2n}} + \frac{A_{2n-2}}{q^{2n-2}} + \frac{A_{2n-3}}{q^{2n-3}} + \ldots + 0(1)\,, \tag{17}$$

where one sees from (12) that the constants $A_2 \ldots A_{2n}$ are real numbers. and $A_1 A_3$ are pure immaginary. On the cut of $f(q)$, one has

$$f(ik+\varepsilon) + f(ik-\varepsilon) = 2[1 - \Delta h(-k^2)]\, f(-ik)\,. \tag{18}$$

One can write a Cauchy formula for the function

$$F(q) = \left[f(q) - 1 - \sum A_p (q)^{-p}\right](iq+\mu)^{\frac{1}{2}}$$

thus getting

$$F(q) = -\frac{1}{\pi}\int_\mu^\infty \frac{1-\Delta h(-y^2)}{(y-\mu)^{-\frac{1}{2}}(iy-q)}\, f(-iy)\,\mathrm{d}y + \frac{1}{\pi}\int_\mu^\infty \frac{1+\sum A_p (iy)^{-p}}{(y-\mu)^{-\frac{1}{2}}(iy-q)}\,\mathrm{d}y\,. \tag{19}$$

In order to define $f(q)$, it is thus only necessary to know it between $-i\infty$ and $-i\mu$. Let us thus define

$$\Phi(x) = f(-ix) - 1 \qquad \text{for } x \geqslant \mu \tag{20}$$

(note that, from (12) $\Phi(x)$ is real). $\Phi(x)$ is thus defined through the Fredholm equation (*)

$$\Phi(x) = \frac{1}{\pi}\int_\mu^\infty \sqrt{\frac{y-\mu}{x+\mu}}\,\frac{\Delta h(-y^2)\,\mathrm{d}y}{x+y} + \sum A_p\left[\frac{1}{(ix)^p} + \psi_p(x)\right] - \\ - \frac{1}{\pi}\int_\mu^\infty \sqrt{\frac{y-\mu}{x+\mu}}\,\frac{1-\Delta h(-y^2)}{x+y}\,\Phi(y)\,\mathrm{d}y\,, \tag{21}$$

(*) Strictly speaking, this equation is not a Fredholm equation. However, it can be shown by a somewhat lengthy argument which will be published elsewhere that it has a unique solution in L^2.

and

$$\psi_p(x) = \frac{1}{\pi}\int_\mu^\infty \sqrt{\frac{y-\mu}{x+\mu}}\,\frac{\mathrm{d}y}{(iy)^p(x+y)}\,.$$

If a bound state exists in the theory it appears generally as a δ-function contribution to Δh. In fact, let us suppose that we impose to $s(q)$ the following supplementary condition: $s(q)$ has a pole of residue g^2 at $q = im$. Then $f(q)$ has a pole at im and (20) is replaced by

$$(20a)\qquad \Phi(x) = \frac{1}{\pi}\int_\mu^\infty \sqrt{\frac{y-\mu}{x+\mu}}\,\frac{\Delta h(-y^2)\,\mathrm{d}y}{x+y} + \sum A_p\left[\frac{1}{(ix^p)} + \psi_p(x)\right] +$$

$$+ \frac{g^2}{x+m}\sqrt{\frac{m-\mu}{x+\mu}}\,\Phi(-m) - \frac{1}{\pi}\int_\mu^\infty \sqrt{\frac{y-\mu}{x+\mu}}\,\frac{1-\Delta h(-y^2)}{x+y}\,\Phi(y)\,\mathrm{d}y\,,$$

for $x \geqslant \mu$.

$\Phi(-m)$ can be deduced from (20a) by inserting $x = m$. The case of several bound states is treated in the same way.

5. – Let us state our results:

Every solution $s(\gamma)$ of our problem may be written in the form (16) where $f(q)$ is defined by eq. (19) and the weight function $f(-ik) = \Phi(k)+1$ in (19) is a solution of the Fredholm eq. (21). $F(q)$ verifies properties a), b), c), d) of Section **3** and is related to the phase-shift, up to a constant factor, by (14).

It is clear that this problem has infinitely many solutions depending on a set of arbitrary parameters $A_1 \ldots A_{2n}$ where n itself is arbitrary ([5]). The value of n fixes the variation of δ:

$$(22)\qquad \delta(\infty) - \delta(0) = n\pi\,.$$

We are thus sure that, for n given, δ passes at least n times through an odd multiple of $\pi/2$ (resonance).

Eq. (21) which is the center of this method is simpler than the equations obtained for the D function when writing ([2])

$$(23)\qquad h(q) = \frac{qN(\nu)}{D(\nu)}\,,$$

([5]) This result is to be compared with the results of CASTILLEJO, DALITZ and DYSON: *Phys. Rev.*, **101**, 453 (1956).

as one easily sees a particular set of N and D functions is

$$D(\nu) = f(-q)\,, \qquad \operatorname{Im} q > 0\,,$$

$$N(\nu) = \frac{1}{2iq}\,[f(q) - f(-q)]\,,$$

one verifies immediately that $D(\nu)$ admits only the cut from 0 to ∞ and $N(\nu)$ only the cut from $-\infty$ to $-\mu^2$. Finally, let us remark that the form (16) of $s(q)$ is well known in potential scattering where $f(q)$ is the Jost function ([6]). Thus expression (16) is well suited to the transition to potential scattering in the low energy limit. In particular, it allows *a priori* to study the existence of a potential as an approximation to low energy scattering by using Gel'fand and Levitan ([7]) equations.

Also we feel that the general structure property (16) of $s(q)$ may prove useful in theoretical considerations.

This method will be applied to the solution of Chew-Mandelstam equations.

* * *

I had illuminating discussions, on this and related subjects, with Mr. G. Mahoux.

([6]) R. Jost and A. Pais: *Phys. Rev.*, **82**, 840 (1951); R. Jost: *Helv. Phys. Acta*, **20**, 256 (1947).

([7]) I. M. Gel'fand and B. M. Levitan: *Dokl. Akad. Nauk SSSR*, **77**, 557 (1951); *Izv. Akad. Nauk SSSR*, **15**, 309 (1951).

RIASSUNTO (*)

Riduciamo il problema di determinare una funzione analitica unitaria la cui discontinuità su un taglio sia nota alla soluzione di un'equazione di Fredholm. Questo metodo conduce a risultati molto più semplici e fisicamente trasparenti che non il metodo N/D di Chew e Mandelstam. Si chiarisce la connessione fra i due metodi. L'ambiguità della soluzione è completamente chiarita. La forma risultante permette la comprensione della struttura della matrice s^* al disotto della soglia anelastica.

(*) *Traduzione a cura della Redazione.*

IL NUOVO CIMENTO Vol. XXI, N. 3 1° Agosto 1961

Anomalous Thresholds of Reaction Amplitudes.

P. G. O. Freund and R. Karplus (*)

Institute for Theoretical Physics, University of Vienna - Vienna

(ricevuto il 14 Giugno 1961)

Summary. — Anomalous thresholds of reaction amplitudes are studied without recourse to a partial wave expansion. It is shown that the behavior of the amplitudes is quite similar to that of the partial wave projections even though the Legendre series does not converge near the anomalous threshold.

The extension of two-particle reaction amplitudes and form factors from the physical domain of their energy and angular dependence to complex and unphysical real values of these arguments on a multi-sheeted Riemann surface has been extensively studied and described ([1-5]). In general the singularities of these functions on the physical sheet are associated with thresholds for the occurrence of new processes in the interaction. There is a class of singularities, however, so-called « anomalous thresholds » or « structure singularities », for which this did not appear to be the case ([6]). A closer investigation,

(*) Fulbright Research Scholar and John Simon Guggenheim Fellow on sabbatical leave from the University of California, Berkeley.

([1]) J. Gunson and J. G. Taylor: *Phys. Rev.*, **119**, 1121 (1961); **121**, 343 (1961).

([2]) R. Oehme: *Phys. Rev.*, **121**, 1810 (1961) and preprint EFINS 61-15 (University of Chicago), which contains a comprehensive review.

([3]) R. Blankenbecler: *Proceedings of the* 1960 *Rochester Conference* (New York, 1961). R. Blankenbecler, M. L. Goldberger, L. S. McDowell and S. B. Treiman: *Singularities of scattering amplitudes on unphysical sheets and their interpretation* (Princeton, 1961).

([4]) W. Zimmermann: *Nuovo Cimento*, **21**, 249 (1961).

([5]) P. G. O. Freund and R. Karplus: *Nuovo Cimento*, **21**, 519 (1961).

([6]) R. Karplus, CH. M. Sommerfield and E. H.Wichmann: *Phys. Rev.*, **111**, 1187 (1958); **114**, 376 (1959); Y. Nambu: *Nuovo Cimento*, **9**, 610 (1958); R. Oehme: *Phys. Rev.*, **111**, 1430 (1958).

has revealed the fact that these singularities are introduced through the unitarity relation, by the expected singular behavior of the matrix elements that connect the initial state to certain intermediate states ([2,7,8]). These singularities usually lie on unphysical sheets of the Riemann surface of the reaction amplitude or form factor, but can make their appearance on the physical sheet if certain conditions are satisfied among the masses of the particles involved.

This rationalization of the existence of anomalous thresholds has been carried out in the context of the partial wave expansion for the scattering amplitude. Since the term-by-term analytic continuation of the partial wave series, however, does not converge to the analytic continuation of the entire amplitude in the vicinity of the anomalous threshold, it is necessary to study the amplitude itself by an independent procedure ([9,10]). To this end, we have considered the integral equation form of the unitarity condition ([3,4]) for an amplitude that is expected to exhibit anomalous behavior. We find that it has indeed an anomalous behavior of a character very similar to that of the partial wave amplitudes ([2]). This result is to be contrasted with the rather different behavior of the amplitude and the partial wave projections at other singularities where the Legendre expansion does not converge: a pole of the amplitude on the physical sheet may give rise to a logarithmic branch point in the partial wave amplitude, while a natural boundary of the amplitude on the second sheet may only give rise to an isolated branch point in the partial wave amplitude ([5]).

In principle the calculation parallels that of OEHME ([2]). We consider three types of spinless particles A, C, B, with masses $m_A < m_C < m_B < 2m_A$, that can undergo the (virtual) reactions

(1*a*) $\quad A + A \to A + A$

(1*b*) $\quad B + B \to B + B$

(1*c*) $\quad A + A \to B + B$

(1*d*) $\quad A + B \to A + B$

(1*e*) $\quad A + B \to C$

([7]) R. OEHME: *Nuovo Cimento*, **13**, 778 (1959).

([8]) S. MANDELSTAM: *Phys. Rev. Lett.*, **4**, 84 (1960); R. BLANKENBECLER and Y. NAMBU: *Nuovo Cimento*, **18**, 595 (1960).

([9]) Since form factors only involve a small number of partial waves, depending on the spins of the particles involved, convergence difficulties cannot arise.

([10]) Mr. R. C. HWA has communicated with us privately concerning the singularities of the amplitude and the problems raised by the non-convergence of the Legendre expansion.

and all others implied by these. Depending on the energy available, certain of the reactions may really take place. When the masses satisfy the additional inequality

$$m_B^2 < m_C^2 + m_A^2 , \tag{2}$$

then the partial wave amplitude of processes (1*b*) and (1*c*) do not exhibit anomalous thresholds, while when inequality (2) is reversed, they do [2,6-8]. Hence we begin by imposing restriction (2) and stating the two coupled unitarity conditions for processes (1*a*) and (1*c*) in the « elastic interval » in which the variable s (the square of the mass of the two-particle system) lies in the range

$$(2m_A)^2 < s < (2m_C)^2 , \tag{3}$$

so that only reaction (1*a*) can really take place. We shall call the two amplitudes (functions of s and scattering angle θ) respectively $\Phi_{AA}(s, \cos\theta)$, and $\Phi_{AB}(s, \cos\theta)$ on the physical sheet, and $\Phi^{(2)}_{AA}(s, \cos\theta)$ and $\Phi^{(2)}_{AB}(s, \cos\theta)$ on the unphysical sheet connected to the physical sheet along the real interval (3). Then the unitarity conditions which allow us to determine the singularities of the functions $\Phi^{(2)}$ when those of the Φ are known, are

$$\Phi^{(2)}_{AA}(s, \cos\theta) = \Phi_{AA}(s, \cos\theta) - \frac{i}{4}\sqrt{\frac{s - 4m_A^2}{s}} \cdot \tag{4}$$

$$\cdot \int_{-1}^{+1} \mathrm{d}\cos\theta' \int_{-1}^{+1} \mathrm{d}\cos\theta'' \Phi_{AA}(s, \cos\theta') \Phi^{(2)}_{AA}(s, \cos\theta'') \frac{\theta(-k(\cos\theta, \cos\theta', \cos\theta''))}{[-k(\cos\theta, \cos\theta', \cos\theta'')]^{\frac{1}{2}}} ,$$

$$\Phi^{(2)}_{AB}(s, \cos\theta) = \Phi_{AB}(s, \cos\theta) - \frac{i}{4}\sqrt{\frac{s - 4m_A^2}{s}} \cdot \tag{5}$$

$$\cdot \int_{-1}^{+1} \mathrm{d}\cos\theta' \int_{-1}^{+1} \mathrm{d}\cos\theta'' \Phi_{AA}(s, \cos\theta') \Phi^{(2)}_{AB}(s, \cos\theta'') \frac{\theta(-(k(\cos\theta, \cos\theta', \cos\theta''))}{[-k(\cos\theta, \cos\theta', \cos\theta'')]^{\frac{1}{2}}} ,$$

or

$$\Phi^{(2)}_{AB}(s, \cos\theta) = \Phi_{AB}(s, \cos\theta) - \frac{i}{4}\sqrt{\frac{s - 4m_A^2}{s}} \cdot \tag{6}$$

$$\cdot \int_{+1}^{-1} \mathrm{d}\cos\theta' \int_{+1}^{-1} \mathrm{d}\cos\theta'' \Phi_{AB}(s, \cos\theta') \Phi^{(2)}_{AA}(s, \cos\theta'') \frac{\theta(-k(\cos\theta, \cos\theta', \cos\theta''))}{[-k(\cos\theta, \cos\theta', \cos\theta'')]^{\frac{1}{2}}} ,$$

where

$$k(x, x'x'') = -1 + x^2 + x'^2 + x''^2 - 2xx'x'' , \quad \theta(-k) = \tfrac{1}{2} - \tfrac{1}{2}k/|k| .$$

For the functions Φ we shall assume a Mandelstam representation ([11]). We therefore introduce the three invariants s,

$$t = m_A^2 + m_B^2 - \tfrac{1}{2}s + 2\cos\theta(\tfrac{1}{4}s - m_A^2)^{\frac{1}{2}}(\tfrac{1}{4}s - m_B^2)^{\frac{1}{2}} \tag{7a}$$

and

$$u = m_A^2 + m_B^2 - \tfrac{1}{2}s - 2\cos\theta(\tfrac{1}{4}s - m_A^2)^{\frac{1}{2}}(\tfrac{1}{4}s - m_B^2)^{\frac{1}{2}} \tag{7b}$$

in terms of which the positions of the singularities are simply described. Thus the amplitude Φ_{AA} which is symmetrical in s, t, and u, has branch points at

$$s = 4(n_A m_A + n_B m_B + n_C m_C)^2\,, \quad n_A, n_B, n_C = 0, 1, 2, \ldots \quad n_A + n_B + n_C \geqslant 1 \tag{8}$$

(the lowest of these, $s = 4m_A^2$, is an isolated branch point ([3,4])) and at the same values for t and u. The amplitude Φ_{AB} has the branch points given in eq. (9) as functions of s, but is, of course, only symmetrical in t and u. As functions of these variables it has poles

$$t = m_C^2 \qquad \text{or} \qquad u = m_C^2\,, \tag{9}$$

the isolated branch points

$$t = (m_A + m_B)^2 \qquad \text{or} \qquad u = (m_A + m_B)^2 \tag{10}$$

and higher singularities. In the $(s\cos\theta)$ space, the poles occur at the points

$$\cos\theta = \cos\theta_C^{\pm}(s) = \pm\frac{m_A^2 + m_B^2 - m_C^2 - s/2}{2(s/4 - m_A^2)^{\frac{1}{2}}(s/4 - m_B^2)^{\frac{1}{2}}}\,. \tag{11}$$

Except for the reduction in extent of the elastic interval (3), the problem of finding $\Phi_{AA}^{(2)}(s, \cos\theta)$ is the same as that considered in our earlier paper ([5]), and we shall accept the solution given there. We therefore turn to the calculation of the function $\Phi_{AB}^{(2)}$. This is a solution of the integral eq. (5) and has the representation (6), which permits an explicit calculation of its properties. It is clear that $\Phi_{AB}^{(2)}$ will have the singularities of the integral in eq. (6) in addition to the singularities of Φ_{AB}; the singularities of the integral in turn depend on the properties of the integrand. We shall be principally concerned with the effect of the poles eq. (11) of Φ_{AB} and postpone consideration of the other singularities.

As shown in the reference quoted earlier ([3,4]), the integral in eq. (6) will

([11]) S. MANDELSTAM: *Phys. Rev.*, **112**, 1344 (1958).

have branch points whenever [12]

$$\cos\theta = \cos\left\{n\cos^{-1}\left[\pm\left(1+\frac{8m_A^2}{s-4m_A^2}\right)+\theta_C^{\pm}(s)\right]\right\}, \tag{12}$$

as long as s is not on the negative real axis. When solved for s at fixed scattering angle θ or at fixed momentum transfer, the singularities cluster around the negative real s-axis independently of the value of m_C. By an adaptation of the reasoning presented earlier [5], therefore, we conclude that the negative real s-axis is a natural boundary of $\Phi_{AB}^{(2)}(s, \cos\theta)$.

In addition to the singularities given by eq. (12), however, it is easy to verify that the integral in eq. (6) has a logarithmic branch point when

$$\cos\theta_C^{\mp}(s) = \pm 1 \tag{13}$$

or

$$s = s_C \equiv -\frac{1}{m_C^2}[m_C^2-(m_B+m_A)^2][m_C^2-(m_B-m_A)^2], \tag{14}$$

that is, when the amplitude Φ_{AB} is singular at the integration end point. Eq. (14) defines a point on the positive real axis

$$0 < s_C < 4m_A^2, \tag{15}$$

whose position is independent of the scattering angle.

The higher singularities of $\Phi_{AB}(s, \cos\theta)$, such as the branch points given by eq. (10), contribute further singularities to the distribution near the negative real s-axis when $\Phi_{AB}^{(2)}(s, \cos\theta)$ is studied at fixed angle or fixed momentum transfer. The additional branch points corresponding to eq. (14), however, occur on the negative real axis, and therefore do not explicitly complicate the behavior of the function for which we have found a natural boundary there.

We therefore arrive at the result that the analytic behavior of $\Phi_{AB}^{(2)}(s, \cos\theta)$ near $s = s_C$ is essentially the same as the behavior at this point of the analytic continuation of the partial wave projections of $\Phi_{AB}^{(1)}(s, \cos\theta)$. The conclusions about the occurrence of anomalous thresholds that have been obtained by following the change in position of s_C considered as a function of slightly complex m_B^2 as the the real part of m_B^2 is increased until

$$\mathrm{Re}\, m_B^2 > m_A^2 + m_C^2 \tag{16}$$

[12] Both the functions $\cos^{-1} z$ and θ_C appearing here are obtained by analytic continuation from the physical range of the variable s without crossing the real axis $s < 4m_A^2$. They therefore have an imaginary part of the same sign.

can therefore be applied to the entire reaction amplitude at all physical angles ([2,7,8]). We shall briefly review these conclusions. As long as inequality (2) is satisfied, $\Phi_{AB}(s, \cos\theta)$ and $\Phi^{(2)}_{AB}(s, \cos\theta)$ have poles at the points

$$s = s_C^{\pm}(\cos\theta)\,, \tag{17}$$

where $s_C^{\pm}(\cos\theta)$ are the solutions of

$$\cos\theta_C^{\pm}(s_C) = \cos\theta\,; \tag{18}$$

in addition, $\Phi^{(2)}_{AB}(s, \cos\theta)$ has the branch point at

$$s = s_C = s_C(1)\,. \tag{19}$$

As $\mathrm{Re}\, m_B^2$ is increased until inequality (16) is satisfied, the singularities move continuously on the two-sheeted surface. Most important, the branch point s_C wanders around the physical threshold and appears as a singularity (« anomalous » threshold) of Φ_{AB} on the physical sheet, still in the interval

$$0 < s_C < 4m_A^2\,. \tag{20}$$

The two pairs of poles $s_C^{\pm}(\cos\theta)$ also change their position. Since they occur on both sheets with the same residues, however, the fact that one pair exchanges sheets (*i.e.* one pole of Φ_{AB} appears on the unphysical sheet and the corresponding pole of $\Phi^{(2)}_{AB}$ appears on the physical sheet) does not explicitly affect the function. For a certain range of angles defined by

$$\frac{m_C^2}{m_B^2 - m_A^2} < \sin\theta < 1\,, \tag{21}$$

the poles occur at complex values of s on the circle ([10])

$$|s - s_C| = [(m_B^2 - m_A^2)^2 - m_C^4]^{\frac{1}{2}}/m_C^2 \tag{22}$$

These results are most clearly displayed in the complex plane of $k = \frac{1}{2}\sqrt{s - 4m_A^2}$

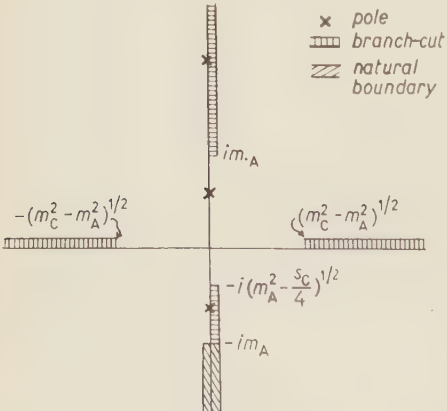

Fig. 1. – Singularities of Φ_{AB} and $\Phi^{(2)}_{A}$ in the complex plane of the variable $k = \frac{1}{2}\sqrt{s - 4m_A^2}$. The masses satisfy the inequality $m_B^2 < m_C^2 + m_A^2$.

The upper and lower half-planes correspond, respectively, to the physical and unphysical sheets we are discussing. In Fig. 1 are shown the locations of singularities in the « normal » case of inequality (2), while in Fig. 2 are shown the locations of singularities in the « anomalous » case of inequality (16). As

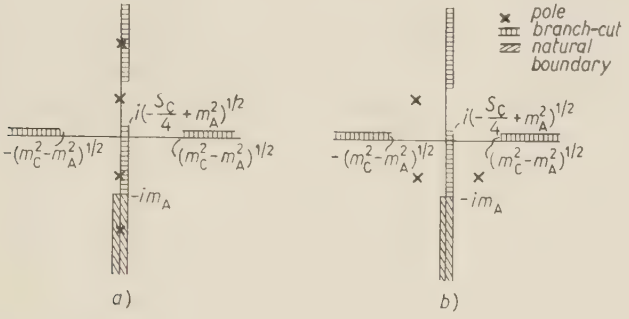

Fig. 2. – *a*) Singularities of Φ_{AB} and $\Phi^{(2)}_{AB}$ in the complex plane of the variable $k=\frac{1}{2}\sqrt{s-4m_A^2}$. The masses satisfy the inequality $m_B^2>m_C^2+m_A^2$. The scattering angle satisfies $\sin\theta<m_C^2/(m_B^2-m_A^2)$. *b*) Singularities of Φ_{AB} and $\Phi^{(2)}_{AB}$ in the complex plane of the variable $k=\frac{1}{2}\sqrt{s-4m_A^2}$. The masses satisfy the inequality $m_B^2>m_C^2+m_A^2$. The scattering angle satisfies $\sin\theta>m_C^2/(m_B^2-m_A^2)$.

we pointed out, the behavior is qualitatively similar to the behavior of the partial wave amplitudes. We add that the natural boundary is unaffected by the variation of m_B^2. It is also clear from Fig. 2 that the continuations of Φ_{AB} unto the upper and lower halves of the second sheet are no longer connected with each other in a direct way. They are only connected by paths that pass through the physical sheet.

A dispersion relation for the amplitude on the physical sheet must take into account the location of the poles in addition to the contribution from the branch-cuts. We therefore have the two cases (neglecting subtractions),

$$\Phi_{AB}(s,\cos\theta)=\int_{-\infty}^{0}\frac{\operatorname{Im}\Phi_{AB}(s',\cos\theta)}{s'-s}\,ds'+\int_{4m_A^2}^{\infty}\frac{\operatorname{Im}\Phi_{AB}(s',\cos\theta)}{s'-s}\,ds'+ \tag{23}$$

$$+\frac{g^2}{t(s,\cos\theta)-m_C^2}+\frac{g^2}{u(s,\cos\theta)-m_C^2},$$

and

$$\Phi^{(2)}_{AB}(s,\cos\theta)=\int_{-\infty}^{s_C}\frac{\operatorname{Im}\Phi^{(2)}_{AB}(s',\cos\theta)}{s'-s}\,ds'+\int_{4m_A^2}^{\infty}\frac{\operatorname{Im}\Phi^{(2)}_{AB}(s',\cos\theta)}{s'-s}\,ds'+ \tag{24}$$

$$+\frac{g^2}{t(s,\cos\theta)-m_C^2}+\frac{g^2}{u(s,\cos\theta)-m_C^2},$$

in the absence of anomalous thresholds, while

$$\Phi_{AB}(s, \cos\theta) = \int_{-\infty}^{0} \frac{\operatorname{Im} \Phi_{AB}(s', \cos\theta)}{s' - s} \, ds' + \int_{s_C}^{\infty} \frac{\operatorname{Im} \Phi_{AB}(s', \cos\theta)}{s' - s} \, ds' + \frac{g^2}{t(s, \cos\theta) - m_C^2} + \frac{g^2}{u(s, \cos\theta) - m_C^2}, \tag{25}$$

and

$$\Phi^{(2)}_{AB}(s, \cos\theta) = \int_{-\infty}^{+\infty} \frac{\operatorname{Im} \Phi^{(2)}_{AB}(s', \cos\theta)}{s' - s} \, ds' + \frac{g^2}{t(s, \cos\theta) - m_C^2} + \frac{g^2}{u(s, \cos\theta) - m_C^2}, \tag{26}$$

in the presence of anomalous thresholds. It must be remembered that $\operatorname{Im} \Phi_{AB}(s, \cos\theta)$ in the interval $s_c < s < 4m_A^2$ is derived from $\Phi^{(2)}_{AB}(s, \cos\theta)$ in the same way as in the partial wave case that has been discussed in detail by OEHME [2].

At fixed momentum transfer one can draw the identical conclusion about anomalous thresholds in the dispersion relations for Φ_{AB} (the only difference here is that the location of the poles, of course, is independent of the mass m_B). This result follows from the fact that no new singularities of $\Phi^{(2)}_{AB}$ other than the branch point s_c cross into the physical sheet through the cut (3) as m_B^2 in varied. For $\Phi^{(2)}_{AB}$, on the other hand, one cannot write a simple dispersion relation at fixed momentum transfer because of the many singularities at complex values of s [3-5].

In spite of the non-convergence of the Legendre series, therefore, the existence and properties of anomalous thresholds of reaction amplitudes parallel closely the corresponding behavior of the partial wave amplitudes. Basically, these properties stem from the angular integral in the unitarity condition (or in the partial wave case, from the integral defining the partial wave projection). Since the reaction amplitude has singularities in the $\cos\theta$ plane, such integrals define multi-valued functions, whose value depends on the choice of the path of integration. Now, in the physical domain on the physical sheet, the integrals must be taken along the real interval

$$C: \{-1 \leqslant \operatorname{Re} \cos\theta \leqslant 1, \quad \operatorname{Im} \cos\theta = 0\}. \tag{27}$$

The analytic continuation from the physical domain then requires appropriate

distortion of the contour C as a singularity approaches it, so that the singularity does not cross it. Usually the singularities do not approach C when s remains on the physical sheet. In the anomalous case of the inequality (16), however, the poles given by eq. (9) approach C on the circle eq. (22) in the s-plane. Continuation inside the circle then requires the contour to be distorted severely. On the real s-axis, finally, the contour resumes its normal shape C (except for the usual infinitesimal detours around the poles) for $s < s_c$, but extends along the real axis outside the interval C for $s > s_c$. It is these latter distortions, which disappear at $s = s_c$, that bring about the singular behavior at this point (see Fig. 3).

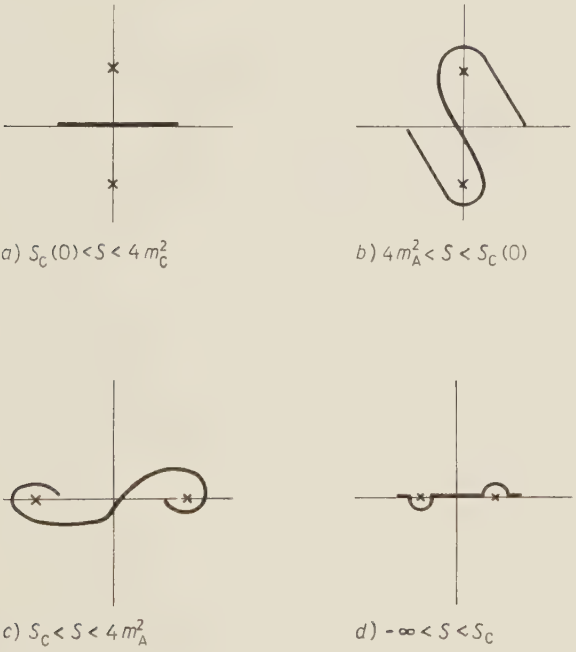

Fig. 3. – Paths of integration in the complex $\cos\theta$-plane for the integrals in eqs. (4), (5), (6) in the anomalous case $m_B^2 > m_C^2 + m_A^2$. Parts a-d refer to different values of the variable s. The crosses show the locations of the poles of Φ_{AB} and $\Phi_{AB}^{(2)}$:

The discussion we have just given makes plausible the appearance of anomalous thresholds without using the device of changing the particle masses. It provides a somewhat more direct connection between these singularities and the physical region. In addition, it makes clear that the analytic continuation of the partial wave projections will differ, near the anomalous thresh-

old, from the partial wave projection of the analytic continuation of the amplitude. Nevertheless, both have anomalous thresholds.

* * *

We have enjoyed stimulating and informative conversations concerning this problem with R. OEHME. One of us (R.K.) is grateful to Professor W. THIRRING for the hospitality of the Institute for Theoretical Physics.

RIASSUNTO (*)

L'ampiezza di scattering ad energia cinetica zero ha un punto di diramazione appartenente a due foglietti. Si dimostra che l'ampiezza sul secondo foglietto (non fisico) ha un limite naturale che termina all'energia totale zero.

(*) *Traduzione a cura della Redazione.*

Radiative Corrections to $\pi^- \to \pi^0 + e^- + \bar{\nu}$ Decay.

G. Da Prato and G. Putzolu

Laboratori Nazionali del C.N.E.N., Frascati - Roma

(ricevuto il 16 Giugno 1961)

Summary. — We have calculated the radiative corrections to the $\pi^- \to \pi^0 + e^- + \bar{\nu}$ decay.

1. – Introduction.

Feynman and Gell-Mann [1] introduced the hypothesis of conserved current to explain the absence of renormalization effects in the V part of the β-decay. In their scheme the weak vector current is identified with the $(+)$ component of the isotopic spin current $J_k^{(+)}$. One of the suggested tests of the theory is an accurate measurement of the decay rate for the leptonic decay of the pion:

$$\pi^- \to \pi^0 + e^- + \bar{\nu} \,. \tag{1}$$

In fact, neglecting electromagnetic corrections, the corresponding matrix element is given by

$$ig\sqrt{2}\left(\bar{e}\gamma^k[1 + i\gamma^5]\nu\right)\left(\pi^0 | J_k^{(+)} | \pi^-\right) \tag{2}$$

and we have a simple connection between the relevant matrix element of the vector current and the electromagnetic form factor of the pion F_π:

$$\left(\pi^0 | J_k^{(+)} | \pi^-\right) = \frac{1}{\sqrt{2}} \left(\pi_k^0 + \pi_k^-\right) F_\pi(k^2) \,, \tag{3}$$

(1) R. P. Feynmann and M. Gell-Mann: *Phys. Rev.*, **109**, 193 (1958).

where $k^2 = (\pi^- - \pi^0)^2$ is the momentum transfer to the lepton pair. In the actual process (1) this momentum transfer is very small, so that one can safely put $F_\pi = 1$. In this work we propose to evaluate the radiative corrections (to order e^2) to process (1). This would be important for a comparison of an accurate experimental result and the prediction of the Feynmann and Gell-Mann theory.

Since it is difficult to introduce the pion form factor in a gauge-invariant way for vertices with virtual pion lines, we will use a local Lagrangian and a Feynman cut-off in the calculation of radiative corrections. The results will not depend critically on this cut-off, since the divergence will be found to be only logarithmic.

2. – Formulation.

In the following we shall use the notations and the conventions of the textbook of BOGOLIUBOV and SHIRKOV (2). Let p_1, p_2, p_3, p_4 be the momenta and m_1, m_2, m_3, $m_4 = 0$ the masses of the π^-, e^-, π^0, $\bar{\nu}$. We put also:

$$\cosh\theta = \frac{(p_1 p_2)}{m_1 m_2}. \tag{4}$$

All the calculations will be performed in the center-of-mass system.

The Lagrangian responsible for the process is

$$\mathscr{L}_1 = \{\pi^- \partial_k \pi^0 - \pi^0 \partial_k \pi^-\}(\bar{e}\gamma^k[1 + i\gamma^5]\nu) + \text{h. c.}. \tag{5}$$

Following the principle of the minimal electromagnetic interaction, the Lagrangian that takes into account the electromagnetic interactions as well, is obtained from the complete Lagrangian without them

$$\mathscr{L}_0 = \mathscr{L}^{(e)}_{\text{free}} + \mathscr{L}^{(\nu)}_{\text{free}} + \mathscr{L}^{(\pi)}_{\text{free}} + \mathscr{L}^{(\gamma)}_{\text{free}} + \mathscr{L}_1, \tag{6}$$

by the substitution

$$\partial_k \varphi(x) \to (\partial_k - ie A_k(x))\varphi(x), \tag{7}$$

where $A(x)$ and $\varphi(x)$ are respectively the field operators of the photon and of the generic charged particle that appears in the process (1).

(2) N. N. BOGOLIUBOV and D. V. SHIRKOV: *Introduction to the Theory of Quantized Fields* (New York, London, 1959).

In this way we obtain for the complete interaction Lagrangian L:

$$\mathscr{L} = \mathscr{L}_1 + e{:}\bar{e}\hat{A}e{:} + ie{:}[\partial^k\pi^* \cdot \pi - \pi^* \partial^k\pi]{:}A_k - e^2{:}\pi^*\pi A_k A^k{:} + \\ + \left[g(\bar{e}\gamma^k[1 + i\gamma^5]\nu)ieA_k\pi^*\pi^0 + \text{h. c.}\right]. \tag{8}$$

The last term is a new direct interaction between the five particles π^-, π^0, e^-, $\bar{\nu}$ and γ.

3. – Feynman diagrams.

Using the Lagrangian (8) we have seven diagrams corresponding to the process (1) up to the order g^2e^2 (Fig. 1).

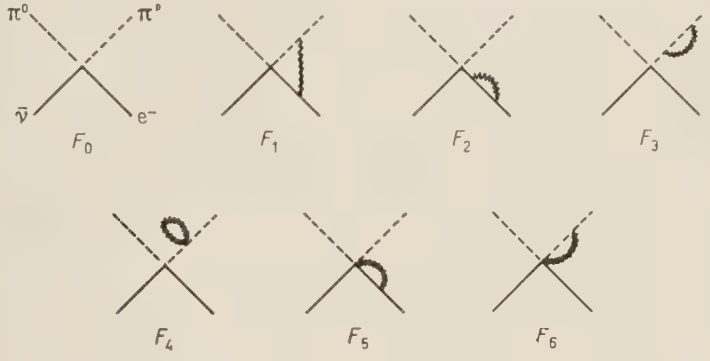

Fig. 1.

Besides them we have also to consider three diagrams (Fig. 2) relative to the same process with bremsstrahlung:

$$\pi^- \to \pi^0 + e^- + \bar{\nu} + \gamma\,. \tag{9}$$

Fig. 2.

They give to the transition probability a contribution of the order g^2e^2, depending on the experimental situation (see Section 5).

4. – Transition probabilities (virtual photons).

We put

$$(e^-, \pi^0, \bar{\nu}\,|\,S-1\,|\,\pi^-) = \delta(p_1-p_2-p_3-p_4)F \tag{10}$$

and we have

$$F = \sum_1^6 {}_h F_h\,, \tag{11}$$

where F_h's refer to the various diagrams of Fig. 1. Calling $\mathrm{d}P_1$ the corresponding differential transition probability, summed over the final spins, we have

$$\mathrm{d}P_1 = \frac{1}{2\pi}\sum_{\text{spin}}|F|^2\delta(p_1-p_2-p_3-p_4)\,\mathrm{d}\boldsymbol{p}_1\,\mathrm{d}\boldsymbol{p}_2\,\mathrm{d}\boldsymbol{p}_3\,, \tag{12}$$

where to the order g^2e^2 we have

$$|F|^2 = |F_0|^2 + 2\mathscr{R}\sum_1^4 {}_h F_0^* F_h\,. \tag{13}$$

4·1. – *Calculation of* F_0.

$$F_0 = \frac{ig}{2(2\pi)^2\sqrt{p_{10}p_{30}}}(\bar{v}_2^+[\hat{p}_1+\hat{p}_3][1+i\gamma^5]v_4^+)\,. \tag{14}$$

$$\sum_{\text{spin}}|F_0|^2 = \frac{g^2}{2(2\pi)^4 p_{10}p_{20}p_{30}p_{10}}\{8(p_1p_2)(p_1p_4) - 4m_2^2(p_1p_4) + [m_2^2-4m_1^2](p_2p_4)\}\,. \tag{15}$$

4·2. – *Calculation of* $(F_1+F_5+F_6)$.

$$F_1 + F_5 + F_6 = \frac{ge^2}{(2\pi)^6}\frac{1}{\sqrt{4p_{10}p_{30}}}\bar{v}_2^+\int \mathrm{d}k\,((2\hat{p}_1-\hat{k})(k^2-2(p_2k)) +$$
$$+ (4m_2-2\hat{p}_2+2\hat{k})(k^2-2(p_1k)) + (2\hat{p}_1-\hat{k})(m_2+\hat{p}_2-\hat{k})(\hat{p}_1+\hat{p}_3-\hat{k})]\cdot$$
$$\cdot\, k^{-2}[k^2-2(p_1k)]^{-1}[k^2-2(p_2k)]^{-1}[1+i\gamma^5]v_4^+\,.$$

This integral shows ultraviolet and infrared divergences; consequently it has been evaluated introducing a Feynman cut-off $\left(-(\lambda^2/(k^2-\lambda^2))\right)$ and a fictitious photon mass λ_m. The same will be made, where necessary, for the other diagrams.

By standard methods one obtains

$$(17)\qquad F_1+F_5+F_6=-\frac{ge^2}{(2\pi)^6}\frac{1}{\sqrt{4p_{10}p_{30}}}\bar{v}_2^+\{2I_1\hat{p}_1[\hat{p}_2+m_2][\hat{p}_1+\hat{p}_3]-$$
$$-I_2[5m_2\hat{p}_1+m_2\hat{p}_3+\hat{p}_2\hat{p}_3+\hat{p}_2\hat{p}_1-2\hat{p}_1\hat{p}_2]-2[4(p_1p_2-m_2\hat{p}_2)]\hat{I}_2-$$
$$-2\hat{p}_1\hat{I}_2[(\hat{p}_1+\hat{p}_3+2m_2]+I_3[4\hat{p}_1+3m_2]-2\hat{I}_4\}(1+i\gamma^5)v_4^+\,,$$

where

$$(18)\qquad \begin{cases} I_1=\dfrac{i\pi^2}{2}\,j_1\,, \\ \hat{I}_2=\dfrac{i\pi^2}{2}\sum\limits_h g^{hh}\gamma^h j_2^h\,, \\ I_3=\dfrac{i\pi^2}{2}\sum\limits_h g^{hh}j_3^{hh}\,, \\ \hat{I}_4=\dfrac{i\pi^2}{2}\sum\limits_{hk} g^{hh}g^{kk}\gamma^h(\hat{p}_2-\hat{p}_1)\gamma^k j_3^{hk}\,. \end{cases}$$

j_1, j_2^h and j_3^{hk} have been defined and evaluated by BEHRENDS, FINKELSTEIN and SIRLIN [3] (formulae (7*a*) and following).

Substituting the expressions for the j's, we obtain

$$(19)\qquad F_1+F_5+F_6=-\frac{ge^2}{(2\pi)^6}\frac{1}{\sqrt{4p_{10}p_{30}}}\frac{i\pi^2}{2}\bar{v}_2^+(Am_2+2B\hat{p}_1)(1+i\gamma^5)v_4^+\,,$$

where

$$(20)\qquad \begin{cases} A=-4I_1(p_1p_2)-2I_{21}[m_1^2-(p_1p_2)]- \\ \qquad\qquad -2I_{22}[4(p_1p_2)-m_2^2-2m_1^2]+3I_3-2I_{42}\,, \\ B=4I_1(p_1p_2)-2I_{21}[3(p_1p_2)+m_1^2]-I_{22}[3m_2^2+4(p_1p_2)]+2I_3-I_{41}\,. \end{cases}$$

I_{21}, I_{22}, I_{41} and I_{42} are defined by the positions:

$$(21)\qquad \begin{cases} \hat{I}_2=I_{21}\,\hat{p}_1+I_{22}\,\hat{p}_2\,, \\ \hat{I}_4=I_{41}\,\hat{p}_1+I_{42}\,\hat{p}_2\,. \end{cases}$$

Finally the contribution of $(F_1+F_5+F_6)$ to the transition probability is

$$(22)\qquad \sum_{\text{spin}} 2\mathscr{R}\,[(F_1+F_5+F_6)\cdot F_0^*]=-\frac{g^2}{4(2\pi)^4}\frac{\alpha}{\pi}[8B(p_1p_2)(p_1p_4)+$$
$$+2(A-B)m_2^2(p_1p_4)-(Am_2^2+4Bm_1^2)(p_2p_4)]\frac{1}{p_{10}p_{20}p_{30}p_{40}}\,,$$

[3] R. H. BEHRENDS, R. J. FINKELSTEIN and A. SIRLIN: *Phys. Rev.*, **101**, 866 (1956).

and the fractional correction $\delta^{(1,5,6)}$ is

$$\delta^{(1,5,6)} = \frac{\sum_{\text{spin}} 2\mathscr{R}[(F_1 + F_5 + F_6)F_0^*]}{\sum_{\text{spin}} |F_0|^2} = \tag{23}$$

$$= \frac{1}{2}\frac{\alpha}{\pi}\frac{8B(p_1p_2)(p_1p_4) + 2(A-B)m_2^2(p_1p_4) - (Am_2^2 + 4Bm_1^2)(p_2p_4)}{8(p_1p_2)(p_1p_4) - 4m_2^2(p_1p_4) + (m_2^2 - 4m_1^2)(p_2p_4)}.$$

4·3. – *Calculation of* F_2, F_3 *and* F_4. – These diagrams describe self-energy effects; after mass and wave function renormalization the diagram F_4 does not give any contribution, while the diagrams F_2 and F_3 give the following fractional corrections to the transition probability:

$$\begin{cases} \delta^{(2)} = -\dfrac{\alpha}{\pi}\left(\dfrac{1}{2}\ln\dfrac{\lambda}{m_2} + \ln\dfrac{\lambda_m}{m_2} - \dfrac{9}{8}\right), \\ \delta^{(3)} = -\dfrac{\alpha}{\pi}\left(-\ln\dfrac{\lambda}{m_1} - \ln\dfrac{\lambda_m}{m_1} - 1\right). \end{cases} \tag{24}$$

5. – Transition probabilities (real photons).

As is well known, when treating approximations to the order g^2e^2, one must consider the corrections due to real photons of energy inferior to a maximum value ε depending upon the experimental resolution, as well as the corrections due to virtual photons. In our case we have assumed $\varepsilon \ll m_2$. We put

$$(e^-, \pi^0, \bar{\nu}, \gamma\,|\,(S-I)\,|\,\pi^-) = \delta(p_1 - p_2 - p_3 - p_4 - k)G\,, \tag{25}$$

where k is the momentum of the emitted photon, and $G = F_7 + F_8 + F_9$ (see Fig. 2).

Calling $\mathrm{d}P_2$ the corresponding differential transition probability, summed over the final spins and polarizations, and integrated over $\boldsymbol{k}$ with $|\boldsymbol{k}| < \varepsilon$, one obtains

$$\mathrm{d}P_2 = \frac{1}{2\pi}\sum_{\text{spin}}\sum_{\substack{\text{pol}\\ |\boldsymbol{k}|<\varepsilon}}\int \mathrm{d}\boldsymbol{k}\,|G|^2\,\delta(p_1 - p_2 - p_3 - p_4 - k)\,\mathrm{d}\boldsymbol{p}_2\,\mathrm{d}\boldsymbol{p}_3\,\mathrm{d}\boldsymbol{p}_4\,. \tag{26}$$

Because $\varepsilon \ll m_2$, we can neglect the diagram F_9, which gives corrections proportional to ε and ε^2; for the correction relative to $(F_7 + F_8)$ one obtains by standard methods

$$\mathrm{d}P_2 = \delta^{(7,8)}\,\frac{1}{2\pi}\sum_{\text{spin}}|F_0|^2\,\delta(p_1 - p_2 - p_3 - p_4)\,\mathrm{d}\boldsymbol{p}_2\,\mathrm{d}\boldsymbol{p}_3\,\mathrm{d}\boldsymbol{p}_4\,, \tag{27}$$

where $\delta^{(7,8)}$, that is consequently the fractional correction due to the bremsstrahlung, is given by

$$\delta^{(7,8)} = -\frac{\alpha}{\pi}\left[2 \ln \frac{2\varepsilon}{\lambda_m}(1 - \theta \cdot \operatorname{ctgh} \theta) - \theta \operatorname{ctgh} \theta - 1 + \right. \tag{28}$$

$$\left. + (p_1 p_2)\int_{-1}^{1} \mathrm{d}z \, \frac{1}{p_z^2} \frac{1}{2v_z} \ln \frac{1+v_z}{1-v_z}\right],$$

where

$$p_z = \tfrac{1}{2}[p_1(1+z) + p_2(1-z)] \qquad \text{and} \qquad v_z = \frac{|\boldsymbol{p}_z|}{p_{z_0}} .$$

6. – Total correction and approximations.

The total percentual correction is given by

$$\delta = \delta^{(1,5,6)} + \delta^{(2)} + \delta^{(3)} + \delta^{(7,8)}, \tag{29}$$

where the $\delta^{(i)}$'s are given from (23), (24) and (28). As it must be, δ does not contain λ_m.

In the very good approximation $m_2 \ll m_1$, $\delta^{(1,5,6)}$ and $\delta^{(7,8)}$ may be written as follows:

$$\begin{cases} \delta^{(4,5,6)} = -\dfrac{\alpha}{\pi}\left[\theta \operatorname{ctgh} \theta \left(\theta - 2 \ln \dfrac{\lambda_m}{m_2} - 5\right) - \ln \dfrac{m_1}{m_2} + \dfrac{5}{2} \ln \dfrac{m_1}{\lambda} - \dfrac{13}{8}\right], \\ \delta^{(7,8)} = -\dfrac{\alpha}{\pi}\left[2 \ln \dfrac{2\varepsilon}{\lambda_m}(1 - \theta \operatorname{ctgh} \theta) + \theta \operatorname{ctgh} \theta - 1\right]. \end{cases} \tag{30}$$

Then

$$\delta = -\frac{\alpha}{\pi}\left[\theta^2 \operatorname{ctgh} \theta - 4\theta \operatorname{ctgh} \theta - \frac{1}{2} \ln \frac{m_1}{m_2} - 3 \ln \frac{\lambda}{m_1} - \frac{1}{2} + \right. \tag{31}$$

$$\left. + \ln \frac{2\varepsilon}{m_1} + \ln \frac{2\varepsilon}{m_2}(1 - 2\theta \operatorname{ctgh} \theta)\right].$$

7. – Integral transition probability.

We call P_0 and P the integral transition probabilities to the order g^2 and $g^2 e^2$, and $\delta p = (P - P_0)/P_0$ the corresponding fractional correction.

By definition:

$$(32)\qquad \begin{cases} P_0 = \dfrac{1}{2\pi}\displaystyle\int \sum_{\text{spin}} |F_0|^2\,\delta(p_1 - p_2 - p_3 - p_4)\,\mathrm{d}\boldsymbol{p}_2\,\mathrm{d}\boldsymbol{p}_3\,\mathrm{d}\boldsymbol{p}_4\,, \\ P = \dfrac{1}{2\pi}\displaystyle\int \sum_{\text{spin}} |F_0|^2(1+\delta)\,\delta(p_1 - p_2 - p_3 - p_4)\,\mathrm{d}\boldsymbol{p}_2\,\mathrm{d}\boldsymbol{p}_3\,\mathrm{d}\boldsymbol{p}_4\,. \end{cases}$$

Performing the integrations considering also the pion's recoil, and neglecting only terms like m_2^2 in comparison with m_1^2, one obtains

$$(33)\qquad P_0 = \frac{g^2}{\pi^3 m_1}\left[\frac{1}{5}(\Delta^2 - m_2^2)^{\frac{5}{2}}(m_1 - 2\Delta) + \frac{1}{3}(\Delta^2 - m_2^2)^{\frac{3}{2}}\left(\frac{5}{4}\Delta^3 - \frac{1}{2}m_1\Delta^2 - \right.\right.$$
$$\left.\left. - \frac{13}{8}m_2^2\Delta + m_1 m_2^2\right) + \frac{1}{8}m_2^2\Delta^2(\Delta - 2m_1)(\Delta^2 - m_2^2)^{\frac{1}{2}}\right],$$

$$(34)\qquad \delta_p = -\frac{\alpha}{\pi}\left[\left(\ln\frac{2\Delta}{m_2}\right)^2 - \frac{167}{30}\ln\frac{2\Delta}{m_2} + \frac{6229}{1800} + \frac{3}{2}\ln\frac{m_2}{m_1} - \right.$$
$$\left. - 3\ln\frac{\lambda}{m_1} + 2\ln\frac{2\varepsilon}{m_2}\left(\frac{107}{60} - \ln\frac{2\Delta}{m_2}\right)\right],$$

where

$$\Delta = \frac{m_1^2 - m_3^2}{2m_1}.$$

Finally one obtains numerically

$$(35)\qquad P_0 = 0.552\ \text{s}^{-1},$$

$$(36)\qquad \delta_p = 0.027 + 0.005\ln\frac{2\varepsilon}{m_2} + 0.007\ln\frac{\lambda}{m_1}.$$

8. Discussion.

The value (35) has been obtained using the following numerical values:

$$(37)\qquad \begin{cases} m_1 = (139.59 \pm 0.05)\ \text{MeV}\ (^4) \\ m_3 = (135.00 \pm 0.05)\ \text{MeV}\ (^4) \\ g m_{\text{proton}}^2 = (1.204 \pm 0.001)\cdot 10^{-5}\ (^5). \end{cases}$$

(4) W. H. Barkas and A. H. Roselfeld: UCRL 8030.
(5) M. Gell-Mann and M. Lévy: *Nuovo Cimento*, **16**, 705 (1960).

From the errors on m_1, m_3 and g follows an error of 1.6% on P_0, essentially determinated by the incertitude on the masses; hence this error is about one half of the correction (36).

In (36) the cut-off for short wavelengths is not cancelled; however, the result depends only logarithmically on this cut-off.

Assuming for example $\varepsilon = (1/20)m_2$ and $\lambda = 10 m_1$ we find

$$\delta p \simeq 0.032 . \tag{38}$$

Finally for the lifetime τ we get

$$\tau = 1.808(1 + 0.032)(1 \pm 0.016)\ \mathrm{s} = (1.866 \pm 0.030)\ \mathrm{s} . \tag{39}$$

* * *

We thank Professor R. Gatto and Doctor N. Cabibbo for their continuous assistance and advice. We are also grateful to Dr. S. Berman for some useful remarks.

RIASSUNTO

Abbiamo calcolato le correzioni relative al decadimento $\pi^- \to \pi^0 + e^- + \bar{\nu}$.

On the Radiative Decay Mode $K^+ \to \pi^+ + \pi^0 + \gamma$.

D. Monti, G. Quareni and A. Quareni Vignudelli

Istituto di Fisica dell'Università - Bologna
Istituto Nazionale di Fisica Nucleare - Sezione di Bologna

(ricevuto il 3 Luglio 1961)

Summary. — A decay mode: $K^+ \to \pi^+ + \pi^0 + \gamma$ has been observed. Up to now, this is the third event supporting such decay mode. The π^+ energy is 79 ± 1.5 MeV. Taking into account the available experimental data, the branching ratio, which corresponds to the energy interval $(55 \div 80)$ MeV of the positive pion, results to be $8 \cdot 10^{-4}$ radiative decays per K^+-decay. A part from fluctuations, the mentioned value might be underestimated by a factor two. In order to justify the experimental branching ratio a direct emission term is needed, in addition to the bremstrahlung term, which alone would account for a ratio of $1.6 \cdot 10^{-4}$.

During a systematic study on the K^+ decay modes by means of photographic emulsions, an unusual event has been observed. A K^+ decays at rest giving, as unique charged product, a pion of 79 MeV. The pion too decays at rest in the emulsion stack giving the decay cascade $\pi \to \mu \to e$. The K^+ belongs to the K^+-beam, as it has been controlled by following its track back and by comparing the behaviour of its ionization with that of other K^+'s decaying at rest in three charged pions (see Fig. 1). The energy of the pion was determined from its range and it agrees with grain count at the beginning of the track (see Fig. 2). No sudden changes in the ionization have been observed; therefore inelastic scattering along the particle path can be excluded. The ionization of the pion has been measured in many points of the track and its behaviour has been compared with that of other identified π-mesons (see Fig. 2). The length of the μ-meson track is 605 μm.

The possibility that this K^+ decays in flight in one of the two usual decay modes: $K^+ \to \pi^+ + \pi^0$ and $K^+ \to \pi^+ + \pi^0 + \pi^0$, is ruled out by kinematical considerations.

The more plausible interpretation of our event is a radiative decay in accord with the scheme: $K^+ \to \pi^+ + \pi^0 + \gamma$.

So far two other anomalous events were observed ([1,2]) which have been interpreted in such a way. However the energies of the pions of the two earlier events coincide so closely, (60 ± 1) MeV and (61.7 ± 1.5) MeV, that one could think to a two-body decay in which a neutral particle of 500 m_e might have been present. The energy of the pion in our event is quite different; (79 ± 1.5) MeV; therefore the interpretation of these anomalous events as radiative decays becomes even more reasonable.

The radiative decay of the K^+ is connected with a rather interesting problem. Because of the $\Delta T = \frac{1}{2}$ selection rule, the $K^+ \to \pi^+ + \pi^0$ decay is thought to go through the electromagnetic interaction. Its amplitude would arise from electromagnetic corrections of order e^2,

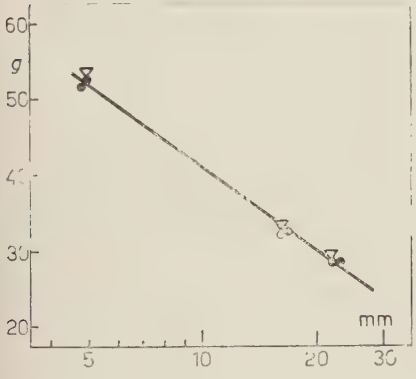

Fig. 1. – The grain density g (in arbitrary units) of K^+-meson tracks *vs.* the range. ● the K^+ undergoing radiative decay; ▽ τ-mesons.

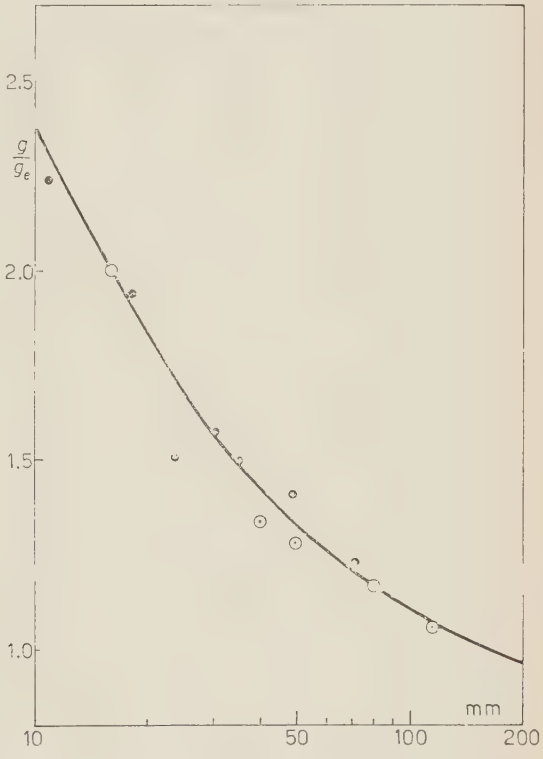

Fig. 2. – The grain density of π-meson tracks *vs.* the range. g_e is the grain density corresponding to the plateau, ● the 79 MeV π^+; ⊙ other π^+'s.

while for the radiative decay $K^+ \to \pi^+ + \pi^0 + \gamma$ the direct emission amplitude whould be of the order e. For this reason GELL-MANN ([3]) suggested that the two processes might have comparable rates. However, this fact is not confirmed

([1]) G. HARRIS, J. LEE, J. OREAR and S. TAYLOR: *Phys. Rev.*, **108**, 1561 (1957).
([2]) D. J. PROWSE and D. EVANS: *Nuovo Cimento*, **8**, 856 (1958).
([3]) M. GELL-MANN: *Nuovo Cimento*, **5**, 758 (1957).

by the experiments. GOOD [1] and more recently CABIBBO and GATTO [5] calculated the radiative rate and they found that it could be, according to the selection rule, as low as the experiments indicate. The energy spectrum of the positive pion is constructed by three additive terms: a direct emission term, the internal Bremsstahlung term (of order e^3) and an interference term. It is not possible to determine exactly the direct term because of the rather large uncertainties, mainly connected with the mass corresponding to the interaction volume, by GOOD, or with a decay constant by CABIBBO and GATTO. Also the sign of the interference term is not known. The spectrum extends from 0 to 108 MeV, the upper limit being the energy of the positive pion in the non radiative decay. Only a small region can be compared with the experimental data. In fact, it is practically impossible to distinguish between the $\pi^+ + \pi^0 + \gamma$ and the $\pi^+ + \pi^0 + \pi^0$ modes when the energy of the π^+ is smaller than 55 MeV, (the maximum energy of the π^+ in the $\pi^+ - \pi^0 + \pi^0$ mode is 53 MeV). Even the most energetic pions of the spectrum have been not recognized because of their low specific ionization, the selection criteria for searching these events being based generally on ionization cut-offs wich each laboratory has established in order to guarantee largely the complete detection of the $\pi^+ + \pi^0 + \pi^0$ decay mode or to inspect the $K_{\mu 3}$ spectrum until about 60 MeV.

The theoretical spectrum was compared with the experimental data in the energy region between 55 and 75 MeV, *i.e.*, 2 events in a sample of 8653 events. Since the internal bremsstrahlung term alone accounts for $1.2 \cdot 10^{-4}$ radiative decays per K^+-decay, the mentioned experimental rate could be explained without invoking the direct emission term or by choosing the negative sign for the interference term. Our additional event does not change appreciably the experimental situation, even though it was found in a very small sample of properly analysed K^+-decays.

We think, however, that the experimental rate was underestimated. The 8653 K^+-decays belong 5000 to the Columbia University group [6,7], 3300 to the Dublin group [8] and 353 to PROWSE and EVANS [2]. Except for this last sample, it appears from the literature that, because of technical reasons, not all decays have been analysed with the same criteria and only a fraction have been inspected in a suitable way as it is required for the detection of the $\pi^+ + \pi^0 + \gamma$ decays.

[1] J. D. GOOD: *Phys. Rev.*, **113**, 352 (1959).

[5] N. CABIBBO and R. GATTO: *Phys. Rev. Lett.*, **5**, 382 (1960).

[6] J. OREAR, G. HARRIS and S. TAYLOR: *Phys. Rev.*, **104**, 1463 (1956).

[7] S. TAYLOR, G. HARRIS, J. OREAR, J. LEE and P. BAUMEL: *Phys. Rev.*, **114**, 359 (1959).

[8] G. ALEXANDER, R. H. W. JOHNSTON and C. O'CEALLAIGH: *Nuovo Cimento*, **6**, 478 (1957).

We try here to summarize the world data in order to get a better and more complete situation of the present experimental situation. The data appears in the Table I; in the column 3, for the properly examined K^+-decays we mean the number of K^+-decays among wich radiative decays could be detected with a reasonable efficiency. The error of the sum of column 3 is no more than symbolic; it represents our estimate of the order of magnitude of the error we made in manipulating other people's data. The two doubtful decays of column 4

TABLE I.

Authors	Number of K^+-decays		Radiative decays	π^- energy (MeV)	Upper energy limit (MeV)
	Total	Properly examined			
ALEXANDER *et al.* [8]	3300	358	0		
TAYLOR *et al.* [7]	3656	2380	1	60 ± 1	83
			2?	$55 \div 83$	
OREAR *et al.* [6]	1249	0	0		
PROWSE and EVANS [5]		353	1	61.7 ± 1.5	80
G-Stack Collaboration [9]		54	0		
RITSON *et al.* [10]	766	37	0		
CRUSSARD *et al.* [11]		63	0		
HOANG *et al.* [12]	173	46	0		
BØGGILD *et al.* [13]	1257	467	0		61
Present work	9000	30	1	79 ± 1.5	80
Total		3788 ± 100	$3+2?$		

[9] G-Stack Collaboration: *Nuovo Cimento*, **2**, 1063 (1955).

[10] D. M. RITSON, A. PEVSNER, S. C. FUNG, M. WIDGOFF, G. T. ZORN, S. GOLDHABER and G. GOLDHABER: *Phys. Rev.*, **101**, 1085 (1956).

[11] J. CRUSSARD, V. FOUCHÉ, J. HENNESSY, G. KAYAS, L. LEPRINCE-RINGUET: *Nuovo Cimento*, **3**, 731 (1956).

[12] T. F. HOANG, M. F. KAPLON and G. YEKUTIELI: *Phys. Rev.*, **102**, 1185 (1956).

[13] J. K. BØGGILD, K. H. HANSEN, J. E. HOOPER and M. SCHARFF: *Nuovo Cimento* **19**, 821 (1961).

give each a secondary which goes out of the stack. The measurements on the track indicate pion masses, but the authors classified the two events as $K_{\mu 3}$ decay modes for very acceptable arguments, based on the relative rate of the two considered processes and on the probability of the measurement deviations.

It is not clear whether one must take into account these two events or not; if not, the corresponding K^+-sample should be furthermore reduced for this kind of inefficiency; if yes, one can note that the rate would become more similar to the rate given by the other laboratories.

In order to take into account also our event, we will consider the energy interval from 55 up to 80 MeV. Therefore one should multiply the number of the observed events by some factor greater than unity, in order to correct for the detection inefficiency which should have been rather important near the upper limit of the energy interval. However the most pessimistic rate $3/3\,788 \simeq 8 \cdot 10^{-4}$ is 5 times greater than the rate accounted for by the internal bremsstrahlung term alone, *i.e.*, $1.6 \cdot 10^{-4}$ radiative decays per K^+ in the range $(55 \div 80)$ MeV. Unfortunately the number of the radiative decays up to now observed is so small that one risks drawing meaningless conclusions. However the aim of our discussion is to show that: i) in order to account for the present experimental rate, the direct term is necessarily required; ii) the mentioned experimental rate being very probably underestimated by a factor 2, it is not hopeless to bring more light on the problem with an appropriate experiment.

* * *

We wish to thank Dr. E. Lofgren and the Radiation Laboratory staff of the University of California for making the exposure possible and in particular Dr. Schmitz for his valuable help during the exposure. We are also grateful to Prof. R. Gatto and Prof. A. Stanghellini for their interest in our research and for many helpful discussions.

RIASSUNTO

È stato osservato un decadimento del tipo $K^+ \to \pi^+ + \pi^0 + \gamma$. Si tratta di un evento molto raro di cui finora esistono solo tre esempi. L'energia del π^+ è 79 ± 1.5 MeV. Tenuto conto dei dati sperimentali finora a disposizione, il rapporto di disintegrazione corrispondente all'intervallo di energia del π^+ $(55 \div 80)$ MeV, risulta $8 \cdot 10^{-4}$ decadimenti radiativi per decadimento di K^+. Si ritiene che, fluttuazioni a parte, il rapporto possa essere sottostimato per un fattore 2. Per spiegare il rapporto sperimentale è indispensabile tener conto di un termine di emissione diretta oltre al termine di bremstrahlung; quest'ultimo da solo giustificherebbe un rapporto di $1.6 \cdot 10^{-4}$.

LETTERE ALLA REDAZIONE

(La responsabilità scientifica degli scritti inseriti in questa rubrica è completamente lasciata dalla Direzione del periodico ai singoli autori)

On the Two-centre Models of Particle Emission in Cosmic Ray Jets.

J. Pernegr, V. Šimák and M. Votruba

Institute of Physics of the Czechoslovak Academy of Sciences - Prague

(ricevuto il 4 Gennaio 1961)

The observation of a two-maxima shape of the angular distribution of secondary particles in high-energy cosmic ray jets has been described by Ciok *et al.* [1] and is supported by a large evidence of Gierula *et al.* [2,3]. For the description of this experimental finding empirical models have been proposed in which the emission of particles is supposed to take place from two independent centres. There are two different two-centre models: 1) the « fire-ball » model of [1,4,5] where the emitting centres are assumed to move separately from the nucleons after collision, and 2) the « isobar » or « excited nucleons » model [6,7] where particles are supposed to be emitted from the moving nucleons which become excited during their interaction.

We should like to contribute to the question of the regions of applicability of both models [6-8]. At first, we are summarizing the basic relations. Assuming forward-backward symmetry the energy balance in the c.m. system of a nucleon-nucleon interaction is given in any type of a two-centre model as follows

$$\gamma_c = \gamma_{\mathcal{N}} + \bar{\gamma} M^* , \tag{1}$$

where γ_c and $\gamma_{\mathcal{N}}$ is the energy of the nucleon before and after collision in units of Mc^2 (and, of course, γ_c is then equal to the Lorentz-factor of transformation from the c.m. system to the L-system), $\bar{\gamma}$ is the Lorentz-factor of the emitting system with respect to the c.m.-frame, $M^* = 3 n_s E_\pi / 4 Mc^2$ (where E_π is usually put equal to 0.5 GeV). Similarly as in [1] we denote by γ_1 and γ_2 the Lorentz-factors of transformation from the emitting systems to the L-system, and by n_s the number of charged secondaries.

In the fire-ball model the derived

(1) P. Ciok, T. Coghen, J. Gierula, R. Holyński, A. Jurak, M. Mięsowicz, T. Saniewska, O. Stanisz and J. Pernegr: *Nuovo Cimento*, **8**, 166 (1958); **10**, 741 (1958).

(2) J. Gierula, M. Mięsowicz and P. Zieliński: *Acta Phys. Pol.*, **19**, 119 (1960); *Nuovo Cimento*, **18**, 102 (1960).

(3) J. Gierula, D. M. Haskin and E. Lohrmann (we are indebted to Prof. Gierula for kindly sending to us the preprint).

(4) G. Cocconi: *Phys. Rev.*, **111**, 1699 (1958).

(5) K. Niu: *Nuovo Cimento*, **10**, 994 (1958).

(6) J. Burmeister, K. Lanius and H. W. Meier: *Nuovo Cimento*, **11**, 12 (1959).

(7) F. J. Farley: *Nuovo Cimento*, **16**, 209 (1960).

(8) E. G. Boos and J. S. Takibaev: *Proc. of the Moscow Cosmic Ray Conf.*, **1**, 82 (1960).

quantities γ_c, $\bar{\gamma}$ and inelasticity K are defined by the formulae:

$$\gamma_c = \sqrt{\gamma_1 \gamma_2}\,, \tag{2}$$

$$\bar{\gamma} = \frac{\gamma_1 + \gamma_2}{2\sqrt{\gamma_1 \gamma_2}}\,, \tag{3}$$

$$K = \frac{\bar{\gamma} M^*}{\gamma_c - 1} = \frac{\bar{\gamma}}{\gamma_c} M^*\,. \tag{4}$$

In the isobar model there are two ways of defining these quantities. The Berlin group ([6]) starting from the energy balance in the L-system and using consequently in eq. (1) the identity $\gamma_{\mathcal{N}} \equiv \bar{\gamma}$ obtained the expressions:

$$\gamma = \sqrt{\tfrac{1}{2}(\gamma_1 + \gamma_2)(1 + M^*)}\,, \tag{5}$$

$$\bar{\gamma}' = \frac{\gamma_c'}{1 + M^*}\,, \tag{6}$$

$$K' = \frac{\gamma_c'}{\gamma_c' - 1} \cdot \frac{M^*}{1 + M^*} = \frac{M^*}{1 + M^*}\,. \tag{7}$$

might express them as follows:

$$n_s'' = \frac{4}{3E_\pi}(2\gamma_2 - 1)\,, \tag{8a}$$

or

$$\gamma_2'' = \frac{M^* + 1}{2}\,. \tag{8b}$$

To compare mutually both modifications of the isobar model and the fire-ball model we introduce (using the equality $\gamma_c \bar{\gamma} = \gamma_c' \bar{\gamma}'$) the parameter Δ given by the formula

$$\Delta = \sqrt{\frac{2\gamma_1\gamma_2}{(\gamma_1 + \gamma_2)(1 + M^*)}}\,. \tag{9}$$

with the help of which we may rewrite conveniently the basic relations; we are summarizing them in Table I.

It is clear that in the case $\Delta = 1$ the fire ball model becomes identical with the isobar model.

In Fig. 1 we plotted the values of Δ

TABLE I.

		γ_c	$\bar{\gamma}$	K	n_s	γ_2
Fire-ball model						
Isobar model	Berlin ([6])	$\gamma_c' = (1/\Delta)\gamma_c$	$\bar{\gamma}' = \Delta\bar{\gamma}$	$K' = \Delta^2 K$	n_s	γ_2
	FARLEY ([7])	γ_c	$\bar{\gamma}$	$\Delta^2 K$	$n_s'' = \Delta^2 n_s$	γ_2
					n_s	$\gamma_2'' = \Delta^2\gamma_2$

Farley's modification of the isobar model ([7]), on the other hand, is based on the angular distribution and maintains therefore the definitions of γ_c and $\bar{\gamma}$ according to eq. (2) and (3); the inelasticity K (γ_1, γ_2, n_s) according to eq. (4) then has to be equal to K' given by eq. (7) which is independent of the angular distribution. To obtain agreement between eq. (4) and (7) a « predicted » multiplicity n_s'' or alternatively a theoretical value of γ_2'' are being used in ([7]); we against γ_c of 80 jets with $n_s \geq 6$ and $N_h \leq 2$, induced by neutral, singly charged and α-primaries which have been collected from this laboratory and from co-operating groups ([9]) as well as from

([9]) Private communication from Prof. M. DANYSZ (Warsaw), Dr. E. FENYVES (Budapest), Prof. J. GIERULA and Prof. M. MIĘSOWICZ (Cracow), Dr. K. LANIUS (Berlin), Dr. G. B. ŽDANOV (Moscow) and Prof. J. ŽDANOV (Leningrad).

literature ([10-13]). It is to be seen that fluctuations can not oppress an obvious trend of increasing Δ with γ_c. In the region of $\gamma_c < 20$ the mean value of $\Delta = 1$ *i.e.* the isobar model seems to fit the data satisfactorily, while at high energies the parameter Δ reaches values far above unity.

whereas the trend of the values of Δ is just opposite, and could not be as high as the observed values of Δ resp. Δ^2 in the high energy region.

The remarkable point of difference between the isobar and fire-ball models is the inelasticity. In Fig. 2 we have drawn the values of K (circles) and K' (crosses)

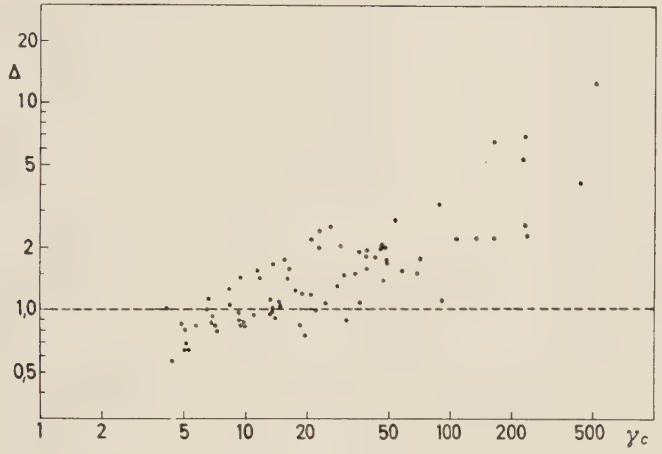

Fig. 1. – Energy dependence of parameter Δ characterizing the difference between the isobar model and the fire-ball model; dashed line for $\Delta = 1$ corresponds to isobar model.

The fact that Δ is a factor of proportionality between γ_c and γ_c' and that Δ^2 relates γ_2 and γ_2'' suggests that the influence of the energy spectrum (II approx. of CASTAGNOLI *et al.* ([14])) on the value of Δ should be considered. This influence, however, had to remain constant or rather to decrease with increasing Δ^2,

for the same collection of jets as in Fig. 1. Again, in the region of $\gamma_c < 20$ the isobar model suits better than the fire-ball model; at high energies, on the other hand, the fire-ball inelasticities K agree reasonably with direct experimental evidence, whereas the values of K' seem to be overestimated.

Following FARLEY (cfr. Fig. 2 in ([7])) we tried to test the applicability of the isobar model comparing the observed values n_s and γ_2 with the theoretical curve drawn according to eq. (9); we divided our collection of jets into two groups with $\gamma_c < 20$ and with $\gamma_c > 20$ (Fig. 3). The points corresponding to jets from the low energy group are cumulated around the curve drawn for the isobar model in agreement with ([7]); it would be difficult, however, to make similar observation for the high energy jets.

From Figs. 1, 2 and 3 we are inclined

([10]) B. EDWARDS, J. LOSTY, D. H. PERKINS, K. PINKAU and J. REYNOLDS: *Phil. Mag.*, 3, 237 (1958).

([11]) M. SCHEIN, D. M. HASKIN, E. LOHRMANN and M. W. TEUCHER: *Phys. Rev.*, 116, 1238 (1959).

([12]) J. G. MCEVAN: *Phys. Rev.*, 115, 1712 (1959).

([13]) R. G. GLASSER, D. M. HASKIN, M. SCHEIN and J. J. LORD: *Phys. Rev.*, 99, 1555 (1955).

([14]) C. CASTAGNOLI, G. CORTINI, C. FRANZINETTI, A. MANFREDINI and D. MORENO: *Nuovo Cimento*, 10, 1539 (1953).

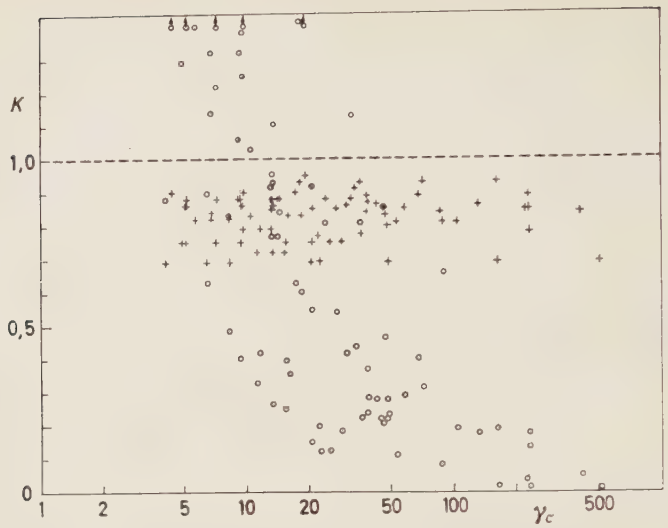

Fig. 2. – The dependence on γ_c of the inelasticity K defined with the help of eq. (4) (fire-ball model)—circles, and of the inelasticity K' according to eq. (7) (isobar model)—crosses.

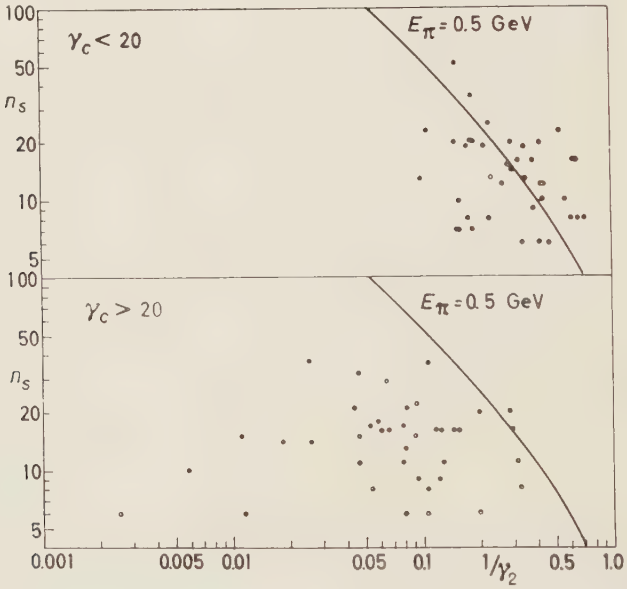

Fig. 3. Observed multiplicity n_s plotted against the values of $1/\gamma_2$. The curve is drawn according to eq. (8) for the isobar model.

to draw the conclusion that the (isobar) model of excited nucleons may describe well the interactions with primary energy below $\sim 10^{12}$ eV ($\gamma_c < 20$), while the region of applicability of the model of « ionized » nucleons (fire-ball model) lies above $\sim 10^{12}$ eV. Fig. 1 shows also that the boundary region between both models is rather broad and suggests that besides primary energy other parameters influence the excitation or « ionization » of the interacting nucleons.

IL NUOVO CIMENTO Vol. XXI, N. 3 1° Agosto 1961

The Knight Shift in the Superconducting State.

R. Suzuki and M. Akano

Department of Physics, Tokyo College of Science - Tokyo

(ricevuto il 19 Gennaio 1961)

Recently several attempts have been made to give the correct explanation of the finite Knight shift for superconductors by using the theory of Bardeen *et al.* and Bogoliubov [1]. These approaches are roughly classified into two groups; the one [2] shows that, by taking account of the significance of the size parameter in the theory, a finite Knight shift is explained phenomenologically, and the other [3] that the frequency shift for superconductors is deduced indirectly to be zero from predicting the exponentially vanishing susceptibility near $T=0$ °K. In particular, anticipating the possibility of the occurrence of paramagnetism in superconducting electrons in the latter case, Yoshida and Schrieffer rearranged the operators in the magnetic interaction and calculated the electronic spin susceptibility for the superconducting ground state. On the other hand, Reif's [4] experimental result shows that the Knight shift in colloidal superconducting mercury is 1.6%, and Knight *et al.* find a Knight shift of only 0.5% for Hg and 0.55% for Sn [5] when extrapolated to $T=0$ °K.

The purpose of the present note is, instead of calculating the susceptibility of electrons directly, to consider an alternative way of computing the shift and to investigate the dependence of the Knight shift on the energy gap appearing in the energy spectrum of superconductors. According to the proposal of Knight [6], the frequency shift of nuclear magnetic resonance is caused by the orientation of spin moments of conduction electrons near the top of the Fermi distribution.

Thus we take the following processes as relevant to the Knight shift; the magnetic interaction of electrons first polarizes the electron gas, and then it couples with the nucleus through the electron-nuclear hyperfine interaction, and vice versa. Hence,

(1) J. Bardeen, L. N. Cooper and J. R. Schrieffer: *Phys. Rev.*, **108**, 1175 (1957); N. N. Bogoliubov: *Nuovo Cimento*, **7**, 804 (1958); and N. N. Bogoliubov, V. V. Tolmachev and D. V. Shirkov: *A New Method in the Theory of Superconductivity* (Moscow, 1958).

(2) R. A. Ferrell: *Phys. Rev. Lett.*, **3**, 262 (1959); P. C. Martin and L. P. Kadanoff: *Phys. Rev. Lett.*, **3**, 322 (1959).

(3) K. Yoshida: *Phys. Rev.*, **110**, 769 (1958); J. R. Schrieffer: *Phys. Rev. Lett.*, **3**, 323 (1959).

(4) F. Reif: *Phys. Rev.*, **106**, 208 (1957).

(5) W. D. Knight, G. M. Androes and R. H. Hammond: *Phys. Rev.*, **104**, 852 (1956); G. M. Androes and W. D. Knight: *Phys. Rev. Lett.*, **2**, 386 (1959).

(6) W. D. Knight: *Solid State Physics* (New York, 1956).

we have the following operator, the expectation value of which for the unperturbed Bogoliubov ground state gives rise to the Knight shift,

$$K = H_{qn}\frac{1}{b}H_{\gamma q} + H_{\gamma q}\frac{1}{b}H_{qn}\,; \qquad b = E_0 - H_0 - H_g + i\eta\,, \tag{1}$$

where H_0 is the energy of the free electron, phonon gas and nucleus, H_g the electron phonon interaction energy, $H_{\gamma q}$ the magnetic energy of electrons, and H_{qn} the hyperfine interaction between nucleus and conduction electrons. Of course, these operators are written in the second quantized form and further transformed by Bogoliubov's technique,

$$H_{\gamma q} = \mu_e g H \{g^+_{kk'}(\alpha^*_{k'0}\alpha_{k0} - \alpha^*_{k'1}\alpha_{k1}) + f^-_{kk'}(\alpha^*_{k'0}\alpha^*_{k1} - \alpha_{k'1}\alpha_{k0})\}\,, \tag{2a}$$

$$H_{qn} = \frac{J}{2N}\sum_{pq}\{I^+_{p-q}[g^+_{pq}\alpha^*_{p1}\alpha_{q0} + \tfrac{1}{2}f^-_{pq}(\alpha^*_{p1}\alpha^*_{-q1} + \alpha_{-p0}\alpha_{q0})] + \text{c.c.} + \tag{2b}$$
$$+ I^z_{p-q}[g^+_{pq}(\alpha^*_{p0}\alpha_{q0} - \alpha^*_{p1}\alpha_{q1}) + f^-_{pq}(\alpha^*_{p0}\alpha^*_{-q1} - \alpha_{-p1}\alpha_{q0})]\}\,,$$

with

$$I^+_p = \sum I_i \exp\,[-iP\cdot R]\,,\ \text{etc.}\,,$$

and

$$f^-_{kk'} = u_k v_{k'} - u_{k'}v_k\,, \qquad g^+_{kk'} = u_k u_{k'} + v_k v_{k'}\,,$$
$$a_{k\uparrow} = u_k\alpha_{k0} + v_k\alpha^*_{k1}\,, \qquad a_{-k\downarrow} = u_k\alpha_{k1} - v_k\alpha^*_{k0}\,,$$

where α^*, α obey the Fermion commutation rule, provided that $u_k^2 + v_k^2 = 1$. If we calculate its expectation value for the unperturbed Bogoliubov ground state, inserting expressions (2) into eq. (1), we have the shift of magnetic energy in the form

$$\Delta H = \frac{2J\mu_l g H}{N}\sum_{l,k}\left|-I^z_{l-k}\frac{1}{E_l - E_k}\langle k\,|\,W\,|\,k\rangle\left\{u_l^2 v_k^2 + u_k^2 v_l^2 - 2(uv)_l(uv)_k\right\}\right|\,. \tag{3}$$

The matrix element $\langle k\,|\,W\,|\,k\rangle$ is the diagonal element of the operator W which is obtaine by approximately replacing the propagator $1/b$ with the operator $[a - Hg(1/a)Hg]^{-1}$, in order to calculate the multiple scattering of phonons by quasi-particles in the intermediate states, except for multiple exchange of phonons, where $a \equiv E_0 - H_0$.

The integral equation for W is suitably rewritted by using scattering matrix, and it is easily proved that the integral equation is approximately solved by the choice of a suitable trial function relevant to the multiple phonon scattering. Thus the trial function is [7]

$$R = \frac{1}{1 \quad q^2\left(\tfrac{1}{2} \cdot \alpha\xi\,(\alpha^2 \quad \xi\text{-})\right)F(\eta)}\,. \tag{4}$$

[7] R. SUZUKI and M. AKANO: *Nuovo Cimento*, **16**, 570 (1959).

Now, substituting Bogoliubov's values for u_k and v_k in eq. (3), the magnetic energy shift is obtained in the form of

$$\Delta H = -\frac{J}{N}(\mu_e^2 gH)(mk_F/2\pi^2)^2 I^2 R(Z_1 - cZ_2)\,, \tag{5}$$

where

$$Z_1 = -\frac{8}{3}(2\pi)^6\gamma\,, \qquad Z_2 = -\frac{\pi}{4}\log\frac{\sqrt{c^2+\bar{\xi}^2}+\bar{\xi}}{\sqrt{c^2+\bar{\xi}^2}-\bar{\xi}}\,.$$

γ being the cut-off energy in order of magnitude of $E_F\cdot 10^{-4}$ or energy gap C_0 at $T=0$ °K. Further, by rewriting the square energy density $(mk_F/2\pi^2)^2$ as $\frac{9}{8}(n/E_p)^2$, the Knight shift is given by

$$\frac{\Delta H}{H} = \frac{3n}{4N}J\frac{3n\mu_e^2}{2E_F}\frac{R}{E_F}(Z_1 - cZ_2)\,. \tag{6}$$

Since, in eq. (6), the second term in brackets involves the energy gap c explicitly and, therefore, vanishes as $c\to 0$, it is thought to be a necessary term for describing the Knight shift for superconductors. On the other hand, the first term depends implicitly on c only via the trial function, and, it will give the Knight shift proportional to the paramagnetic susceptibility $\chi_p = 3n\mu_e^2/2E_F$ as $c\to 0$. In order to check up our result with experiments, it is necessary that one normalizes the contribution from the first term to the values (2.5%) for mercury, or (0.75%) for tin at the transition temperature or at $c=0$, since the zero-order interaction responsible for the Knight shift in the normal metals hardly gives the contributions to that in the superconducting state. Then we have

$$Z_1 = \frac{\alpha\pi}{4}C_0\,, \tag{7}$$

where α is determined from Reif's measurements to give about 2.0 for mercury or 2.3 for tin, and C_0 is the energy gap at absolute zero. The feature of eq. (6) is shown in Fig. 1, in which the constant factors are adjusted by the values depending on elements; for example,

$$E_F(\mathrm{Hg}) = 6.84\ \mathrm{eV}\,, \quad C_0 = 2.0 \sim 3.5kT_0 = 0.71 \sim 1.25\cdot 10^{-3}\ \mathrm{eV}\,, \quad J(\mathrm{Hg}) \approx 0.24\ \mathrm{eV}\,,$$

and

$$E_F(\mathrm{Sn}) = 9.64\ \mathrm{eV}\,, \quad C_0 = 2.0 \sim 3.5kT_0 = 0.65 \sim 1.13\cdot 10^{-3}\ \mathrm{eV}\,, \quad J(\mathrm{Sn}) \approx 0.74\ \mathrm{eV}\ [8]\,.$$

In Fig. 1, the lower curves for the respective metals are drawn for the energy gap $3.5kT_c$ and the upper ones for $2.0kT_c$. The cross signs indicate the experimental values when $C_0 = \bar{\xi}$, where $\bar{\xi}$ is in the range of $\frac{1}{2} \leqslant (\bar{\xi}/c) \leqslant 1$. These curves are given

[8] See reference [4].

for $g^2F(\beta)=0.5$, but the change of this value gives rise to only a slight shift against the drawn curves.

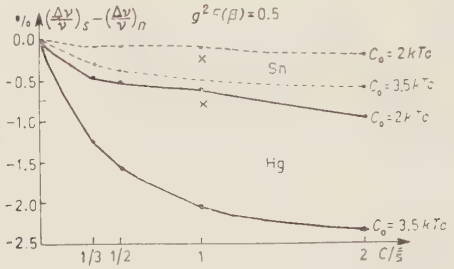

Fig. 1. The Knight shifts for superconducting metals.

In conclusion, our method may not necessarily be ingenious for describing the Knight shift in the superconducting state, but it will be, at least, possible to say that, so long as the Knight shift for superconductors is considered to be dependent on the energy gap, it does not vanish, when extrapolated to the maximum gap, contrary to the results of cited papers. However, when the integral equation for W can be analytically solved and the detailed dependence of the energy gap on temperature is more clarified, more correct result will be obtained.

Y^{*0} Effects in the Reaction $K^- + p \to \Sigma + \pi$ on Complex Nuclei (*).

Y. Eisemberg and G. Yekutieli
The Weizmann Institute of Science - Rehovoth

P. Abrahamson and D. Kessler
Israel Atomic Energy Establishment - Rehovoth

(ricevuto il 16 Aprile 1961)

The existence of a $\Lambda^0\pi$ resonant state (refered to as Y*) has been demonstrated recently by several groups ([1-3]). In these experiments the reactions

$$K^- + p \to \Lambda^0 + \pi^- \ ([1,2]),$$

and

$$K_2^0 + p \to \Lambda^0 + \pi^0 + \pi^- \ ([3]),$$

were studied, and a strong correlation between the Λ^0-hyperon and the pions was observed. Thus, the existence of Y* was established. Since fast K beams were used by the above groups, the main production reactions which presumably occured were: $K^- + p \to Y^{*\pm} + \pi^{\mp}$ with the subsequent decay: $Y^{*\pm} \to \Lambda^0 + \pi^{\pm}$. The mass of $Y^{*\pm}$ turned out to be about 1385 MeV and its full width at half maximum was given as 30 ([2,3]) to 60 ([1]) MeV.

The production of Y* by K^--captures at rest on free hydrogen is prohibited. However, Y* production in K^- captures at rest in deuterium is possible; *i.e.* $K^- + (np) \to Y^* + p \to \Lambda^0 + \pi^- + p$. Indeed, the Deuterium Bubble Chamber group recently studied the influence of the $\Lambda^0\pi$ resonance on correlation in the $K^- + d \to \Lambda^0 + \pi^- + p$ reaction and have found large effects ([4]). They estimate about one third of all events of the above type are associated with the Y* channel. It should be noticed that in all above experiments (except ref. ([3])) the charged Y*-decay was studied: $Y^{*\pm} \to \Lambda^0 + \pi^{\pm}$. In the K_2^0 experiment ([3]), however, 18 examples of $Y^{*0} \to \Lambda^0 + \pi^0$ were observed.

In the present experiment we studied the effects of Y^{*0} production in the absorption of K^--mesons at rest and in flight (average kinetic energy, $\bar{T}_K = 50$ MeV) on complex nuclei in

(*)Supported in part by the European Office, USAF, Contract AF 61 (052)-371.

([1]) M. Alston, L. W. Alvarez, P. Eberhard, M. L. Good, W. Graziano, H. K. Ticho and S. G. Wojcicki: *Phys. Rev. Lett.*, **5**, 520 (1960).

([2]) M. Ferro-Luzzi, J. P. Berge, J. Kirz J. J. Murray, A. H. Rosenfeld and M. Watson *Bull. Am. Phys. Soc.*, **5**, 509 (1960).

([3]) H. J. Martin, L. B. Leipuner, W. Chinowsky, F. T. Shively and R. K. Adair: *Phys. Rev. Lett.*, **6**, 283 (1961).

([4]) O. I. Dahl, N. Horwitz, D. H. Miller, J. J. Murray and P. G. White: *Phys. Rev. Lett.*, **6**, 142 (1961).

nuclear emulsions. Since Y* has I-spin one, the only possible decay modes of Y^{*0} into Σ-hyperons is: $Y^{*0} \to \Sigma^{\pm} + \pi^{\mp}$. This reaction is relatively easy to study in emulsions. In a nuclear emulsions stack, exposed to the 300 MeV/c K^- beam at Berkeley, we analyzed the stars from which a $\Sigma^{\pm}$ and a pion were emitted. No dip cut-off was applied to the stars in flight. However, for the stars at rest we accepted only events in which the pion dip was less than $\sim 30°$. In Figures 1*a* and 2*a* we have plotted the variable M, for the stars at rest [5] and in flight, respectively, according to the invariant relation

$$M^2 = (W_\Sigma + W_\pi)^2 - (\boldsymbol{P}_\Sigma + \boldsymbol{P}_\pi)^2 ,$$

where W_i is the total energy and $\boldsymbol{P}_i$ is the vector momentum of each particle. For comparison, we give in Fig. 1*b* and 2*b* the distribution of the quantity $W = W_\Sigma + W_\pi$. The typical error on the value of M was ± 6 MeV. In a few events, only an upper limit could be determined. These are marked with an arrow in the figures.

It is clear from Fig. 1 and 2 that there is a marked peak in the M-distribution, in the neighborhood of 1 400 MeV, superimposed upon a broad background. We should like to argue now that this peak can not be explained in terms of the direct reaction:

$$K^- + p \to \Sigma + \pi ,$$

and that it must be due to Y^{*0} production, namely: $K^- + \mathcal{N}$ (bound) $\to Y^{*0}$ and $Y^{*0} \to \Sigma + \pi$.

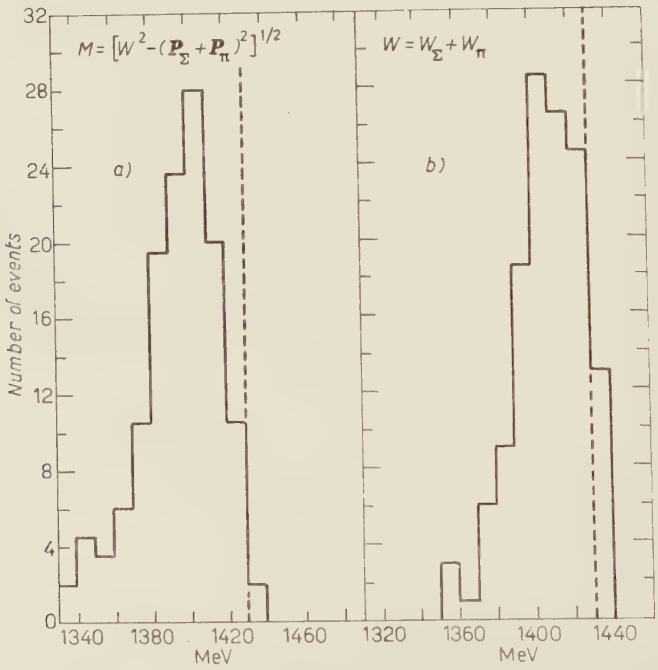

Fig. 1. – K^- absorption at rest on complex nuclei (130 events). *a*) Invariant mass (M) distribution. *b*) Total Σ and π energy (W) distribution. The broken line indicates the maximum possible energy.

[5] We have included in Fig. 1*a* 37 events found by F. C. GILBERT, C. E. VIOLET and R. S. WHITE: *Phys. Rev.*, **107**, 228 (1957).

We first examine the K^--captures at rest and compare the total energy distribution W (Fig. 1*b*) of the $(\Sigma+\pi)$ pairs to the expected distribution of the quantity M. If indeed all pion-hyperon pairs are due to the direct reaction, the M-distribution is expected to be wider than the total energy distribution and shifted to lower energy values. Using the model of CAPPS (6) for K^--absorption, we estimate that a point representing a typical pair on the total energy plot, will be shifted on the M-plot to lower energies by about 25 MeV with a spread of the same order. On the other hand, if an M-distribution narrower than the W-distribution is observed, it must be due to the decay of a Y*⁰ particle. It turns out indeed, in the present experiment (see Fig. 1 and 2), that the basis of the mass distribution is wider, but its peak is higher and more pronounced than the W-distribution. This observation strongly suggests that the observed mass distribution is a superposition of two distributions: a wide distribution due to direct production of $\Sigma+\pi$ pairs, and a narrow resonance peak due to Y*⁰ decays. It is estimated that about $\frac{1}{3}$ of the $(\Sigma+\pi)$ pairs in K^--captures at rest are due to Y*-decays. The M-distribution of the directly produced pairs is asymmetric towards higher M-values. Therefore the mass of the Y*⁰ is expected to be somewhat lower than 1 400 MeV (the peak value of our observed mass distribution), in better agreement with the values quoted for the mass of the charged Y*.

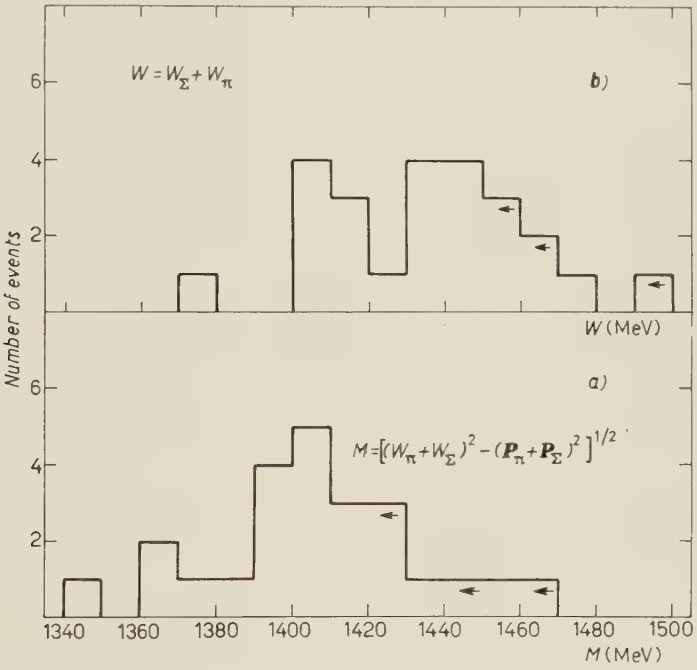

Fig. 2. – K^- interactions in flight on complex nuclei (24 events). *a*) Invariant mass (M) distribution. *b*) Total Σ and π energy (W) distribution.

Similar considerations are applied to the case of K^--capture in flight. In this

(6) R. H. CAPPS: *Phys. Rev.*, **107**, 239 (1957).

case, because of the wider energy range available for the direct reaction, the difference between the mass distributions for the Y*-decay pairs and the directly produced ones is expected to be considerable. Again comparing the total energy distribution of $(\Sigma+\pi)$ pairs produced in flight to the M-distribution, (Fig. 2*b* and 2*a*), one can, in spite of the poor statistics, detect the wide distribution of the directly produced pairs and the peak of Y^{*0}-decay.

In conclusion, we should like to summarize our results:

1) The existence of $Y^{*0}\to\Sigma^{\pm}+\pi^{\mp}$ may be regarded as established.

2) The mass of Y^{*0} seems to be greater than the mass of $Y^{*\pm}$ by $(10\div15)$ MeV.

3) The width of the resonance at half maximum should be less than our observed width (~ 40 MeV), which includes the natural width and also our experimental spread.

4) Very roughly, about $\frac{1}{3}$ of all $\Sigma^{\pm}+\pi^{\mp}$ production in K^--absorption on emulsion proceed via the Y* channel.

5) We should like to suggest the so called « multi-nucleon » K^--captures at rest, $K^-+2\mathcal{N}\to$ hyperon + nucleon, are produced in a two-step process [7] via Y*:

$$K^-+\mathcal{N}\,(\text{bound})\to Y^*$$

and

$$Y^*+\text{nucleon}\to\text{hyperon}+\text{nucleon}\,.$$

* * *

We are very grateful to G. Goldhaber and S. Goldhaber for calling our attention to the problem and for participating in the early stage of the experiment, and to H. J. Lipkin and I. Talmi for many interesting and stimulating discussions. Are sincere thanks are due to K. Gottstein who lent us the stack and to the Bevatron crew who performed the exposure. Without their effort this experiment would not have been possible.

The help of A. Avni, M. Friedman and R. Gottesman in the measurements is greatly appreciated.

[7] Y. Eisenberg, M. Friedman, G. Alexander and D. Kessler: *Nuovo Cimento*, in press (1961).

Leptonic Decay of a Σ-Hyperon.

B. Bhowmik

Department of Physics, University of Delhi - Delhi

(ricevuto il 16 Maggio 1961)

According to the universal V-A interaction theory ([1,2]) of weak interaction, hyperons are expected to decay in the leptonic mode in a few percent of all modes, provided there is no strong renormalisation effect. Two clear cases of Λ^0-decay in the leptonic mode with electron secondary have been observed by Berkeley bubble chamber groups ([3,4]) but no event with μ^--secondary has been recorded. The observed rate is almost an order of magnitude less than the predicted rate. The evidence for leptonic decay ([5-7]) of the Σ-hyperon is poor. One probable case of decay in flight of $\Sigma^\pm \to e^\pm$ or $\mu^\pm$ has been reported earlier from emulsion work ([8]). The purpose of this note is to report what appears to be a clear case of leptonic decay of a Σ^--hyperon with e^- as the charged secondary.

The event was found amongst 91 Σ-hyperon decays obtained during the course of an analysis of K^--stars in two emulsion stacks exposed to the magnetically separated Berkeley K^--beam. Details of exposure and scanning procedure have been given elsewhere ([9]). A K^--meson incident from the beam direction and identified by g^*-range measurement comes apparently to rest in the expected region of stopping K^--mesons. Three tracks are produced at its end, a grey track 55.05 mm range, a black track 381 μm range and a short prong 3.9 μm range (see photograph). The grey track is identified as π^+ meson by its terminal behavior characteristic of π-μ-e decay, the muon having a range of 620 μm. The black track is presumably due to a stable particle since no decay secondary could be associated at its end. Using the constant sagitta measurements we get a mass $= 825^{+907}_{-355}$ MeV. This track is therefore labelled as proton. The short prong is not amenable to any

([1]) R. P. Feynman and M. Gell-Mann: *Phys. Rev.*, **109**, 193 (1958).

([2]) E. C. G. Sudarshan and R. E. Marshak: *Phys. Rev.*, **109**, 1860 (1958).

([3]) F. S. Crawford, Jr., M. Cresti, M. L. Good and H. K. Ticho: *Phys. Rev. Lett.*, **1**, 337 (1958).

([4]) P. Nordin, J. Orear, L. Reed, A. H. Rossenfeld, F. T. Solmitz, H. D. Taft and R. D. Tripp: *Phys. Rev. Lett.*, **1**, 380 (1958).

([5]) D. A. Glaser: *Proc. Conf. on High Energy Physics* (Kiev, 1959), p. 242.

([6]) K. Gottstein: *Proc. Conf. of High Energy Physics* (Rochester, 1960), p. 430.

([7]) M. Schwartz: loc. cit. p. 726, see discussion.

([8]) J. Hornbostel and E. O. Salant: *Phys. Rev.*, **102**, 502 (1956).

([9]) B. Bhowmik, P. C. Jain and P. C. Mathur: *Nuovo Cimento*, **20**, 857 (1961).

measurement for its identification. However, at its end a flat light track of plateau ionisation $g^* = 1.15 \pm 0.08$ is associated. On the scattering of the secondary we estimate its $p\beta = 28.5 \pm 6.8$ MeV/c.

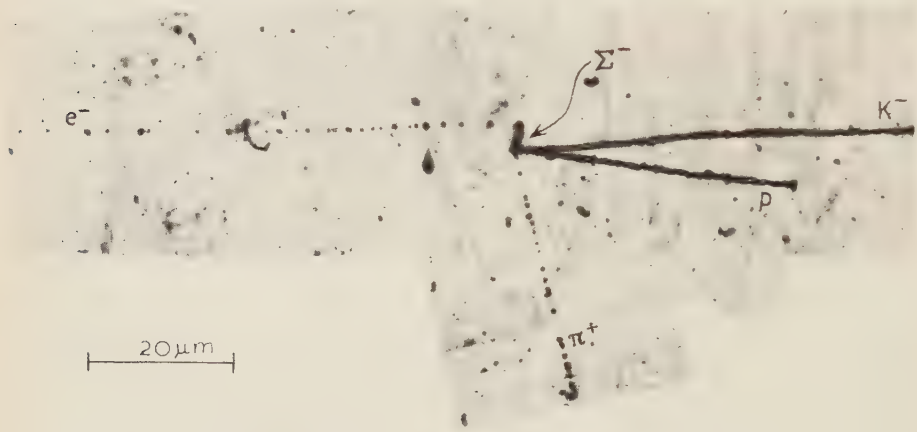

Fig. 1. – Leptonic decay of a Σ^--hyperon, $\Sigma^- \rightarrow n + e^- + \bar{\nu}$.

The secondary is therefore identified as an electron. One can consider the unstable prong as an example of β-decay of an excited nucleus. This possibility is discounted on the ground that the observed energy 28.0 ± 6.8 MeV of the light secondary is very much higher than the upper limit of the kinetic energy of electrons emitted from known β-emitters amongst the light nuclei. The other possibilities are that the prong is a case of leptonic decay of either (i) a π-meson, (ii) a K-meson (iii) or a Σ-hyperon. Possibilities (i) and (ii) are eliminated from the terminal behaviour of the incident K^--meson. There is definite sign of interaction at its end with the production of a fast π^+-meson of kinetic energy 65.65 MeV. This completely rules out the production of a second π-meson, and also the possibility of re-emergence of the incident K^--meson, which might subsequently undergo β-decay. We therefore interpret the unstable prong as decay of a Σ^--hyperon, produced by the capture of the K^--meson by a bound proton according to the reaction $K^- + p \rightarrow \Sigma^- + \pi^+ + Q$. The assignment of the charge of the hyperon is based on the fact that Σ and π must have opposite charge. This criterion has been applied with considerable success in case of interactions with bound nucleons although it is absolute only in the case of free hydrogen capture. Only one case has been reported ([10]) so far where both the partners have the same sign of the charge. This is expected in case of two nucleon collision where a Σ^--hyperon can be produced in association with π^--meson according to the reaction $K^- + n + n \rightarrow \Sigma^- + p + \pi^-$. Since no such postulated reaction is possible for the production of $\Sigma\pi$ event with both signs positive we conclude that the π^+-meson must have a Σ^- partner. The charge assignment is therefore unique.

The negative hyperon can decay only in flight. To calculate the rest system energy of the decay electron, the space angle between the two tracks and the velocity of the hyperon at the

([10]) M. Nikolić, Y. Eisenberg, W. Koch M. Schneeberger and H. Winzeler: *Helv. Phys. Acta*, **33**, 221 (1960).

decay point are required. The measured space angle is 108.7° but the energy of the hyperon cannot be estimated by any direct measurement on the prong. However, an indirect estimate can be made from the knowledge of the space angle between the $\Sigma\pi$ pair. The total kinetic energy $T_\pi + T_\Sigma$ lies within narrow limits when the pair is emitted making space angle $> 110°$. For $\Sigma^+\pi^-$ pair it has been determined [11] as 87.0 MeV. Our estimated value for $\Sigma^-\pi^+$ pair is (79.3 ± 2.1) MeV. Since the space angle between the $\Sigma^-\pi$ pair in the present case is 148.4° the wide angle criterion is clearly satisfied. We ignore the presence of the short proton track of 8 MeV which essentially is an evaporation prong. The kinetic energy for the Σ-hyperon therefore is (14 ± 2) MeV and the corresponding rest system energy of the electron for the measured space angle is 30.1 MeV. The transformation to rest system is insensitive to primary velocity.

The leptonic decay of a Σ^--hyperon with an electron secondary having energy $(30 + 7)$ MeV cannot be due to the rare (frequency $\sim 10^{-9}$) strangeness conserving decay mode $\Sigma^- \to \Sigma^0 + e^- + \bar{\nu}$, since the maximum energy of the electron in this mode could only be 4.5 MeV. For strangeness conserving Λ^0 mode and the strangeness violating neutron mode the upper limit of the energy is 79 and 229 MeV respectively. The event may therefore belong to either of the modes. The expected frequency for the two modes are $1.8 \cdot 10^{-4}$ and $5.8 \cdot 10^{-2}$, respectively, and on this ground we prefer to label the event as the decay of a Σ^--hyperon in strangeness violating neutron mode according to the scheme:

$$\Sigma^- \to n + e^- + \bar{\nu} .$$

Weak interaction of mesons and baryons must be reduced to the weak interactions of a minimum number of particles and the Sakata [12] model precisely does this by assuming only three particles Λ^0, n and p among the strongly interacting particles as elementary. Among the various well defined corollaries of the principle of minimal weak interaction we have a prediction that $\Delta S = \Delta Q$ is permitted whereas $\Delta S = -\Delta Q$ is forbidden which necessarily means that the decay process $\Sigma^- \to n + e^- + \bar{\nu}$ is allowed whereas $\Sigma^+ \not\to n + e^+ + \nu$ is forbidden. These predictions are consequences of such deep-seated formulation of the theory that observation of a single case of Σ^+-decay with μ^+ secondary will completely overthrow the theory. In the case of electronic mode, observation of secondary with energy greater than 72 MeV (the maximum for Λ^0 mode) will establish unambiguously the existence of the mode $\Sigma^+ \to n + e^+ + \nu$ and violate the prediction. A crucial test of the validity of the theory is therefore provided by the observation of stangeness violating leptonic Σ^--decay and the absence of Σ^+-decay.

In our sample we have 28 Σ-decays in flight into light particles of which 8 have been identified as $\Sigma^+ \to \pi^+$, 7 as $\Sigma^- \to \pi^-$ and one as $\Sigma^- \to e^-$; the remaining 12 are are unidentified $\Sigma^\pm$-decays. We distribute them equally between the two charges according to the statistics of the identified sample which gives us in all 14 Σ^--decays. The observed frequency of Σ^- leptonic decay from our sample therefore is 7.3 per cent. This is consistent with the predicted rate, although on world statistics the observed rate is almost an order of magnitude less. This gap arises partly due to the detection inefficiency in the experimental set up. Slow secondary electrons are generally confused with

[11] S. C. Freden: H. N. Kornblum and R. S. White: *Nuovo Cimento*, **16**, 611 (1960).

[12] S. Sakata: *Prog. Theor. Phys. (Kyoto)*, **16**, 686 (1956).

background electron, whereas in case of fast electrons above 100 MeV the discrimination between electron and pion is poor. From this consideration only $\frac{1}{3}$ of the phase space is usable for analysis, therefore the observed rate should be increased by a factor of three.

The observed Σ^--decay rate based on world emulsion data is about 1/200 which corrected for detection efficiency becomes 1.5 per cent. This is not inconsistent with the theoretical rate particularly in view of the fact that certain approximations are involved in the calculation of theoretical rates. There are indications ([13]) that the effective coupling constant is much smaller than unity, and when this approximation is removed the true theoretical rate may be down by several times. However, there is no ambiguity regarding the theoretical prediction of Σ^+ leptonic decay rate which must necessarily be zero. More than 1000 Σ^+-decays have been observed in emulsion work without recording a single leptonic decay. Neglecting detection inefficiency which affects decays in flight into light particles forming only 20 per cent of total decays, the limit for Σ^+ leptonic decay rate can be set as less than 0.1 per cent.

* * *

Our thanks are due to Mrs. JYOTIRMOYEE BHOWMIK who found the event and made numerous careful measurements. We are indebted to Professor E. J. LOFGREN for exposure facilities and to Professor D. J. PROWSE for making the exposure for us. We thank Professor C. F. POWELL for the processing facility at Bristol. We are grateful to the Department of Atomic Energy for financial support of the research project.

Note added in proof.

Since this letter was with the printers a clear example of electronic decay of Σ^--hyperon has been reported from K^--capture stars in hydrogen bubble chamber ([14]). Another case of strangeness violating Σ^- leptonic decay in the mode $\Sigma^- \to n + e^- + \bar{\nu}$ was observed in propane bubble chamber ([15]) irradiated with 2 GeV π^- beam. However the conclusions regarding low leptonic decay rates of hyperons drawn in reference ([14]) is in variance with our finding. We believe that the experimental decay rates corrected for scanning loss are consistent with the predicted rate from UFI theory. This conclusion is further supported by our work ([16]) on leptonic decay of Λ^0-hyperon in the mode $\Lambda^0 \to p + e^- + \bar{\nu}$. Our Λ^0 leptonic decay rate on the basis of two events is 1.3% as against theoretical decay rate of 1.6 %. We therefore suspect strong scanning bias as the cause of low observed decay rate quoted by HUMPHREY *et al.* ([14]).

([13]) I. OKUN: *Ann. Rev. Nucl. Sci.*, **9**, 61 (1959).

([14]) W. E. HUMPHERY, J. KIRZ, A. H. ROSENFELD, J. LEITNER and Y. I. RHEE: *Phys. Rev. Lett.*, **6**, 478 (1961).

([15]) P. FRANZINI and J. STEINBERGER: *Phys. Rev. Lett.*, **6**, 281 (1961).

([16]) B. BHOWMIK, D. P. GOYAL and N. K. YAMDAGNI: *Leptonic decay of Λ^0-hyperon*, *Nuovo Cimento*: to be published.

Remark on the Radiative Muon Decay in the Theory with an Intermediate Vector Meson.

Z. Bialynicka-Birula (*)

Department of Physics and Astronomy, University of Rochester - Rochester, N. Y.

(ricevuto il 19 Maggio 1961)

It is well known that there is a great difficulty in explaining the lack of the radiative muon decay in a theory with an intermediate charged vector meson. Such a theory was discussed by many authors (1). Experiments provide the upper limit for the ratio of this decay to the usual muon decay (2).

$$\varrho = \frac{R(\mu \to e + \gamma)}{R(\mu \to e + \nu + \bar{\nu})} < 1.2 \cdot 10^{-6} .$$

This problem was examined by several authors (3). The usual theory with an intermediate meson is non-renormalizable and therefore they had to introduce a cut-off Λ (4) in order to compute ϱ even in the lowest order of perturbation theory. The result is strongly dependent on Λ. If the vector meson has no anomalous magnetic moment one must take Λ equal approximately 0.2 of the vector meson mass to obtain ϱ in agreement with experiment. One can obtain a reasonable value of Λ if the anomalous magnetic moment 0.75 is given to the vector meson.

The purpose of this note is to test another possibility of introducing the charged vector meson into the theory of weak interactions. The following form of free Lagrangian for the meson φ_μ is assumed

$$\mathscr{L}_0 = -\partial^\mu \varphi_\nu^+ \partial_\mu \varphi^\nu + M^2 \varphi_\mu^+ \varphi^\mu , \tag{1}$$

(*) On leave of absence from the Institute of Physics, Polish Academy of Sciences, Warsaw, Poland.

(1) J. Schwinger: *Ann. Phys.*, **2**, 407 (1957); R. P. Feynman and M. Gell-Mann: *Phys. Rev.*, **109**, 193 (1958); E. C. G. Sudarshan and R. E. Marshak: *Phys. Rev.*, **109**, 1860 (1958).

(2) The lowest limit was obtained by S. Frankel, V. Hagopian, J. Halpern and A. L. Whetstone: *Phys. Rev.*, **118**, 589 (1960).

(3) G. Feinberg: *Phys. Rev.*, **110**, 1482 (1958); Ph. Meyer and G. Salzman: *Nuovo Cimento*, **14**, 1310 (1959); M. E. Ebel and F. J. Ernst: *Nuovo Cimento*, **15**, 173 (1960).

(4) The result is of course dependent on the form of the cut-off factor. In all papers mentioned in (3) it was chosen to be $\Lambda^2/(\Lambda^2 + p^2)$.

which leads to the meson propagator in the form

$$\langle 0 \mid T\varphi_\mu(x)\varphi_\nu^+(y) \mid 0\rangle = ig_{\mu\nu}\Delta_F(x-y)\,, \tag{2}$$

instead of the usually adopted form $i(g_{\mu\nu} - M^{-2}\partial_\mu\partial_\nu)\Delta_F(x-y)$. The choice of such a Lagrangian makes the theory of weak interactions fully renormalizable, introducing however an indefinite metric into the Hilbert space. As long as there are no vector mesons in the initial and final states our scheme gives unique and finite transition amplitudes for every weak process. To deal with the vector mesons appearing in the final or initial states this scheme must be supplemented by some methods of handling states with negative norm as for example the one proposed by E. C. G. SUDARSHAN [5].

From the Lagrangian (1) one may derive the electromagnetic interaction of the meson φ_μ by assuming the « minimal » electromagnetic interaction. This procedure does not give however the interaction of the meson magnetic moment and the corresponding interaction term must be added separately. The electromagnetic Lagrangian for the vector meson has finally the form

$$\mathscr{L}_{\mathrm{em}}^{vm} = ie\varphi_\nu^+ \overleftrightarrow{\partial}_\mu \varphi^\nu A^\mu - e^2 A_\mu A^\mu \varphi_\nu^+ \varphi^\nu + ie(1+\lambda)\varphi_\nu^+ \varphi_\mu F^{\nu\mu}\,, \tag{3}$$

where λ is an anomalous magnetic moment in the units of the vector meson magneton. The inclusion of this interaction does not spoil the renormalizability of our theory.

The probability for the process $\mu \to e + \gamma$ is computed from the following diagrams:

Fig. 1.

The Lagrangian giving contribution to this process has the form

$$\mathscr{L} = M\sqrt{G}\bar{\psi}_{(e)}\gamma'_\lambda(1 - i\gamma'_5)\psi_{(\nu)}\varphi^\lambda + M\sqrt{G}\bar{\psi}_{(\nu)}\gamma'_\lambda(1 - i\gamma'_5)\psi_{(\mu)}\varphi^\lambda + \mathscr{L}_{\mathrm{em}}\,. \tag{4}$$

The divergent contributions cancel in the sum as a result of gauge invariance of the theory. The transition amplitude was computed in the approximation in which (m_e/m_μ) and $(m_\mu/M)^2$ were neglected in comparison with unity. The result is

$$S_{i\to f} = \delta_4(p - q - k)(1 + 3\lambda)C\bar{u}_{(e)}(\bar{q})(1 + i\gamma'_5)\gamma'_{\mu\nu}k^\mu e^\nu(\bar{k})(1 + i\gamma'_5)u_{(\mu)}(\bar{p})\,, \tag{5}$$

where $u_{(e)}(\bar{q})$ and $u_{(\mu)}(\bar{p})$ are the wave functions of electron and muon with momenta $\bar{q}$ and $\bar{p}$ respectively, $e^\nu(\bar{k})$ describes the polarization of the photon, C is a constant depending on e, G, m_μ and m_e only. This amplitude does not vanish unless we put

[5] E. C. G. SUDARSHAN: *Phys. Rev.* (to be published).

$\lambda = -\frac{1}{3}$. The value of ϱ obtained for $\lambda=0$ is 10^3 times larger than the experimental upper limit.

No interactions are known which could produce a large anomalous magnetic moment of the vector meson and therefore our result should be regarded as a negative one. There are two ways of saving the above proposed theory of the weak interactions: to assume the existence of two different kinds of neutrinos or to consider the magnetic moment $1+\lambda = \frac{2}{3}$ to be the normal one for this kind of meson.

* * *

The author is greatly indebted to Dr. I. Bialynicki-Birula for suggesting the problem and continuous help and to Dr. E. C. G. Sudarshan for discussions.

Sur les relations entre charges et spin.

F. Lurçat

Institut de Physique, Faculté des Sciences - Lille

L. Michel

Physique Théorique et Hautes Energies - Orsay

(ricevuto il 6 Giugno 1961)

Une des énigmes que pose actuellement l'étude des particules élémentaires est la suivante (1): parmi les trois (2) espèces de charges strictement conservées (3): la charge électrique q, la charge baryonique (4) b et la charge leptonique (5) l, la charge électrique est la seule que puissent posséder les mésons, qui sont des particules de spin entier. Par contre, il n'existe aucune particule de spin demi-entier sans charge, soit baryonique, soit leptonique. Cela peut être résumé en une formule:

$$(1) \qquad (-1)^{2j} = (-1)^{b+l},$$

vraie pour tout état physique (j désigne le moment cinétique).

Nous nous proposons de montrer comment une relation de cette forme (équation (7)) peut apparaître comme conséquence d'axiomes admis ou admissibles par de nombreux physiciens (axiomes a, b, c, d).

a) Les observables en mécanique quantique sont représentées par des opérateurs hermitiens $A = A^*$, sur un espace d'Hilbert $\mathcal{H}$.

b) Il existe un système complet d'observables commutatives.

Pour déduire de a) et b) les propriétés qui nous seront nécessaires, nous suivrons l'excellent exposé de Jauch (6) auquel

(1) Voir par exemple D. H. Wilkinson in: *Turning points in physics* (Amsterdam, 1959), p. 169.

(2) Nous laissons au lecteur le soin de généraliser au cas où il existerait plusieurs charges pour les leptons (par exemple: νe d'une part, $\mu\nu'$ d'autre part).

(3) Pour la discussion des preuves expérimentales de la conservation des charges, voir: G. Feinberg and M. Goldhaber: *Proc. Nat. Acad. Sci. U.S.A.*, **45**, 1301 (1959).

(4) Le concept de charge nucléonique semble avoir été introduit par E. Wigner: *Proc. Am. Phil. Soc.*, **93**, 521 (1949). La généralisation aux hypérons, après la découverte de ces derniers, était évidente.

(5) Le concept de charge leptonique semble avoir été introduit par E. Fermi vers 1950 (non publié). La charge leptonique attribuée à chaque lepton a varié au cours des dix dernières années (voir par ex.: E. J. Konopinski and H. M. Mahmoud: *Phys. Rev.*, **92**, 1045 (1953); Ya. B. Zeldovich: *Doklady Akad. Nauk USSR*, **91**, 1317 (1953)); actuellement elle semble fixée à la même valeur pour e^-, μ^-, ν.

(6) J. M. Jauch: *Helv. Phys. Acta*, **33**, 711 (1960).

nous renvoyons le lecteur pour plus de détails.

Résumons d'abord les notions mathématiques utilisées:

Si $\mathscr{D}$ est un ensemble d'opérateurs sur $\mathscr{H}$ tel que $D_1 \in \mathscr{D}$, $D_2 \in \mathscr{D}$ implique $\alpha D_1 \in \mathscr{D}$, $D_1 + D_2 \in \mathscr{D}$, $D_1 D_2 \in \mathscr{D}$, $D_1^* \in \mathscr{D}$ (α est un nombre complexe), il est appelé une $*$-algèbre.

On appelle commutant [7] d'un ensemble d'opérateurs $\mathscr{M}$ l'ensemble $\mathscr{M}'$ des opérateurs bornés commutant avec tous les opérateurs de $\mathscr{M}$. On pose $\mathscr{M}'' = (\mathscr{M}')'$, etc.

Si $\mathscr{M}$ et $\mathscr{N}$ sont des ensembles d'opérateurs bornés, $\mathscr{M}'' \supset \mathscr{M}$; de plus, l'inclusion $\mathscr{N} \supset \mathscr{M}$ entraîne $\mathscr{M}' \supset \mathscr{N}'$; en particulier, si $\mathscr{N} = \mathscr{M}''$, $\mathscr{M}' \supset (\mathscr{M}'')' = \mathscr{M}'''$; et puisqu'on a aussi $\mathscr{M}''' = (\mathscr{M}')'' \supset \mathscr{M}'$, on a $\mathscr{M}' = \mathscr{M}'''$.

Si $\mathscr{M}$ est une $*$-algèbre et si $\mathscr{M} = \mathscr{M}''$, $\mathscr{M}$ est appelée algèbre de von Neumann.

Soit $\mathscr{O}$ l'ensemble des observables: puisque ce sont des opérateurs hermitiens, $\mathscr{O}'$ est une $*$-algèbre et $\mathscr{O}'$ et $\mathscr{O}''$ sont des algèbres de von Neumann que nous noterons $\mathscr{N}'$ et $\mathscr{N}$. On dit que $\mathscr{N}$ est l'algèbre de von Neumann engendrée par $\mathscr{O}$.

Jauch [6] montre que l'axiome b) équivaut à:

b') Il existe une sous-algèbre abélienne $\mathscr{B}$ de $\mathscr{N}$ qui est maximale, c'est-à-dire $\mathscr{B}' = \mathscr{B}$.

De $\mathscr{B} \subset \mathscr{N}$ résulte $\mathscr{B}' \supset \mathscr{N}'$; donc le commutant $\mathscr{N}'$ est abélien. On dit alors (référence [8], p. 120) que l'algèbre $\mathscr{N}$ est discrète. De plus, $\mathscr{N}' \subset \mathscr{B}' = \mathscr{B}$ implique que $\mathscr{N}'$ est le centre de $\mathscr{N}$ (c'est-à-dire $\mathscr{N}' \cap \mathscr{N}$).

$\mathscr{N}'$ contient en particulier les opérateurs Q, B, L correspondant aux charges électrique, baryonique et leptonique. Nous faisons l'hypothèse physique que $\mathscr{N}'$ est engendré par Q, B, L.

La décomposition spectrale de $\mathscr{N}'$ détermine une somme directe [9]

$$\mathscr{H} = \oplus_\lambda \mathscr{H}(\lambda),$$

d'espaces d'Hilbert $\mathscr{H}(\lambda)$. Seuls les éléments de ces espaces (et non tout élément de $\mathscr{H}$) représentent des états physiques. Deux états représentés par des vecteurs appartenant à des $\mathscr{H}(\lambda)$ différents sont dits séparés par une règle de supersélection. Les règles de supersélection étant ainsi obtenues indépendamment de l'invariance relativiste, la règle obtenue usuellement à partir de l'invariance par rapport à $\mathscr{L}_0$ (supersélection entre les états de spin entier et demi-entier) doit être incluse dans les précédentes; d'où l'existence d'une relation entre $(-1)^{2j}$ et les charges. Afin de préciser la nature de cette relation, nous allons maintenant formuler l'invariance relativiste, en nous limitant ici au sous-groupe connexe $\mathscr{L}_0$ de $\mathscr{L}$, groupe de Lorentz inhomogène (autrement dit, nous ne considérerons pas les réflexions d'espace et de temps).

c) Il existe un isomorphisme entre $\mathscr{L}_0$ et un sous-groupe du groupe des automorphismes de $\mathscr{N}$. Les charges étant invariantes par les transformations de $\mathscr{L}_0$, les automorphismes de $\mathscr{N}$ correspondants laissent fixes les éléments de $\mathscr{N}'$. Nous pouvons alors utiliser le théorème énoncé à la ref. [8], p. 255-256.

Tout automorphisme A d'une algèbre de von Neumann discrète $\mathscr{N}$, qui laisse fixes les éléments du centre de cette algèbre, peut s'écrire:

$$A \xrightarrow{A} UAU^{-1}, \tag{2}$$

où U est un opérateur unitaire appartenant à $\mathscr{N}$.

Quels sont tous les opérateurs uni-

[7] Pour la définition précise de la commutation avec un opérateur non borné, voir la référence [8].

[8] J. Dixmier: *Les algèbres d'opérateurs dans l'espace hilbertien (algèbres de von Neumann)* (Paris, 1957).

[9] Ici, pour notre $\mathscr{N}'$; Jauch (réf. [6]) envisage la cas plus général d'une intégrale directe.

taires qui réalisent l'automorphisme A? Si U_1 et U_2 sont deux tels opérateurs, $U_1 U_2^{-1}$ est un élément unitaire de $\mathcal{N}'$. Appellons $\mathcal{C}$ l'ensemble des opérateurs unitaires de $\mathcal{N}'$. $\mathcal{N}'$ étant une $*$-algèbre, $\mathcal{C}$ est un groupe. Appelons $\mathcal{U}$ l'ensemble des U pour tous les $A \in \mathcal{L}_0$: $\mathcal{U}$ est un groupe homomorphe à $\mathcal{L}_0$. Les U qui correspondent à l'identité de $\mathcal{L}_0$ sont les éléments de $\mathcal{C}$, sous-groupe invariant de $\mathcal{U}$.

Notons que $\mathcal{C}$ est dans le centre de $\mathcal{U}$; d'après l'axiome c) le quotient $\mathcal{U}/\mathcal{C}$ est isomorphe à $\mathcal{L}_0$; nous noterons cela:

$$(3) \qquad \begin{cases} \mathcal{C} \subset \text{centre } (\mathcal{U}) , \\ \mathcal{U}/\mathcal{C} \sim \mathcal{L}_0 . \end{cases}$$

Il existe plusieurs solutions au problème: étant donné deux groupes $\mathcal{C}$ abélien et $\mathcal{L}_0$, trouver tous les groupes $\mathcal{U}$ tels que $\mathcal{C}$ soit dans le centre de $\mathcal{U}$ et $\mathcal{U}/\mathcal{C} \sim \mathcal{L}_0$ (relation (3)). On dit aussi: trouver toutes les extensions centrales de $\mathcal{L}_0$ par $\mathcal{C}$. Nous exposerons ailleurs la solution de ce problème [10].

Les restrictions à un $\mathcal{H}(\lambda)$ de Q, B, L et des éléments de $\mathcal{C}$ sont des multiples de l'identité qui sont respectivement de la forme: q, b, l et $\exp[if(q, b, l)]$ où f est une fonction réelle. Les $\mathcal{H}(\lambda)$ peuvent être étiquetés par les triplets d'entiers (q, b, l). La méthode usuelle pour obtenir ces résultats, c'est d'exiger l'invariance par rapport au groupe de jauge $\mathcal{A}$, dont les éléments sont

$$(4) \qquad \exp[i(\alpha_q Q + \alpha_b B + \alpha_l L)] ,$$

(les α sont des nombres réels modulo 2π). Les représentations linéaires irréductibles de $\mathcal{A}$ sont en effet

$$(5) \qquad \exp[i(\alpha_q q + \alpha_b b + \alpha_l l)] ,$$

et sont caractérisées par les triplets d'entiers q, b, l.

[10] F. LURÇAT et L. MICHEL: à paraître.

En fait, dans les théories usuelles, on ne considère pas le groupe $\mathcal{C}$, et on se contente d'utiliser le groupe de jauge $\mathcal{A}$. Ceci nous amène à poser:

d) Les transformations de Lorentz (éléments de $\mathcal{L}_0$) sont représentées à une transformation de jauge près.

Dans le langage utilisé précédemment, cela revient à dire que le groupe d'invariance de la théorie est un groupe $\mathcal{E}$, qui est une extension centrale de $\mathcal{L}_0$ par $\mathcal{A}$.

Pour le groupe $\mathcal{A}$ défini par (4), on montre [10] que les extensions inéquivalentes sont caractérisées par un élément d'ordre 2 (racine carrée de l'unité) de $\mathcal{A}$, qui correspond à la « rotation de 2π ». Le groupe $\mathcal{A}$ possède 8 racines carrées de l'unité, qui sont

$$(6) \qquad \exp[i\pi(\varepsilon_q Q + \varepsilon_b B + \varepsilon_l L)] ,$$

avec $\varepsilon = 0$ ou 1.

Par suite, pour un état de moment cinétique j, de charges q, b, l, on a la relation

$$(7) \qquad (-1)^{2j} = (-1)^{\varepsilon_q q + \varepsilon_b b + \varepsilon_l l} .$$

Les relations (7) et (1) doivent être compatibles quels que soient j, b, l; cette condition détermine de façon unique le groupe $\mathcal{E}$:

$$(8) \qquad \varepsilon_q = 0 , \qquad \varepsilon_b = \varepsilon_l = 1 .$$

On peut remarquer que, contrairement à ce qui semble généralement admis, ce groupe n'est pas le produit direct de $\mathcal{L}_0$ par $\mathcal{A}$ (qui correspondrait à $\varepsilon_q = \varepsilon_b = \varepsilon_l = 0$). Nous reviendrons ultérieurement sur les conséquences physiques de ce fait.

* * *

L'un de nous (F. L.) remercie M. JEAN de l'avoir accueilli au Laboratoire de Physique Nucléaire d'Orsay, Groupe I.

IL NUOVO CIMENTO Vol. XXI, N. 3 1° Agosto 1961

Some Remarks on Low Energy Pion Phenomena.

J. K. Walker

Ecole Normale Supérieure, Laboratoire de l'Accélérateur Linéaire - Orsay (S. et O.)

(ricevuto il 9 Giugno 1961)

It would appear that in the last two years the anomalies that once existed in the relationship between pion photoproduction and scattering via the Panofsky ratio have gradually dissolved to the point that there exists a reasonable agreement within the field. The purpose of the present note is to show that when the experimental data are re-analysed according to better theoretical prescriptions there emerge certain small but not insignificant discrepancies in the data.

Following the suggestion of Baldin [1] we have analysed the reactions

$$\gamma + p \to n + \pi^+, \tag{1}$$

$$\gamma + n \to p + \pi^-, \tag{2}$$

in such a way that there should be good agreement with the predictions of the Chew-Goldberger-Low-Nambu and Robinson (C.G.L.N.R.) theory [2]. The basis of the method is that the comparison is made in a region of the kinematic variables such that the momentum transfer is fixed and equal to that occurring at the threshold of the reactions (1) and (2). In this way it is possible to eliminate the contribution under the dispersion integrals of the unobservable energy region. It has been shown that this is an important qualification [3] as the π-π interaction can produce appreciable contributions to the amplitudes which have not been included in the C.G.L.N.R. theory.

1. – π^+ photoproduction data.

The cross-section for the process (1) can be written in the form

$$\frac{d\sigma}{d\Omega} = \eta\omega \left[1 + \frac{\mu}{M} v\right]^{-2} |T^+|^2 ,$$

in the notation employed by Bernardini [4]; we require that the momentum transfer at any photon energy v should be equal to that at threshold, *i.e.* we require [5].

$$v(\omega - \cos\theta) = 0.93 .$$

---

[1] A. M. Baldin: *Proc. of the 1960 Annual International Conference on High Energy Physics at Rochester*, p. 325.

[2] C. S. Robinson: Technical Report, no. 8, Office of Naval Research, 1834 (05).

[3] B. De Tollis, E. Ferrari and H. Manczik: *Nuovo Cimento*, **18**, 198 (1960).

[4] G. Bernardini: *Proc. of the CERN Symposium* (1956), p. 251.

[5] At the Rochester Conference 1960, Baldin reported a similar comparison with experimental data but it appears that he used π^0-meson kinematics in the case of π^+-meson photoproduction. Secondly, his comparison did not include the interesting energy region where there appears to be a «resonance».

We have analysed the available experimental data and extracted $|T^+|^2$ at the appropriate value of θ at each given ν ([6]), the result of this is shown in Fig. 1. It should be noted that the data of Beneventano *et al.* have been at Illinois ([13]). Plotted also is the prediction of the C.G.L.N.R. theory with values of f^2 and ω_0^* as shown. A good agreement both in absolute magnitude and energy dependence is obtained from threshold up to the $(\frac{3}{2}\,\frac{3}{2})$ resonance at

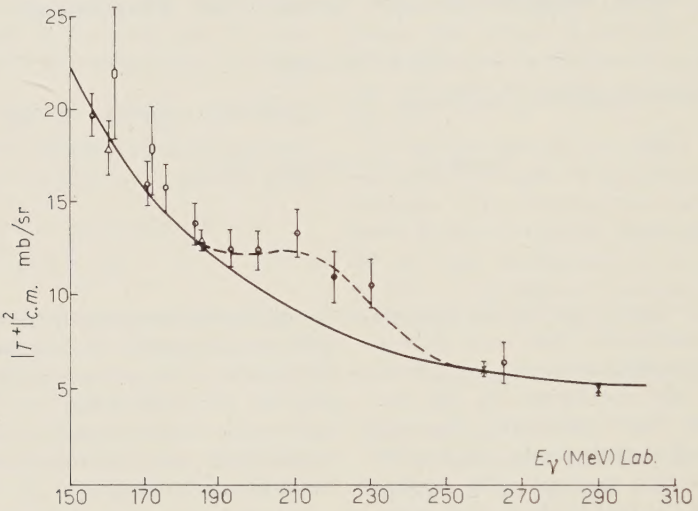

Fig. 1. – Beneventano *et al.* ([7]); Leiss *et al.* ([8]); Knapp *et al.* ([9]); Walker *et al.* ([10]); Adamovich *et al.* ([11]); Barbara *et al.* ([12]): —— C.G.L.N.R. with $f^2=0.081$ and $\omega_0=2.08$, – – – Best fit (Eye).

increased in absolute magnitude by 10% to take account of a recent recalibration

([6]) Where experimental data are reported at values of the kinematic variables other than those required here we have only accepted these data when the difference in differential cross-section between the two conditions is less than 1% under the assumption of a reasonable angular distribution.

([7]) M. Beneventano, G. Bernardini, D. Carlson-Lee, G. Stoppini and L. Tau: *Nuovo Cimento*, **4**, 323 (1956).

([8]) J. Leiss and A. S. Penner: *Proc. of the 1960 Annual International Conference on High Energy Physics at Rochester.*

([9]) E. Knapp, R. W. Kenney and V. Perez-Mendez: *Phys. Rev.*, **114**, 605 (1958).

([10]) J. K. Walker, J. G. Rutherglen, D. Miller and J. M. Peterson: to be published.

([11]) *Proc. of the 1960 Annual International Conference on High Energy Physics at Rochester*, p. 330.

([12]) *Proc. of the 1959 Annual International Conference on High Energy Physics at Kiev*, p. 41.

300 MeV. A suggestion of a bump in the experimental data occurs at around 215 MeV where there is a $\sim(30\pm10)\%$ absolute discrepancy with the theory. It is difficult to conclude whether this is due to a systematic experimental error (the experimental evidence relies entirely on one experiment) or to a true « resonance » occurring in the production amplitude. It is clear that new experimental data are highly desirable to verify or otherwise the existence of this phenomenon.

It may be relevant to note at this stage that recent Russian work ([11]) on the angular distribution of this reaction at 185 MeV is in disagreement with the

([13]) *Proc. of the 1960 Annual International Conference on High Energy Physics at Rochester*, p. 26.

experimental data of Beneventano *et al.* by about $(35 \pm 10)\%$ at backward angles. It must therefore be concluded, that the possibility of an experimental error of this magnitude cannot be completely ruled out.

The extrapolation of the experimental data to threshold would appear to be unambiguous and gives a value for $|T^+|$ of 22.0 μb/sr with an estimated accuracy of $\pm 5\%$.

2. – π^-/π^+ ratio.

The photoproduction of charged pions from deuterium has been studied extensively by several investigators. We have used the experimental results of Beneventano *et al.* [7], Hogg and Bellamy [14], Sands *et al.* [15] and Rutherglen and Walker [16] which appear to constitute a reasonably self consistent set of data. Best fits by eye, as the proper analytic variation is unknown, were made to this data in the entire angular region and the values of ratio were extracted at the required values of θ. The variation of the π^-/π^+ ratio as a function of γ-ray energy is shown plotted in Fig. 2. The uncertainties shown are reasonable limits allowed by the fits to the experimental data. Also shown in Fig. 2 is the C.G.L.N.R. prediction evaluated under the same conditions as before. The corrections for final state interactions, both nuclear and Coulomb, have been calculated by Baldin [17] and their effect on the C.G.L.N.R. theory is shown by the dashed line. The agreement is seen to be approximate and nowhere within the range investigated does the discrepancy exceed 13%. The predicted energy variation of the ratio does seem to be in discord with that found experimentally. As the basic theory should be good to about 5% and the final state interactions' correction takes account of effects which produce a $\geqslant 10\%$ correction then it is just possible, although rather unlikely, that the experimental data can be properly described within the framework of the present theory.

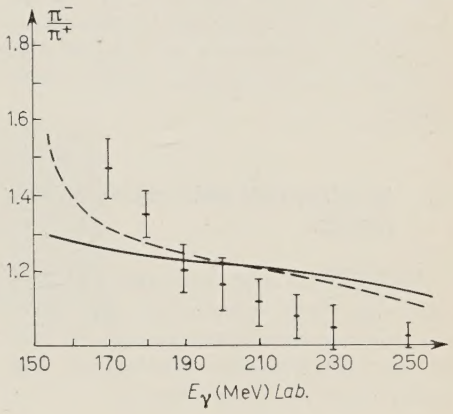

Fig. 2. – —— C.G.L.N.R. theory; – – – Corrected for final state effects.

It has been shown [3] that the π-π interaction gives an important contribution to the π^-/π^+ ratio. Therefore, it would seem desirable to adjust the parameters in the π-π contribution so that a good fit to the experimental data is obtained in this region of kinematic variables where the evaluation of the C.G.L.N.R. theory is thought to be correct, and not at a fixed angle in the c.m. system which is the procedure which has previously been followed.

It is clear from Fig. 2 that it is difficult to extrapolate the experimental data to threshold in a rigorous way. However, it would appear that a value 15% to 20% higher than that of 1.30 predicted by the C.G.L.N.R. theory, is not unreasonable.

---

[14] W. R. Hogg and E. H. Bellamy: *Proc. Phys. Soc.*, **72**, 895 (1958).

[15] M. Sands, J. G. Teasdale and R. L. Walker: *Phys. Rev.*, **95**, 592 (1954); **101**, 1159 (1956).

[16] J. G. Rutherglen and J. K. Walker: *Proc. Phys. Soc.*, **76**, 431 (1960).

[17] A. M. Baldin: *Nuovo Cimento*, **8**, 569 (1958).

The fact that the above conclusion is not substantiated by the experimental data of Kharlamov *et al.* [18] who claim that $\pi^-/\pi^+ = (1.30 \pm 10)\%$ in the energy interval 156 to 172.5 MeV is thought to represent the difficulty of interpretation of final state interactions in this energy region.

3. – Panofsky ratio and S-wave scattering lengths.

Within the last year the Panofsky ratio has been remeasured with great accuracy by several groups and reported at the 1960 Rochester Conference. The mean value of all the data is

$$P = (1.53 \pm 1)\% .$$

Finally, the S-wave scattering lengths appear to have been treated in the most complete fashion by Hamilton and Woolcock [19] who obtain:

$$a_1 - a_3 = 0.245 \pm 0.007 .$$

4. – Conclusion.

When we use the above values of P, $a_3 - a_1$, and $|T^+|^2$ to calculate the π^-/π^+ ratio we obtain the value 1.2 ± 0.1. This value has to be compared with the threshold value of the π^-/π^+ ratio which we have already discussed. It is clearly in adequate agreement with the C.G.L.N.R. predictions and the data of Adamovich *et al.* However, there is room for improvement in the agreement of this threshold value with that obtained from the rest of the experimental data.

In conclusion, we may say that although the description of low energy pion phenomena has reached a relatively satisfactory state, with reasonable internal consistency being displayed, there still exist certain discrepancies which remain to be clarified.

([18]) S. Kharlamov, M. Adamovich and V. Larionova: *Žurn. Èks. Teor. Fiz.*, **36**, 946 (1959).

([19]) J. Hamilton and W. S. Woolcock: *Phys. Rev.*, **118**, 291 (1960).

Direttore responsabile: G. POLVANI Tipografia Compositori - Bologna

Questo fascicolo è stato licenziato dai torchi il 18-VIII-1961